Physikalisch
Technische
Bundesanstalt

PTB-Bericht

Ulrike Ankerhold

Catalogue of X-ray spectra and their characteristic data –ISO and DIN radiation qualities, therapy and diagnostic radiation qualities, unfiltered X-ray spectra–

PTB-Dos-34
Braunschweig, April 2000

ISSN 0341-6674
ISBN 3-89701-513-7

PTB

Recommended citation format:
Ankerhold, Ulrike. Catalogue of X-ray spectra and their characteristic data : ISO and DIN radiation qualities, therapy and diagnostic radiation qualities, unfiltered X-ray spectra. Physikalisch-Technische Bundesanstalt (PTB), 2000.
Available by: https://doi.org/10.7795/110.20190315B

Verfügbar unter: https://doi.org/10.7795/110.20190315B

Physikalisch-Technische Bundesanstalt

Dosimetrie

PTB-Bericht Dos-34

Catalogue of X-ray spectra and their characteristic data

— ISO and DIN radiation qualities, therapy and diagnostic radiation qualities, unfiltered X-ray spectra —

by

Ulrike Ankerhold

Verfügbar unter: https://doi.org/10.7795/110.20190315B

Abstract

The pulse height spectra of the radiation qualities of the low air-kerma rate, narrow-spectrum, wide-spectrum and high air-kerma rate ISO series, the A-, B- and C-series according to the German DIN standard 6818-1, several diagnostic and therapy radiation qualities and unfiltered X-ray spectra were measured using a Ge spectrometer and a special experimental set-up. The spectra were unfolded to obtain the fluence spectra. The values for the characteristic parameters (first and second half-value layer, mean photon energy, 10 % percentile, kerma factor, conversion coefficients from air kerma, K_a, to the operational radiation protection quantities $H_p(10)$, $H_p(0{,}07)$, $H^*(10)$ and $H'(0{,}07,\vec{\Omega})$) were determined for each radiation quality and each unfiltered X-ray spectrum using these fluence spectra. All data given are normalised to reference conditions. For each radiation quality and each unfiltered X-ray spectrum the fluence spectrum is shown in a graph together with two other curves. One curve is the fluence spectrum weighted with the energy-dependent kerma factors; the second is the fluence spectrum weighted with the energy-dependent conversion coefficients from fluence to personal dose equivalent, $H_p(10)$.

Zusammenfassung

Die Impulshöhenspektren von den Strahlungsqualitäten der Low-air-kerma-rate-, Narrow-spectrum-, Wide-spectrum- and High-air-kerma-rate-ISO-Serien, der A-, B- und C-Serien der deutschen Norm DIN 6818-1, mehrerer diagnostischer und Therapie-Strahlungsqualitäten und ungefilterter Röntgenspektren wurden mit einem Ge-Spektrometer und einem speziellen Messaufbau gemessen. Die Spektren wurden entfaltet zur Bestimmung der Fluenzspektren. Für jede Strahlungsqualität und jedes ungefilterte Röntgenspektrum wurden die Werte der charakteristischen Parameter (erste und zweite Halbwertschichtdicke, mittlere Photonenenergie, 10 % Percentile, Kermafaktor, Konversionsfaktoren zur Umrechnung der Luftkerma, K_a, in die Messgrößen im Strahlenschutz $H_p(10)$, $H_p(0{,}07)$, $H^*(10)$ und $H'(0{,}07,\vec{\Omega})$) mit Hilfe der Fluenzspektren bestimmt. Alle Spektren und somit alle charakteristischen Daten sind auf Bezugsbedingungen normiert worden. Für jede Strahlungsqualität und für jedes ungefilterte Röntgenspektrum ist das Fluenzspektrum zusammen mit zwei weiteren Kurven in einem Bild dargestellt. Eine Kurve stellt das Fluenzspektrum gewichtet mit den monoenergetischen Kermafaktoren dar; die zweite Kurve ist das Fluenzspektrum gewichtet mit den monoenergetischen Konversionsfaktoren zur Umrechnung der Fluenz in die Tiefen-Personendosis, $H_p(10)$.

General remark:

In accordance with ISO 31-0 [1], a comma on the line is used in this report as the decimal sign.

Contents

Verfügbar unter: https://doi.org/10.7795/110.20190315B

Verfügbar unter: https://doi.org/10.7795/110.20190315B

1. Introduction

Dosemeter systems generally show an energy dependence of their response often very strong at low photon energies. It is, therefore, necessary to calibrate dosemeters and to perform type testing using different photon spectra. X-radiation qualities, i.e. real photon spectra produced under standard experimental conditions, specified in the standards ISO 4037-1 [2], DIN 6818-1 [3], IEC 61267 [4] (DIN EN 61267 [5]), DIN 6817 [6], DIN 6809-4 [7] and DIN 6809-5 [8] are used for calibration and type testing purposes. In the standards they are characterised by the parameters X-ray tube voltage, filtration, mean photon energy, first half-value layer and, partly, second half-value layer and 10 % percentile.

With the introduction of the new concept of radiation protection quantities, which was developed by the ICRU (International Commission on Radiation Units and Measurements) [9], further characteristic values have to be determined for each radiation quality. The new concept contains the two quantities for individual monitoring, the personal dose equivalents $H_p(10)$ and $H_p(0,07)$, and the two quantities for area monitoring, the ambient dose equivalent, $H^*(10)$, and the directional dose equivalent, $H'(0,07,\vec{\Omega})$. These operational quantities are now accepted worldwide and were integrated into international standards. According to the international standard ISO 4037-3 [10], the calibration of dosemeters and the determination of their response as a function of photon energy and, if specified, of the angle of radiation incidence in terms of the operational quantities is to be based on the quantity air kerma free-in-air, K_a. It is therefore indispensable to know the conventionally true values of the conversion coefficients from air kerma, K_a, to the new quantities for each radiation quality used for calibration.

The characteristic parameters, first and second half-value layer, can be determined using ionisation chambers [11]. However, to determine the mean photon energy, the 10 % percentile, the kerma factor and the conversion coefficients mentioned in the previous paragraph, the fluence spectra of the radiation qualities have to be known.

It is a prerequisite for measuring X-ray spectra that the X-ray facilities used are adjusted to produce very low dose rates. However, most X-ray units commercially available are designed to generate as high dose rates as possible, and low dose rates cannot be achieved. This is certainly one reason why only few publications giving measured fluence spectra exist. Measured spectra of some selected X-radiation qualities together with their values of the characteristic parameters (first and second half-value layer, mean photon energy) were published by Peaple *et al.* [12], Iles *et al.* [13], Read *et al.* [14] and, recently, by Ankerhold *et al.* [15]. A comprehensive catalogue of many measured fluence spectra and tables with the values of the characteristic parameters (first and second half-value layer, mean photon energy and homogeneity coefficient) were published 20 years ago by Seelentag *et al.* [16]. The fluence spectra contained in that catalogue are frequently used to determine the charateristic data of radiation qualities, which then were integrated into international or national standards.

If published spectra are used, it is to be considered that the spectral distribution of nominally the same X-ray quality, but generated by different X-ray facilities, will always show small differences due to differences between the X-ray units (different tube anode angle, anode roughening, high-voltage waveform, inherent filtration, etc.). Due to technical improvements of the X-ray facilities, e.g. reducing the ripple of the voltage, the spectral distribution of the X-ray spectra generated has changed in the last 20 years, as shown by the comparison between several fluence spectra of the ISO narrow-spectrum series measured by Seelentag *et al*. [16] and more recent measurements [12][13][14][15]. Furthermore, fluence spectra of the same radiation quality and generated by the same X-ray facility can also show spectral differences. Due to the energy

Verfügbar unter: https://doi.org/10.7795/110.20190315B

dependence of air absorption, the fluence spectra change when the distance between the measuring position and the focus of the X-ray tube or, which is the same, the air density is changed [15]. The air absorption and the specific differences of the X-ray units may result in great spectral changes of the X-ray spectra of the radiation qualities with a low mean photon energy. However with increasing X-ray tube voltage, the spectral differences decrease [15].

Therefore and because of the strong energy dependence of the monoenergetic conversion coefficients from air kerma, K_a, to $H_p(10)$ and $H^*(10)$ [17][18], in particular for low photon energies E, it is most important to know the fluence spectra generated by the X-ray facility used to determine the conversion coefficients. This is emphasized by the comparison of the conversion coefficients from K_a to $H_p(10)$ determined using the fluence spectra measured by Seelentag *et al.* [16] and Ankerhold *et al.* [15], which show differences of up to 88 %. Compared with the conversion coefficients, the influence of spectral differences on the parameters mean photon energy, first and second half-value layer and 10 % percentile are much smaller [15].

These considerations were a starting point for the measurements of the fluence spectra of all radiation qualities 'R' used for calibration and type testing of dosemeters and for the determination of the characteristic data of these spectra (first and second half-value layer, mean photon energy, 10 % percentile, kerma factor, conversion coefficients from K_a to $H_p(10)$, $H_p(0{,}07)$, $H^*(10)$ and $H'(0{,}07,\vec{\Omega})$, respectively). The fluence spectra of the radiation qualities specified in the standards ISO 4037-1 [2] and DIN 6818-1 [3] and unfiltered X-ray spectra were measured at a distance of 1,0 m and 2,5 m. The additional measurement of the fluence spectra of these radiation qualities at a distance of 2,5 m is necessary for the following reason: for calibration in terms of $H_p(10)$, personal dosemeters are irradiated on a slab phantom (300 mm x 300 mm x 150 mm) [19][20]. In order to irradiate the whole phantom surface homogeneously, the distance between the focus of the X-ray tube and the phantom has to be about 2,5 m [21]. Therefore, to determine the conventionally true conversion coefficients from air kerma, K_a, to $H_p(10)$ for these radiation qualities 'R', the fluence spectra at this distance have to be known. The fluence spectra of the diagnostic radiation qualities specified in standard IEC 61267 [4] (DIN EN 61267 [5]) and by Engelke *et al.* [22] were measured at a distance of 1,0 m. The fluence spectra of the therapy radiation qualities given in standards DIN 6817 [6], DIN 6809-4 [7] and DIN 6809-5 [8] were determined at the specified distance (0,3 m and 1,0 m, respectively).

For comparison and discussion, all spectra and thus all characteristic data given were normalised to reference conditions. All fluence spectra measured are available for downloading as ASCII files in the Internet on the homepage of the "Area and Personal Dosimetry" Section of the Physikalisch-Technische Bundesanstalt (http:\\www.ptb.de) so that characteristic data not contained in this report can be determined and radiation calculations using the fluence spectra be performed.

Unfiltered X-ray spectra were measured for the two following reasons: firstly they are well suitable for testing theoretical model calculations and secondly the spectrum of any radiation quality can be calculated using the unfiltered X-ray spectrum with the correct X-ray tube voltage and the exponential attentuation law with the filtration chosen.

The catalogue is subdivided into five sections: In the next section, the experimental set-up and the unfolding procedure, which have been presented in detail by Ankerhold *et al.* [15], are briefly described. In the third section, the determination of the characteristic data using the fluence spectra is explained. The uncertainties of the characteristic data considered in this report are also discussed. The fourth section gives the tables with the characteristic values determined. In the fifth section a graph is presented for each radiation quality and each unfiltered X-ray spectrum considered in this report, showing the fluence spectrum not weighted and weighted with the kerma factor and the fluence-to-personal dose equivalent conversion coefficient, respectively.

2. Experiment

Pulse height spectra of the following radiation qualities were measured: the radiation qualities of the ISO low air-kerma rate series (L), the ISO narrow-spectrum series (N), the ISO wide-spectrum series (W) and the ISO high air-kerma rate series (H) according to ISO 4037-1 [2] as well as of the DIN A-, B-, and C-series according to the German standard DIN 6818-1 [3], therapy radiation qualities according to DIN 6817 [6], DIN 6809-4 [7] and DIN 6809-5 [8] and diagnostic radiation qualities according to IEC 61267 [4] (DIN EN 61267 [5]) and Engelke *et al.* [22]. In addition, the pulse height spectra of unfiltered X-ray spectra were measured.

The experimental set-up and the measurements of the pulse height spectra have been described in detail by Ankerhold *et al.* [15]. Therefore only a general outline of the mesurements is given in the following; however, the few differences from the measurements performed by Ankerhold *et al.* [15] are described in detail.

The measurements of the pulse height spectra were performed in two different X-ray units of the PTB in Braunschweig. For the radiation qualities and the unfiltered X-ray spectra with a tube voltage equal to or lower than 120 kV, a 120 kV facility with a MB 121/1 type tube manufactured by AEG, and for the radiation qualities and the unfiltered X-ray spectra with a tube voltage higher than 120 kV, a 420 kV facility with a MB 420/1 type AEG tube were used. Both X-ray tubes have a tungsten anode with a 20° angle. In both X-ray units, directly behind the X-ray tube, a PTW monitor chamber (model No. 786) is installed with three Kapton® (polyimide) foils serving as entrance and exit windows and as center electrode. Filters according to ISO 4037-1 [2] and DIN 6818-1 [3] were used to produce the spectra of the radiation qualities of the ISO and DIN series. For the therapy radiation qualities, filters according to DIN 6817 [6] and for the diagnostic radiation qualities, filters according to IEC 61267 [4] and Engelke *et al.* [22] were used. In IEC 61267 each diagnostic radiation quality 'RQR' is defined by the first half-value layer and a given approximate X-ray tube voltage and not by the specification of the X-ray tube voltage and the filtration. According to this standard, for each radiation quality 'RQR', the tube voltage has to be adjusted and the total filtration of the X-ray beam has to be chosen in such a way that the particular first half-value layer is realized. However, the radiation qualities 'RQR' specified in IEC 61267 correspond to the radiation qualities 'DV' specified by Engelke *et al.* [22]. Therefore, the filtration and the X-ray tube voltages given by Engelke *et al.* were used. The radiation qualities RQR 2, RQR 4, RQR 6 and RQR 7 are not given by Engelke *et al*. But to produce these radiation qualities, the filtration and the X-ray tube voltages for generating these radiation qualities can be derived from the 'DV' radiation qualities given by Engelke *et al.* [22].

The inherent filtration of the 120 kV X-ray facility is given by the window of the X-ray tube of 1,0 mm Be and by the monitor chamber of a total thickness of 250 µm Kapton®. The inherent filtration of the 420 kV X-ray unit is given by the window of the tube of 7 mm Be and 250 µm Kapton® of the monitor chamber. For each radiation quality considered in this report Table 2.1 to Table 2.4 give the thickness of the total filtration, consisting of the additional filtration required by the standards mentioned plus 4 mm Al for the radiation quality of the ISO-series and therapy radiation qualities and 2,5 mm Al for the diagnostic radiation qualities as an adjustment of the inherent filtration to 4 mm Al and 2,5 mm Al, respectively, where required. The purity of the filter materials is 99,98 % for Al and 99,99 % for Cu, Sn and Pb. The unfiltered X-ray spectra are only filtered by the inherent filtration of the X-ray units.

Verfügbar unter: https://doi.org/10.7795/110.20190315B

Table 2.1: Total filtration to produce the radiation qualities specified in ISO 4037-1 [2] and DIN 6818-1 [3] using the 120 kV X-ray facility. The designation of each quality is composed of the letter of the radiation quality series and a number which gives the voltage of the X-ray tube in kV.

Radiation quality							Total filtration according to ISO 4037-1 [2] and DIN 6818-1 [3] in mm for		
Low air-kerma rate series	Narrow-spectrum series		Wide-spectrum series		High air-kerma rate series				
	ISO	DIN	ISO	DIN	ISO	DIN	Al	Cu	Sn
		A 7,5		B 7,5		C 7,5	—	—	—
L-10							0,3	—	—
	N-10	A 10		B 10			0,1	—	—
					H-10	C 10	—	—	—
	N-15	A 15		B 15			0,5	—	—
L-20							2,0	—	—
	N-20	A 20		B 20			1,0	—	—
					H-20	C 20	0,15	—	—
	N-25						2,0	—	—
L-30							4,0	0,18	—
	N-30	A 30					4,0	—	—
				B 30			2,0	—	—
					H-30	C 30	0,5	—	—
L-35							4,0	0,25	—
	N-40	A 40					4,0	0,21	—
				B 40			4,0	—	—
						C 40	1,0	—	—
L-55							4,0	1,2	—
	N-60	A 60					4,0	0,6	—
			W-60	B 60			4,0	0,3	—
					H-60	C 60	3,9	—	—
L-70							4,0	2,5	—
	N-80	A 80					4,0	2,0	—
			W-80	B 80			4,0	0,5	—
						C 80	7,2	—	—
L-100							4,0	0,5	2,0
	N-100	A 100					4,0	5,0	—
					H-100	C 100	4,0	0,15	—
			W-110	B 110			4,0	2,0	—
	N-120	A 120					4,0	5,0	1,0

Table 2.2: Total filtration to produce the radiation qualities specified in ISO 4037-1 [2] and DIN 6818-1 [3] using the 420 kV X-ray unit. The designation of each quality is composed of the letter of the radiation quality series and a number which gives the voltage of the X-ray tube in kV.

Radiation quality							Total filtration according to ISO4037-1 [2] and DIN 6818-1 [3] in mm for			
Low air-kerma rate series	Narrow-spectrum series		Wide-spectrum series		High air-kerma rate series					
	ISO	DIN	ISO	DIN	ISO	DIN	Al	Cu	Sn	Pb
L-125							4,0	1,0	4,0	—
	N-150	A 150					4,0	—	2,5	—
			W-150	B 150			4,0	—	1,0	—
						C 150	4,0	0,5	—	—
L-170							4,0	1,0	3,0	1,5
	N-200	A 200					4,0	2,0	3,0	1,0
			W-200	B 200			4,0	—	2,0	—
					H-200	C 200	4,0	1,0	—	—
L-210							4,0	0,5	2,0	3,5
L-240							4,0	0,5	2,0	5,5
	N-250	A 250					4,0	—	2,0	3,0
			W-250	B 250			4,0	—	4,0	—
					H-250	C 250	4,0	1,6	—	—
					H-280		4,0	3,0	—	—
	N-300	A 300					4,0	—	3,0	5,0
			W-300	B 300			4,0	—	6,5	—
					H-300	C 300	4,0	2,2	—	—

Verfügbar unter: https://doi.org/10.7795/110.20190315B

Table 2.3: Total filtration to generate the therapy and diagnostic radiation qualities considered in this report using the 120 kV X-ray facility. The X-ray tube voltage and the distance between the focus of the X-ray tube and the front of the Ge detector (see Figure 2.1) are listed for each radiation quality. The qualities TW 7,5 to TW 50 are defined for a distance of 0,3 m; the therapy radiation qualities SH 50, SH 70, TH 70, TH 100 and TH 120 are defined for 1,0 m distance [6].

Therapy radiation quality	Diagnostic radiation quality		X-ray tube voltage in kV	Distance between the focus of the X-ray tube and the point of measurement in m	Total filtration according to Engelke *et al.* [22] and DIN 6817 [6] in mm for Al
DIN 6817 [6]	IEC 61267 [4]	Engelke *et al.* [22]			
TW 7,5			7,5	0,3	—
TW 10			10		—
TW 15			15		0,05
TW 20			20		0,15
		DV 20	20	1,0	2,5
TW 30			30	0,3	0,3
		DV 30	30	1,0	2,5
TW 40			40	0,3	0,5
	RQR 2	DV 40 *	40	1,0	2,5
	RQA 2	DN 2	40		6,5
TW 50			50	0,3	1,0
SH 50			50	1,0	4,0
	RQR 3	DV 50	50		2,5
	RQA 3	DN 3	50		12,5
	RQR 4	DV 60 *	60		2,5
	RQA 4	DN 4	60		18,5
SH 70			70		4,0
TH 70			70		2,4
	RQR 5	DV 70	70		2,5
	RQA 5	DN 5	70		23,5
	RQR 6	DV 80 *	80		2,5
	RQA 6	DN 6	80		28,5
	RQR 7	DV 90 *	90	1,0	2,5
	RQA 7	DN 7	90		32,5
TH 100			100		4,5
	RQR 8	DV 100	100		2,5
	RQA 8	DN 8	100		36,5
TH 120			120		6,0
	RQR 9	DV 120	120		2,5
	RQA 9	DN 9	120		42,5
	RQT		120		24,5

* Radiation quality not specified by Engelke *et al.* [22].

Verfügbar unter: https://doi.org/10.7795/110.20190315B

Table 2.4: Total filtration to generate the therapy and diagnostic radiation qualities considered in this report using the 420 kV X-ray facility. The tube voltage and the distance between the focus of the X-ray tube and the front of the Ge detector (see Figure 2.1) are listed for each radiation quality.

Therapy radiation quality	Diagnostic radiation quality		X-ray tube voltage in kV	Distance between the focus of the X-ray tube and the point of measurement in m	Total filtration according to Engelke *et al.* [22] and DIN 6817 [6] in mm for	
DIN 6817 [6]	IEC 61267 [4]	Engelke *et al.* [22]			Al	Cu
TH 140			140	1,0	9,0	—
TH 150			150		4,0	0,5
	RQR 10	DV 150	150		2,5	—
	RQA 10	DN 10	150		50,0	—
TH 200			200		4,0	1,0
TH 250			250		4,0	1,6
TH 280			280		4,0	3,0

The pulse height spectra were measured with a commercial ORTEC Ge detector (model No. GLP-25300/13-P) equipped with a planar high-purity Ge crystal (effective diameter: 24,4 mm, effective length: 15,4 mm) and a Be foil 250 µm thick (diameter: 52,0 mm) serving as entrance window. A separate ORTEC bias supply (model No. 659) was used as high-voltage supply. The electronic measuring system consists of a preamplifier integrated in the liquid N_2-cooled Ge detector system, an ORTEC amplifier (model No. 671) and a multichannel buffer of ORTEC make (model No. 926) together with an ORTEC interface card (model No. 918A) with a maximum of 4096 channels.

A diagrammatic view of the experimental set-up used for the measurements of the pulse height spectra is shown in Figure 2.1. The X-ray beam is collimated with a pair of diaphragms before and behind the monitor chamber, producing a beam diameter of 1,75 cm at 0,5 m distance from the focus, of 3,5 cm at 1,0 m distance and of 8,8 cm at 2,5 m distance. The spectrometer crystal is surrounded by a lead cylinder (outer diameter: 160 mm, wall thickness: 30 mm, front plate: 40 mm). In its head, in front of the Ge crystal, an interchangeable lead collimator with an aperture (diameter: 1,13 mm, length: 60 mm) is installed. This serves to reduce the number of photons entering the detector and to eliminate both edge effects and the influence of scattered radiation. A laser beam was used to accurately align the collimator and the Ge spectrometer system on the beam axis.

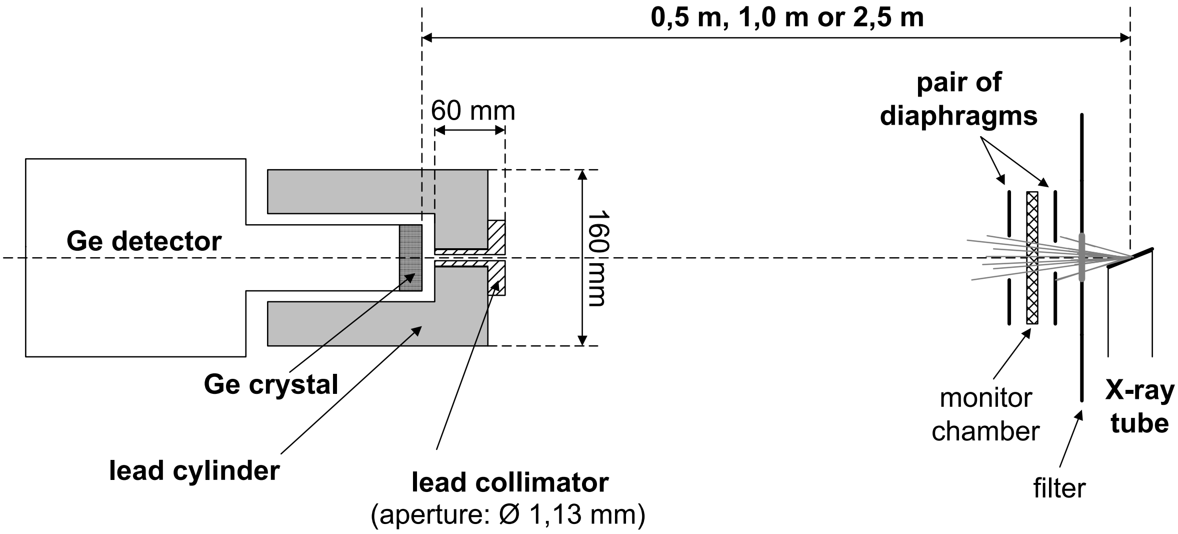

Figure 2.1: Diagrammatic view of the experimental set-up for the measurements of the pulse height spectra.

Measurements of the pulse height spectra were performed at 0,5 m, 1,0 m and 2,5 m distance between the focus of the X-ray tube and the front of the Ge detector (see Figure 2.1) with a small statistical uncertainty (typical measuring time of about 1 h for more than 420 000 counts). The current of the X-ray tube was typically adjusted to 0,1 mA or lower to prevent pile-up. Only for measuring the spectra of the radiation qualities of the ISO low air-kema rate series with a X-ray tube voltage higher than 120 kV was a current between 0,5 mA and 2 mA used. From each pulse height spectrum a background spectrum with a small statistical uncertainty (measuring time: about 48 h) was substracted.

With the line spectra of the radionuclides Co-57, Am-241 and Fe-55 measured with the experimental set-up shown in Figure 2.1, however with a lead collimator having a greater aperture (diameter: 5 mm), resolutions (full width at half maximum = FWHM) of 280 eV at 5,9 keV, 290 eV at 60 keV, 520 eV at 122 keV and 750 eV at 276 keV were determined.

The therapy radiation qualities TW 7,5 to TW 50 are defined for a distance of 0,3 m between the focus of the X-ray tube and the measuring point (see Table 2.3). This distance could not, however, be adjusted with the experimental set-up on the X-ray facility used. Therefore the spectra of these radiation qualities were measured at a distance of 0,5 m and converted into spectra with 0,3 m distance according to the ‘inverse’ exponential attenuation law (air path reduced by 0,2 m); see Ankerhold *et al.* [15].

For the unfolding of the pulse height spectra, three response matrices of the Ge detector with different maximum energy and energy resolution were calculated, as described in detail by Ankerhold *et al.* [15]: one matrix for photon energies up to 60 keV (channel width: 0,2 keV), another matrix for energies up to 150 keV (channel width: 0,5 keV) and one for energies up to 300 keV (channel width: 1,0 keV). All pulse height spectra measured were unfolded with the help of these response matrices. The unfolding procedure has been described in detail by Ankerhold *et al.* [15].

Verfügbar unter: https://doi.org/10.7795/110.20190315B

3. Determination of the characteristic data

3.1 Preparatory procedures

The procedures to prepare the fluence spectra so that the characteristic data can be determined, have been described in detail by Ankerhold *et al.* [15]. In this section only a brief description of the procedures is given.

The fluence spectra obtained after unfolding extend from 2 keV to an energy of at least 4 keV above the theoretical maximum photon energy. To calculate the characteristic parameters (first and second half-value layer (1st HVL, 2nd HVL), mean photon energy $\overline{E}_{\mathrm{ph}}$, 10 % percentile, kerma factor $k_{\Phi}(\mathrm{R})$, conversion coefficients $h_{\mathrm{p}K}(10;\mathrm{R},\alpha)$, $h_{\mathrm{p}K}(0{,}07;\mathrm{R})$, $h_K^*(10;\mathrm{R})$ and $h_K'(0{,}07;\mathrm{R},\alpha)$), each fluence spectrum was cut off at a minimum energy E_{min} and a maximum energy E_{max}.

The minimum energy E_{min} of the fluence spectrum is chosen in the manner described in detail by Ankerhold *et al.* [15]. The maximum energy E_{max} of the fluence spectrum is 1 keV above the theoretical maximum energy, which is attributable to the X-ray tube voltage adjusted, for the following reason: In the spectra a non-zero fluence contribution is observed up to about 400 eV above the theoretical maximum energy. This strange effect can be observed in all fluence spectra independently of the unfolding algorithm used [15]. This is not due to systematic errors of the high voltage measurement of the X-ray facilities (standard uncertainty of the 120 kV X-ray facility: 10 V, standard uncertainty of the 420 kV X-ray unit: 100 V). An explanation for this effect could not be found. In Section 3.7 the influence of this effect on the characteristic data of the spectra considered in this report is discussed in detail.

The environmental parameter air density, ρ, influences the spectra, in particular the low-energy spectra. To compare and discuss the characteristic data of the radiation qualities and the unfiltered X-ray spectra, the same air density has to be valid for all spectra. The fluence spectra were, therefore, normalised to reference conditions (air density ρ_0 = 1,1974·10^{-3} g/cm^3, air pressure p_0 = 101,3 kPa, air temperature T_0 = 293,15 K, relative air humidity r_0 = 0,65) by the method described in Ref. [15]. All characteristic data given in this report are normalised to these reference conditions.

For the determination of the characteristic parameters with exception of the mean photon energy, $\overline{E}_{\mathrm{ph}}$, after the procedures decribed in the previous paragraphs the fluence spectra were weighted with the energy-dependent kerma factor $k_{\Phi}(E)$, i.e. the weighted fluence spectra are given by the product $\Phi_E(E) \cdot k_{\Phi}(E)$. $\Phi_E(E)$ is the spectral fluence; the monoenergetic $k_{\Phi}(E)$ values were calculated by the following equation:

$$k_{\Phi}(E) = E \cdot \frac{\mu_{\mathrm{tr}}(E)}{\rho}. \tag{3.1}$$

Instead of the mass energy transfer coefficient $\mu_{\mathrm{tr}}(E)/\rho$ for air, the monoenergetic mass energy absorption coefficient $\mu_{\mathrm{en}}(E)/\rho$ for air has been used as the differences are negligible for the photon energies considered in this report. The $\mu_{\mathrm{en}}(E)/\rho$ values were taken from Hubbell *et al.* [23] and subjected to double logarithmic interpolation (two-point interpolation on a log-log scale).

Verfügbar unter: https://doi.org/10.7795/110.20190315B

3.2 First and second half-value layer

The first half-value layer (1^{st} HVL) is the "thickness of the specified material which attenuates the beam of radiation to an extent such that the air kerma rate is reduced to half of its original value" [2]. The second half-value layer (2^{nd} HVL) is the thickness of the specified material which increases the first half-value layer (1^{st} HVL) such that the air kerma rate is reduced from half to one fourth of its original value [24].

Assuming exponential attenuation of the photons by the filter material aluminium or copper, the 1^{st} HVL and the 2^{nd} HVL were calculated using the exponential attenuation law

$$\Phi_E^*(E) \cdot k_\Phi(E) = \Phi_E(E) \cdot k_\Phi(E) \cdot \mathrm{e}^{-\left(\frac{\mu(E)}{\rho}\right) \cdot \rho \cdot d}, \tag{3.2}$$

where $\Phi_E^*(E)$ and $\Phi_E(E)$ are the fluence spectra behind and before the absorption layer. The product $\Phi_E(E) \cdot k_\Phi(E)$ may be called "spectral air kerma" meaning the ratio of the proportion of air kerma, that is produced by photons in the energy interval E to $E + \mathrm{d}E$, and this energy interval $\mathrm{d}E$. $\Phi_E(E) \cdot k_\Phi(E)$ was calculated as described in Section 3.1. $\mu(E)/\rho$ is the monoenergetic mass attenuation coefficient of aluminium or copper, ρ the density of aluminium and copper, respectively, taken from the database of the Photcoef program [25] and d the thickness of the Al or Cu absorption layer. The monoenergetic mass attenuation coefficients $\mu(E)/\rho$, calculated by the Photcoef program [25], were subjected to double logarithmic interpolation (two-point interpolation on a log-log scale).

The values of the first and second half-value layer for reference conditions determined using Equation 3.2 are listed in Section 4 for each radiation quality and unfiltered X-ray spectrum.

3.3 Mean photon energy

The mean photon energy $\overline{E}_{\mathrm{ph}}$ is defined by [2]:

$$\overline{E}_{\mathrm{ph}} = \frac{\int_{E_{\mathrm{min}}}^{E_{\mathrm{max}}} E \cdot \Phi_E(E)\,\mathrm{d}E}{\int_{E_{\mathrm{min}}}^{E_{\mathrm{max}}} \Phi_E(E)\,\mathrm{d}E} \tag{3.3}$$

with the spectral fluence $\Phi_E(E)$ and E_{max} and E_{min} as discussed in Section 3.1. In Section 4 the values of the mean photon energy $\overline{E}_{\mathrm{ph}}$ calculated with the fluence spectra according to Equation 3.3 are listed. All values are determined for reference conditions.

3.4 10 % percentile

The 10 % percentile of a radiation quality or an unfiltered X-ray spectrum is defined as the photon energy $E_{10\,\%}$, which gives the energy boundary in the spectrum, so that 10 % of the total air kerma, K_a, of the radiation quality is produced by photons with an energy lower than $E_{10\,\%}$. The 10 % percentile of each spectrum was calculated using the following equation:

$$\frac{\int_{E_{\min}}^{E_{10\,\%}} \Phi_E(E) \cdot k_\Phi(E)\,\mathrm{d}E}{\int_{E_{\min}}^{E_{\max}} \Phi_E(E) \cdot k_\Phi(E)\,\mathrm{d}E} = 0{,}1 \tag{3.4}$$

with $E_{\min}$, $E_{\max}$ and $\Phi_E(E) \cdot k_\Phi(E)$ as discussed in Section 3.1. For the radiation qualities and unfiltered X-ray spectra considered in this report, the values of the 10 % percentile for reference conditions are listed in Section 4.

3.5 Kerma factor

The kerma factor, k_Φ(R), of a radiation quality or an unfiltered X-ray spectrum ‘R’, i.e. averaged over the fluence spectrum denoted ‘R’, is defined as the quotient of the total air kerma, K_a, and the total fluence of the spectrum. It is given by following equation:

$$k_\Phi(\mathrm{R}) = \frac{\int_{E_{\min}}^{E_{\max}} k_\Phi(E) \cdot \Phi_E(E)\,\mathrm{d}E}{\int_{E_{\min}}^{E_{\max}} \Phi_E(E)\,\mathrm{d}E} \tag{3.5}$$

with $E_{\max}$, $E_{\min}$ and $\Phi_E(E) \cdot k_\Phi(E)$ as discussed in Section 3.1. $\Phi_E(E)$ is the spectral fluence. The kerma factors, k_Φ(R), for the radiation qualities and unfiltered X-ray spectra considered in this report are listed in Section 4. They are given for reference conditions.

3.6 Conversion coefficients

3.6.1 Conversion coefficient $h_{pK}(10;\mathrm{R},\alpha)$ for the slab phantom

The quantity $H_p(10)$ is defined as the personal dose equivalent in ICRU soft tissue at a depth of 10 mm in the body at the location where the personal dosemeter is worn [26]. For calibration purposes, this definition has been extended to phantoms [19][20]. For the slab phantom, conversion coefficients $h_{pK}(10;\mathrm{R},\alpha)$ from air kerma K_a to $H_p(10)$ at different angles of incidence, α, between the monodirectional calibration photon field and the normal on the slab phantom front face were determined for each radiation quality and each unfiltered X-ray spectrum 'R' considered in this report.

Conversion coefficients $h_{pK}(10;E,\alpha)$ for monodirectional and monoenergetic photon radiation of energy E and the slab phantom are laid down in ICRP Publication 74 [17] and ICRU Report 57 [18] for the angles of incidence α of 0°, 15°, 30°, 45°, 60° and 75° in the following manner: For some photon energies between 10 keV and 100 MeV values of $h_{pK}(10;E,\alpha = 0°)$ and for the angles of incidence α = 15°, 30°, 45°, 60° and 75° ratios of $h_{pK}(10;E,\alpha)/h_{pK}(10;E,0°)$ are listed. The following interpolations between these basic values are recommended by ICRP Publication 74 [17] and ICRU Report 57 [18]: For the monoenergetic conversion coefficients $h_{pK}(10;E,0°)$, a four-point (cubic) Lagrangian interpolation on a linear(x-axis)-log(y-axis) scale is to be used. The ratios $h_{pK}(10;E,\alpha)/h_{pK}(10;E,0°)$ should be subjected to four-point (cubic) Lagrangian interpolation on a linear-linear scale. After the interpolation the conversion coefficients for $\alpha \neq 0°$ are given by multiplication of the respective ratio by the $h_{pK}(10;E,0°)$ value. By definition, the monoenergetic conversion coefficients have no uncertainty [17][18].

The conversion coefficients calculated using the basic values and the interpolation instructions given in ICRP Publication 74 [17] and ICRU Report 57 [18] were used as far as possible. However, for the angles of incidence α of 0°, 15°, 30° and 45°, conversion coefficients are given in ICRP Publication 74 and ICRU Report 57 only for photon energies equal to or larger than 10 keV and, for the angles of 60° and 75°, only for energies equal to or larger than 12,5 keV and 15 keV, respectively. For the conversion coefficients $h_{pK}(10;E<E_{\mathrm{ICRP}},\alpha)$, E_{ICRP} denoting the lowest photon energy given by ICRP 74 and ICRU 57, an extrapolation was therefore performed from E_{ICRP} down to 3 keV in the following way:

$$h_{pK}(10;E<E_{\mathrm{ICRP}},\alpha) = h_{pK}(10;E_{\mathrm{ICRP}},\alpha)\cdot\frac{\exp\left(-\left(\frac{\mu(E)}{\rho}\right)_{\mathrm{ICRU,en}}\cdot\rho_{\mathrm{ICRU}}\cdot\frac{d_0}{\cos\alpha}\right)}{\exp\left(-\left(\frac{\mu(E_{\mathrm{ICRP}})}{\rho}\right)_{\mathrm{ICRU,en}}\cdot\rho_{\mathrm{ICRU}}\cdot\frac{d_0}{\cos\alpha}\right)}, \tag{3.6}$$

where $(\mu(E)/\rho)_{\mathrm{ICRU,en}}$ is the monoenergetic mass energy absorption coefficient of ICRU tissue, d_0 = 10 mm and ρ_{ICRU} = 1,0 g/cm^3 the density of ICRU tissue given in ICRU Report 46 [27]. The coefficients $(\mu(E)/\rho)_{\mathrm{ICRU,en}}$ were calculated by the Photcoef program [25] and subjected to double logarithmic interpolation (two-point interpolation on a log-log scale). The monoenergetic mass energy absorption coefficient was used because generally a broad-beam geometry prevails in the case of irradiation. In Table 3.1 the monoenergetic conversion coefficients $h_{pK}(10;E,\alpha)$ calculated according to Equation 3.6 for photon energies E from 3 keV to $E = E_{ICRP}$ = 10 keV, 12,5 keV and 15 keV for the angles of incidence α of 0°, 15°, 30°, 45°, 60° and 75° are listed. The basic values, $h_{pK}(10;E_{ICRP},\alpha)$, for the extrapolation (Equation 3.6) are plotted in bold type in Table 3.1. In addition, the conversion coefficients $h_{pK}(10;E,\alpha)$ are plotted in italics in Table 3.1; they were calculated according to the instructions given in ICRP Publication 74 [17] and ICRU Report 57 [18].

Table 3.1: Monoenergetic conversion coefficients $h_{pK}(10;E,\alpha)$ in Sv/Gy for the angles of incidence α of 0°, 15°, 30°, 45°, 60° and 75°. For photon energies from 3 keV to E_{ICRP} = 10 keV and for the angles of 60° and 75° up to E_{ICRP} = 12,5 keV and E_{ICRP} = 15 keV, respectively, $h_{pK}(10;E,\alpha)$ values were calculated according to Equation 3.6. The conversion coefficients, $h_{pK}(10;E_{ICRP},\alpha)$, which are the basis for the extrapolation using Equation 3.6, are plotted in bold type. The $h_{pK}(10;E,\alpha)$ values plotted in roman for energies higher than E_{ICRP} are given in ICRP Publication 74 [17] and ICRU Report 57 [18], additional values in italics have been calculated according the instructions given in ICRP Publication 74 [17] and ICRU Report 57 [18].

Photon energy E in keV	$h_{pK}(10;E,\alpha)$ in Sv/Gy for angles of incidence α of					
	0°	15°	30°	45°	60°	75°
3,0	$<1\cdot10^{-6}$	$<1\cdot10^{-6}$	$<1\cdot10^{-6}$	$<1\cdot10^{-6}$	$<1\cdot10^{-6}$	$<1\cdot10^{-6}$
4,0						
5,0						
6,0						
7,0	$0,13\cdot10^{-5}$					
8,0	$1,07\cdot10^{-4}$	$8,13\cdot10^{-5}$	$2,99\cdot10^{-5}$	$0,38\cdot10^{-5}$		
9,0	$1,63\cdot10^{-3}$	$1,36\cdot10^{-3}$	$6,94\cdot10^{-4}$	$1,78\cdot10^{-4}$	$0,38\cdot10^{-5}$	
10,0	**$9,00\cdot10^{-3}$**	**$8,00\cdot10^{-3}$**	**$5,00\cdot10^{-3}$**	**$2,00\cdot10^{-3}$**	$1,17\cdot10^{-4}$	
11,0	*$3,07\cdot10^{-2}$*	*$2,81\cdot10^{-2}$*	*$1,95\cdot10^{-2}$*	*$9,23\cdot10^{-3}$*	$1,16\cdot10^{-3}$	$0,33\cdot10^{-5}$
12,0	*$7,16\cdot10^{-2}$*	*$6,63\cdot10^{-2}$*	*$4,91\cdot10^{-2}$*	*$2,58\cdot10^{-2}$*	$5,52\cdot10^{-3}$	$0,66\cdot10^{-4}$
12,5	$9,80\cdot10^{-2}$	$9,10\cdot10^{-2}$	$6,90\cdot10^{-2}$	$3,80\cdot10^{-2}$	**$1,00\cdot10^{-2}$**	$0,21\cdot10^{-3}$
13,0	*$1,30\cdot10^{-1}$*	*$1,22\cdot10^{-1}$*	*$9,48\cdot10^{-2}$*	*$5,53\cdot10^{-2}$*	*$1,69\cdot10^{-2}$*	$0,55\cdot10^{-3}$
14,0	*$1,98\cdot10^{-1}$*	*$1,89\cdot10^{-1}$*	*$1,54\cdot10^{-1}$*	*$9,97\cdot10^{-2}$*	*$3,83\cdot10^{-2}$*	$2,55\cdot10^{-3}$
15,0	$2,64\cdot10^{-1}$	$2,55\cdot10^{-1}$	$2,17\cdot10^{-1}$	$1,52\cdot10^{-1}$	$6,89\cdot10^{-2}$	**$7,92\cdot10^{-3}$**
16,0	*$3,39\cdot10^{-1}$*	*$3,29\cdot10^{-1}$*	*$2,88\cdot10^{-1}$*	*$2,15\cdot10^{-1}$*	*$1,11\cdot10^{-1}$*	*$1,76\cdot10^{-2}$*
17,0	*$4,11\cdot10^{-1}$*	*$3,99\cdot10^{-1}$*	*$3,58\cdot10^{-1}$*	*$2,80\cdot10^{-1}$*	*$1,59\cdot10^{-1}$*	*$3,20\cdot10^{-2}$*
17,5	$4,45\cdot10^{-1}$	$4,32\cdot10^{-1}$	$3,91\cdot10^{-1}$	$3,12\cdot10^{-1}$	$1,85\cdot10^{-1}$	$4,09\cdot10^{-2}$
18,0	*$4,81\cdot10^{-1}$*	*$4,68\cdot10^{-1}$*	*$4,27\cdot10^{-1}$*	*$3,45\cdot10^{-1}$*	*$2,12\cdot10^{-1}$*	*$5,11\cdot10^{-2}$*
19,0	*$5,49\cdot10^{-1}$*	*$5,36\cdot10^{-1}$*	*$4,95\cdot10^{-1}$*	*$4,08\cdot10^{-1}$*	*$2,65\cdot10^{-1}$*	*$7,46\cdot10^{-2}$*
20,0	$6,11\cdot10^{-1}$	$6,00\cdot10^{-1}$	$5,58\cdot10^{-1}$	$4,66\cdot10^{-1}$	$3,18\cdot10^{-1}$	$1,02\cdot10^{-2}$

The conversion coefficient $h_{\mathrm{p}K}(10;\mathrm{R},\alpha)$ for a radiation quality or an unfiltered X-ray spectrum 'R' and an angle of incidence α is then given by

$$h_{\mathrm{p}K}(10;\mathrm{R},\alpha) = \frac{\int_{E_{\min}}^{E_{\max}} \Phi_E(E)\cdot k_\Phi(E)\cdot h_{\mathrm{p}K}(10;E,\alpha)\,\mathrm{d}E}{\int_{E_{\min}}^{E_{\max}} \Phi_E(E)\cdot k_\Phi(E)\,\mathrm{d}E}\ , \tag{3.7}$$

with $E_{\min}$, $E_{\max}$ and $\Phi_E(E)\cdot k_\Phi(E)$ as discussed in Section 3.1. In Section 4 the conversion coefficients $h_{\mathrm{p}K}(10;\mathrm{R},\alpha)$ for the angles of incidence α of 0°, 15°, 30°, 45°, 60° and 75° calculated in this manner are listed. They are determined for reference conditions.

The following has to be considered when tabulated conversion coefficients $h_{\mathrm{p}K}(10;\mathrm{R},\alpha)$ are used: The spectral distribution of the radiation qualities, in particular those with an appreciable portion of low-energy photons, depends significantly on the total beam filtration (thickness of filters, air path, air density, etc.) and the X-ray facility used (X-ray tube anode angle, sputtering of anode material on the tube window, voltage waveform, etc.). Furthermore, the monoenergetic conversion coefficients $h_{\mathrm{p}K}(10;E,\alpha)$ are strongly energy-dependent, in particular for low photon energies. As a result of both dependencies, the conversion coefficients $h_{\mathrm{p}K}(10;\mathrm{R},\alpha)$ for a radiation quality 'R' may differ by up to several ten percent from one X-ray facility to another, and also due to changes in the air path or air density when the same X-ray unit is used, see the discussion in Section 3.7. The conversion coefficients $h_{\mathrm{p}K}(10;\mathrm{R},\alpha)$ of spectra with an appreciable portion of low-energy photons (E less than about 20 keV) presented in this catalogue should therefore be used only for calibrations in terms of $H_\mathrm{p}(10)$, if the uncertainties due to differences in the X-ray facilities and the air paths are considered. To reduce these uncertainties, either the conversion coefficients of the X-ray unit used have to be determined in the manner described in this report, or a secondary standard chamber for directly measuring the conventionally true value of $H_\mathrm{p}(10)$ has to be used. Such a chamber was developed by Ankerhold *et al.* [28].

3.6.2 Conversion coefficient $h_{\mathrm{p}K}(0,07;\mathrm{R})$ for the rod phantom

The quantity $H_\mathrm{p}(0,07)$ is defined as the personal dose equivalent in ICRU soft tissue at a depth of 0,07 mm in the body at the location where the personal dosemeter is worn [26]. For calibration purposes, this definition is extended to phantoms [19][20]. For the rod phantom, the conversion coefficient $h_{\mathrm{p}K}(0,07;\mathrm{R})$ from air kerma, K_a, to $H_\mathrm{p}(0,07)$ was determined for each radiation quality and each unfiltered X-ray spectrum 'R' considered in this report.

The conversion coefficients $h_{\mathrm{p}K}(0,07;\mathrm{R})$ listed in this report are angle-independent for the following reason: The standard ISO 4037-3 [10] states that "due to the small magnitude of the angular variation of the conventionally true value of $H_\mathrm{p}(0,07)$ it is assumed that $H_\mathrm{p}(0,07)$ for the rod phantom is independent of the direction of radiation incidence for angles up to 60°. Rotations over angles larger than 60° are not considered in this standard." Therefore, the $h_{\mathrm{p}K}(0,07;\mathrm{R})$ values calculated with the conversion coefficients $h_{\mathrm{p}K}(0,07;E)$ for monodirectional and monoenergetic

Verfügbar unter: https://doi.org/10.7795/110.20190315B

photon radiation E, which are given for the rod phantom in ISO 4037-3, are valid for all angles of incidence, α, from 0° to 60°. The angle α is formed by the monodirectional photon field and the normal to the rod surface (perpendicular to the longitudinal rod axis). Between the basic values of $h_{pK}(0{,}07;E)$ given in ISO 4037-3 [10], four-point (cubic) Lagrangian interpolation on a linear(x-axis)-log(y-axis) scale as used for the interpolation of the $h_{pK}(10;\mathrm{R},0°)$ basic values (see Section 3.6.1) was carried out. By definition, the monoenergetic conversion coefficients have no uncertainty [17][18].

Conversion coefficients $h_{pK}(0{,}07;E)$ given in ISO 4037-3 [10] and subjected to the interpolation described in the previous paragraph were used as far as possible for determining the conversion coefficients $h_{pK}(0{,}07;\mathrm{R})$. However, in ISO 4037-3 [10], conversion coefficients $h_{pK}(0{,}07;E)$ are given only for photon energies equal to or larger than 5 keV. For the conversion coefficients $h_{pK}(0{,}07;E<E_{\mathrm{ISO}})$ (E_{ISO} = 5 keV), an extrapolation, quite analogous to Equation 3.6 (see Section 3.6.1), was therefore performed from E_{ISO} down to 3 keV, i.e. E_{min} for low-energy photon spectra, in the following way:

$$h_{pK}(0{,}07;E<E_{\mathrm{ISO}}) = h_{pK}(0{,}07;E_{\mathrm{ISO}}) \cdot \frac{\exp\left(-\left(\dfrac{\mu(E)}{\rho}\right)_{\mathrm{ICRU,en}} \cdot \rho_{\mathrm{ICRU}} \cdot d_0\right)}{\exp\left(-\left(\dfrac{\mu(E_{\mathrm{ISO}})}{\rho}\right)_{\mathrm{ICRU,en}} \cdot \rho_{\mathrm{ICRU}} \cdot d_0\right)}, \qquad (3.8)$$

with $(\mu(E)/\rho)_{\mathrm{ICRU,en}}$ and ρ_{ICRU} as given in Section 3.6.1 and d_0 = 0,07 mm.

In Table 3.2 the monoenergetic conversion coefficients $h_{pK}(0{,}07;E)$ given in ISO 4037-3 [10] and subjected to four-point Lagrangian interpolation on a linear(x-axis)-log(y-axis) scale as described in the previous paragraph are plotted in italics, and additionally the values for E = 3 keV and 4 keV calculated according to Equation 3.8 are listed. The basic value, $h_{pK}(0{,}07;E_{\mathrm{ISO}})$, for the extrapolation (Equation 3.8) is plotted in bold type in Table 3.2.

Table 3.2: Monoenergetic conversion coefficients $h_{pK}(0{,}07;E)$ in Sv/Gy. For the photon energies E = 3 keV and 4 keV, the $h_{pK}(0{,}07;E)$ values were calculated according to Equation 3.8. The conversion coefficient $h_{pK}(0{,}07;\ E_{ISO})$ (E_{ISO} = 5 keV) which is the basis for the extrapolation (see Equation 3.8) is plotted in bold type. The $h_{pK}(0{,}07;E)$ values plotted in roman for energies larger than E_{ISO} = 5 keV are given in ISO 4037-3 [10], additional values in italics were subjected to four-point Lagrangian interpolation on a linear(x-axis)-log(y-axis) scale. The conversion coefficients $h_{pK}(0{,}07;E)$ are valid for all angles of incidence from 0° to 60°.

Photon energy E in keV	$h_{pK}(0{,}07;E)$ in Sv/Gy
3,0	0,306
4,0	0,595
5,0	**0,760**
6,0	0,840
7,0	*0,891*
8,0	0,920
9,0	*0,940*
10,0	0,950
11,0	*0,956*
12,0	*0,959*
12,5	0,960
13,0	*0,964*
14,0	*0,971*
15,0	0,980
16,0	*0,987*
17,0	*0,993*
18,0	*0,999*
19,0	*1,00*
20,0	1,01

The conversion coefficient $h_{pK}(0{,}07;\mathrm{R})$ for a radiation quality or an unfiltered X-ray spectrum ‘R’ results from

$$h_{pK}(0{,}07;\mathrm{R}) = \frac{\int_{E_{\min}}^{E_{\max}} \Phi_E(E)\cdot k_\Phi(E)\cdot h_{pK}(0{,}07;E)\,\mathrm{d}E}{\int_{E_{\min}}^{E_{\max}} \Phi_E(E)\cdot k_\Phi(E)\,\mathrm{d}E}\ , \tag{3.9}$$

with $E_{\min}$, $E_{\max}$ and $\Phi_E(E)\cdot k_\Phi(E)$ as discussed in Section 3.1. The $h_{pK}(0{,}07;\mathrm{R})$ values calculated in this way are listed in Section 4 for all radiation qualities and unfiltered X-ray spectra considered in this report. They are determined for reference conditions.

In contrast to the monoenergetic conversion coefficients $h_{pK}(10;E,\alpha)$, the conversion coefficients $h_{pK}(0{,}07;E)$ show only a small energy dependence. Therefore, differences of the spectral distribution of nominally the same radiation quality due to changes in the air density or the use of different X-ray facilities influence the $h_{pK}(0{,}07;\mathrm{R})$ values only slightly, as discussed in Section 3.7. Thus the $h_{pK}(0{,}07;\mathrm{R})$ values of all spectra, also those with an appreciable portion of low-energy photons, can be used for determining the correct $H_p(0{,}07)$ values for radiation qualities generated with an X-ray facility not used for the measurements described in this catalogue.

3.6.3 Conversion coefficient $h_K^*(10;\mathrm{R})$

The quantity $H^*(10)$, the ambient dose equivalent at a point of interest in a real radiation field, is defined as the dose equivalent that would be produced by the corresponding expanded and aligned field, in the ICRU sphere at a depth of 10 mm, on the radius vector opposing the direction of the aligned field [26]. As a result of the imaginary alignment and expansion of the radiation field, the contributions from all directions of radiation add up. The value of $H^*(10)$ is therefore independent of the directional distribution of the radiation in the actual field. The conversion coefficient $h_K^*(10;\mathrm{R})$ from air kerma, K_a, to $H^*(10)$ was determined for each radiation quality and each unfiltered X-ray spectrum 'R' considered in this report.

Conversion coefficients $h_K^*(10;E)$ for monodirectional and monoenergetic radiation (expanded and aligned radiation fields) and the ICRU sphere are listed in ICRP Publication 74 [17] and ICRU Report 57 [18] for some photon energies E. The interpolation between these monoenergetic $h_K^*(10;E)$ basic values is to be carried out in accordance with the recommendation of ICRP Publication 74 and ICRU Report 57 using a four-point (cubic) Lagrangian interpolation on a linear(x-axis)-log(y-axis) scale. In Figure 3.1 the conversion coefficients $h_K^*(10;E)$ calculated with these basic values and this interpolation instruction are plotted as a function of photon energy E. In particular for low photon energies the conversion coefficients $h_K^*(10;E)$ show a strong energy dependence. However, only a few basic values of $h_K^*(10;E)$ are given in ICRP Publication 74 [17] and ICRU Report 57 [18] for the low energies so that the four-point Lagrangian interpolation on a linear(x-axis)-log(y-axis) scale results in a strange energy dependence of $h_K^*(10;E)$ with "curves" for energies between 10 keV and 30 keV (see Figure 3.1). When four-point Lagrangian interpolation on a linear-linear scale is used, the energy dependence of the $h_K^*(10;E)$ values seems, however, to be much smoother as shown in Figure 3.1. The conversion coefficients $h_K^*(10;E)$ for energies greater than 30 keV calculated on a linear-linear scale are identical with those determined on a linear-log scale.

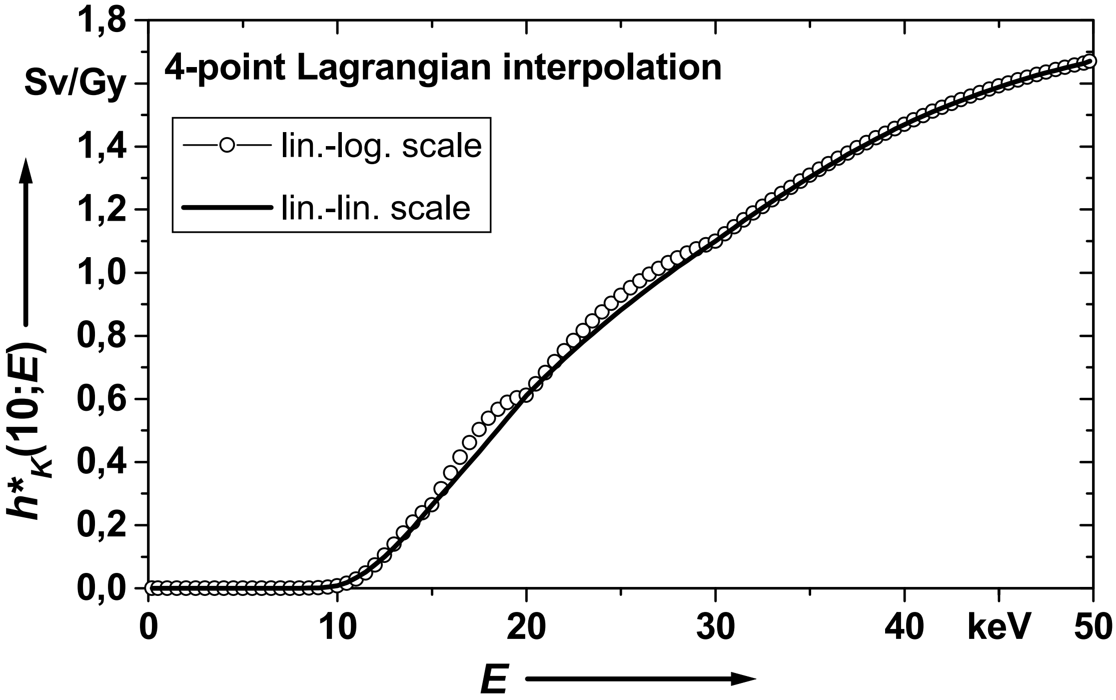

Figure 3.1: Monoenergetic conversion coefficients $h_K^*(10;E)$ in Sv/Gy as a function of photon energy E. The $h_K^*(10;E)$ values were calculated with the set of basic values given in ICRP Publication 74 [17] and ICRU Report 57 [18] and four-point Lagrangian interpolation on a linear(x-axis)-log(y-axis) scale and a linear-linear scale, respectively.

Because of these results the monoenergetic conversion coefficients $h_K^*(10;E)$ were calculated using the set of basic values listed in ICRP Publication 74 [17] and ICRU Report 57 [18] and four-point Lagrangian interpolation on a linear-linear scale. By definition, the monoenergetic conversion coefficients have no uncertainty [17][18]. These $h_K^*(10;E)$ values were used as far as possible. However, conversion coefficients are given in ICRP Publication 74 and ICRU Report 57 only for photon energies equal to or larger than 10 keV. For the conversion coefficients $h_K^*(10;E < E_{\mathrm{ICRP}})$ ($E_{\mathrm{ICRP}} = 10\,\mathrm{keV}$), an extrapolation, quite analogous to the extrapolation described in Section 3.6.1, was therefore performed from E_{ICRP} down to 3 keV in the following way:

$$h_K^*(10;E < E_{\mathrm{ICRP}}) = h_K^*(10;E_{\mathrm{ICRP}}) \cdot \frac{\exp\left(-\left(\frac{\mu(E)}{\rho}\right)_{\mathrm{ICRU,en}} \cdot \rho_{\mathrm{ICRU}} \cdot d_0\right)}{\exp\left(-\left(\frac{\mu(E_{\mathrm{ICRP}})}{\rho}\right)_{\mathrm{ICRU,en}} \cdot \rho_{\mathrm{ICRU}} \cdot d_0\right)}, \tag{3.10}$$

with $(\mu(E)/\rho)_{\mathrm{ICRU,en}}$ and ρ_{ICRU} as given in Section 3.6.1 and $d_0 = 10$ mm.

Verfügbar unter: https://doi.org/10.7795/110.20190315B

In Table 3.3 the monoenergetic conversion coefficients $h_K^*(10;E)$ calculated with Equation 3.10 for photon energies E from 3 keV to $E = E_{\mathrm{ICRP}}$ = 10 keV are listed. The basic value, $h_K^*(10;E_{\mathrm{ICRP}})$, for the extrapolation (see Equation 3.10) is plotted in Table 3.3 in bold type. In addition, conversion coefficients $h_K^*(10;E)$ listed in ICRP Publication 74 [17] and ICRU Report 57 [18] and subjected to the interpolation described in the previous paragraph are given in Table 3.3.

Table 3.3: Monoenergetic conversion coefficients $h_K^*(10;E)$ in Sv/Gy. For photon energies from 3 keV to 10 keV, the $h_K^*(10;E)$ values were calculated according to Equation 3.10. The conversion coefficient $h_K^*(10;E_{\mathrm{ICRP}})$ (E_{ICRP} = 10 keV), which is the basis for the extrapolation (see Equation 3.10), is plotted in bold type. The $h_K^*(10;E)$ values plotted in roman for energies larger than E_{ICRP} are given in ICRP Publication 74 [17] and ICRU Report 57 [18]; additional values in italics are calculated using the set of basic values given in ICRP Publication 74 and ICRU Report 57 and a four-point Lagrangian interpolation on a linear-linear scale.

Photon energy E in keV	$h_K^*(10;E)$ in Sv/Gy
3,0	$<1\cdot10^{-6}$
4,0	
5,0	
6,0	
7,0	$0{,}12\cdot10^{-5}$
8,0	$9{,}50\cdot10^{-5}$
9,0	$1{,}45\cdot10^{-3}$
10,0	$\mathbf{8{,}00\cdot10^{-3}}$
11,0	*$3{,}31\cdot10^{-2}$*
12,0	*$7{,}37\cdot10^{-2}$*
13,0	*$1{,}27\cdot10^{-1}$*
14,0	*$1{,}90\cdot10^{-1}$*
15,0	$2{,}60\cdot10^{-1}$
16,0	*$3{,}26\cdot10^{-1}$*
17,0	*$3{,}95\cdot10^{-1}$*
18,0	*$4{,}66\cdot10^{-1}$*
19,0	*$5{,}38\cdot10^{-1}$*
20,0	$6{,}10\cdot10^{-1}$

The conversion coefficient $h_K^*(10;\mathrm{R})$ for a radiation quality or an unfiltered X-ray spectrum ‘R’ is given by

$$h_K^*(10;\mathrm{R}) = \frac{\int_{E_{\min}}^{E_{\max}} \Phi_E(E)\cdot k_\Phi(E)\cdot h_K^*(10;E)\,\mathrm{d}E}{\int_{E_{\min}}^{E_{\max}} \Phi_E(E)\cdot k_\Phi(E)\,\mathrm{d}E}\,, \tag{3.11}$$

with E_{min}, E_{max} and $\Phi_E(E)\cdot k_\Phi(E)$ as discussed in Section 3.1. The $h_K^*(10;\mathrm{R})$ values calculated in this manner are listed in Section 4 for the radiation qualities and unfiltered X-ray spectra considerd in this report. They are determined for reference conditions.

Because of the strong energy dependence of the monoenergetic conversion coefficients $h_K^*(10;E)$ in particalur for low photon energies, the same problem is encountered when tabulated $h_K^*(10;E)$ values are used, as discussed in Section 3.6.1 for the use of $h_{pK}(10;\mathrm{R},\alpha)$ values: The conversion coefficients $h_K^*(10;\mathrm{R})$ may differ from one X-ray facility to another by up to several ten percent and also when the air path or the air density using the same X-ray unit is changed. Therefore the $h_K^*(10;\mathrm{R})$ values for radiation qualities with an appreciable portion of low-energy photons (E less than about 20 keV) listed in this catalogue should be used only for calibrations in terms of $H^*(10)$, if the uncertainties due to differences in the X-ray facilities and the air paths are considered. To reduce these uncertainties, either the conversion coefficients of the X-ray unit used have to be determined in the manner as described in this report or a secondary standard chamber for directly measuring the conventionally true value of $H^*(10)$ has to be used.

3.6.4 Conversion coefficient $h'_K(0{,}07;\mathrm{R},\alpha)$

The quantity $H'(0{,}07,\vec{\Omega})$, the directional dose equivalent at a point of interest in a real radiation field, is defined as the dose equivalent that would be produced by the corresponding expanded radiation field, in the ICRU sphere at a depth of 0,07 mm, on a radius in a specified direction $\vec{\Omega}$ [26]. The conversion coefficients $h'_K(0{,}07;\mathrm{R},\alpha)$ from air kerma, K_a, to $H'(0{,}07,\vec{\Omega})$ for different angles α were determined for each radiation quality and each unfiltered X-ray spectrum 'R' considered in this report. The angle of incidence α is the angle between the specified direction $\vec{\Omega}$ and a radius vector opposing an expanded monodirectional radiation field as shown in Figure 3.2.

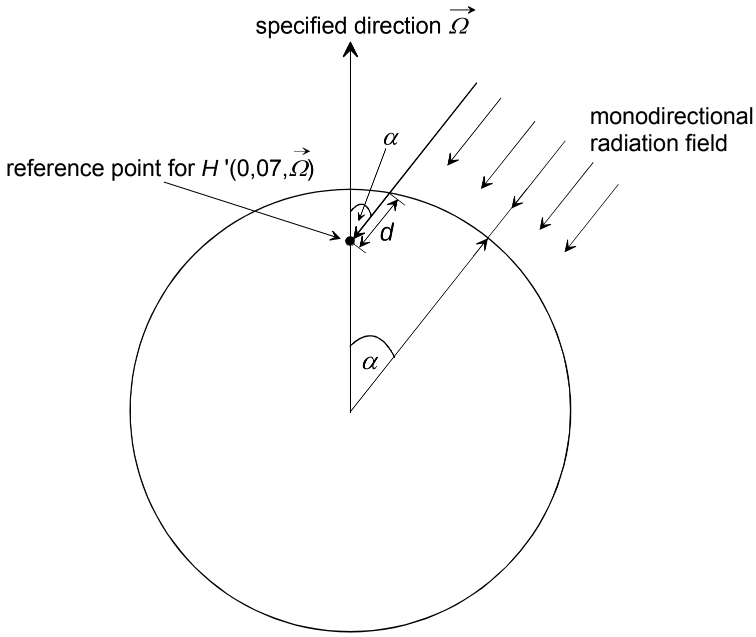

Figure 3.2: Definition of the angle of incidence α used for the conversion coefficients $h'_K(0{,}07;E,\alpha)$ and $h'_K(0{,}07;\mathrm{R},\alpha)$

In ICRP Publication 74 [17] and ICRU Report 57 [18] basic values of the conversion coefficient $h'_K(0{,}07;E,0°)$ and the ratios $h'_K(0{,}07;E,\alpha)/h'_K(0{,}07;E,0°)$ (α = 0°, 15°, 45°, 60°, 75°, 90° and 180°) for monodirectional and monoenergetic photon radiation of energy E (expanded radiation field) are listed together with the following interpolation instruction: The interpolation for calculating the $h'_K(0{,}07;E,0°)$ values is to be carried out using four-point Lagrangian interpolation on a linear(x-axis)-log(y-axis) scale; the ratios $h'_K(0{,}07;E,\alpha)/h'_K(0{,}07;E,0°)$ are to be subjected to four-point Lagrangian interpolation on a linear-linear scale. The $h'_K(0{,}07;E,\alpha)$ values for α unequal to 0° are then given by multiplication of the two values. The monoenergetic conversion coefficients $h'_K(0{,}07;E,\alpha)$ for α = 0°, 15°, 30°, 45°, 60°, 75°, 90° and 180° calculated in this manner are plotted in Figure 3.3 for energies up to 50 keV and in Figure 3.4 up to 300 keV. In the energy range between 5 keV and 20 keV, the $h'_K(0{,}07;E,\alpha)$ values for α below 90° show a very strange energy dependence with “curves”. Besides for energies from 10 keV to 20 keV, the $h'_K(0{,}07;E,60°)$ values are greater than those for α lower than 60°. These energy dependencies seem not to be intended by ICRP and ICRU. The reason is the same as for the strange energy dependence of the $h^*_K(10;E)$ values at low photon energies. The number of basic values given by ICRP Publication 74 [17] and ICRU Report 57 [18] in the low energy range are too small, so the recommended interpolation yields in this energy dependence.

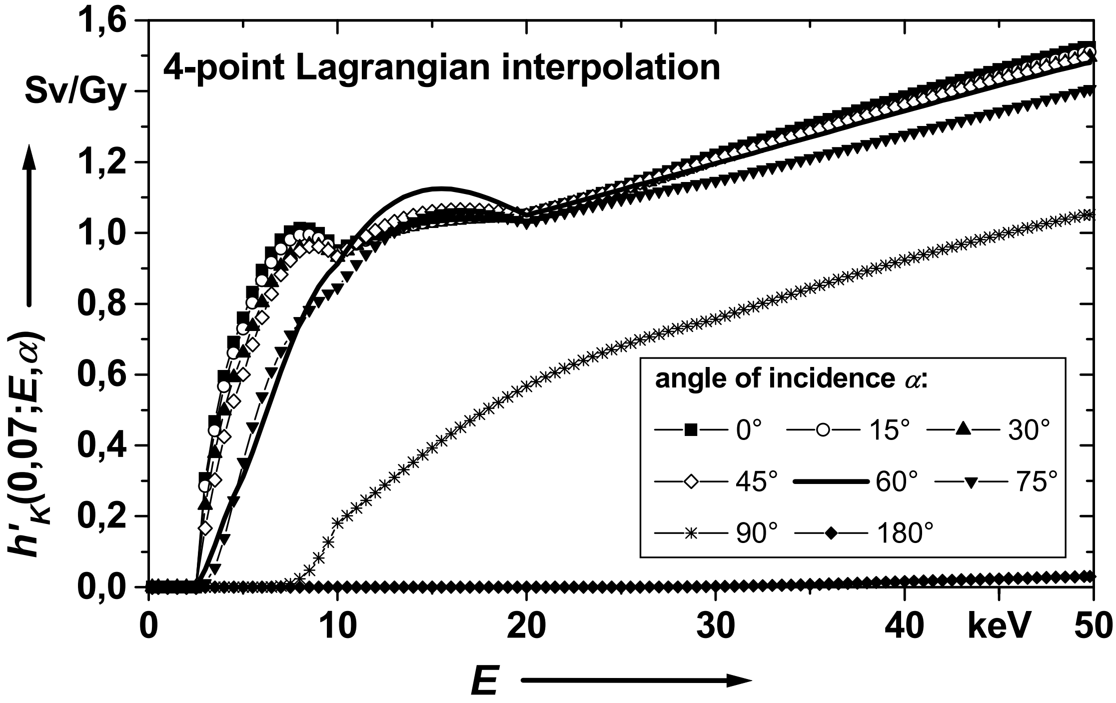

Figure 3.3: Monoenergetic conversion coefficients $h'_K(0{,}07;E,\alpha)$ in Sv/Gy for photon energies up to 50 keV and angles of incidence α of 0°, 15°, 30°, 45°, 60°, 75°, 90° and 180°. The $h'_K(0{,}07;E,\alpha)$ values were calculated using the set of basic values listed in ICRP Publication 74 [17] and ICRU Report 57 [18] and the interpolation instruction recommended (see text).

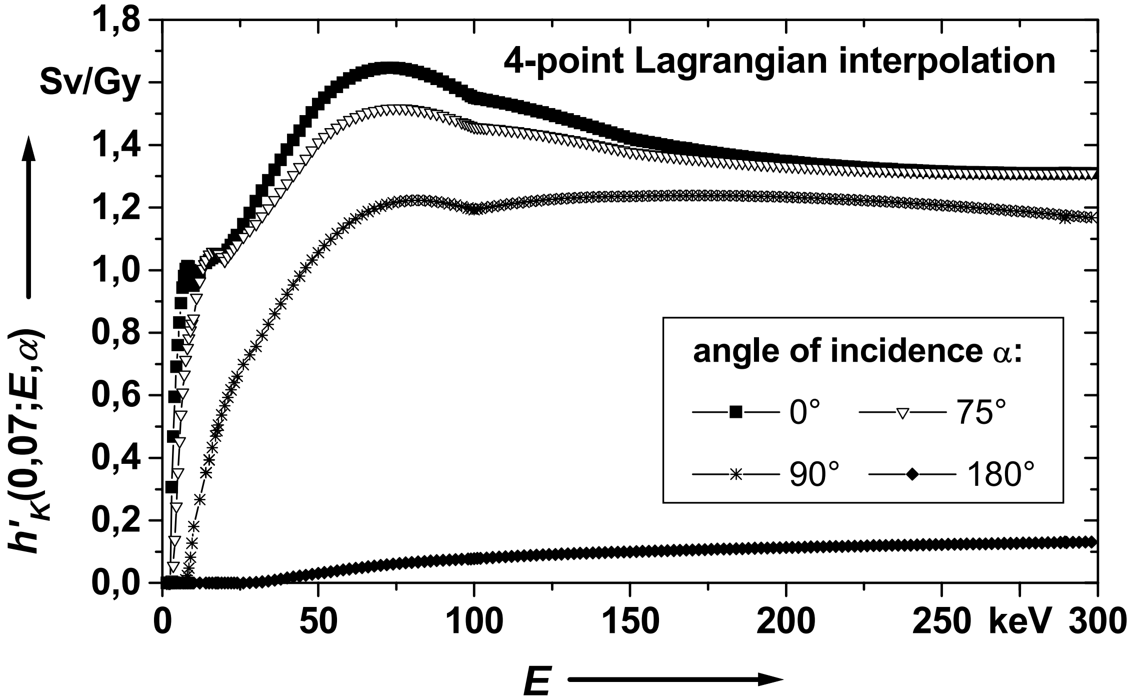

Figure 3.4: Monoenergetic conversion coefficients $h'_K(0{,}07;E,\alpha)$ in Sv/Gy for the angles of incidence α of 0°, 75°, 90° and 180° as a function of photon energy E. The $h'_K(0{,}07;E,\alpha)$ values were calculated using the set of basic values given in ICRP Publication 74 [17] and ICRU Report 57 [18] and a four-point Lagrangian interpolation as recommended (see text).

Different interpolation formulae were tested using the set of basic values given in ICRP Publication 74 [17] and ICRU Report 57 [18] to get a smooth energy dependence of the monoenergetic conversion coefficients $h'_K(0{,}07;E,\alpha)$ in line with the ICRP/IRCU intention. Using the $h'_K(0{,}07;E,\alpha)$ basic values (α = 0°, 15°, 30°, 45°, 60°, 75°, 90°, 180°) given in ICRP 74 and ICRU 57, an additional value for $\alpha = 75°$ and $E = 5\,\mathrm{keV}$, which is derived from the $h'_K(0{,}07;\ 5\,\mathrm{keV},\alpha)$ values for α below 75° listed in ICRP 74 and ICRU 57 (see Table 3.4), and carrying out a simple two-point interpolation on a linear-linear scale, the general energy dependence seems to be in line with the ICRP/IRCU intention. In Figure 3.5 the $h'_K(0{,}07;E,\alpha)$ values calculated in this manner are plotted for energies up to 50 keV and in Figure 3.6 for energies up to 300 keV. For all energies the $h'_K(0{,}07;E{,}60°)$ values are equal to or smaller than those with an angle of incidence α smaller than 60°. The bends in the energy dependence result from the two-point interpolation. Using the set of basic values given in ICRP Publication 74 [17] and ICRU Report 57 [18] in spite of the bends, two-point interpolation on a linear-linear scale seems to be the best choice to derive the monoenergetic conversion coefficients $h'_K(0{,}07;E,\alpha)$. In Table 3.4 $h'_K(0{,}07;E,\alpha)$ values determined in this manner are plotted in italics. By definition, the monoenergetic conversion coefficients have no uncertainty [17] [18].

Verfügbar unter: https://doi.org/10.7795/110.20190315B

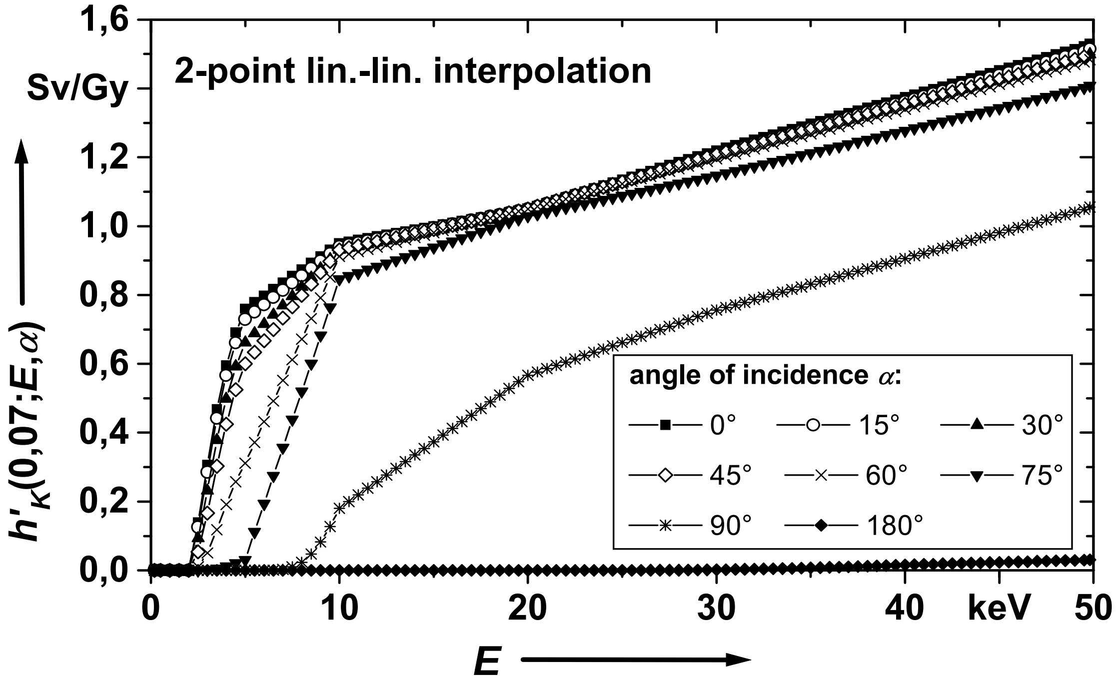

Figure 3.5: Monoenergetic conversion coefficients $h'_K(0{,}07;E,\alpha)$ in Sv/Gy for the angles of incidence α of 0°, 15°, 30°, 45°, 60°, 75°, 90° and 180° and photon energies up to 50 keV. The $h'_K(0{,}07;E,\alpha)$ values were calculated using the $h'_K(0{,}07;E,\alpha)$ basic values given in ICRP Publication 74 [17] and ICRU Report 57 [18], an additional $h'_K(0{,}07;E,\alpha)$ value for α = 75° and E = 5 keV (see Table 3.4) and two-point interpolation on a linear-linear scale.

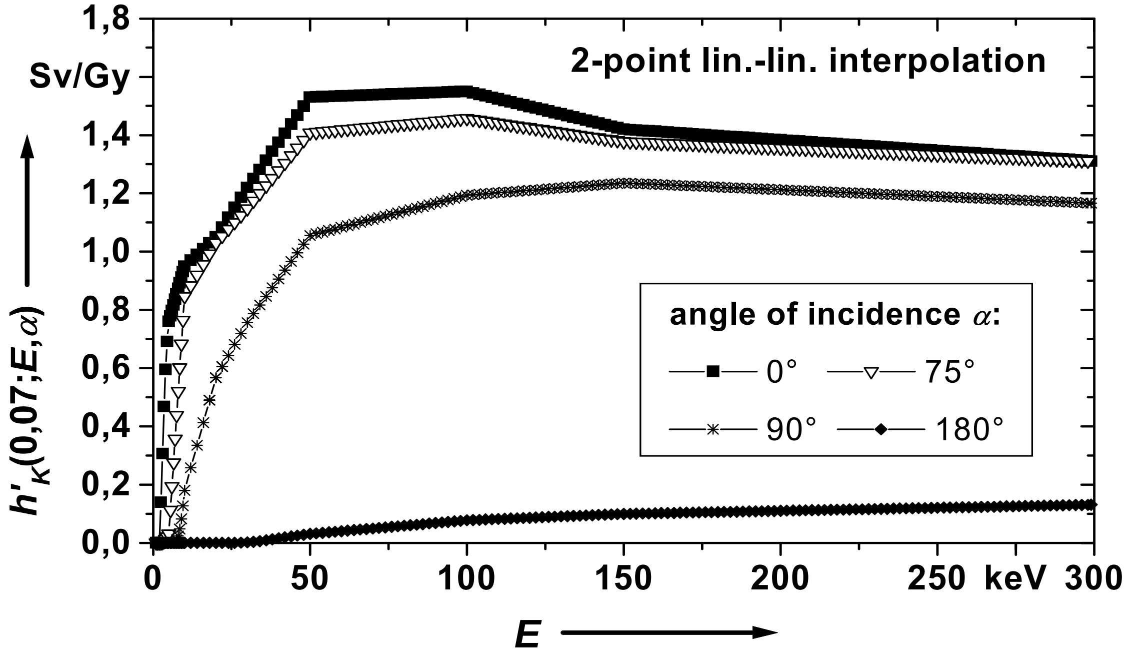

Figure 3.6: Monoenergetic conversion coefficients $h'_K(0{,}07;E,\alpha)$ in Sv/Gy for the angles of incidence α of 0°, 75°, 90° and 180° as a function of photon energy E. The $h'_K(0{,}07;E,\alpha)$ values were calculated using the $h'_K(0{,}07;E,\alpha)$ basic values given in ICRP Publication 74 [17] and ICRU Report 57 [18], an additional $h'_K(0{,}07;E,\alpha)$ value for α = 75° and E = 5 keV (see Table 3.4) and two-point interpolation on a linear-linear scale.

The $h'_K(0{,}07;E,\alpha)$ values calculated with the $h'_K(0{,}07;E,\alpha)$ basic values listed in ICRP Publication 74 [17] and ICRU Report 57 [18], an additional $h'_K(0{,}07;E,\alpha)$ value for $\alpha = 75°$ and $E = 5$ keV and two-point interpolation on a linear-linear scale were used as far as possible to determine the $h'_K(0{,}07;\mathrm{R},\alpha)$ values. However, for the angles of 0°, 15°, 30°, 45° and 60° conversion coefficients are given in ICRP Publication 74 and ICRU Report 57 only for photon energies equal to or larger than 5 keV, for the angles of 75° and 90° only for energies equal to or larger than 10 keV and for 180° only for photon energies equal to or larger than 50 keV. To get a correct interpolation for $\alpha = 75°$, an additional value (see Table 3.4) for 5 keV, which is not given in ICRP Publication 74 and ICRU Report 57, was derived from the $h'_K(0{,}07;\ 5\ \mathrm{keV},\alpha)$ values for α smaller than 75° listed in ICRP 74 and ICRU 57. For the conversion coefficients $h'_K(10;E < E_{\mathrm{ICRP}},\alpha)$, denoting the lowest energy given in ICRP 74 and ICRU 57 as E_{ICRP} with the exception of $\alpha = 75°$, for which E_{ICRP} is set to 5 keV, an extrapolation was performed from E_{ICRP} down to 3 keV in the following way (see also Section 3.6.1):

$$h'_K(0{,}07;E<E_{\mathrm{ICRP}},\alpha) = h'_K(0{,}07;E_{\mathrm{ICRP}},\alpha)\cdot\frac{\exp\left(-\left(\frac{\mu(E)}{\rho}\right)_{\mathrm{ICRU,en}}\cdot\rho_{\mathrm{ICRU}}\cdot d\right)}{\exp\left(-\left(\frac{\mu(E_{\mathrm{ICRP}})}{\rho}\right)_{\mathrm{ICRU,en}}\cdot\rho_{\mathrm{ICRU}}\cdot d\right)}, \qquad (3.12)$$

with $(\mu(E)/\rho)_{\mathrm{ICRU,en}}$ and ρ_{ICRU} as given in Section 3.6.1. d is the distance between the surface of the ICRU sphere and the reference point at 0,07 mm depth, at which the directional dose equivalent is determined, and is demonstrated in Figure 3.2. The distance d depends on the angle of incidence α. The diameter of the ICRU sphere is 300,0 mm. For the determination of d, the following cases have to be distinguished:

$\underline{\alpha = 0°}$: $d = 0{,}07$ mm;

$\underline{0° < \alpha < 180°}$: $\delta = \arcsin\left((1-\frac{0{,}07}{150})\cdot\sin(180°-\alpha)\right)$

$$\gamma = \alpha - \delta$$

$$d = r_{\mathrm{ICRU}}\cdot\frac{\sin\gamma}{\sin(180°-\alpha)} \quad ; \quad r_{\mathrm{ICRU}} = 150\ \mathrm{mm}$$

$\underline{\alpha = 180°}$: $d = 300$ mm - 0,07 mm;

In Table 3.4 the monoenergetic conversion coefficients $h'_K(0{,}07;E,\alpha)$ calculated with the aid of Equation 3.12 for photon energies E from 3 keV to $E = E_{\mathrm{ICRP}} = 5$ keV, 10 keV and 50 keV for the angles of incidence α of 0°, 15°, 30°, 45°, 60°, 75°, 90° and 180° are listed. The basic values, $h'_K(0{,}07;E_{\mathrm{ICRP}},\alpha)$, for the extrapolation (see Equation 3.12) are plotted in Table 3.4 in bold type.

Verfügbar unter: https://doi.org/10.7795/110.20190315B

Table 3.4: Monoenergetic conversion coefficients $h'_K(0{,}07;E,\alpha)$ in Sv/Gy for the angles of incidence α of 0°, 15°, 30°, 45°, 60°, 75°, 90° and 180°. For the angles of incidence of 0°, 15°, 30°, 45°, 60° and 75° for photon energies up to E_{ICRP} = 5 keV, for the angle of 90° up to E_{ICRP} = 10 keV and for the angle of 180° up to E_{ICRP} = 50 keV the $h'_K(0{,}07;E,\alpha)$ values were calculated with Equation 3.12. The conversion coefficients $h'_K(0{,}07;E_{ICRP},\alpha)$ forming the basis for the extrapolation are plotted in bold type (see Equation 3.12). The $h'_K(0{,}07;E,\alpha)$ values plotted in roman for energies higher than E_{ICRP} are given in ICRP Publication 74 [17] and ICRU Report 57 [18]; additional values in italics were calculated using the $h'_K(0{,}07;E,\alpha)$ basic values given in ICRP 74 and ICRU 57, an additional value for E = 5 keV for α = 75° (see the text) and two-point interpolation on a linear-linar scale.

Photon energy E in keV	$h'_K(0{,}07;E,\alpha)$ in Sv/Gy for angles of incidence α of							
	0°	15°	30°	45°	60°	75°	90°	180°
3,0	0,306	0,285	0,232	0,166	0,051	$9{,}07\cdot10^{-4}$	$<1\cdot10^{-6}$	$<1\cdot10^{-6}$
4,0	0,595	0,566	0,498	0,425	0,191	0,012		
5,0	**0,760**	**0,730**	**0,661**	**0,600**	**0,312**	**0,030**		
6,0	*0,798*	*0,772*	*0,715*	*0,667*	*0,432*	*0,193*	$8{,}34\cdot10^{-5}$	
8,0	*0,874*	*0,856*	*0,823*	*0,799*	*0,672*	*0,519*	0,0237	
10,0	0,950	0,941	0,931	0,931	0,912	0,846	**0,181**	
12,0	*0,970*	*0,962*	*0,953*	*0,955*	*0,940*	*0,882*	*0,258*	
14,0	*0,990*	*0,984*	*0,974*	*0,979*	*0,967*	*0,919*	*0,335*	
15,0	*1,00*	*0,995*	*0,985*	*0,991*	*0,981*	*0,937*	*0,374*	
20,0	1,05	1,05	1,04	1,05	1,05	1,03	0,567	
30,0	1,22	1,21	1,21	1,21	1,20	1,15	0,756	$1{,}89\cdot10^{-3}$
40,0	1,38	1,36	1,35	1,35	1,34	1,28	0,906	$1{,}59\cdot10^{-2}$
50,0	1,53	1,51	1,50	1,50	1,48	1,41	1,06	**0,0306**
60,0	*1,53*	*1,52*	*1,51*	*1,51*	*1,49*	*1,42*	*1,08*	*0,0400*
70,0	*1,54*	*1,52*	*1,51*	*1,51*	*1,50*	*1,43*	*1,11*	*0,0494*
80,0	*1,54*	*1,53*	*1,52*	*1,52*	*1,51*	*1,44*	*1,14*	*0,0587*
90,0	*1,55*	*1,53*	*1,53*	*1,53*	*1,51*	*1,45*	*1,17*	*0,0681*
100,0	1,55	1,53	1,53	1,53	1,52	1,46	1,19	0,0775

The conversion coefficient $h'_K(0{,}07;\mathrm{R},\alpha)$ for a radiation quality or an unfiltered X-ray spectrum 'R' results from

$$h'_K(0{,}07;\mathrm{R},\alpha)=\frac{\int_{E_{\min}}^{E_{\max}}\Phi_E(E)\cdot k_\Phi(E)\cdot h'_K(0{,}07;E,\alpha)\,\mathrm{d}E}{\int_{E_{\min}}^{E_{\max}}\Phi_E(E)\cdot k_\Phi(E)\;\mathrm{d}E}, \tag{3.13}$$

with $E_{\min}$, $E_{\max}$ and $\Phi_E(E)\cdot k_\Phi(E)$ as discussed in Section 3.1. The $h'_K(0{,}07;\mathrm{R},\alpha)$ values calculated with Equation 3.13 are listed in Section 4 for the radiation qualities and unfiltered X-ray spectra considered in this report. They are determined for reference conditions.

For energies greater than 10 keV the conversion coefficients $h'_K(0{,}07;E,\alpha)$ show a small energy dependence. Therefore the influence of differences in the spectral distribution due to the use of different X-ray units or a change of the air path or the air density to the $h'_K(0{,}07;\mathrm{R},\alpha)$ values of a radiation quality 'R', which includes an appreciable protion of photons with an energy larger than 10 keV, is small. Thus the values of almost all radiation qualities presented in this catalogue can be directly used for calibration purposes in terms of the directional dose equivalent $H'(0{,}07,\vec{\Omega})$, as discussed for the use of the $h_{pK}(0{,}07;\mathrm{R})$ values in Section 3.6.2.

3.7 Analysis of the uncertainties of the characteristic data

The characteristic data are influenced by the choice of the minimum and maximum cut-off energies $E_{\min}$ and $E_{\max}$ (see Section 3.1), the air density, ρ, the accuracy of the high-voltage adjustment of the X-ray facility, the statistics of the pulse height spectra and the unfolding method. The influences of these parameters on the data presented in this report are discussed with the aid of a sensitivity study [29] in this section. This means, that the influence of each of these parameters is analysed in the following way: the value of only one parameter, e.g. the air density, is changed, the values of the other parameters are kept unchanged and then the characteristic data are determined. The comparison of these data with those presented in Section 4 show the influence of the changed parameter on the characteristic data.

The statistical uncertainty of the characteristic data is negligible because of the large number of counts measured for each pulse height spectrum (see Section 2). To check the correctness of unfolding several pulse height spectra were unfolded using two different algorithms, see [15]. The fluence spectra produced by the two algorithms are identical.

The pulse height spectra were measured with a very low tube current (below 0,1 mA) to prevent pile-up events (see Section 2). A possible dependence of the spectral distribution on the X-ray tube current was investigated with several spectra of the ISO narrow-spectrum series and the ISO low air-kerma rate series. They could be measured without any pile-up events both with higher tube currents (0,1 mA to 1,5 mA) and with currents below 0,1 mA. No differences in the spectral distribution could be observed when the current was reduced below 0,1 mA.

The standard uncertainty of the high-voltage adjustment of the X-ray units used is about 10 V for the 120 kV X-ray facility and about 100 V for the 420 kV X-ray unit. These small uncertainties of the high-voltage adjustment are smaller than the channel width of the response matrices used and of the resolution of the fluence spectra, respectively. These small uncertainties therefore do not influence the values presented.

To get an estimate of the influence of the accuracy of the tube voltage adjustment to the characteristic data, the deviations due to changes in the tube potential (theoretical maximum energy of the fluence spectrum) by ± 5 % were calculated. The two following assumptions were made for this investigation: Firstly, the relative change of the tube potential and the relative change of the mean photon energy are equal. Secondly, for the purpose of calculating the deviations of the values of the characteristic parameters of a radiation quality ‘R’, the respective value can be replaced by the monoenergetic one for the mean photon energy. For the calculation of the deviations of the characteristic data, the mean photon energies $\overline{E}_{\mathrm{ph}}$ of 24 fluence spectra with maximum energies from 7,5 keV to 300 keV were used to cover the whole energy range considered in this report. The spectra were subdivided into four groups according to their mean photon energies: the first group includes all spectra with $\overline{E}_{\mathrm{ph}}$ = 6,0 to 14,0 keV, the second group contains all spectra with $\overline{E}_{\mathrm{ph}}$ = 14,0 to 25,5 keV, in the third group all spectra with $\overline{E}_{\mathrm{ph}}$ = 25,5 to 58,0 keV are combined, and all spectra with $\overline{E}_{\mathrm{ph}}$ = 58,0 to 249,0 keV belong to the fourth group. In Table 3.5a and Table 3.5b, for each energy group, the relative deviations in percent of the values of the characteristic parameters (first and second half-value layer (1st HVL, 2nd HVL), mean photon energy $\overline{E}_{\mathrm{ph}}$, 10 % percentile, kerma factor k_{Φ}(R), conversion coefficients $h_{\mathrm{p}K}$(0,07;R), $h_K^*(10;\mathrm{R})$, $h_{\mathrm{p}K}(10;\mathrm{R},\alpha)$ (α = 0°, 45° and 75°) and $h'_K(0{,}07;\mathrm{R},\alpha)$ (α = 0°, 45°, 75° and 180°)) due to a change in the tube potential by ± 5 % are listed. The deviations of the angle-dependent quantities $h_{\mathrm{p}K}(10;\mathrm{R},\alpha)$ and $h'_K(0{,}07;\mathrm{R},\alpha)$ were calculated only for some angles of incidence α. The relative deviations at the angles of incidence in between can be concluded from the values listed. The relative deviation of the mean photon energy $\overline{E}_{\mathrm{ph}}$ and the 10 % percentile is given by the change of the tube potential by ± 5 %.

Table 3.5a: Relative deviations in % of the values of the characteristic parameters (first and second half-value layer (1st HVL, 2nd HVL), mean photon energy $\overline{E}_{\mathrm{ph}}$, 10 % percentile, kerma factor k_{Φ}(R) and conversion coefficient $h_{\mathrm{p}K}$(0,07;R) and $h_K^*(10;\mathrm{R})$) when the X-ray tube potential changes by ± 5 %.

<table>
<tr><th>$\overline{E}_{\mathrm{ph}}$ in keV of the radiation quality ‘R’</th><th>Δ1st HVL in %</th><th>Δ2nd HVL in %</th><th>$\Delta\overline{E}_{\mathrm{ph}}$ in %</th><th>Δ(10 % percentile) in %</th><th>Δk_{Φ}(R) in %</th><th>$\Delta h_{\mathrm{p}K}$(0,07;R) in %</th><th>$\Delta h_K^*(10;\mathrm{R})$ in %</th></tr>
<tr><td>6,0 – 14,0</td><td rowspan="3">10 – 15</td><td rowspan="3">10 – 15</td><td rowspan="4">5</td><td rowspan="4">5</td><td>10 – 20</td><td rowspan="2">0,5 – 1</td><td>20 – 200 [a]</td></tr>
<tr><td>14,0 – 25,5</td><td rowspan="2">5 – 10</td><td>6 – 20</td></tr>
<tr><td>25,5 – 58,0</td><td rowspan="2">0,1 – 0,5</td><td>1 – 6</td></tr>
<tr><td>58,0 – 249,0</td><td>2 – 10</td><td>2 – 10</td><td>1 – 5</td><td>0,2 – 1</td></tr>
</table>

[a] No relative deviations were determined for values of $h_K^*(10;\mathrm{R})$ below $1\cdot10^{-4}$ Sv/Gy.

Table 3.5b: Relative deviations in % of the values of the conversion coefficients $h_{\mathrm{p}K}(10;\mathrm{R},\alpha)$ (α = 0°, 45° and 75°) and $h'_K(0{,}07;\mathrm{R},\alpha)$ (α = 0°, 45°, 75° and 180°) when the X-ray tube potential changes by ± 5 %.

<table>
<tr><th rowspan="2">$\overline{E}_{\mathrm{ph}}$ in keV of the radiation quality ‘R’</th><th colspan="3">$\Delta h_{\mathrm{p}K}(10;\mathrm{R},\alpha)$ in %</th><th colspan="4">$\Delta h'_K(0{,}07;\mathrm{R},\alpha)$ in %</th></tr>
<tr><th>α = 0°</th><th>α = 45°</th><th>α = 75°</th><th>α = 0°</th><th>α = 45°</th><th>α = 75°</th><th>α = 180°</th></tr>
<tr><td>6,0 – 14,0</td><td>20 – 200 [a]</td><td>25 – 300 [a]</td><td>50 – 500 [a]</td><td rowspan="3">1 – 3,5 [a]</td><td rowspan="3">1,5 – 4 [a]</td><td>3,5 – 5,5 [a]</td><td>—</td></tr>
<tr><td>14,0 – 25,5</td><td>7 – 20</td><td>8 – 25</td><td>15 – 50</td><td rowspan="2">1,5 – 3,5</td><td>—</td></tr>
<tr><td>25,5 – 58,0</td><td>1,5 – 7</td><td>1,5 – 8</td><td>1,5 – 15</td><td rowspan="2">2 – 7</td></tr>
<tr><td>58,0 – 249,0</td><td colspan="3">0,2 – 1,5</td><td colspan="3">0,1 – 1,5</td></tr>
</table>

[a] No relative deviations were determined for values of $h_{\mathrm{p}K}(10;\mathrm{R},\alpha)$ and $h'_K(0{,}07;\mathrm{R},\alpha)$ below $1\cdot10^{-4}$ Sv/Gy.

The conversion coefficients $h_{pK}(10;\mathrm{R},\alpha)$ and $h_K^*(10;\mathrm{R})$ show very large variations for spectra with a low mean photon energy. This is due to the large energy dependence of the monoenergetic conversion coefficients $h_{pK}(10;E,\alpha)$ and $h_K^*(10;E)$, in particular for low photon energies. The relative deviations of the conversion coefficients $h_{pK}(0,07;\mathrm{R})$ in the whole energy range is, however, only small because of the small energy dependence of the monoenergetic conversion coefficient $h_{pK}(0,07;E)$. As shown in Table 3.5a and Table 3.5b, the relative deviations of the characteristic data due to a change of the tube potential by ± 5 % decrease with increasing mean photon energy. Because of the two assumptions made for the calculation of the deviations, the values given in the tables are only approximated values, but they show the general dependence of the characteristic data on the tube potential. The relative deviations listed in Tables 3.5a and 3.5b demonstrate the requirements to be met by the X-ray unit used: the tube potential must be the same for the determination of the values $H_p(10)$ and $H^*(10)$ using the conversion coefficients $h_{pK}(10;\mathrm{R},\alpha)$ and $h_K^*(10;\mathrm{R})$, respectively, and the calibration measurements and, in addition, the tube potential must be stable during the measurements, see also [21].

For determining the characteristic data, the fluence spectra were cut off at a minimum energy E_{min} and a maximum energy E_{max}, as described in Section 3.1. The error in determining E_{min} is less than ± 20 %, see [15]. To determine the influence of this error on the characteristic data, the relative deviations caused by a variation of E_{min} by ± 20 % were calculated for the same parameters (1st HVL, 2nd HVL, $\overline{E}_{ph}$, 10 % percentile, kerma factor $k_\Phi(\mathrm{R})$, $h_{pK}(0,07;\mathrm{R})$, $h_K^*(10;\mathrm{R})$, $h_{pK}(10;\mathrm{R},\alpha)$, $h'_K(0,07;\mathrm{R},\alpha)$) considered in Tables 3.5a and 3.5b. For this investigation 60 fluence spectra (46 different radiation qualities with and without additional filtration) determined for distances between the focus of the X-ray tube and the spectrometer of 2,5 m, 1,0 m and 0,3 m and with maximum energies from 7,5 keV to 300 keV were used to cover the whole energy range considered in this report. These fluence spectra make up a representative set of spectra, so the relative deviations determined allow conclusions to be drawn for the deviations of the characteristic data of the other radiation qualities considered in this report. They were subdivided in four groups according to their mean photon energies as described in the previous paragraph. For each group the relative deviations in percent by ± 20 % variation of E_{min} are listed for each characteristic parameter in Table 3.6a and Table 3.6b. For the conversion coefficients $h_{pK}(10;\mathrm{R},\alpha)$ the deviations are listed only for angles of incidence α of 0°, 45° and 75° and for $h'_K(0,07;\mathrm{R},\alpha)$ only for α of 0°, 45°, 75° and 180°. For the angles of incidence in between, the deviations can be concluded from the values listed. The relative deviations give the maximum uncertainties due to the choice of the minimum cut-off energy E_{min} for determining the characteristic data. They decrease with increasing mean photon energy. The maximum relative deviation is about 1,5 %.

Verfügbar unter: https://doi.org/10.7795/110.20190315B

Table 3.6a: Relative deviations in % of the values of the characteristic parameters (first and second half-value layer (1st HVL, 2nd HVL), mean photon energy $\overline{E}_{\mathrm{ph}}$, 10 % percentile, kerma factor k_{Φ}(R), conversion coefficient $h_{\mathrm{p}K}$(0,07;R) and $h_K^*(10;\mathrm{R})$) due to a variation of the minimum cut-off energy $E_{\min}$ by ± 20 %.

<table>
<tr><th>$\overline{E}_{\mathrm{ph}}$ in keV of the radiation quality ‘R’</th><th>Δ1st HVL in %</th><th>Δ2nd HVL in %</th><th>$\Delta \overline{E}_{\mathrm{ph}}$ in %</th><th>Δ(10 % percentile) in %</th><th>Δk_{Φ}(R) in %</th><th>$\Delta h_{\mathrm{p}K}$(0,07;R) in %</th><th>$\Delta h_K^*(10;\mathrm{R})$ in %</th></tr>
<tr><td>6,0 – 14,0</td><td rowspan="3">0,4 – 1,5</td><td rowspan="3">0,3 – 0,8</td><td>0,3 –1</td><td rowspan="2">0,5 – 1,5</td><td rowspan="3">0,3 – 1,5</td><td rowspan="2">0,1 – 0,5</td><td rowspan="3">0,4 – 1,5 [a]</td></tr>
<tr><td>14,0 – 25,5</td><td>0,1 – 0,3</td></tr>
<tr><td>25,5 – 58,0</td><td>—</td><td>0,2 – 0,5</td><td rowspan="2">—</td></tr>
<tr><td>58,0 – 249,0</td><td>0,1 – 0,4</td><td>0,1 – 0,3</td><td>—</td><td>—</td><td>0,1 – 0,3</td><td>0,1 – 0,4</td></tr>
</table>

[a] For $h_K^*(10;\mathrm{R})$ values below $1 \cdot 10^{-4}$ Sv/Gy, no relative deviations were determined.

Table 3.6b: Relative deviations in % of the values of the conversion coefficients $h_{\mathrm{p}K}(10;\mathrm{R},\alpha)$ ($\alpha = 0°$, 45° and 75°) and $h'_K(0{,}07;\mathrm{R},\alpha)$ ($\alpha = 0°$, 45°, 75° and 180°) due to a variation of the minimum cut-off energy $E_{\min}$ by ± 20 %.

<table>
<tr><th rowspan="2">$\overline{E}_{\mathrm{ph}}$ in keV of the radiation quality ‘R’</th><th colspan="3">$\Delta h_{\mathrm{p}K}(10;\mathrm{R},\alpha)$ in %</th><th colspan="4">$\Delta h'_K(0{,}07;\mathrm{R},\alpha)$ in %</th></tr>
<tr><th>α = 0°</th><th>α = 45°</th><th>α = 75°</th><th>α = 0°</th><th>α = 45°</th><th>α = 75°</th><th>α = 180°</th></tr>
<tr><td>6,0 – 14,0</td><td colspan="3" rowspan="3">0,4 – 1,5 [a]</td><td rowspan="4">0,1 – 0,7 [a]</td><td colspan="3" rowspan="4">0,1 – 1 [a]</td></tr>
<tr><td>14,0 – 25,5</td></tr>
<tr><td>25,5 – 58,0</td></tr>
<tr><td>58,0 – 249,0</td><td colspan="3">0,1 – 0,4</td></tr>
</table>

[a] No relative deviations were determined for values of $h_{\mathrm{p}K}(10;\mathrm{R},\alpha)$ and $h'_K(0{,}07;\mathrm{R},\alpha)$ below $1 \cdot 10^{-4}$ Sv/Gy.

In the spectra the fluence contribution is zero only for energies higher than about 400 eV above the theoretical maximum energy given by the adjusted X-ray tube voltage. Due to this extension in the fluence spectra, the maximum cut-off energy $E_{\max}$ was set to 1 keV above the theoretical maximum energy (see Section 3.1 and [15]). To investigate the influence of this effect on the values of the characteristic parameters considered in this report, the characteristic data of the representative spectra (described in the previous paragraph) were determined both with a maximum cut-off energy $E_{\max}$ of 1 keV above the theoretical maximum energy (including the extension) and with $E_{\max}$, which is identical with the theoretical maximum energy (cutting off the extension). The comparison of the values calculated in this manner shows that the influence by this effect is less than 0,5 % with the exception of the conversion coefficients $h_{\mathrm{p}K}(10;\mathrm{R},\alpha)$ and $h^*(10;\mathrm{R})$ of the spectra with a mean photon energy lower than 14 keV, for which this effect leads to relative deviations of 0,5 to 2 %.

The environmental parameter air density, ρ, influences the fluence spectra, in particular the spectra with an appreciable portion of low-energy photons. To get an estimate of the influence of the air density on the characteristic data, the relative deviations between the values for reference conditions

Verfügbar unter: https://doi.org/10.7795/110.20190315B

and those based on an air density differing by ± 10 % were determined. The variation of the reference air density by ± 10 % is equivalent to the air density range recommended by ISO 4037-3 [10] for “standard test conditions”. For the investigation of the influence of the air density, the representative set of fluence spectra as described in the previous paragraph was used. The spectra were again subdivided into four groups according to their mean photon energies. However, the unfiltered X-ray spectra with a mean photon energy $\overline{E}_{ph}$ equal to or larger than 14,0 keV are combined in a separate group because of their wide spectral distribution with an appreciable portion of low-energy photons, which causes great sensitivity to air density variations. In Tables 3.7a and 3.7b the relative deviations in percent of the values of the characteristic parameters by changing the reference air density by ± 10 % are listed. For each mean photon energy group the minimum and maximum deviation for each characteristic parameter is given.

Table 3.7a: Relative deviations in % of the values of the characteristic parameters (first and second half-value layer (1st HVL, 2nd HVL), mean photon energy $\overline{E}_{ph}$, 10 % percentile, kerma factor k_{Φ}(R), conversion coefficient h_{pK}(0,07;R) and $h_K^*(10;\mathrm{R})$) for a ± 10 % change of the reference air density.

<table>
<tr><th>$\overline{E}_{ph}$ in keV of the radiation quality ‘R’</th><th>Δ1st HVL in %</th><th>Δ2nd HVL in %</th><th>$\Delta\overline{E}_{ph}$ in %</th><th>Δ(10 % percentile) in %</th><th>Δk_{Φ}(R) in %</th><th>Δh_{pK}(0,07;R) in %</th><th>$\Delta h_K^*(10;\mathrm{R})$ in %</th></tr>
<tr><td>6,0 – 14,0</td><td>2,5 – 5</td><td>1,5 – 5,5</td><td rowspan="2">0,3 – 1,5</td><td rowspan="2">1 – 4,5</td><td>3 – 7</td><td rowspan="2">0,2 – 1,5</td><td>2,5 – 11 [a]</td></tr>
<tr><td>14,0 – 25,5</td><td>0,3 – 3</td><td>0,3 – 2</td><td>0,4 – 2,5</td><td>0,6 – 2,5</td></tr>
<tr><td>25,5 – 58,0</td><td rowspan="2">0,2 – 1</td><td rowspan="2">0,2 – 0,5</td><td rowspan="2">0,1 – 0,3</td><td>0,4 – 1</td><td>0,1 – 0,4</td><td>—</td><td>0,1 – 0,6</td></tr>
<tr><td>58,0 – 249,0</td><td>—</td><td>—</td><td>—</td><td>—</td></tr>
<tr><td>Unfiltered spectra ($\overline{E}_{ph} \geq$ 14,0 keV)</td><td>3,5 – 10</td><td>3,5 – 9,5</td><td>1,5 – 2,5</td><td>1,5 – 3,5</td><td>4 – 7</td><td>0,5 – 1</td><td>5 – 13</td></tr>
</table>

[a] For $h_K^*(10;\mathrm{R})$ values below $1{\cdot}10^{-4}$ Sv/Gy, no relative deviations were determined.

Table 3.7b: Relative deviations in % of the values of the conversion coefficients $h_{pK}(10;\mathrm{R},\alpha)$ (α = 0°, 45°, and 75°) and $h'_K(0{,}07;\mathrm{R},\alpha)$ (α = 0°, 45°, 75° and 180°) for a ± 10 % change of the reference air density.

<table>
<tr><th rowspan="2">$\overline{E}_{ph}$ in keV of the radiation quality ‘R’</th><th colspan="3">$\Delta h_{pK}(10;\mathrm{R},\alpha)$ in %</th><th colspan="4">$\Delta h'_K(0{,}07;\mathrm{R},\alpha)$ in %</th></tr>
<tr><th>α = 0°</th><th>α = 45°</th><th>α = 75°</th><th>α = 0°</th><th>α = 45°</th><th>α = 75°</th><th>α = 180°</th></tr>
<tr><td>6,0 – 14,0</td><td>2,5 – 12 [a]</td><td>2,5 – 25 [a]</td><td>3 – 13 [a]</td><td rowspan="3">0,3 – 0,7 [a]</td><td rowspan="3">0,3 – 1 [a]</td><td rowspan="3" colspan="2">0,3 – 1,5 [a]</td></tr>
<tr><td>14,0 – 25,5</td><td>0,5 – 3</td><td>0,5 – 3,5</td><td>0,5 – 4,5</td></tr>
<tr><td>25,5 – 58,0</td><td colspan="2">0,1 – 0,8</td><td>0,1 – 0,8</td></tr>
<tr><td>58,0 – 249,0</td><td colspan="2">—</td><td>—</td><td>0,1 – 0,3</td><td colspan="3">0,1 – 0,3</td></tr>
<tr><td>Unfiltered spectra ($\overline{E}_{ph} \geq$ 14,0 keV)</td><td colspan="2">5,5 – 13</td><td>6 – 14</td><td>0,4 – 1</td><td colspan="3">0,4 – 1,5</td></tr>
</table>

[a] No relative deviations were determined for values of $h_{pK}(10;\mathrm{R},\alpha)$ and $h'_K(0{,}07;\mathrm{R},\alpha)$ below $1{\cdot}10^{-4}$ Sv/Gy.

As shown in Table 3.7a and Table 3.7b, with increasing mean photon energy the influence of the air density on the characteristic data decreases. The greatest deviations due to a variation of the reference air density by ± 10 % are shown by the conversion coefficients $h_{pK}(10;R,\alpha)$ and $h_K^*(10;R)$ for the spectra with an appreciable portion of low-energy photons. This results from the great energy dependence of the monoenergetic conversion coefficients. Therefore, as shown in Tables 3.7a and 3.7b, it is necessary in particular for the low-energy radiation qualities, to maintain nearly the same air density, for which the conversion coefficients are determined, throughout the calibration measurements, see also [21]. The unfiltered X-ray spectra have an appreciable portion of low-energy photons, so their characteristic data show great deviations due to the variation of the air density; the deviations are smaller with increasing mean photon energy.

The extent of the influence of the air density on the fluence spectra is dependent on the distance between the focus of the X-ray tube and the spectrometer, at which the spectrum was measured (compare the values listed in Section 4.1.2 and Section 4.1.3). With increasing air path the influence of the air density increases as well. However, this influence on the data is within the deviation ranges given in Tables 3.7a and 3.7b, so that this effect is not demonstrated in a separate table.

For each measurement of a fluence spectrum the temperature and air pressure were measured and then the air density was calculated (see Section 3.1 and [15]), so that the maximum uncertainty of the air density of each measurement of a spectrum is about ± 1 % and smaller. Considering the relative deviations of the values of the characteristic parameters due to a ± 10 % variation of the reference air density (see Table 3.7a and Table 3.7b), a change of the air density by ± 1 % has only a small influence on the characteristic data. Altogether, the choice of E_{min} and E_{max}, which was set to 1 keV above the theoretical maximum energy (see Section 3.1), and an uncertainty of the air density of ± 1 % result in an overall relative uncertainty of the values of the characteristic parameters for the radiation qualities with a mean photon energy lower than 14,0 keV and all unfiltered X-ray spectra considered in this report of about up to 2 %. For the radiation qualities with a mean photon energy higher than 14,0 keV, the total relative uncertainty is about up to 1 %.

Verfügbar unter: https://doi.org/10.7795/110.20190315B

4. Tables with the characteristic data

4.1 Data for the ISO low air-kerma rate series, the ISO narrow-spectrum series, the ISO wide-spectrum series, the ISO high air-kerma rate series and the DIN A-, B- and C-series as well as for several unfiltered X-ray spectra

4.1.1 Introduction

In Sections 4.1.2 and 4.1.3 for each radiation quality 'R' of the ISO low air-kerma rate series (L), the ISO narrow-spectrum series (N), the ISO wide-spectrum series (W), the ISO high air-kerma rate series (H) and of the A-, B- and C-series according to the German standard DIN 6818-1 [3] the values for the following characteristic parameters are listed:

- first and second half-value layer (1^{st} HVL, 2^{nd} HVL),
- mean photon energy $\overline{E}_{ph}$,
- 10 % percentile,
- kerma factor k_{Φ}(R),
- conversion coefficient $h_{pK}(10;R,\alpha)$ from air kerma, K_a, to the personal dose equivalent, $H_p(10)$, for the slab phantom at an angle of incidence α,
- conversion coefficient $h_{pK}(0{,}07;R)$ from air kerma, K_a, to the personal dose equivalent, $H_p(0{,}07)$, for the rod phantom and all angles of incidence α below 60°,
- conversion coefficient $h_K^*(10;R)$ from air kerma, K_a, to the ambient dose equivalent, $H^*(10)$,
- conversion coefficient $h'_K(0{,}07;R,\alpha)$ from air kerma, K_a, to the directional dose equivalent, $H'(0{,}07,\vec{\Omega})$, at an angle of incidence α.

In addition, the values for these characteristic parameters of the unfiltered X-ray spectra with tube voltages of 7,5 kV to 300 kV are given. In Section 4.1.2 the data of the spectra measured at a distance between the focus of the X-ray tube and the front of the Ge detector of 1,0 m are given; in Section 4.1.3 those for a distance of 2,5 m are listed. All data are valid for reference conditions (see Section 3.1). The unfiltered X-ray spectra with a tube voltage higher than 120 kV could not be measured at a distance of 1,0 m because the tube current could not be sufficiently reduced.

As shown in Tables 2.1 to 2.4 some radiation qualities are specified in several series and therefore have more than one designation. The radiation qualities A 10, A 15 and A 20 are identical with B 10, B 15 and B 20, respectively. The qualities A 7,5, B 7,5 and C 7,5 are identical with the unfiltered X-ray spectrum generated with 7,5 kV tube voltage. The quality C 10 is identical with the unfiltered X-ray spectrum with a tube voltage of 10 kV. For clear arrangement, however, in the tables of one series, the characteristic data of every radiation quality of this series are listed, so some values are appear in several tables.

4.1.2 Data for a reference distance of 1,0 m

4.1.2.1 ISO low air-kerma rate series

Table 4.1: Data for the radiation qualities of the low air-kerma rate series (L) specified in ISO 4037-1 [2]: first and second half-value layers (1^{st} HVL, 2^{nd} HVL) in mm with the absorber materials Al and Cu, mean photon energies $\overline{E}_{ph}$ in keV, 10 % percentiles in keV, kerma factors $k_{\Phi}(R)$ in $pGy \cdot cm^2$, conversion coefficients $h_{pK}(0{,}07;R)$ from air kerma, K_a, to the personal dose equivalent, $H_p(0{,}07)$, for the rod phantom and conversion coefficients from air kerma, K_a, to the ambient dose equivalent, $H^*(10)$, for the ICRU sphere. The $h_{pK}(0{,}07;R)$ values are valid for all angles of incidence $\alpha \leq 60°$ (see Section 3.6.2). The $h_K^*(10;R)$ values are given for an expanded and aligned radiation field. The reference distance is 1,0 m.

Radiation quality	1^{st} HVL in mm		2^{nd} HVL in mm		$\overline{E}_{ph}$	10 % percentile	$k_{\Phi}(R)$	$h_{pK}(0{,}07;R,\alpha)$	$h_K^*(10;R)$
	Al	Cu	Al	Cu	in keV	in keV	in $pGy \cdot cm^2$	in Sv/Gy	in Sv/Gy
L-10	0,0682	0,00589	0,0710	0,00971	9,0	7,8	9,66	0,936	0,00210
L-20	0,446	0,0143	0,483	0,0152	17,3	14,6	2,44	0,992	0,393
L-30	1,56	0,0482	1,62	0,0503	26,7	23,2	0,967	1,04	0,937
L-35	2,18	0,0687	2,29	0,0727	30,4	25,8	0,745	1,06	1,09
L-55	6,14	0,248	6,30	0,261	47,8	41,2	0,356	1,11	1,62
L-70	9,11	0,483	9,21	0,505	60,6	52,5	0,302	1,14	1,73
L-100	13,49	1,22	13,54	1,25	86,8	76,5	0,333	1,16	1,70
L-125	15,79	1,98	15,82	2,02	109,4	98,0	0,415	1,17	1,62
L-170	18,51	3,40	18,55	3,46	148,5	134,0	0,595	1,16	1,49
L-210	20,34	4,52	20,36	4,55	184,6	167,0	0,777	1,15	1,42
L-240	21,50	5,19	21,51	5,22	211,4	192,0	0,914	1,15	1,38

Table 4.2: Conversion coefficients $h_{pK}(10;L,\alpha)$ in Sv/Gy from air kerma, K_a, to the personal dose equivalent, $H_p(10)$, for the slab phantom and the radiation qualities of the low air-kerma rate series (L) specified in ISO 4037-1 [2]; the reference distance is 1,0 m.

Radiation quality	$h_{pK}(10;L,\alpha)$ in Sv/Gy for angles of incidence α of					
	0°	15°	30°	45°	60°	75°
L-10	0,00236	0,00204	0,00116	0,000385	$<1\cdot10^{-4}$	$<1\cdot10^{-4}$
L-20	0,405	0,394	0,354	0,279	0,164	0,0382
L-30	0,944	0,926	0,888	0,796	0,633	0,328
L-35	1,11	1,09	1,05	0,958	0,788	0,451
L-55	1,69	1,67	1,63	1,51	1,31	0,877
L-70	1,88	1,85	1,82	1,70	1,49	1,05
L-100	1,87	1,86	1,81	1,72	1,53	1,13
L-125	1,76	1,75	1,72	1,64	1,49	1,10
L-170	1,61	1,60	1,58	1,52	1,40	1,09
L-210	1,52	1,51	1,50	1,45	1,36	1,08
L-240	1,47	1,47	1,46	1,42	1,33	1,08

Table 4.3: Conversion coefficients $h'_K(0{,}07;\mathrm{R},\alpha)$ in Sv/Gy from air kerma, K_a, to the directional dose equivalent, $H'(0{,}07,\vec{\Omega})$, for the ICRU sphere and the radiation qualities of the low air-kerma rate series (L) specified in ISO 4037-1 [2] (expanded radiation field); the reference distance is 1,0 m.

Radiation quality	$h'_K(0{,}07;\mathrm{R},\alpha)$ in Sv/Gy for angles of incidence α of							
	0°	15°	30°	45°	60°	75°	90°	180°
L-10	0,907	0,893	0,871	0,857	0,778	0,663	0,0833	$<1\cdot10^{-4}$
L-20	1,02	1,02	1,01	1,01	1,01	0,971	0,447	
L-30	1,16	1,15	1,15	1,15	1,14	1,10	0,686	0,000465
L-35	1,22	1,21	1,20	1,20	1,19	1,15	0,750	0,00238
L-55	1,48	1,46	1,45	1,45	1,44	1,36	1,01	0,0263
L-70	1,53	1,52	1,51	1,51	1,49	1,42	1,08	0,0403
L-100	1,54	1,53	1,53	1,53	1,51	1,44	1,16	0,0656
L-125	1,52	1,51	1,51	1,51	1,49	1,44	1,20	0,0816
L-170	1,43	1,41	1,41	1,41	1,41	1,38	1,23	0,0982
L-210	1,39	1,38	1,38	1,38	1,38	1,36	1,22	0,107
L-240	1,37	1,37	1,37	1,37	1,37	1,35	1,21	0,113

4.1.2.2 ISO narrow-spectrum series and DIN A-series

Table 4.4: Data for the radiation qualities of the narrow-spectrum series (N) specified in ISO 4037-1 [2] and the A-series according to DIN 6818-1 [3]: first and second half-value layers (1st HVL, 2nd HVL) in mm with the absorber materials Al and Cu, mean photon energies $\overline{E}_{ph}$ in keV, 10 % percentiles in keV, kerma factors $k_{\Phi}(R)$ in pGy·cm², conversion coefficients $h_{pK}(0{,}07;R)$ from air kerma, K_a, to the personal dose equivalent, $H_p(0{,}07)$, for the rod phantom and conversion coefficients $h_K^*(10;R)$ from air kerma, K_a, to the ambient dose equivalent, $H^*(10)$, for the ICRU sphere. The $h_{pK}(0{,}07;R)$ values are valid for all angles of incidence $\alpha \leq 60°$ (see Section 3.6.2). The $h_K^*(10;R)$ values are given for an expanded and aligned radiation field. The reference distance is 1,0 m.

Radiation quality		1st HVL in mm		2nd HVL in mm		$\overline{E}_{ph}$	10 % percentile	$k_{\Phi}(R)$	$h_{pK}(0{,}07;R,\alpha)$	$h_K^*(10;R)$
ISO	DIN	Al	Cu	Al	Cu	in keV	in keV	in pGy·cm²	in Sv/Gy	in Sv/Gy
	A 7,5	0,0268	0,00797	0,0284	0,00842	6,6	5,6	18,60	0,861	$<1\cdot10^{-4}$
N-10	A 10	0,0548	0,00846	0,0596	0,0124	8,5	7,0	11,07	0,922	0,00110
N-15	A 15	0,157	0,00580	0,177	0,00636	12,4	9,8	5,11	0,959	0,0872
N-20	A 20	0,344	0,0113	0,396	0,0126	16,3	12,4	2,87	0,983	0,307
N-25		0,662	0,0206	0,746	0,0230	20,3	15,8	1,78	1,01	0,566
N-30	A 30	1,16	0,0357	1,28	0,0394	24,6	19,6	1,18	1,03	0,810
N-40	A 40	2,63	0,0850	2,83	0,0927	33,3	27,0	0,638	1,07	1,19
N-60	A 60	5,85	0,234	6,21	0,263	47,9	37,5	0,365	1,11	1,59
N-80	A 80	9,90	0,578	10,08	0,622	65,2	54,5	0,302	1,15	1,74
N-100	A 100	12,96	1,09	13,06	1,15	83,3	70,5	0,325	1,16	1,71
N-120	A 120	14,98	1,67	15,04	1,73	100,4	87,0	0,380	1,17	1,65
N-150	A 150	16,49	2,30	16,56	2,41	118,2	99,0	0,456	1,16	1,58
N-200	A 200	19,40	3,92	19,45	3,99	164,8	143,0	0,676	1,16	1,46
N-250	A 250	21,36	5,10	21,40	5,14	207,3	181,0	0,893	1,15	1,39
N-300	A 300	22,94	5,96	22,98	6,00	248,4	216,0	1,11	1,14	1,35

Verfügbar unter: https://doi.org/10.7795/110.20190315B

Verfügbar unter: https://doi.org/10.7795/110.20190315B

Table 4.5: Conversion coefficients $h_{pK}(10;\mathrm{R},\alpha)$ in Sv/Gy from air kerma, K_a, to the personal dose equivalent, $H_p(10)$, for the slab phantom and the radiation qualities of the narrow-spectrum series (N) specified in ISO 4037-1 [2] and the A-series according to DIN 6818-1 [3]; the reference distance is 1,0 m.

Radiation quality		$h_{pK}(10;\mathrm{R},\alpha)$ in Sv/Gy for angles of incidence α of					
ISO	DIN	0°	15°	30°	45°	60°	75°
	A 7,5	$<1\cdot10^{-4}$	$<1\cdot10^{-4}$	$<1\cdot10^{-4}$	$<1\cdot10^{-4}$	$<1\cdot10^{-4}$	$<1\cdot10^{-4}$
N-10	A 10	0,00127	0,00109	0,000605	0,000193		
N-15	A 15	0,0883	0,0832	0,0653	0,0392	0,0130	0,000756
N-20	A 20	0,316	0,306	0,270	0,206	0,114	0,0237
N-25		0,574	0,562	0,521	0,436	0,298	0,103
N-30	A 30	0,815	0,800	0,761	0,668	0,512	0,239
N-40	A 40	1,21	1,19	1,15	1,06	0,880	0,527
N-60	A 60	1,66	1,64	1,60	1,49	1,29	0,861
N-80	A 80	1,89	1,87	1,83	1,72	1,51	1,07
N-100	A 100	1,88	1,87	1,82	1,73	1,53	1,12
N-120	A 120	1,80	1,79	1,75	1,67	1,51	1,11
N-150	A 150	1,72	1,71	1,68	1,61	1,46	1,10
N-200	A 200	1,56	1,56	1,54	1,49	1,38	1,08
N-250	A 250	1,48	1,47	1,46	1,42	1,33	1,08
N-300	A 300	1,42	1,42	1,41	1,38	1,30	1,07

Table 4.6: Conversion coefficients $h'_K(0{,}07;\mathrm{R},\alpha)$ in Sv/Gy from air kerma, K_a, to the directional dose equivalent, $H'(0{,}07,\vec{\Omega})$, for the ICRU sphere and the radiation qualities of the narrow-spectrum series (N) specified in ISO 4037-1 [2] and the A-series according to DIN 6818-1 [3] (expanded radiation field); the reference distance is 1,0 m.

Radiation quality		$h'_K(0{,}07;\mathrm{R},\alpha)$ in Sv/Gy for angles of incidence α of							
ISO	DIN	0°	15°	30°	45°	60°	75°	90°	180°
	A 7,5	0,814	0,790	0,739	0,696	0,486	0,267	0,00180	$<1\cdot10^{-4}$
N-10	A 10	0,885	0,868	0,839	0,818	0,706	0,566	0,0532	
N-15	A 15	0,967	0,959	0,948	0,948	0,929	0,867	0,250	
N-20	A 20	1,01	1,00	0,993	0,993	0,987	0,945	0,396	
N-25		1,05	1,05	1,04	1,04	1,04	1,01	0,532	
N-30	A 30	1,12	1,11	1,11	1,11	1,11	1,07	0,635	0,00020
N-40	A 40	1,26	1,24	1,24	1,24	1,23	1,18	0,790	0,00510
N-60	A 60	1,46	1,45	1,43	1,43	1,42	1,35	0,991	0,0251
N-80	A 80	1,53	1,52	1,51	1,51	1,49	1,42	1,10	0,0447
N-100	A 100	1,54	1,53	1,52	1,52	1,51	1,44	1,15	0,0623
N-120	A 120	1,54	1,52	1,52	1,52	1,51	1,45	1,19	0,0764
N-150	A 150	1,49	1,48	1,48	1,48	1,47	1,42	1,21	0,0861
N-200	A 200	1,41	1,40	1,40	1,40	1,40	1,37	1,22	0,103
N-250	A 250	1,38	1,37	1,37	1,37	1,37	1,35	1,21	0,112
N-300	A 300	1,35	1,34	1,34	1,34	1,35	1,33	1,19	0,121

4.1.2.3 ISO wide-spectrum series and DIN B-series

Table 4.7: Data for the radiation qualities of the wide-spectrum series (W) specified in ISO 4037-1 [2] and the B-series according to DIN 6818-1 [3]: first and second half-value layers (1st HVL, 2nd HVL) in mm with the absorber materials Al and Cu, mean photon energies $\overline{E}_{\mathrm{ph}}$ in keV, 10 % percentiles in keV, kerma factors $k_{\Phi}(\mathrm{R})$ in $\mathrm{pGy \cdot cm^2}$, conversion coefficients $h_{\mathrm{p}K}(0{,}07;\mathrm{R})$ from air kerma, K_{a}, to the personal dose equivalent, $H_{\mathrm{p}}(0{,}07)$, for the rod phantom and conversion coefficients $h_K^*(10;\mathrm{R})$ from air kerma, K_{a}, to the ambient dose equivalent, $H^*(10)$, for the ICRU sphere. The $h_{\mathrm{p}K}(0{,}07;\mathrm{R})$ values are valid for all angles of incidence $\alpha \leq 60°$ (see Section 3.6.2). The $h_K^*(10;\mathrm{R})$ values are given for an expanded and aligned radiation field. The reference distance is 1,0 m.

Radiation quality		1st HVL in mm		2nd HVL in mm		$\overline{E}_{\mathrm{ph}}$	10 % percentile	$k_{\Phi}(\mathrm{R})$	$h_{\mathrm{p}K}(0{,}07;\mathrm{R},\alpha)$	$h_K^*(10;\mathrm{R})$
ISO	DIN	Al	Cu	Al	Cu	in keV	in keV	in $\mathrm{pGy \cdot cm^2}$	in Sv/Gy	in Sv/Gy
	B 7,5	0,0268	0,00797	0,0284	0,00842	6,6	5,6	18,60	0,861	$<1 \cdot 10^{-4}$
	B 10	0,0548	0,00846	0,0596	0,0124	8,5	7,0	11,07	0,922	0,00110
	B 15	0,157	0,00580	0,177	0,00636	12,4	9,8	5,11	0,959	0,0872
	B 20	0,344	0,0113	0,396	0,0126	16,3	12,4	2,87	0,983	0,307
	B 30	0,863	0,0268	1,02	0,0315	22,9	16,8	1,42	1,02	0,687
	B 40	1,72	0,0539	2,03	0,0649	29,8	21,2	0,838	1,05	0,998
W-60	B 60	4,80	0,180	5,34	0,215	44,8	32,5	0,410	1,10	1,50
W-80	B 80	7,42	0,349	8,10	0,433	56,5	40,0	0,332	1,13	1,66
W-110	B 110	12,11	0,933	12,42	1,08	79,1	59,5	0,323	1,16	1,71
W-150	B 150	15,10	1,78	15,45	2,03	104,2	79,0	0,405	1,16	1,62
W-200	B 200	17,88	3,00	18,03	3,24	137,5	107,0	0,547	1,16	1,52
W-250	B 250	19,86	4,14	19,97	4,34	172,3	135,0	0,716	1,15	1,44
W-300	B 300	21,38	5,03	21,47	5,18	205,4	161,0	0,885	1,15	1,39

Table 4.8: Conversion coefficients $h_{pK}(10;\mathrm{R},\alpha)$ in Sv/Gy from air kerma, K_a, to the personal dose equivalent, $H_p(10)$, for the slab phantom and the radiation qualities of the wide-spectrum series (W) specified in ISO 4037-1 [2] and the B-series according to DIN 6818-1 [3]; the reference distance is 1,0 m.

Radiation quality		$h_{pK}(10;\mathrm{R},\alpha)$ in Sv/Gy for angles of incidence α of					
ISO	DIN	0°	15°	30°	45°	60°	75°
	B 7,5	$<1\cdot10^{-4}$	$<1\cdot10^{-4}$	$<1\cdot10^{-4}$	$<1\cdot10^{-4}$	$<1\cdot10^{-4}$	$<1\cdot10^{-4}$
	B 10	0,00127	0,00109	0,000605	0,000193		
	B 15	0,0883	0,0832	0,0653	0,0392	0,0130	0,000756
	B 20	0,316	0,306	0,270	0,206	0,114	0,0237
	B 30	0,693	0,679	0,640	0,551	0,404	0,172
	B 40	1,01	0,990	0,951	0,860	0,693	0,380
W-60	B 60	1,55	1,53	1,49	1,38	1,19	0,778
W-80	B 80	1,77	1,75	1,71	1,60	1,39	0,960
W-110	B 110	1,87	1,86	1,82	1,72	1,52	1,10
W-150	B 150	1,77	1,76	1,72	1,64	1,48	1,10
W-200	B 200	1,64	1,63	1,61	1,55	1,42	1,09
W-250	B 250	1,54	1,54	1,52	1,47	1,37	1,08
W-300	B 300	1,48	1,47	1,46	1,42	1,33	1,08

Table 4.9: Conversion coefficients $h'_K(0{,}07;\mathrm{R},\alpha)$ in Sv/Gy from air kerma, K_a, to the directional dose equivalent, $H'(0{,}07,\vec{\Omega})$, for the ICRU sphere and the radiation qualities of the wide-spectrum series (W) specified in ISO 4037-1 [2] and the B-series according to DIN 6818-1 [3] (expanded radiation field); the reference distance is 1,0 m.

Radiation quality		$h'_K(0{,}07;\mathrm{R},\alpha)$ in Sv/Gy for angles of incidence α of							
ISO	DIN	0°	15°	30°	45°	60°	75°	90°	180°
	B 7,5	0,814	0,790	0,739	0,696	0,486	0,267	0,00180	$<1\cdot10^{-4}$
	B 10	0,885	0,868	0,839	0,818	0,706	0,566	0,0532	
	B 15	0,967	0,959	0,948	0,948	0,929	0,867	0,250	
	B 20	1,01	1,00	0,993	0,993	0,987	0,945	0,396	
	B 30	1,08	1,08	1,07	1,07	1,07	1,04	0,582	0,000102
	B 40	1,18	1,18	1,17	1,17	1,17	1,12	0,711	0,00228
W-60	B 60	1,41	1,40	1,39	1,39	1,37	1,31	0,941	0,0197
W-80	B 80	1,49	1,48	1,47	1,47	1,45	1,38	1,04	0,0340
W-110	B 110	1,54	1,53	1,52	1,52	1,50	1,44	1,14	0,0587
W-150	B 150	1,51	1,50	1,49	1,49	1,48	1,43	1,19	0,0781
W-200	B 200	1,45	1,44	1,44	1,44	1,43	1,39	1,22	0,0945
W-250	B 250	1,40	1,39	1,39	1,39	1,39	1,37	1,22	0,105
W-300	B 300	1,37	1,37	1,37	1,37	1,38	1,35	1,20	0,113

4.1.2.4 ISO high air-kerma rate series and DIN C-series

Table 4.10: Data for the radiation qualities of the high air-kerma rate series (H) specified in ISO 4037-1 [2] and the C-series according to DIN 6818-1 [3]: first and second half-value layers (1st HVL, 2nd HVL) in mm with the absorber materials Al and Cu, mean photon energies $\overline{E}_{\mathrm{ph}}$ in keV, 10 % percentiles in keV, kerma factors $k_{\Phi}(\mathrm{R})$ in pGy·cm², conversion coefficients $h_{\mathrm{p}K}(0{,}07;\mathrm{R})$ from air kerma, K_{a}, to the personal dose equivalent, $H_{\mathrm{p}}(0{,}07)$, for the rod phantom and conversion coefficients $h_K^*(10;\mathrm{R})$ from air kerma, K_{a}, to the ambient dose equivalent, $H^*(10)$, for the ICRU sphere. The $h_{\mathrm{p}K}(0{,}07;\mathrm{R})$ values are valid for all angles of incidence $\alpha \le 60°$ (see Section 3.6.2). The $h_K^*(10;\mathrm{R})$ values are given for an expanded and aligned radiation field. The reference distance is 1,0 m.

Radiation quality		1st HVL in mm		2nd HVL in mm		$\overline{E}_{\mathrm{ph}}$	10 % percentile	$k_{\Phi}(\mathrm{R})$	$h_{\mathrm{p}K}(0{,}07;\mathrm{R},\alpha)$	$h_K^*(10;\mathrm{R})$
ISO	DIN	Al	Cu	Al	Cu	in keV	in keV	in pGy·cm²	in Sv/Gy	in Sv/Gy
	C 7,5	0,0268	0,00797	0,0284	0,00842	6,6	5,6	18,60	0,861	$<1\cdot 10^{-4}$
H-10	C 10	0,0439	0,00907	0,0499	0,0117	8,0	6,2	12,7	0,905	0,000646
H-20	C 20	0,128	0,00655	0,172	0,00853	13,1	8,4	5,23	0,954	0,0972
H-30	C 30	0,364	0,0123	0,563	0,0175	19,5	10,2	2,33	0,988	0,383
	C 40	0,815	0,0256	1,17	0,0363	25,4	14,8	1,32	1,02	0,684
H-60	C 60	2,53	0,0839	3,38	0,121	38,0	22,5	0,595	1,07	1,19
	C 80	4,59	0,176	5,87	0,268	48,8	28,5	0,418	1,10	1,46
H-100	C 100	6,43	0,294	7,95	0,462	57,3	33,0	0,364	1,12	1,57
	C 150	11,07	0,808	12,16	1,21	78,0	50,0	0,347	1,15	1,67
H-200	C 200	14,19	1,54	15,11	2,28	99,3	59,0	0,408	1,16	1,61
H-250	C 250	16,55	2,42	17,28	3,24	121,5	71,0	0,495	1,16	1,54
H-280		18,38	3,26	18,83	3,88	144,6	98,0	0,592	1,16	1,49
H-300	C 300	18,29	3,22	18,88	4,00	143,2	92,0	0,590	1,15	1,49

Table 4.11: Conversion coefficients $h_{pK}(10;\mathrm{R},\alpha)$ in Sv/Gy from air kerma, K_a, to the personal dose equivalent, $H_p(10)$, for the slab phantom and the radiation qualities of the high air-kerma rate series (H) specified in ISO 4037-1 [2] and the C-series according to DIN 6818-1 [3]; the reference distance is 1,0 m.

Radiation quality		$h_{pK}(10;\mathrm{R},\alpha)$ in Sv/Gy for angles of incidence α of					
ISO	DIN	0°	15°	30°	45°	60°	75°
	C 7,5	<1·10^-4	<1·10^-4	<1·10^-4	<1·10^-4	<1·10^-4	<1·10^-4
H-10	C 10	0,000726	0,000620	0,000341	0,000107		
H-20	C 20	0,0995	0,0953	0,0806	0,0568	0,0277	0,00486
H-30	C 30	0,389	0,379	0,347	0,285	0,190	0,0684
	C 40	0,692	0,678	0,640	0,556	0,417	0,196
H-60	C 60	1,22	1,20	1,16	1,06	0,887	0,539
	C 80	1,52	1,50	1,46	1,36	1,16	0,768
H-100	C 100	1,67	1,65	1,61	1,51	1,31	0,896
	C 150	1,81	1,79	1,76	1,66	1,47	1,06
H-200	C 200	1,75	1,74	1,71	1,62	1,46	1,09
H-250	C 250	1,67	1,66	1,64	1,57	1,43	1,09
H-280		1,60	1,60	1,58	1,52	1,40	1,09
H-300	C 300	1,60	1,59	1,58	1,52	1,40	1,09

Table 4.12: Conversion coefficients $h'_K(0{,}07;\mathrm{R},\alpha)$ in Sv/Gy from air kerma, K_a, to the directional dose equivalent, $H'(0{,}07,\vec{\Omega})$, for the ICRU sphere and the radiation qualities of the high air-kerma rate series (H) specified in ISO 4037-1 [2] and the C-series according to DIN 6818-1 [3] (expanded radiation field); the reference distance is 1,0 m.

Radiation quality		$h'_K(0{,}07;\mathrm{R},\alpha)$ in Sv/Gy for angles of incidence α of							
ISO	DIN	0°	15°	30°	45°	60°	75°	90°	180°
	C 7,5	0,814	0,790	0,739	0,696	0,486	0,267	0,00180	<1·10^-4
H-10	C 10	0,863	0,844	0,808	0,781	0,639	0,475	0,0341	
H-20	C 20	0,953	0,944	0,929	0,926	0,889	0,813	0,221	
H-30	C 30	1,02	1,01	1,00	1,00	0,996	0,951	0,420	
	C 40	1,09	1,09	1,08	1,08	1,08	1,04	0,573	0,000732
H-60	C 60	1,27	1,26	1,25	1,25	1,24	1,19	0,797	0,00901
	C 80	1,39	1,38	1,37	1,37	1,36	1,30	0,928	0,0212
H-100	C 100	1,46	1,44	1,43	1,43	1,42	1,35	1,00	0,0318
	C 150	1,52	1,50	1,50	1,50	1,48	1,42	1,12	0,0570
H-200	C 200	1,49	1,48	1,48	1,48	1,47	1,41	1,17	0,0751
H-250	C 250	1,46	1,45	1,45	1,45	1,44	1,40	1,20	0,0882
H-280		1,43	1,42	1,42	1,42	1,42	1,38	1,21	0,0978
H-300	C 300	1,43	1,42	1,42	1,42	1,42	1,38	1,20	0,0977

Verfügbar unter: https://doi.org/10.7795/110.20190315B

4.1.2.5 Unfiltered X-ray spectra

Table 4.13: Data for unfiltered X-ray spectra: first and second half-value layers (1st HVL, 2nd HVL) in mm with the absorber materials Al and Cu, mean photon energies $\overline{E}_{\mathrm{ph}}$ in keV, 10 % percentiles in keV, kerma factors $k_{\Phi}(\mathrm{R})$ in pGy·cm², conversion coefficients $h_{\mathrm{p}K}(0,07;\mathrm{R})$ from air kerma, K_{a}, to the personal dose equivalent, $H_{\mathrm{p}}(0,07)$, for the rod phantom and conversion coefficients $h_K^*(10;\mathrm{R})$ from air kerma, K_{a}, to the ambient dose equivalent, $H^*(10)$, for the ICRU sphere. The $h_{\mathrm{p}K}(0,07;\mathrm{R})$ values are valid for all angles of incidence $\alpha \leq 60°$ (see Section 3.6.2). The $h_K^*(10;\mathrm{R})$ values are given for an expanded and aligned radiation field. The reference distance is 1,0 m

Unfiltered X-ray spectra tube voltage in kV	1st HVL in mm		2nd HVL in mm		$\overline{E}_{\mathrm{ph}}$	10 % percentile	$k_{\Phi}(\mathrm{R})$	$h_{\mathrm{p}K}(0,07;\mathrm{R},\alpha)$	$h_K^*(10;\mathrm{R})$
	Al	Cu	Al	Cu	in keV	in keV	in pGy·cm²	in Sv/Gy	in Sv/Gy
7,5	0,0268	0,00797	0,0284	0,00842	6,6	5,6	18,60	0,861	$<1\cdot10^{-4}$
10	0,0439	0,00907	0,0499	0,0117	8,0	6,2	12,7	0,905	0,000646
15	0,0727	0,00697	0,0895	0,00956	10,1	7,0	8,38	0,933	0,0203
20	0,0846	0,00716	0,109	0,00997	11,5	7,6	7,05	0,940	0,0459
25	0,0904	0,00737	0,121	0,0106	12,7	7,8	6,30	0,943	0,0661
30	0,0937	0,00753	0,128	0,0112	13,9	8,0	5,77	0,946	0,0814
35	0,0959	0,00763	0,134	0,0116	15,1	8,2	5,37	0,947	0,0935
40	0,0975	0,00772	0,139	0,0120	16,2	8,2	5,04	0,949	0,104
50	0,103	0,00786	0,153	0,0127	18,8	8,4	4,40	0,953	0,126
55	0,102	0,00788	0,151	0,0129	19,9	8,4	4,25	0,953	0,131
60	0,103	0,00777	0,155	0,0130	21,2	8,5	4,04	0,954	0,139
70	0,106	0,00787	0,165	0,0137	23,7	8,5	3,66	0,956	0,156
80	0,109	0,00800	0,175	0,0144	26,4	8,5	3,33	0,958	0,173
90	0,114	0,00817	0,197	0,0154	29,5	8,5	2,97	0,960	0,197
100	0,115	0,00833	0,205	0,0162	32,2	8,5	2,74	0,963	0,214
110	0,119	0,00853	0,225	0,0173	34,9	8,5	2,50	0,965	0,235
120	0,123	0,00879	0,249	0,0187	37,6	8,5	2,30	0,969	0,256

Table 4.14: Conversion coefficients $h_{pK}(10;\mathrm{R},\alpha)$ in Sv/Gy from air kerma, K_a, to the personal dose equivalent, $H_p(10)$, for the slab phantom and unfiltered X-ray spectra; the reference distance is 1,0 m.

Unfiltered X-ray spectra tube voltage in kV	$h_{pK}(10;\mathrm{R},\alpha)$ in Sv/Gy for angles of incidence α of					
	0°	15°	30°	45°	60°	75°
7,5	$<1\cdot10^{-4}$	$<1\cdot10^{-4}$	$<1\cdot10^{-4}$	$<1\cdot10^{-4}$	$<1\cdot10^{-4}$	$<1\cdot10^{-4}$
10	0,000726	0,000620	0,000341	0,000107		
15	0,0205	0,0190	0,0144	0,00810	0,00234	0,000118
20	0,0469	0,0447	0,0371	0,0254	0,0118	0,00198
25	0,0673	0,0648	0,0560	0,0416	0,0232	0,00598
30	0,0827	0,0800	0,0707	0,0548	0,0336	0,0109
35	0,0950	0,0920	0,0825	0,0656	0,0425	0,0157
40	0,105	0,102	0,0924	0,0749	0,0503	0,0202
50	0,128	0,124	0,114	0,0947	0,0668	0,0299
55	0,133	0,130	0,119	0,100	0,0717	0,0333
60	0,141	0,138	0,127	0,108	0,0782	0,0374
70	0,159	0,155	0,144	0,124	0,0919	0,0462
80	0,177	0,173	0,162	0,140	0,106	0,0555
90	0,202	0,198	0,186	0,162	0,125	0,0679
100	0,220	0,215	0,203	0,179	0,140	0,0781
110	0,242	0,238	0,225	0,199	0,158	0,0903
120	0,265	0,260	0,248	0,220	0,176	0,103

Verfügbar unter: https://doi.org/10.7795/110.20190315B

Table 4.15: Conversion coefficients $h'_K(0{,}07;\mathrm{R},\alpha)$ in Sv/Gy from air kerma, K_a, to the directional dose equivalent, $H'(0{,}07,\vec{\Omega})$, for the ICRU sphere and unfiltered X-ray spectra (expanded radiation field); the reference distance is 1,0 m.

Unfiltered X-ray spectra tube voltage in kV	$h'_K(0{,}07;\mathrm{R},\alpha)$ in Sv/Gy for angles of incidence α of							
	0°	15°	30°	45°	60°	75°	90°	180°
7,5	0,814	0,790	0,739	0,696	0,486	0,267	0,00180	$<1\cdot10^{-4}$
10	0,863	0,844	0,808	0,781	0,639	0,475	0,0341	
15	0,911	0,897	0,874	0,861	0,781	0,668	0,115	
20	0,924	0,911	0,891	0,880	0,813	0,711	0,145	
25	0,930	0,918	0,898	0,889	0,827	0,729	0,162	
30	0,935	0,923	0,904	0,895	0,835	0,740	0,172	
35	0,938	0,927	0,908	0,900	0,841	0,747	0,179	
40	0,941	0,930	0,911	0,903	0,846	0,753	0,185	
50	0,950	0,938	0,921	0,914	0,859	0,769	0,200	0,000191
55	0,950	0,939	0,921	0,914	0,859	0,768	0,201	0,000268
60	0,953	0,942	0,924	0,917	0,863	0,773	0,206	0,000360
70	0,959	0,948	0,931	0,924	0,871	0,782	0,216	0,000573
80	0,965	0,954	0,937	0,930	0,878	0,790	0,226	0,000845
90	0,973	0,962	0,945	0,938	0,888	0,801	0,240	0,00122
100	0,979	0,968	0,951	0,945	0,895	0,809	0,249	0,00160
110	0,986	0,975	0,959	0,952	0,904	0,818	0,262	0,00208
120	0,994	0,983	0,967	0,961	0,914	0,829	0,275	0,00261

4.1.3 Data for a reference distance of 2,5 m

4.1.3.1 ISO low air-kerma rate series

Table 4.16: Data for the radiation qualities of the low air-kerma rate series (L) specified in ISO 4037-1 [2]: first and second half-value layers (1st HVL, 2nd HVL) in mm with the absorber materials Al and Cu, mean photon energies $\overline{E}_{ph}$ in keV, 10 % percentiles in keV, kerma factors k_{Φ}(R) in pGy·cm^2, conversion coefficients h_{pK}(0,07;R) from air kerma, K_a, to the personal dose equivalent, H_p(0,07), for the rod phantom and conversion coefficients $h_K^*(10;\mathrm{R})$ from air kerma, K_a, to the ambient dose equivalent, H^*(10), for the ICRU sphere. The h_{pK}(0,07;R) values are valid for all angles of incidence $\alpha \leq 60°$ (see Section 3.6.2). The $h_K^*(10;\mathrm{R})$ values are given for an expanded and aligned radiation field. The reference distance is 2,5 m.

Radiation quality	1st HVL in mm		2nd HVL in mm		$\overline{E}_{ph}$	10 % percentile	k_{Φ}(R)	$h_{pK}(0{,}07;\mathrm{R},\alpha)$	$h_K^*(10;\mathrm{R})$
	Al	Cu	Al	Cu	in keV	in keV	in pGy·cm^2	in Sv/Gy	in Sv/Gy
L-10	0,0732	0,00488	0,0755	0,00720	9,2	8,2	9,23	0,939	0,00267
L-20	0,446	0,0144	0,489	0,0154	17,4	14,6	2,43	0,992	0,396
L-30	1,56	0,0483	1,63	0,0504	26,7	23,2	0,965	1,04	0,938
L-35	2,18	0,0689	2,30	0,0728	30,5	25,8	0,744	1,06	1,10
L-55	6,15	0,249	6,30	0,261	47,8	41,2	0,356	1,11	1,62
L-70	9,11	0,484	9,22	0,506	60,6	52,5	0,301	1,14	1,73
L-100	13,49	1,22	13,55	1,26	86,9	76,5	0,333	1,16	1,70
L-125	15,79	1,98	15,82	2,02	109,5	98,0	0,416	1,17	1,61
L-170	18,51	3,40	18,56	3,47	148,6	134,0	0,596	1,16	1,49
L-210	20,33	4,50	20,35	4,55	184,2	167,0	0,775	1,15	1,42
L-240	21,49	5,18	21,51	5,21	211,1	192,0	0,913	1,15	1,38

Verfügbar unter: https://doi.org/10.7795/110.20190315B

Table 4.17: Conversion coefficients $h_{pK}(10;\mathrm{R},\alpha)$ in Sv/Gy from air kerma, K_a, to the personal dose equivalent, $H_p(10)$, for the slab phantom and the radiation qualities of the low air-kerma rate series (L) specified in ISO 4037-1 [2]; the reference distance is 2,5 m.

Radiation quality	$h_{pK}(10;\mathrm{L},\alpha)$ in Sv/Gy for angles of incidence α of					
	0°	15°	30°	45°	60°	75°
L-10	0,00300	0,002604	0,00150	0,000510	$<1\cdot10^{-4}$	$<1\cdot10^{-4}$
L-20	0,407	0,396	0,356	0,281	0,167	0,0390
L-30	0,944	0,927	0,889	0,797	0,634	0,328
L-35	1,11	1,09	1,05	0,959	0,789	0,452
L-55	1,69	1,67	1,63	1,51	1,31	0,878
L-70	1,88	1,85	1,82	1,70	1,49	1,05
L-100	1,87	1,86	1,81	1,72	1,53	1,13
L-125	1,76	1,75	1,72	1,64	1,49	1,10
L-170	1,61	1,60	1,58	1,52	1,40	1,09
L-210	1,52	1,52	1,50	1,45	1,36	1,08
L-240	1,47	1,47	1,46	1,42	1,33	1,08

Table 4.18: Conversion coefficients $h'_K(0{,}07;\mathrm{R},\alpha)$ in Sv/Gy from air kerma, K_a, to the directional dose equivalent, $H'(0{,}07,\vec{\Omega})$, for the ICRU sphere and the radiation qualities of the low air-kerma rate series (L) specified in ISO 4037-1 [2] (expanded radiation field); the reference distance is 2,5 m.

Radiation quality	$h'_K(0{,}07;\mathrm{R},\alpha)$ in Sv/Gy for angles of incidence α of							
	0°	15°	30°	45°	60°	75°	90°	180°
L-10	0,915	0,902	0,882	0,871	0,802	0,697	0,0972	$<1\cdot10^{-4}$
L-20	1,02	1,02	1,00	1,00	1,00	0,968	0,447	
L-30	1,16	1,15	1,15	1,15	1,14	1,10	0,686	0,000468
L-35	1,22	1,21	1,20	1,20	1,19	1,15	0,750	0,00240
L-55	1,48	1,46	1,45	1,45	1,44	1,37	1,01	0,0263
L-70	1,53	1,52	1,51	1,51	1,49	1,42	1,08	0,0404
L-100	1,54	1,53	1,53	1,53	1,51	1,44	1,16	0,0656
L-125	1,52	1,51	1,51	1,51	1,49	1,44	1,20	0,0816
L-170	1,43	1,41	1,41	1,41	1,41	1,38	1,23	0,0983
L-210	1,39	1,38	1,38	1,38	1,38	1,36	1,22	0,107
L-240	1,37	1,37	1,37	1,37	1,37	1,35	1,21	0,113

4.1.3.2 ISO narrow-spectrum series and DIN A-series

Table 4.19: Data for the radiation qualities of the narrow-spectrum series (N) specified in ISO 4037-1 [2] and the A-series according to DIN 6818-1 [3]: first and second half-value layers (1st HVL, 2nd HVL) in mm with the absorber materials Al and Cu, mean photon energies $\overline{E}_{\mathrm{ph}}$ in keV, 10 % percentiles in keV, kerma factors $k_{\Phi}(\mathrm{R})$ in pGy · cm², conversion coefficients $h_{\mathrm{p}K}(0{,}07;\mathrm{R})$ from air kerma, K_{a}, to the personal dose equivalent, $H_{\mathrm{p}}(0{,}07)$, for the rod phantom and conversion coefficients $h_K^*(10;\mathrm{R})$ from air kerma, K_{a}, to the ambient dose equivalent, $H^*(10)$, for the ICRU sphere. The $h_{\mathrm{p}K}(0{,}07;\mathrm{R})$ values are valid for all angles of incidence $\alpha \leq 60°$ (see Section 3.6.2). The $h_K^*(10;\mathrm{R})$ values are given for an expanded and aligned radiation field. The reference distance is 2,5 m.

Radiation quality		1st HVL in mm		2nd HVL in mm		$\overline{E}_{\mathrm{ph}}$	10 % percentile	$k_{\Phi}(\mathrm{R})$	$h_{\mathrm{p}K}(0{,}07;\mathrm{R},\alpha)$	$h_K^*(10;\mathrm{R})$
ISO	DIN	Al	Cu	Al	Cu	in keV	in keV	in pGy · cm²	in Sv/Gy	in Sv/Gy
	A 7,5	0,0324	0,00955	0,0334	0,00982	6,9	6,2	16,51	0,883	$<1\cdot10^{-4}$
N-10	A 10	0,0647	0,00662	0,0680	0,0110	8,9	7,6	9,99	0,933	0,00180
N-15	A 15	0,173	0,00613	0,191	0,00662	12,7	10,0	4,81	0,961	0,102
N-20	A 20	0,362	0,0119	0,412	0,0131	16,5	12,8	2,78	0,985	0,323
N-25		0,677	0,0211	0,760	0,0235	20,4	16,0	1,75	1,01	0,576
N-30	A 30	1,17	0,0361	1,29	0,0398	24,7	19,6	1,17	1,03	0,814
N-40	A 40	2,65	0,0856	2,84	0,0932	33,3	27,0	0,635	1,07	1,20
N-60	A 60	5,87	0,235	6,22	0,264	47,9	37,5	0,365	1,11	1,59
N-80	A 80	9,92	0,580	10,09	0,623	65,3	54,5	0,302	1,15	1,74
N-100	A 100	12,97	1,09	13,07	1,15	83,3	70,5	0,325	1,16	1,71
N-120	A 120	14,99	1,67	15,04	1,74	100,4	87,0	0,380	1,17	1,65
N-150	A 150	16,49	2,30	16,57	2,41	118,4	99,0	0,457	1,16	1,58
N-200	A 200	19,40	3,91	19,43	3,99	164,6	142,0	0,675	1,16	1,46
N-250	A 250	21,35	5,08	21,39	5,14	207,3	180,0	0,893	1,15	1,39
N-300	A 300	22,92	5,94	22,96	5,99	247,5	216,0	1,10	1,14	1,35

Table 4.20: Conversion coefficients $h_{pK}(10;\mathrm{R},\alpha)$ in Sv/Gy from air kerma, K_a, to the personal dose equivalent, $H_p(10)$, for the slab phantom and the radiation qualities of the narrow-spectrum series (N) specified in ISO 4037-1 [2] and the A-series according to DIN 6818-1 [3]; the reference distance is 2,5 m.

Radiation quality		$h_{pK}(10;\mathrm{R},\alpha)$ in Sv/Gy for angles of incidence α of					
ISO	DIN	0°	15°	30°	45°	60°	75°
	A 7,5	$<1\cdot10^{-4}$	$<1\cdot10^{-4}$	$<1\cdot10^{-4}$	$<1\cdot10^{-4}$	$<1\cdot10^{-4}$	$<1\cdot10^{-4}$
N-10	A 10	0,00202	0,00174	0,000985	0,000324		
N-15	A 15	0,104	0,0977	0,0773	0,0469	0,0160	0,000967
N-20	A 20	0,333	0,323	0,286	0,219	0,123	0,0261
N-25		0,583	0,571	0,531	0,444	0,305	0,107
N-30	A 30	0,819	0,804	0,765	0,673	0,516	0,243
N-40	A 40	1,21	1,19	1,15	1,06	0,883	0,530
N-60	A 60	1,66	1,64	1,60	1,49	1,29	0,862
N-80	A 80	1,89	1,87	1,83	1,72	1,51	1,07
N-100	A 100	1,88	1,87	1,82	1,73	1,53	1,12
N-120	A 120	1,80	1,79	1,75	1,67	1,51	1,11
N-150	A 150	1,72	1,71	1,68	1,61	1,46	1,10
N-200	A 200	1,56	1,56	1,54	1,49	1,38	1,08
N-250	A 250	1,48	1,47	1,46	1,42	1,33	1,08
N-300	A 300	1,42	1,42	1,41	1,38	1,30	1,07

Table 4.21: Conversion coefficients $h'_K(0{,}07;\mathrm{R},\alpha)$ in Sv/Gy from air kerma, K_a, to the directional dose equivalent, $H'(0{,}07,\vec{\Omega})$, for the ICRU sphere and the radiation qualities of the narrow-spectrum series (N) specified in ISO 4037-1 [2] and the A-series according to DIN 6818-1 [3] (expanded radiation field); the reference distance is 2,5 m.

Radiation quality		$h'_K(0{,}07;\mathrm{R},\alpha)$ in Sv/Gy for angles of incidence α of							
ISO	DIN	0°	15°	30°	45°	60°	75°	90°	180°
	A 7,5	0,830	0,808	0,761	0,723	0,535	0,334	0,00340	$<1\cdot10^{-4}$
N-10	A 10	0,902	0,887	0,863	0,847	0,760	0,639	0,0747	
N-15	A 15	0,972	0,964	0,955	0,955	0,939	0,881	0,267	
N-20	A 20	1,01	1,00	0,993	0,993	0,990	0,949	0,406	
N-25		1,05	1,05	1,05	1,05	1,05	1,02	0,536	
N-30	A 30	1,12	1,11	1,11	1,11	1,11	1,07	0,637	0,000207
N-40	A 40	1,26	1,25	1,24	1,24	1,23	1,18	0,791	0,00518
N-60	A 60	1,46	1,45	1,43	1,43	1,42	1,35	0,992	0,0252
N-80	A 80	1,53	1,52	1,51	1,51	1,49	1,42	1,10	0,0448
N-100	A 100	1,54	1,53	1,52	1,52	1,51	1,44	1,15	0,0624
N-120	A 120	1,54	1,52	1,52	1,52	1,51	1,45	1,19	0,0764
N-150	A 150	1,49	1,48	1,48	1,48	1,47	1,42	1,21	0,0861
N-200	A 200	1,41	1,40	1,40	1,40	1,40	1,37	1,22	0,103
N-250	A 250	1,38	1,37	1,37	1,37	1,37	1,35	1,21	0,112
N-300	A 300	1,35	1,34	1,34	1,34	1,35	1,33	1,19	0,121

4.1.3.3 ISO wide-spectrum series and DIN B-series

Table 4.22: Data for the radiation qualities of the wide-spectrum series (W) specified in ISO 4037-1 [2] and the B-series according to DIN 6818-1 [3]: first and second half-value layers (1^{st} HVL, 2^{nd} HVL) in mm with the absorber materials Al and Cu, mean photon energies $\overline{E}_{ph}$ in keV, 10 % percentiles in keV, kerma factors $k_{\Phi}(R)$ in $pGy \cdot cm^2$, conversion coefficients $h_{pK}(0,07;R)$ from air kerma, K_a, to the personal dose equivalent, $H_p(0,07)$, for the rod phantom and conversion coefficients $h_K^*(10;R)$ from air kerma, K_a, to the ambient dose equivalent, $H^*(10)$, for the ICRU sphere. The $h_{pK}(0,07;R)$ values are valid for all angles of incidence $\alpha \leq 60°$ (see Section 3.6.2). The $h_K^*(10;R)$ values are given for an expanded and aligned radiation field. The reference distance is 2,5 m.

Radiation quality		1^{st} HVL in mm		2^{nd} HVL in mm		$\overline{E}_{ph}$	10 % percentile	$k_{\Phi}(R)$	$h_{pK}(0,07;R,\alpha)$	$h_K^*(10;R)$
ISO	DIN	Al	Cu	Al	Cu	in keV	in keV	in $pGy \cdot cm^2$	in Sv/Gy	in Sv/Gy
	B 7,5	0,0324	0,00955	0,0334	0,00982	6,9	6,2	16,51	0,883	$<1 \cdot 10^{-4}$
	B 10	0,0647	0,00662	0,0680	0,0110	8,9	7,6	9,99	0,933	0,00180
	B 15	0,173	0,00613	0,191	0,00662	12,7	10,0	4,81	0,961	0,102
	B 20	0,362	0,0119	0,412	0,0131	16,5	12,8	2,78	0,985	0,323
	B 30	0,886	0,0275	1,04	0,0322	23,1	17,0	1,39	1,02	0,697
	B 40	1,75	0,0550	2,06	0,0658	29,9	21,4	0,828	1,05	1,01
W-60	B 60	4,82	0,181	5,36	0,216	44,9	32,5	0,409	1,10	1,50
W-80	B 80	7,43	0,350	8,10	0,434	56,6	40,0	0,331	1,13	1,66
W-110	B 110	12,12	0,934	12,42	1,08	79,1	59,5	0,323	1,16	1,71
W-150	B 150	15,15	1,79	15,48	2,04	104,6	79,0	0,406	1,16	1,62
W-200	B 200	17,91	3,01	18,04	3,25	137,9	108,0	0,549	1,16	1,52
W-250	B 250	19,86	4,14	19,98	4,34	172,4	135,0	0,717	1,15	1,44
W-300	B 300	21,37	5,02	21,47	5,18	205,0	161,0	0,883	1,15	1,39

Verfügbar unter: https://doi.org/10.7795/110.20190315B

Table 4.23: Conversion coefficients $h_{pK}(10;\mathrm{R},\alpha)$ in Sv/Gy from air kerma, K_a, to the personal dose equivalent, $H_p(10)$, for the slab phantom and the radiation qualities of the wide-spectrum series (W) specified in ISO 4037-1 [2] and the B-series according to DIN 6818-1 [3]; the reference distance is 2,5 m.

Radiation quality		$h_{pK}(10;\mathrm{R},\alpha)$ in Sv/Gy for angles of incidence α of					
ISO	DIN	0°	15°	30°	45°	60°	75°
	B 7,5	$<1\cdot10^{-4}$	$<1\cdot10^{-4}$	$<1\cdot10^{-4}$	$<1\cdot10^{-4}$	$<1\cdot10^{-4}$	$<1\cdot10^{-4}$
	B 10	0,00202	0,00174	0,000985	0,000324		
	B 15	0,104	0,0977	0,0773	0,0469	0,0160	0,000967
	B 20	0,333	0,323	0,286	0,219	0,123	0,0261
	B 30	0,704	0,690	0,650	0,562	0,414	0,178
	B 40	1,02	0,999	0,960	0,868	0,701	0,386
W-60	B 60	1,55	1,53	1,49	1,38	1,19	0,780
W-80	B 80	1,77	1,75	1,71	1,60	1,39	0,960
W-110	B 110	1,87	1,86	1,82	1,72	1,52	1,10
W-150	B 150	1,76	1,76	1,72	1,64	1,48	1,10
W-200	B 200	1,64	1,63	1,61	1,55	1,42	1,09
W-250	B 250	1,54	1,54	1,52	1,47	1,37	1,08
W-300	B 300	1,48	1,47	1,46	1,42	1,33	1,08

Table 4.24: Conversion coefficients $h'_K(0{,}07;\mathrm{R},\alpha)$ in Sv/Gy from air kerma, K_a, to the directional dose equivalent, $H'(0{,}07,\vec{\Omega})$, for the ICRU sphere and the radiation qualities of the wide-spectrum series (W) specified in ISO 4037-1 [2] and the B-series according to DIN 6818-1 [3] (expanded radiation field); the reference distance is 2,5 m.

Radiation quality		$h'_K(0{,}07;\mathrm{R},\alpha)$ in Sv/Gy for angles of incidence α of							
ISO	DIN	0°	15°	30°	45°	60°	75°	90°	180°
	B 7,5	0,830	0,808	0,761	0,723	0,535	0,334	0,00340	$<1\cdot10^{-4}$
	B 10	0,902	0,887	0,863	0,847	0,760	0,639	0,0747	
	B 15	0,972	0,964	0,955	0,955	0,939	0,881	0,267	
	B 20	1,01	1,00	0,993	0,993	0,990	0,949	0,406	
	B 30	1,09	1,08	1,08	1,08	1,08	1,05	0,587	0,000110
	B 40	1,19	1,18	1,17	1,17	1,17	1,13	0,715	0,00235
W-60	B 60	1,41	1,40	1,39	1,39	1,37	1,31	0,942	0,0198
W-80	B 80	1,50	1,48	1,47	1,47	1,45	1,38	1,04	0,0341
W-110	B 110	1,54	1,53	1,52	1,52	1,50	1,44	1,14	0,0587
W-150	B 150	1,51	1,50	1,49	1,49	1,48	1,43	1,19	0,0784
W-200	B 200	1,45	1,44	1,44	1,44	1,43	1,39	1,22	0,0947
W-250	B 250	1,40	1,39	1,39	1,39	1,39	1,37	1,22	0,105
W-300	B 300	1,37	1,37	1,37	1,37	1,37	1,35	1,20	0,113

4.1.3.4 ISO high air-kerma rate series and DIN C-series

Table 4.25: Data for the radiation qualities of the high air-kerma rate series (H) specified in ISO 4037-1 [2] and the C-series according to DIN 6818-1 [3]: first and second half-value layers (1st HVL, 2nd HVL) in mm with the absorber materials Al and Cu, mean photon energies $\overline{E}_{ph}$ in keV, 10 % percentiles in keV, kerma factors k_{Φ}(R) in pGy·cm^2, conversion coefficients h_{pK}(0,07;R) from air kerma, K_a, to the personal dose equivalent, H_p(0,07), for the rod phantom and conversion coefficients $h_K^*(10;\mathrm{R})$ from air kerma, K_a, to the ambient dose equivalent, H^*(10), for the ICRU sphere. The h_{pK}(0,07;R) values are valid for all angles of incidence $\alpha \leq 60°$ (see Section 3.6.2). The $h_K^*(10;\mathrm{R})$ values are given for an expanded and aligned radiation field. The reference distance is 2,5 m.

Radiation quality		1st HVL in mm		2nd HVL in mm		$\overline{E}_{ph}$	10 % percentile	k_{Φ}(R)	$h_{pK}(0{,}07;\mathrm{R},\alpha)$	$h_K^*(10;\mathrm{R})$
ISO	DIN	Al	Cu	Al	Cu	in keV	in keV	in pGy·cm^2	in Sv/Gy	in Sv/Gy
	C 7,5	0,0324	0,00955	0,0334	0,00982	6,9	6,2	16,51	0,883	$<1\cdot10^{-4}$
H-10	C 10	0,0586	0,00786	0,0629	0,00122	8,7	7,2	10,60	0,927	0,00136
H-20	C 20	0,169	0,00695	0,228	0,00866	14,0	9,2	4,36	0,963	0,143
H-30	C 30	0,441	0,0144	0,636	0,0197	20,1	11,6	2,10	0,995	0,439
	C 40	0,884	0,0277	1,24	0,0385	25,8	15,4	1,25	1,02	0,717
H-60	C 60	2,61	0,0868	3,44	0,122	38,1	23,0	0,584	1,07	1,21
	C 80	4,69	0,181	5,93	0,272	48,9	29,0	0,413	1,10	1,47
H-100	C 100	6,52	0,299	8,00	0,466	57,4	33,0	0,361	1,12	1,58
	C 150	11,10	0,811	12,17	1,21	78,1	50,0	0,347	1,15	1,67
H-200	C 200	14,22	1,55	15,12	2,28	99,4	59,0	0,408	1,16	1,61
H-250	C 250	16,53	2,42	17,28	3,23	121,6	71,0	0,495	1,16	1,54
H-280		18,42	3,28	18,85	3,89	145,1	98,0	0,594	1,16	1,49
H-300	C 300	18,29	3,22	18,87	3,98	143,1	92,0	0,589	1,15	1,49

Verfügbar unter: https://doi.org/10.7795/110.20190315B

Table 4.26: Conversion coefficients $h_{pK}(10;\mathrm{R},\alpha)$ in Sv/Gy from air kerma, K_a, to the personal dose equivalent, $H_p(10)$, for the slab phantom and the radiation qualities of the high air-kerma rate series (H) specified in ISO 4037-1 [2] and the C-series according to DIN 6818-1 [3]; the reference distance is 2,5 m.

Radiation quality		$h_{pK}(10;\mathrm{R},\alpha)$ in Sv/Gy for angles of incidence α of					
ISO	DIN	0°	15°	30°	45°	60°	75°
	C 7,5	$<1\cdot10^{-4}$	$<1\cdot10^{-4}$	$<1\cdot10^{-4}$	$<1\cdot10^{-4}$	$<1\cdot10^{-4}$	$<1\cdot10^{-4}$
H-10	C 10	0,00153	0,00132	0,000738	0,000239		
H-20	C 20	0,146	0,141	0,120	0,0863	0,0434	0,00787
H-30	C 30	0,445	0,435	0,400	0,330	0,224	0,0822
	C 40	0,724	0,710	0,672	0,586	0,443	0,211
H-60	C 60	1,24	1,22	1,18	1,08	0,902	0,549
	C 80	1,54	1,52	1,48	1,37	1,18	0,777
H-100	C 100	1,68	1,66	1,62	1,52	1,32	0,902
	C 150	1,81	1,79	1,76	1,66	1,47	1,06
H-200	C 200	1,75	1,74	1,71	1,62	1,46	1,09
H-250	C 250	1,67	1,66	1,63	1,57	1,43	1,09
H-280		1,60	1,60	1,58	1,52	1,40	1,09
H-300	C 300	1,60	1,60	1,58	1,52	1,40	1,09

Table 4.27: Conversion coefficients $h'_K(0{,}07;\mathrm{R},\alpha)$ in Sv/Gy from air kerma, K_a, to the directional dose equivalent, $H'(0{,}07,\vec{\Omega})$, for the ICRU sphere and the radiation qualities of the high air-kerma rate series (H) specified in ISO 4037-1 [2] and the C-series according to DIN 6818-1 [3] (expanded radiation field); the reference distance is 2,5 m.

Radiation quality		$h'_K(0{,}07;\mathrm{R},\alpha)$ in Sv/Gy for angles of incidence α of							
ISO	DIN	0°	15°	30°	45°	60°	75°	90°	180°
	C 7,5	0,830	0,808	0,761	0,723	0,535	0,334	0,00340	$<1\cdot10^{-4}$
H-10	C 10	0,892	0,876	0,848	0,830	0,728	0,595	0,0610	
H-20	C 20	0,970	0,962	0,950	0,950	0,925	0,862	0,271	
H-30	C 30	1,03	1,03	1,02	1,02	1,01	0,975	0,455	
	C 40	1,10	1,10	1,09	1,09	1,09	1,05	0,590	0,000815
H-60	C 60	1,28	1,27	1,26	1,26	1,25	1,20	0,806	0,00928
	C 80	1,40	1,39	1,38	1,38	1,36	1,30	0,936	0,0216
H-100	C 100	1,46	1,44	1,43	1,43	1,42	1,35	1,01	0,0321
	C 150	1,52	1,50	1,50	1,50	1,48	1,42	1,12	0,0571
H-200	C 200	1,49	1,48	1,48	1,48	1,47	1,41	1,17	0,0753
H-250	C 250	1,46	1,45	1,44	1,44	1,44	1,40	1,20	0,0882
H-280		1,43	1,42	1,42	1,42	1,42	1,38	1,21	0,0980
H-300	C 300	1,43	1,42	1,42	1,42	1,42	1,38	1,20	0,0976

4.1.3.5 Unfiltered X-ray spectra

Table 4.28a: Data for unfiltered X-ray spectra generated with an X-ray tube voltage of up to 120 kV: first and second half-value layers (1st HVL, 2nd HVL) in mm with the absorber materials Al and Cu, mean photon energies $\overline{E}_{ph}$ in keV, 10 % percentiles in keV, kerma factors $k_{\Phi}(R)$ in $pGy \cdot cm^2$, conversion coefficients $h_{pK}(0{,}07;R)$ from air kerma, K_a, to the personal dose equivalent, $H_p(0{,}07)$, for the rod phantom and conversion coefficients $h_K^*(10;R)$ from air kerma, K_a, to the ambient dose equivalent, $H^*(10)$, for the ICRU sphere. The $h_{pK}(0{,}07;R)$ values are valid for all angles of incidence $\alpha \leq 60°$ (see Section 3.6.2). The $h_K^*(10;R)$ values are given for an expanded and aligned radiation field. The reference distance is 2,5 m.

Unfiltered X-ray spectra tube voltage in kV	1st HVL in mm		2nd HVL in mm		$\overline{E}_{ph}$ in keV	10 % percentile in keV	$k_{\Phi}(R)$ in $pGy \cdot cm^2$	$h_{pK}(0{,}07;R,\alpha)$ in Sv/Gy	$h_K^*(10;R)$ in Sv/Gy
	Al	Cu	Al	Cu					
7,5	0,0324	0,00955	0,0334	0,00982	6,9	6,2	16,51	0,883	$<1 \cdot 10^{-4}$
10	0,0586	0,00786	0,0629	0,00122	8,7	7,2	10,60	0,927	0,00136
15	0,100	0,00583	0,119	0,00736	11,0	8,4	6,80	0,946	0,0388
20	0,121	0,00656	0,163	0,00860	12,9	8,4	5,42	0,953	0,0893
25	0,134	0,00713	0,199	0,00994	14,6	8,4	4,61	0,958	0,131
30	0,143	0,00755	0,230	0,0112	16,2	8,4	4,05	0,962	0,163
35	0,150	0,00786	0,257	0,0122	17,7	8,4	3,65	0,964	0,188
40	0,154	0,00812	0,281	0,0132	19,3	8,4	3,34	0,966	0,210
50	0,165	0,00860	0,335	0,0151	22,3	8,4	2,81	0,971	0,253
55	0,168	0,00877	0,358	0,0160	23,7	8,4	2,66	0,972	0,265
60	0,173	0,00887	0,388	0,0168	25,1	8,5	2,49	0,974	0,282
70	0,183	0,00929	0,454	0,0189	28,0	8,5	2,21	0,978	0,314
80	0,193	0,00975	0,536	0,0213	31,0	8,5	1,98	0,981	0,347
90	0,203	0,0103	0,635	0,0242	34,1	8,5	1,76	0,985	0,385
100	0,219	0,0110	0,770	0,0280	36,9	8,5	1,61	0,989	0,416
110	0,240	0,0118	0,947	0,0329	39,8	8,5	1,44	0,994	0,461
120	0,260	0,0126	1,12	0,0380	42,3	8,5	1,35	0,997	0,487

Table 4.28b: Data for unfiltered X-ray spectra generated with an X-ray tube voltage higher than 120 kV: first and second half-value layers (1st HVL, 2nd HVL) in mm with the absorber materials Al and Cu, mean photon energies $\overline{E}_{\mathrm{ph}}$ in keV, 10 % percentiles in keV, kerma factors k_{Φ}(R) in pGy · cm^2, conversion coefficients $h_{\mathrm{p}K}$(0,07;R) from air kerma, K_{a}, to the personal dose equivalent, H_{p}(0,07), for the rod phantom and conversion coefficients $h_K^*(10;\mathrm{R})$ from air kerma, K_{a}, to the ambient dose equivalent, H*(10), for the ICRU sphere. The $h_{\mathrm{p}K}$(0,07;R) values are valid for all angles of incidence $\alpha \leq 60°$ (see Section 3.6.2). The $h_K^*(10;\mathrm{R})$ values are given for an expanded and aligned radiation field. The reference distance is 2,5 m.

Unfiltered X-ray spectra tube voltage in kV	1st HVL in mm		2nd HVL in mm		$\overline{E}_{\mathrm{ph}}$	10 % percentile	k_{Φ}(R)	$h_{\mathrm{p}K}(0{,}07;\mathrm{R},\alpha)$	$h_K^*(10;\mathrm{R})$
	Al	Cu	Al	Cu	in keV	in keV	in pGy · cm^2	in Sv/Gy	in Sv/Gy
125	0,606	0,0222	2,25	0,0773	45,9	9,5	45,90	1,02	0,701
140	0,753	0,0268	2,86	0,106	49,5	10,0	0,867	1,03	0,766
150	0,864	0,0295	3,32	0,131	51,7	10,0	0,821	1,03	0,805
170	1,09	0,0376	4,26	0,191	55,9	10,0	0,756	1,04	0,868
200	1,59	0,0564	5,94	0,337	61,9	10,0	0,684	1,05	0,961
210	1,79	0,0652	6,52	0,400	63,7	10,0	0,666	1,06	0,991
240	2,44	0,0965	8,17	0,626	69,1	10,0	0,630	1,07	1,06
250	2,77	0,115	8,79	0,728	70,9	10,0	0,616	1,07	1,09
280	3,57	0,167	10,29	1,04	76,1	10,0	0,599	1,08	1,14
300	4,15	0,213	11,20	1,27	79,4	11,0	0,592	1,09	1,17

Verfügbar unter: https://doi.org/10.7795/110.20190315B

Table 4.29: Conversion coefficients $h_{pK}(10;\mathrm{R},\alpha)$ in Sv/Gy from air kerma, K_a, to the personal dose equivalent, $H_p(10)$, for the slab phantom and unfiltered X-ray spectra; the reference distance is 2,5 m.

Unfiltered X-ray spectra tube voltage in kV	$h_{pK}(10;\mathrm{R},\alpha)$ in Sv/Gy for angles of incidence α of					
	0°	15°	30°	45°	60°	75°
7,5	$<1\cdot10^{-4}$	$<1\cdot10^{-4}$	$<1\cdot10^{-4}$	$<1\cdot10^{-4}$	$<1\cdot10^{-4}$	$<1\cdot10^{-4}$
10	0,00153	0,00132	0,000738	0,000239		
15	0,0391	0,0365	0,0280	0,0161	0,00486	0,000250
20	0,0914	0,0875	0,0738	0,0518	0,0251	0,00436
25	0,134	0,129	0,113	0,0860	0,0497	0,0133
30	0,166	0,161	0,144	0,114	0,0720	0,0241
35	0,191	0,186	0,169	0,137	0,0912	0,0347
40	0,213	0,207	0,190	0,157	0,108	0,0447
50	0,256	0,250	0,232	0,196	0,141	0,0650
55	0,269	0,262	0,244	0,208	0,152	0,0723
60	0,287	0,280	0,261	0,224	0,166	0,0813
70	0,320	0,314	0,294	0,255	0,193	0,0990
80	0,355	0,348	0,328	0,287	0,221	0,118
90	0,395	0,387	0,367	0,323	0,253	0,140
100	0,428	0,421	0,400	0,355	0,281	0,159
110	0,476	0,468	0,446	0,399	0,319	0,186
120	0,505	0,496	0,474	0,425	0,344	0,204
125	0,728	0,717	0,688	0,622	0,508	0,307
140	0,798	0,786	0,756	0,688	0,568	0,351
150	0,841	0,829	0,798	0,728	0,605	0,380
170	0,910	0,898	0,868	0,796	0,668	0,429
200	1,01	1,00	0,969	0,894	0,760	0,502
210	1,04	1,03	1,00	0,926	0,790	0,526
240	1,12	1,11	1,08	1,00	0,862	0,586
250	1,15	1,14	1,11	1,03	0,893	0,611
280	1,21	1,20	1,17	1,09	0,949	0,660
300	1,24	1,23	1,20	1,12	0,983	0,690

Verfügbar unter: https://doi.org/10.7795/110.20190315B

Table 4.30: Conversion coefficients $h'_K(0{,}07;\mathrm{R},\alpha)$ in Sv/Gy from air kerma, K_a, to the directional dose equivalent, $H'(0{,}07,\vec{\Omega})$, for the ICRU sphere and unfiltered X-ray spectra (expanded radiation field); the reference distance is 2,5 m.

Unfiltered X-ray spectra tube voltage in kV	$h'_K(0{,}07;\mathrm{R},\alpha)$ in Sv/Gy for angles of incidence α of							
	0°	15°	30°	45°	60°	75°	90°	180°
7,5	0,830	0,808	0,761	0,723	0,535	0,334	0,00340	
10	0,892	0,876	0,848	0,830	0,728	0,595	0,0610	
15	0,938	0,927	0,911	0,905	0,858	0,771	0,170	
20	0,951	0,941	0,926	0,922	0,882	0,804	0,212	$<1\cdot10^{-4}$
25	0,959	0,950	0,935	0,933	0,895	0,821	0,238	
30	0,966	0,957	0,943	0,941	0,905	0,833	0,256	
35	0,973	0,964	0,950	0,948	0,913	0,842	0,270	
40	0,978	0,969	0,955	0,953	0,918	0,848	0,280	0,000132
50	0,991	0,982	0,969	0,967	0,934	0,865	0,304	0,000431
55	0,995	0,986	0,972	0,971	0,938	0,869	0,308	0,000602
60	1,00	0,991	0,978	0,976	0,944	0,875	0,317	0,000807
70	1,01	1,00	0,988	0,987	0,955	0,886	0,334	0,00127
80	1,02	1,01	0,998	0,997	0,966	0,897	0,351	0,00185
90	1,03	1,02	1,01	1,01	0,979	0,911	0,372	0,00256
100	1,04	1,03	1,02	1,02	0,990	0,922	0,388	0,00335
110	1,06	1,05	1,04	1,04	1,01	0,941	0,414	0,00437
120	1,07	1,06	1,05	1,05	1,02	0,949	0,427	0,00527
125	1,13	1,13	1,12	1,12	1,10	1,04	0,556	0,00851
140	1,16	1,15	1,14	1,14	1,12	1,07	0,595	0,0109
150	1,17	1,16	1,15	1,15	1,14	1,08	0,618	0,0126
170	1,20	1,19	1,18	1,18	1,16	1,10	0,656	0,0160
200	1,23	1,22	1,21	1,21	1,19	1,14	0,715	0,0216
210	1,24	1,23	1,22	1,22	1,21	1,15	0,735	0,0235
240	1,27	1,25	1,25	1,25	1,23	1,17	0,782	0,0291
250	1,28	1,27	1,26	1,26	1,25	1,19	0,805	0,0313
280	1,30	1,28	1,28	1,28	1,27	1,21	0,844	0,0369
300	1,31	1,30	1,29	1,29	1,28	1,22	0,868	0,0405

Verfügbar unter: https://doi.org/10.7795/110.20190315B

4.2 Data for therapy and diagnostic radiation qualities

4.2.1 Introduction

In Sections 4.2.2 and 4.2.3 the values for the following characteristic parameters are listed for each spectrum 'R' of the therapy and several diagnostic radiation qualities:

- first and second half-value layer (1st HVL, 2nd HVL),
- mean photon energy $\overline{E}_{\mathrm{ph}}$,
- 10 % percentile,
- kerma factor k_{Φ}(R),
- conversion coefficient $h_{\mathrm{pK}}(10;\mathrm{R},\alpha)$ from air kerma, K_{a}, to the personal dose equivalent, $H_{\mathrm{p}}(10)$, for the slab phantom at an angle of incidence α,
- conversion coefficient $h_{\mathrm{pK}}(0{,}07;\mathrm{R})$ from air kerma, K_{a}, to the personal dose equivalent, $H_{\mathrm{p}}(0{,}07)$, for the rod phantom and all angles of incidence α below 60°,
- conversion coefficient $h_K^*(10;\mathrm{R})$ from air kerma, K_{a}, to the ambient dose equivalent, $H^*(10)$,
- conversion coefficient $h_K'(0{,}07;\mathrm{R},\alpha)$ from air kerma, K_{a}, to the directional dose equivalent, $H'(0{,}07,\vec{\Omega})$, at an angle of incidence α.

The reference distances, for which the therapy radiation qualities are defined (see DIN 6817 [6]) and the characteristic data are determined, are given in the tables. The pulse height spectra of the low-energy therapy radiation qualities TW 7,5 to TW 50 could not be measured at the specified distance of 0,3 cm between the focus of the X-ray tube and the front of the Ge detector. They were measured at 0,5 m distance and were converted into fluence spectra with 0,3 m air path (see Section 2). The pulse height spectra of the diagnostic radiation qualities are measured at a distance of 1,0 m. All data given are valid for reference conditions.

The therapy radiation qualities TH 150, TH 200, TH 250 and TH 280 are identical with the qualities C 150, H-200, H-250 and H-280. However, for clear arrangement, the charateristic values of these radiation qualities are given also in the following tables.

4.2.2 Therapy radiation qualities

Table 4.31: Data for the therapy radiation qualities according to DIN 6817 [6]: first and second half-value layers (1st HVL, 2nd HVL) in mm with the absorber materials Al and Cu, mean photon energies $\overline{E}_{\mathrm{ph}}$ in keV, 10 % percentiles in keV, kerma factors $k_{\Phi}(\mathrm{R})$ in pGy·cm², conversion coefficients $h_{\mathrm{p}K}(0{,}07;\mathrm{R})$ from air kerma, K_{a}, to the personal dose equivalent, $H_{\mathrm{p}}(0{,}07)$, for the rod phantom and conversion coefficients $h_K^*(10;\mathrm{R})$ from air kerma, K_{a}, to the ambient dose equivalent, $H^*(10)$, for the ICRU sphere. The $h_{\mathrm{p}K}(0{,}07;\mathrm{R})$ values are valid for all angles of incidence $\alpha \le 60°$ (see Section 3.6.2). The $h_K^*(10;\mathrm{R})$ values are given for an expanded and aligned radiation field. The reference distance is given for each radiation quality.

Radiation quality	Reference distance in m	1st HVL in mm		2nd HVL in mm		$\overline{E}_{\mathrm{ph}}$ in keV	10 % percentile in keV	$k_{\Phi}(\mathrm{R})$ in pGy·cm²	$h_{\mathrm{p}K}(0{,}07;\mathrm{R},\alpha)$ in Sv/Gy	$h_K^*(10;\mathrm{R})$ in Sv/Gy
		Al	Cu	Al	Cu					
TW 7,5	0,3	0,0216	0,00649	0,0240	0,00714	6,2	5,0	21,30	0,832	$<1\cdot10^{-4}$
TW 10	0,3	0,0324	0,00797	0,0394	0,00981	7,5	5,4	15,2	0,875	0,000361
TW 15	0,3	0,0704	0,00701	0,0883	0,00959	10,1	6,8	8,51	0,930	0,0200
TW 20	0,3	0,113	0,00668	0,150	0,00891	12,6	8,4	5,70	0,951	0,0790
TW 30	0,3	0,203	0,00859	0,350	0,0128	17, 7	9,0	3,17	0,973	0,244
TW 40	0,3	0,425	0,0144	0,763	0,0236	23,0	10,0	1,86	0,997	0,465
TW 50	0,3	0,961	0,0303	1,49	0,0471	28,8	15,0	1,10	1,03	0,767
SH 50	1,0	2,20	0,0710	2,77	0,0932	34,2	22,2	0,674	1,06	1,12
SH 70	1,0	2,97	0,102	4,08	0,156	41,7	23,5	0,530	1,08	1,27
TH 70	1,0	2,23	0,0735	3,30	0,120	39,1	20,5	0,621	1,06	1,14
TH 100	1,0	4,50	0,178	6,40	0,329	52,3	26,5	0,426	1,10	1,43
TH 120	1,0	6,05	0,277	8,18	0,519	59,2	30,0	0,385	1,12	1,53
TH 140	1,0	8,15	0,458	10,10	0,804	67,4	35,5	0,360	1,13	1,61
TH 150	1,0	11,07	0,808	12,16	1,21	78,0	50,0	0,347	1,15	1,67
TH 200	1,0	14,19	1,54	15,11	2,28	99,3	59,0	0,408	1,16	1,61
TH 250	1,0	16,55	2,42	17,28	3,24	121,5	71,0	0,495	1,16	1,54
TH 280	1,0	18,38	3,26	18,83	3,88	144,6	98,0	0,592	1,16	1,49

Verfügbar unter: https://doi.org/10.7795/110.20190315B

Table 4.32: Conversion cefficients $h_{pK}(10;\mathrm{R},\alpha)$ in Sv/Gy from air kerma, K_a, to the personal dose equivalent, $H_p(10)$, for the slab phantom and therapy radiation qualities specified in DIN 6817 [6]. The reference distance is given for each radiation quality.

<table>
<tr><th rowspan="2">Radiation quality</th><th rowspan="2">Reference distance in m</th><th colspan="6">$h_{pK}(10;\mathrm{R},\alpha)$ in Sv/Gy for angles of incidence α of</th></tr>
<tr><th>0°</th><th>15°</th><th>30°</th><th>45°</th><th>60°</th><th>75°</th></tr>
<tr><td>TW 7,5</td><td>0,3</td><td>$<1\cdot10^{-4}$</td><td>$<1\cdot10^{-4}$</td><td>$<1\cdot10^{-4}$</td><td>$<1\cdot10^{-4}$</td><td rowspan="2">$<1\cdot10^{-4}$</td><td rowspan="2">$<1\cdot10^{-4}$</td></tr>
<tr><td>TW 10</td><td>0,3</td><td>0,000405</td><td>0,000346</td><td>0,000190</td><td>0,00006</td></tr>
<tr><td>TW 15</td><td>0,3</td><td>0,0201</td><td>0,0187</td><td>0,0142</td><td>0,00804</td><td>0,00237</td><td>0,000130</td></tr>
<tr><td>TW 20</td><td>0,3</td><td>0,0808</td><td>0,0773</td><td>0,0650</td><td>0,0455</td><td>0,0219</td><td>0,00382</td></tr>
<tr><td>TW 30</td><td>0,3</td><td>0,248</td><td>0,241</td><td>0,218</td><td>0,175</td><td>0,113</td><td>0,0389</td></tr>
<tr><td>TW 40</td><td>0,3</td><td>0,471</td><td>0,460</td><td>0,428</td><td>0,363</td><td>0,261</td><td>0,115</td></tr>
<tr><td>TW 50</td><td>0,3</td><td>0,777</td><td>0,763</td><td>0,724</td><td>0,639</td><td>0,494</td><td>0,252</td></tr>
<tr><td>SH 50</td><td>1,0</td><td>1,14</td><td>1,12</td><td>1,08</td><td>0,988</td><td>0,814</td><td>0,478</td></tr>
<tr><td>SH 70</td><td>1,0</td><td>1,31</td><td>1,29</td><td>1,25</td><td>1,15</td><td>0,966</td><td>0,604</td></tr>
<tr><td>TH 70</td><td>1,0</td><td>1,17</td><td>1,15</td><td>1,11</td><td>1,02</td><td>0,842</td><td>0,506</td></tr>
<tr><td>TH 100</td><td>1,0</td><td>1,50</td><td>1,48</td><td>1,45</td><td>1,34</td><td>1,15</td><td>0,763</td></tr>
<tr><td>TH 120</td><td>1,0</td><td>1,62</td><td>1,60</td><td>1,56</td><td>1,46</td><td>1,27</td><td>0,865</td></tr>
<tr><td>TH 140</td><td>1,0</td><td>1,72</td><td>1,71</td><td>1,67</td><td>1,57</td><td>1,37</td><td>0,963</td></tr>
<tr><td>TH 150</td><td>1,0</td><td>1,81</td><td>1,79</td><td>1,76</td><td>1,66</td><td>1,47</td><td>1,06</td></tr>
<tr><td>TH 200</td><td>1,0</td><td>1,75</td><td>1,74</td><td>1,71</td><td>1,62</td><td>1,46</td><td>1,09</td></tr>
<tr><td>TH 250</td><td>1,0</td><td>1,67</td><td>1,66</td><td>1,64</td><td>1,57</td><td>1,43</td><td>1,09</td></tr>
<tr><td>TH 280</td><td>1,0</td><td>1,60</td><td>1,60</td><td>1,58</td><td>1,52</td><td>1,40</td><td>1,09</td></tr>
</table>

Table 4.33: Conversion coefficients $h'_K(0{,}07;\mathrm{R},\alpha)$ in Sv/Gy from air kerma, K_a, to the directional dose equivalent, $H'(0{,}07,\vec{\Omega})$, for the ICRU sphere and the therapy radiation qualities specified in DIN 6817 [6] (expanded radiation field). The reference distance is given for each radiation quality.

Radiation quality	Reference distance in m	$h'_K(0{,}07;\mathrm{R},\alpha)$ in Sv/Gy for angles of incidence α of							
		0°	15°	30°	45°	60°	75°	90°	180°
TW 7,5	0,3	0,795	0,769	0,713	0,664	0,434	0,202	0,00105	$<1\cdot10^{-4}$
TW 10	0,3	0,835	0,813	0,769	0,733	0,555	0,364	0,0200	
TW 15	0,3	0,908	0,894	0,870	0,856	0,772	0,656	0,113	
TW 20	0,3	0,946	0,936	0,920	0,915	0,871	0,790	0,198	
TW 30	0,3	0,990	0,983	0,972	0,972	0,951	0,893	0,325	
TW 40	0,3	1,04	1,04	1,03	1,03	1,02	0,976	0,456	0,000375
TW 50	0,3	1,12	1,12	1,11	1,11	1,11	1,07	0,609	0,00202
SH 50	1,0	1,24	1,23	1,22	1,22	1,21	1,17	0,764	0,00583
SH 70	1,0	1,31	1,30	1,29	1,29	1,29	1,22	0,836	0,0124
TH 70	1,0	1,26	1,25	1,24	1,24	1,23	1,18	0,780	0,00910
TH 100	1,0	1,39	1,37	1,37	1,37	1,35	1,29	0,927	0,0232
TH 120	1,0	1,44	1,42	1,41	1,41	1,40	1,34	0,989	0,0322
TH 140	1,0	1,48	1,47	1,46	1,46	1,44	1,38	1,05	0,0433
TH 150	1,0	1,52	1,50	1,50	1,50	1,48	1,42	1,12	0,0570
TH 200	1,0	1,49	1,48	1,48	1,48	1,47	1,41	1,17	0,0751
TH 250	1,0	1,46	1,45	1,45	1,45	1,44	1,40	1,20	0,0882
TH 280	1,0	1,43	1,42	1,42	1,42	1,42	1,38	1,21	0,0978

4.2.3 Diagnostic radiation qualities

Table 4.34: Data for diagnostic radiation qualities specified in IEC 61267 [4] and by Engelke *et al.* [22]: first and second half-value layers (1st HVL, 2nd HVL) in mm with the absorber materials Al and Cu, mean photon energies $\overline{E}_{\mathrm{ph}}$ in keV, 10 % percentiles in keV, kerma factors $k_{\Phi}(\mathrm{R})$ in pGy·cm², conversion coefficients $h_{\mathrm{p}K}(0{,}07;\mathrm{R})$ from air kerma, K_{a}, to the personal dose equivalent, $H_{\mathrm{p}}(0{,}07)$, for the rod phantom and conversion coefficients $h_K^*(10;\mathrm{R})$ from air kerma, K_{a}, to the ambient dose equivalent, $H^*(10)$, for the ICRU sphere. The $h_{\mathrm{p}K}(0{,}07;\mathrm{R})$ values are valid for all angles of incidence $\alpha \le 60°$ (see Section 3.6.2). The $h_K^*(10;\mathrm{R})$ values are given for an expanded and aligned radiation field. The reference distance is 1,0 m.

Radiation quality		1st HVL in mm		2nd HVL in mm		$\overline{E}_{\mathrm{ph}}$	10 % percentile	$k_{\Phi}(\mathrm{R})$	$h_{\mathrm{p}K}(0{,}07;\mathrm{R},\alpha)$	$h_K^*(10;\mathrm{R})$
IEC 61267	Engelke *et al.*	Al	Cu	Al	Cu	in keV	in keV	in pGy·cm²	in Sv/Gy	in Sv/Gy
	DV 20	0,477	0,0152	0,512	0,0161	17,7	15,0	2,33	0,994	0,419
	DV 30	0,950	0,0295	1,10	0,0341	23,5	17,6	1,33	1,02	0,726
RQR 2		1,36	0,0426	1,72	0,0541	28,2	18,8	0,966	1,04	0,897
RQR 3	DV 50	1,72	0,0545	2,30	0,0754	32,4	19,8	0,783	1,05	1,01
RQR 4		2,02	0,0652	2,84	0,0979	36,0	20,5	0,679	1,06	1,09
RQR 5	DV 70	2,29	0,0758	3,37	0,123	39,4	21,0	0,611	1,07	1,16
RQR 6		2,59	0,0879	3,96	0,155	42,8	21,5	0,561	1,07	1,21
RQR 7		2,91	0,101	4,57	0,193	46,0	22,0	0,524	1,08	1,26
RQR 8	DV 100	3,23	0,116	5,19	0,238	48,8	22,5	0,496	1,08	1,30
RQR 9	DV 120	3,88	0,150	6,37	0,343	53,9	23,0	0,462	1,09	1,36
RQR 10	DV 150	5,01	0,222	8,15	0,560	61,0	25,0	0,434	1,11	1,43
RQA 2	DN 2	2,13	0,0677	2,41	0,0777	31,5	23,8	0,731	1,06	1,09
RQA 3	DN 3	3,67	0,127	4,05	0,145	39,1	29,8	0,492	1,08	1,37
RQA 4	DN 4	5,24	0,202	5,70	0,234	46,1	34,5	0,389	1,10	1,54
RQA 5	DN 5	6,64	0,287	7,16	0,340	52,3	38,5	0,344	1,12	1,63
RQA 6	DN 6	7,96	0,391	8,50	0,468	58,2	42,5	0,322	1,13	1,68
RQA 7	DN 7	9,03	0,495	9,57	0,596	63,2	46,5	0,314	1,14	1,70
RQA 8	DN 8	9,93	0,600	10,47	0,731	67,8	49,5	0,314	1,15	1,71
RQA 9	DN 9	11,37	0,821	11,97	1,04	76,5	55,5	0,328	1,15	1,70
RQA 10	DN 10	12,97	1,17	13,66	1,58	88,1	59,0	0,361	1,16	1,66
RQT		10,01	0,630	10,89	0,861	70,6	47,0	0,328	1,15	1,69

Verfügbar unter: https://doi.org/10.7795/110.20190315B

Verfügbar unter: https://doi.org/10.7795/110.20190315B

Table 4.35: Conversion coefficients $h_{pK}(10;R,\alpha)$ in Sv/Gy from air kerma, K_a, to the personal dose equivalent $H_p(10)$ for the slab phantom and diagnostic radiation qualities specified in IEC 61267 [4] and by Engelke *et al*. [22]. The reference distance is 1,0 m.

Radiation quality		$h_{pK}(10;R,\alpha)$ in Sv/Gy for angles of incidence α of					
IEC 61267	Engelke *et al*.	0°	15°	30°	45°	60°	75°
	DV 20	0,431	0,419	0,379	0,302	0,182	0,0439
	DV 30	0,733	0,718	0,679	0,589	0,439	0,193
RQR 2		0,905	0,889	0,850	0,760	0,600	0,313
RQR 3	DV 50	1,03	1,01	0,970	0,877	0,710	0,399
RQR 4		1,11	1,10	1,06	0,962	0,790	0,463
RQR 5	DV 70	1,18	1,17	1,13	1,03	0,854	0,515
RQR 6		1,25	1,23	1,19	1,09	0,913	0,564
RQR 7		1,30	1,28	1,25	1,15	0,965	0,608
RQR 8	DV 100	1,35	1,33	1,29	1,19	1,01	0,647
RQR 9	DV 120	1,42	1,41	1,37	1,27	1,08	0,710
RQR 10	DV 150	1,51	1,49	1,45	1,35	1,17	0,789
RQA 2	DN 2	1,10	1,09	1,05	0,956	0,785	0,452
RQA 3	DN 3	1,39	1,37	1,33	1,24	1,05	0,664
RQA 4	DN 4	1,60	1,58	1,54	1,43	1,23	0,814
RQA 5	DN 5	1,73	1,70	1,66	1,55	1,35	0,916
RQA 6	DN 6	1,80	1,78	1,74	1,63	1,42	0,988
RQA 7	DN 7	1,84	1,82	1,78	1,67	1,46	1,03
RQA 8	DN 8	1,86	1,84	1,80	1,69	1,49	1,06
RQA 9	DN 9	1,85	1,84	1,80	1,70	1,50	1,08
RQA 10	DN 10	1,81	1,80	1,76	1,67	1,49	1,09
RQT		1,83	1,81	1,77	1,67	1,47	1,05

Table 4.36: Conversion coefficients $h'_K(0{,}07;\mathrm{R},\alpha)$ in Sv/Gy from air kerma, K_a, to the directional dose equivalent $H'(0{,}07,\vec{\Omega})$ for the ICRU sphere and diagnostic radiation qualities specified in IEC 61267 [4] and by Engelke *et al*. [22] (expanded radiation field). The reference distance is 1,0 m.

Radiation quality		$h'_K(0{,}07;\mathrm{R},\alpha)$ in Sv/Gy for angles of incidence α of							
IEC 1267	Engelke *et al*.	0°	15°	30°	45°	60°	75°	90°	180°
	DV 20	1,02	1,02	1,01	1,01	1,01	0,977	0,461	$<1\cdot10^{-4}$
	DV 30	1,09	1,09	1,08	1,08	1,08	1,05	0,599	$1{,}28\cdot10^{-4}$
RQR 2		1,15	1,14	1,14	1,14	1,14	1,10	0,669	0,00156
RQR 3	DV 50	1,20	1,19	1,18	1,18	1,18	1,13	0,719	0,00414
RQR 4		1,23	1,22	1,22	1,22	1,21	1,16	0,756	0,00682
RQR 5	DV 70	1,26	1,25	1,24	1,24	1,24	1,19	0,786	0,00936
RQR 6		1,29	1,27	1,27	1,27	1,26	1,21	0,813	0,0121
RQR 7		1,31	1,30	1,29	1,29	1,28	1,23	0,838	0,0149
RQR 8	DV 100	1,33	1,31	1,31	1,31	1,30	1,24	0,861	0,0176
RQR 9	DV 120	1,36	1,34	1,34	1,34	1,33	1,27	0,899	0,0228
RQR 10	DV 150	1,39	1,38	1,37	1,37	1,36	1,30	0,951	0,0310
RQA 2	DN 2	1,22	1,21	1,20	1,20	1,20	1,15	0,749	0,00340
RQA 3	DN 3	1,34	1,32	1,32	1,32	1,31	1,25	0,869	0,0124
RQA 4	DN 4	1,43	1,42	1,41	1,41	1,39	1,33	0,963	0,0220
RQA 5	DN 5	1,48	1,47	1,45	1,45	1,44	1,37	1,02	0,0260
RQA 6	DN 6	1,51	1,49	1,48	1,48	1,47	1,39	1,06	0,0364
RQA 7	DN 7	1,52	1,51	1,50	1,50	1,48	1,41	1,08	0,0419
RQA 8	DN 8	1,53	1,51	1,50	1,50	1,49	1,42	1,10	0,0470
RQA 9	DN 9	1,53	1,52	1,51	1,51	1,50	1,43	1,13	0,0560
RQA 10	DN 10	1,52	1,51	1,50	1,50	1,49	1,43	1,16	0,0666
RQT		1,52	1,51	1,50	1,50	1,48	1,42	1,10	0,0495

5. Graphical representation of the spectra

5.1 Explanation of the figures

In this section the fluence spectra of all radiation qualities listed in Tables 2.1 to 2.4 of Section 2 and of the unfiltered X-ray spectra considered in Section 4.1 are presented. The energy distribution of the fluence of each radiation quality and unfiltered X-ray spectrum is shown in a figure together with two other curves. One is the spectral fluence weighted with the energy-dependent kerma factors $k_{\Phi}(E)$ (see Section 3.1) and represents the contribution to the total air kerma, K_a, from photons at the respective energies. Similarly, the second curve is the fluence spectrum weighted with the energy-dependent fluence-to-personal dose equivalent conversion coefficients, $h_{p\Phi}(10;E,0°)$, and gives the contribution from photons at the respective energies to the total personal dose equivalent, $H_p(10)$, at the angle of incidence, α, of 0°. The value of $h_{p\Phi}(10;E,0°)$ is given by

$$h_{p\Phi}(10;E,0°) = h_{pK}(10;E,0°) \cdot k_{\Phi}(E) \qquad (5.1)$$

with the conversion coefficient $h_{pK}(10;E,0°)$ from air kerma, K_a, to the personal dose equivalent, $H_p(10)$, at the photon energy E and $\alpha = 0°$ (see Section 3.6.1).

For the low-energy therapy radiation qualities TW 7,5 to TW 50 the reference distance is 0,3 m for the fluence and weighted fluence spectra shown. The plotted unfiltered X-ray spectra generated with an X-ray tube voltage higher than 120 kV are given for a reference distance of 2,5 m because at a distance of 1,0 m they could not be measured (see Section 2). For all other fluence and weighted fluence spectra shown the reference distance is 1,0 m. The additional representation of the spectra measured at 2,5 m distance was dispensed with.

In the graphs the right axis gives the value of the spectral fluence, $\Phi_E(E)$, normalised to its maximum value, $\Phi_E(E)_{max}$, and is written as $\Phi_E/\Phi_{E,max}$. The left axis represents the values of the product $h_{p\Phi}(10;E,0°)\cdot\Phi_E(E)$ and $k_{\Phi}(E)\cdot\Phi_E(E)$, respectively, normalised to the maximum value of the spectral fluence, $\Phi_E(E)_{max}$. In the figures the expression $h_{p\Phi}(10;E,0°)\cdot\Phi_E(E)/\Phi_E(E)_{max}$ is written as $h_{p\Phi}\cdot\Phi_E/\Phi_{E,max}$ and the expression $k_{\Phi}(E)\cdot\Phi_E(E)/\Phi_E(E)_{max}$ is given by $k_{\Phi}\cdot\Phi_E/\Phi_{E,max}$. The minimum and maximum boundary of the energy range of the spectra shown is E_{min} and E_{max} as discussed in Section 3.1. The name of the radiation quality is given in each figure in bold type. In the figures showing the unfiltered X-ray spectra the tube voltage is plotted in bold type. Figure captions were dispensed with because with the information given in this paragraph all figures are self-explanatory.

Verfügbar unter: https://doi.org/10.7795/110.20190315B

5.2 ISO low air-kerma rate series

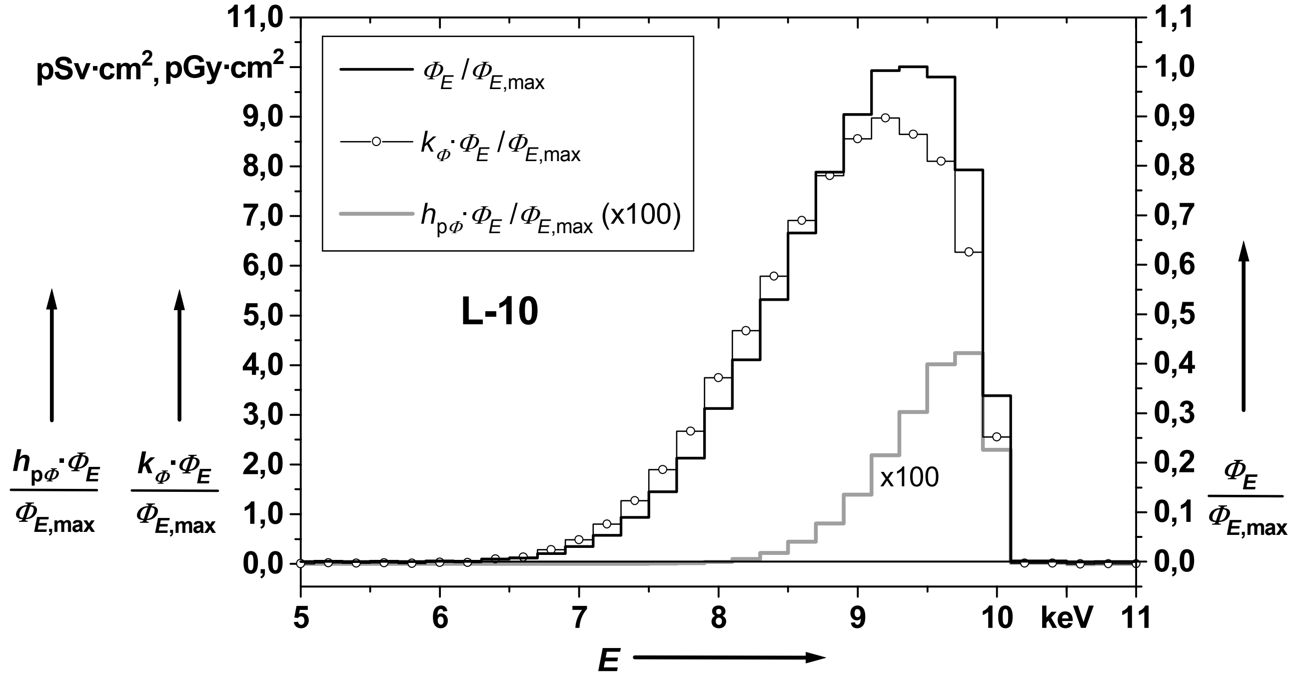

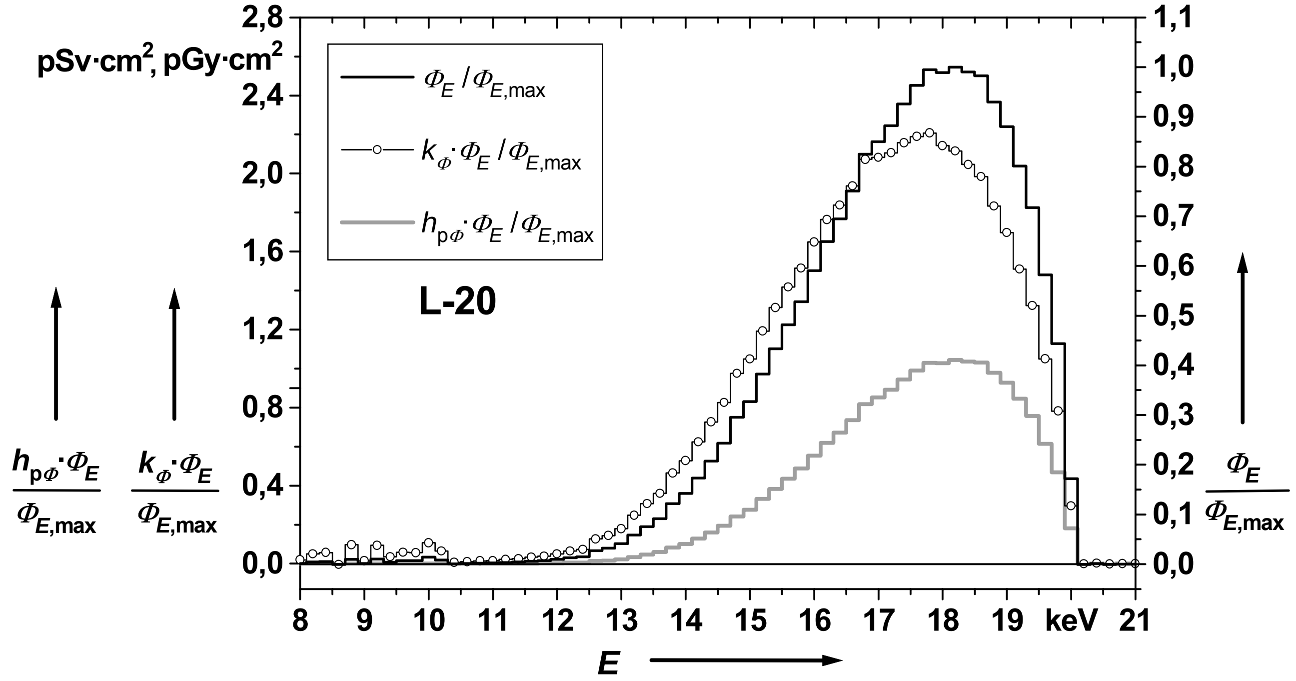

Verfügbar unter: https://doi.org/10.7795/110.20190315B

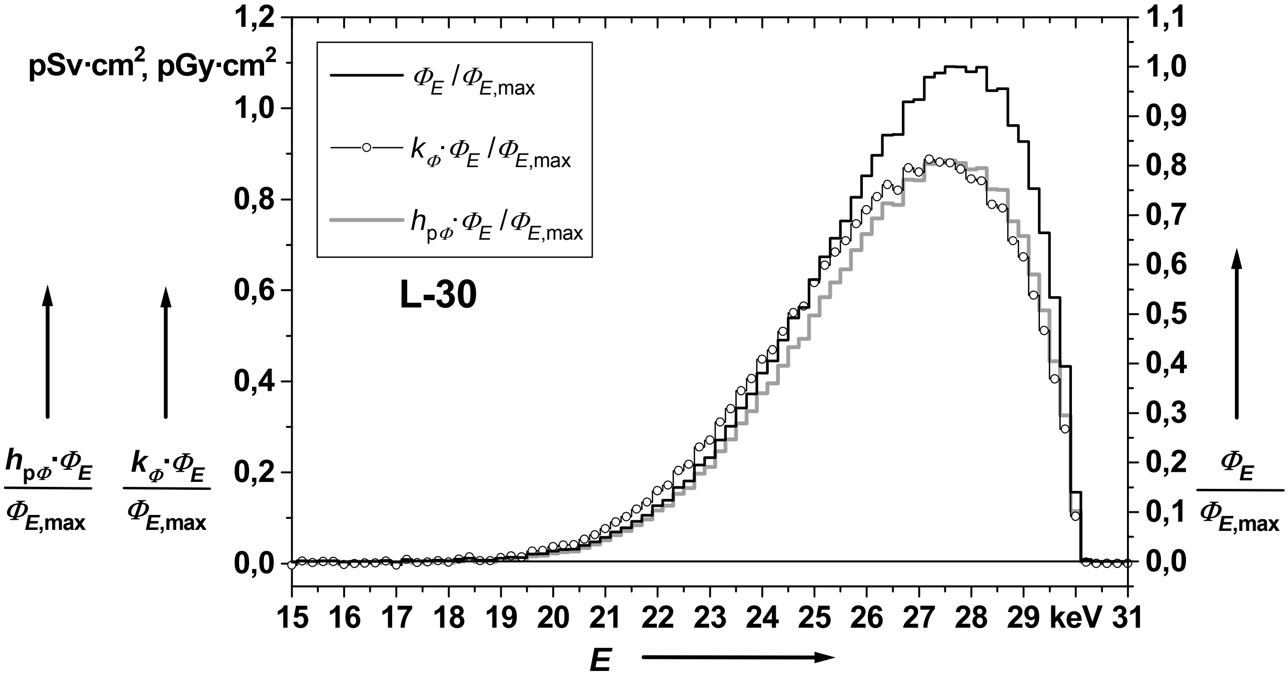

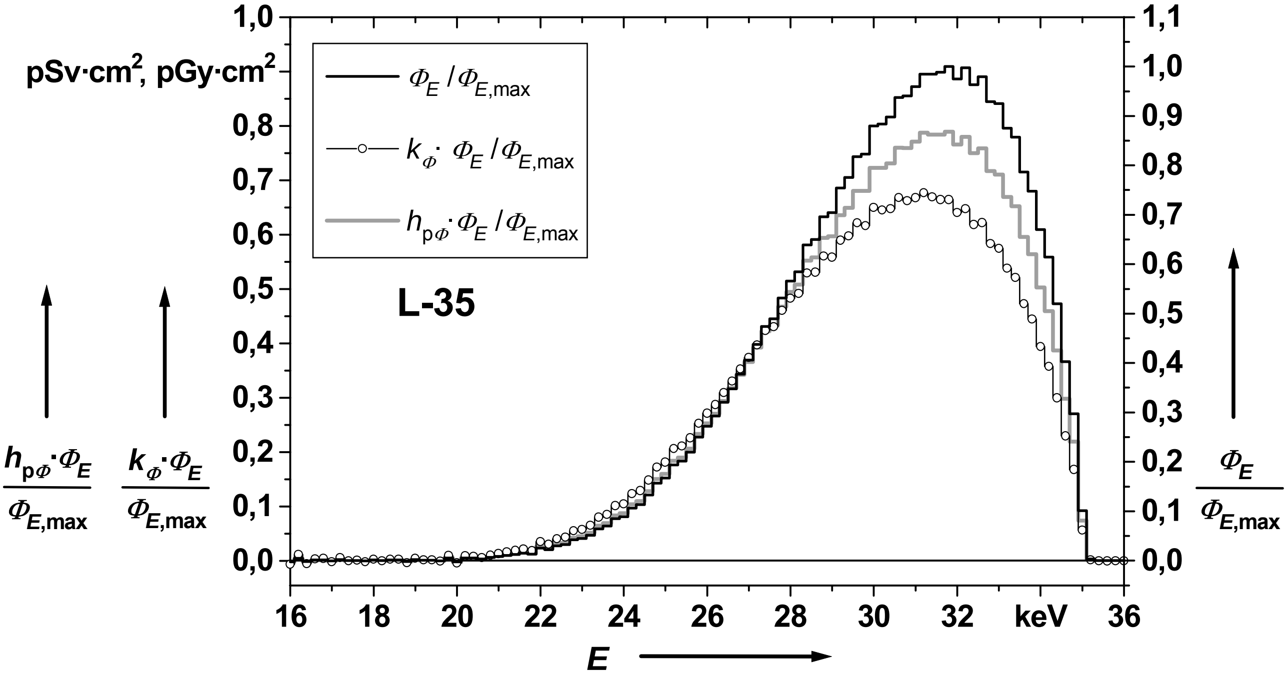

Verfügbar unter: https://doi.org/10.7795/110.20190315B

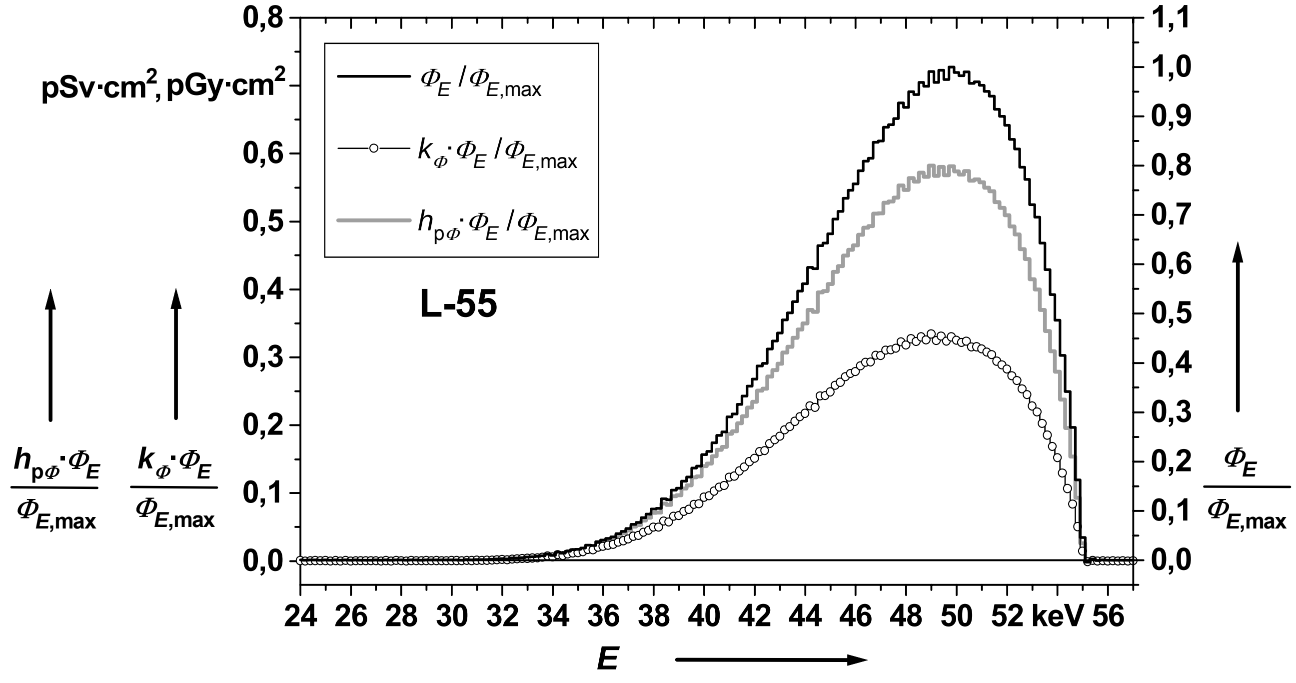

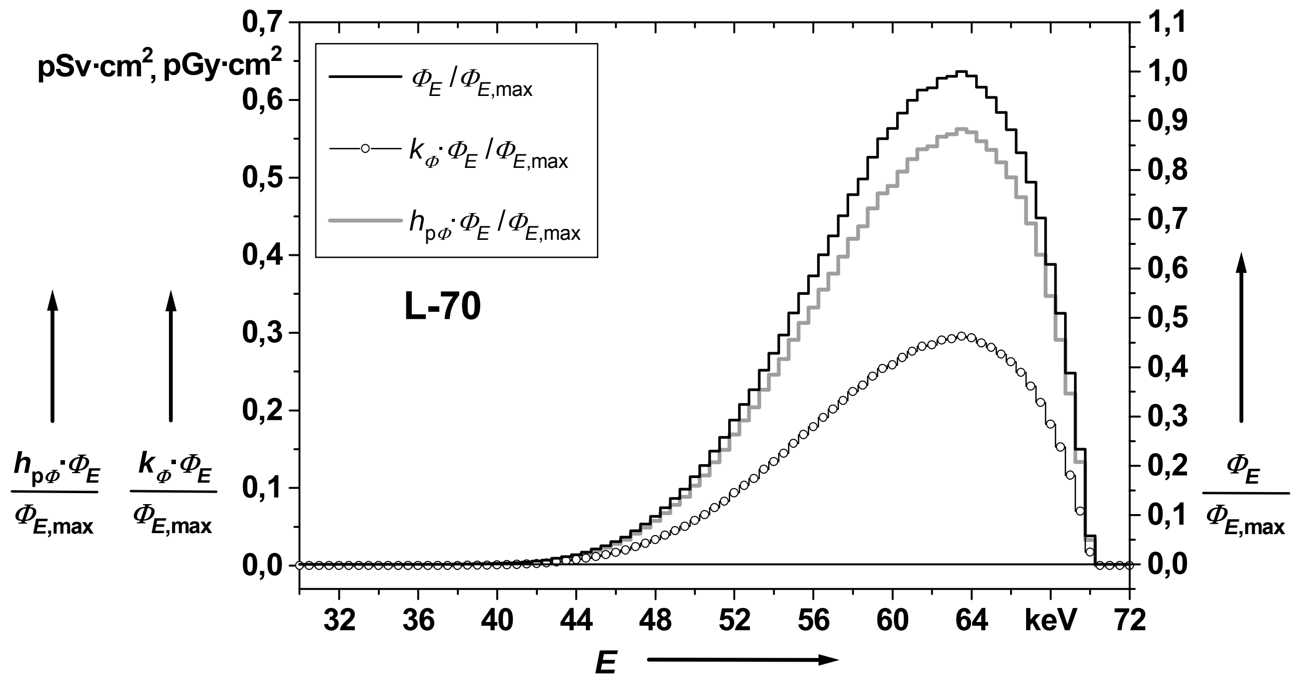

Verfügbar unter: https://doi.org/10.7795/110.20190315B

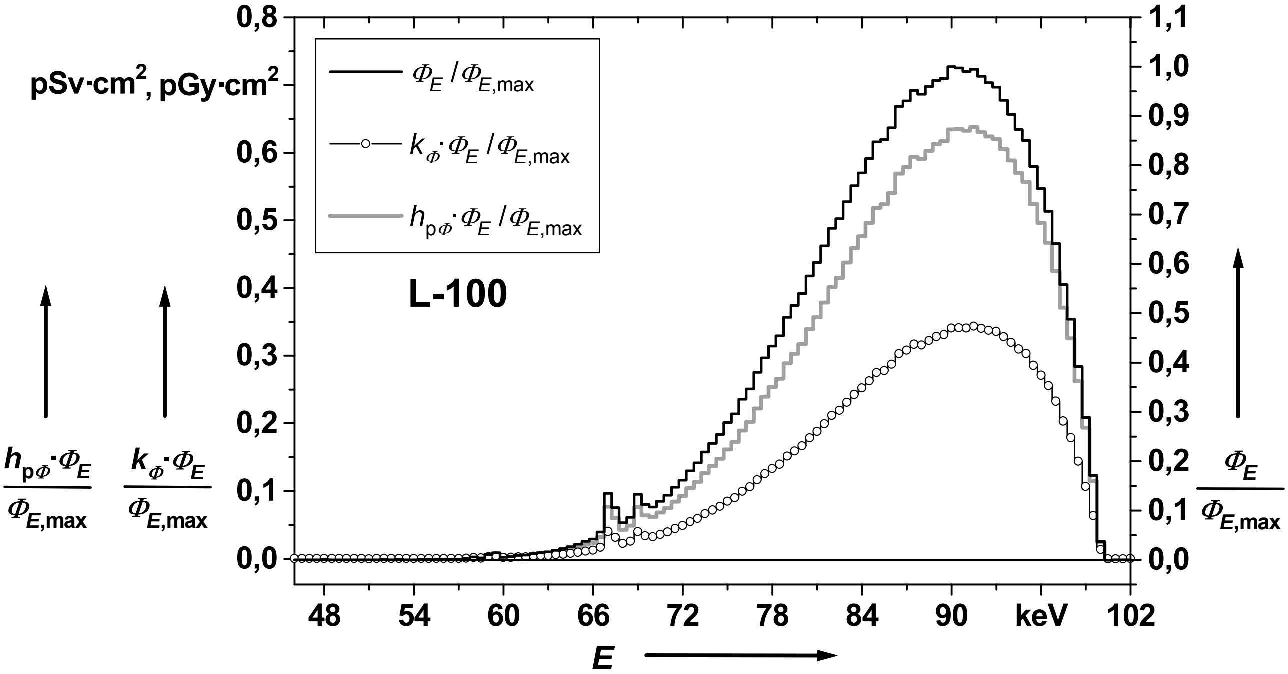

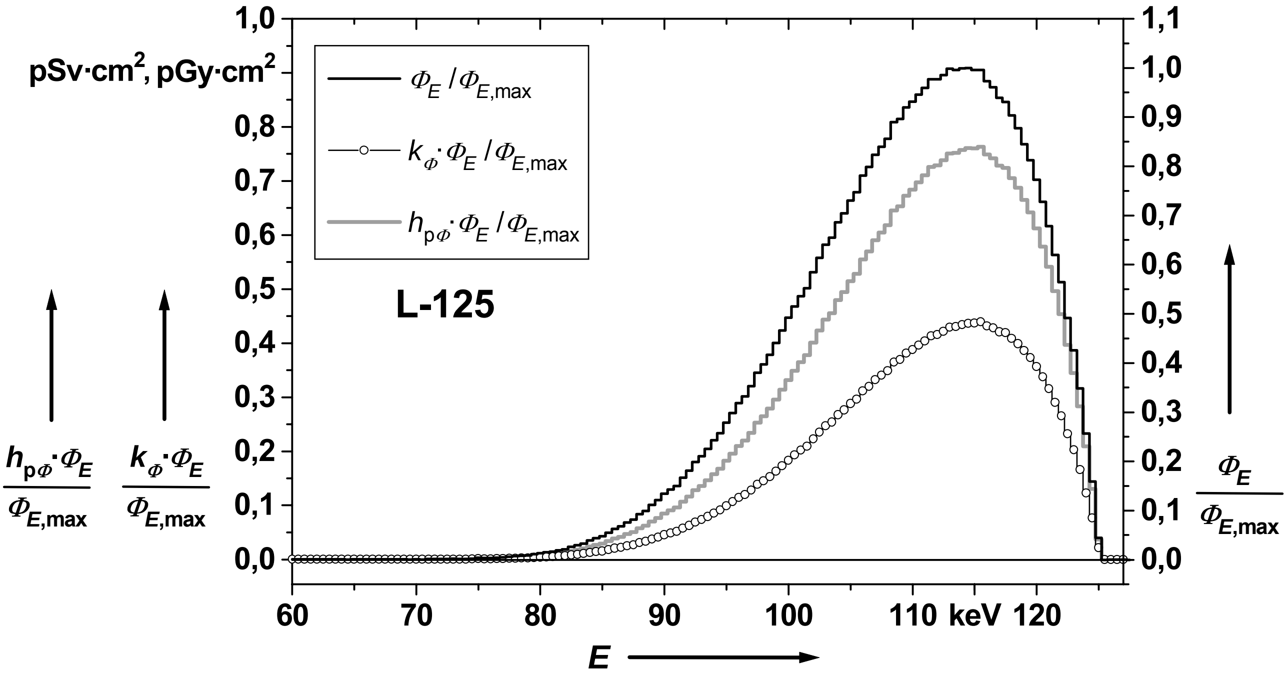

Verfügbar unter: https://doi.org/10.7795/110.20190315B

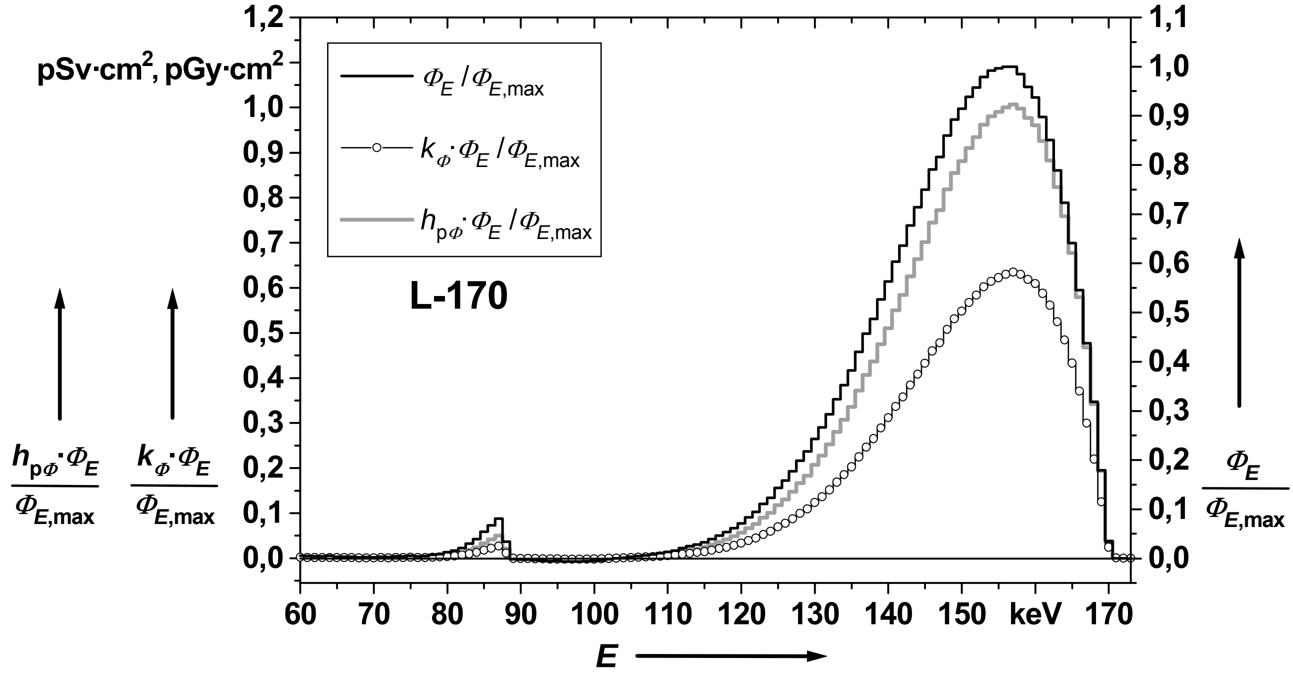

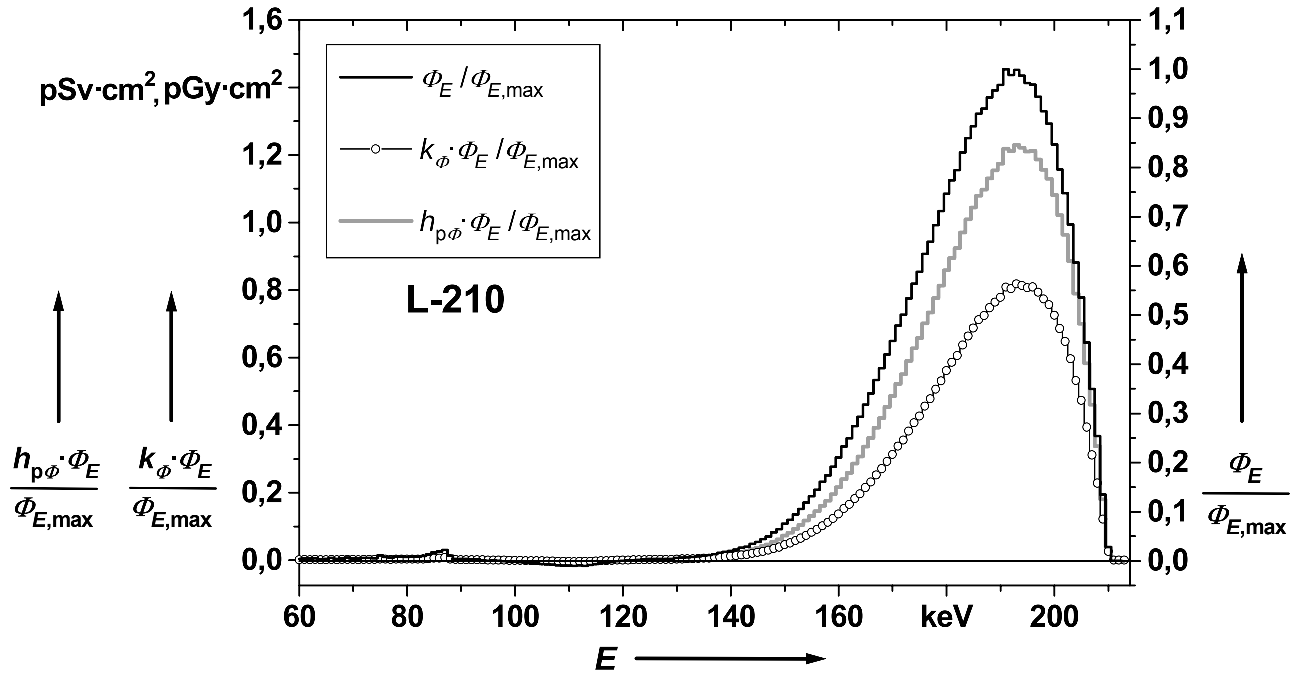

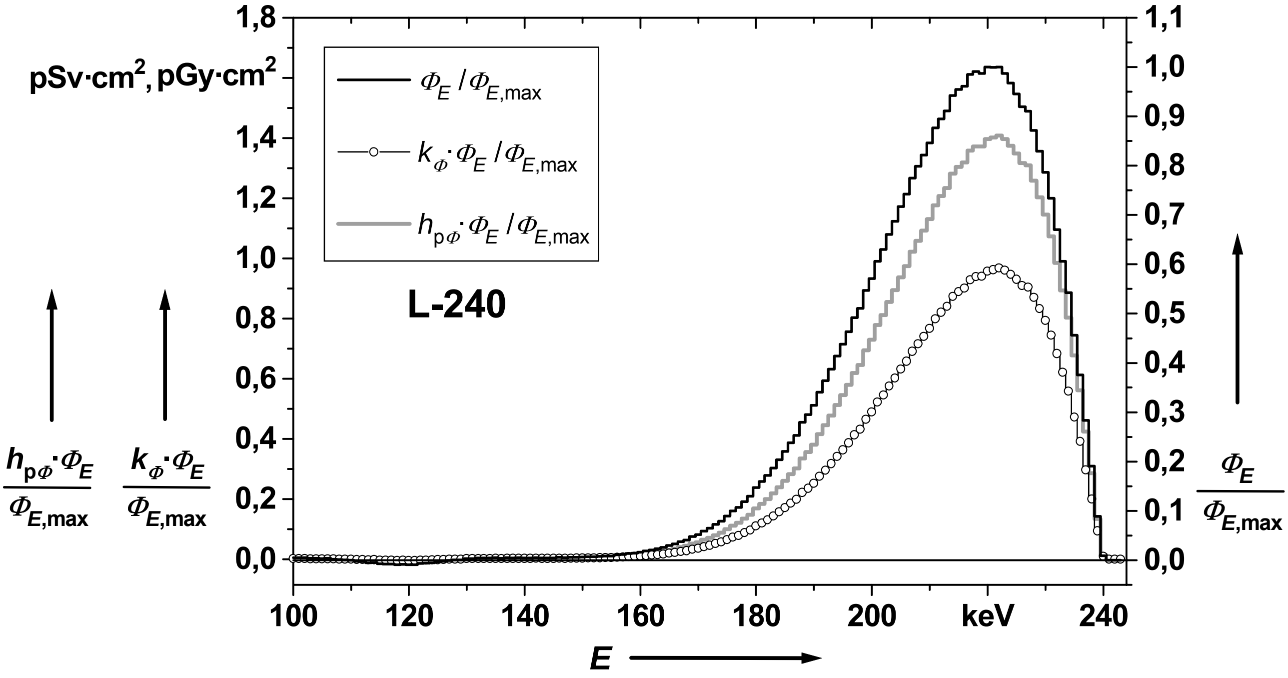

5.3 ISO narrow-spectrum and DIN A-series

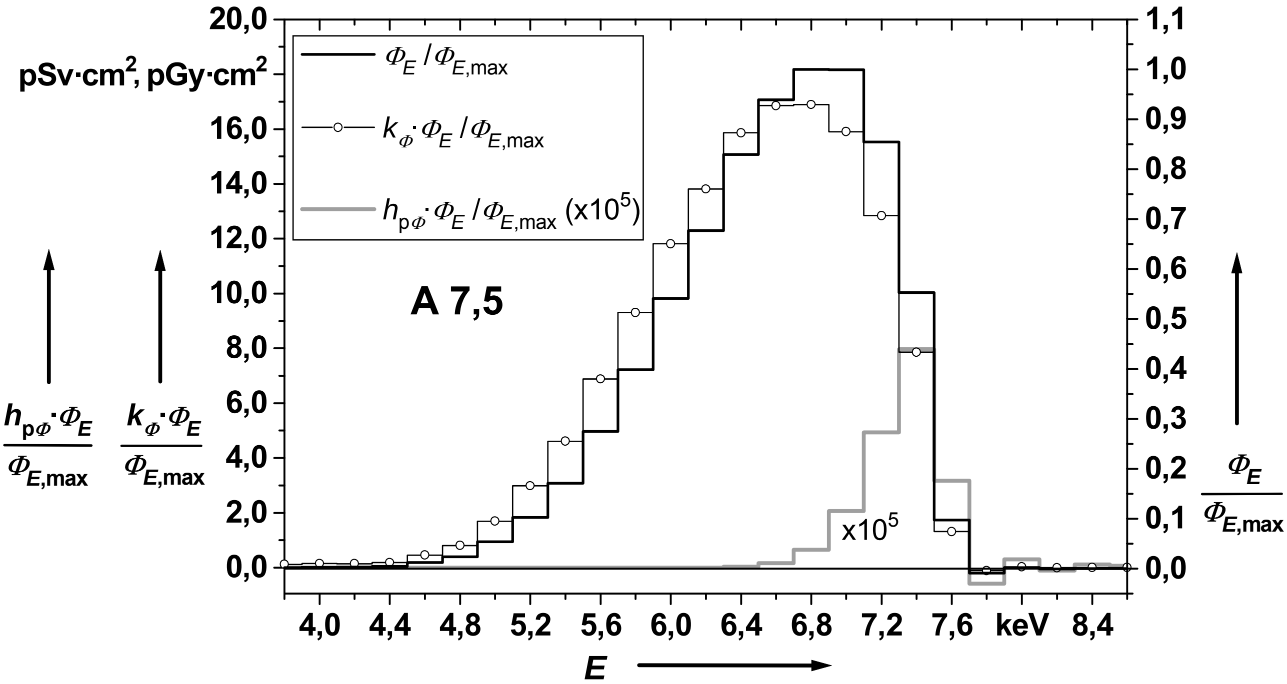

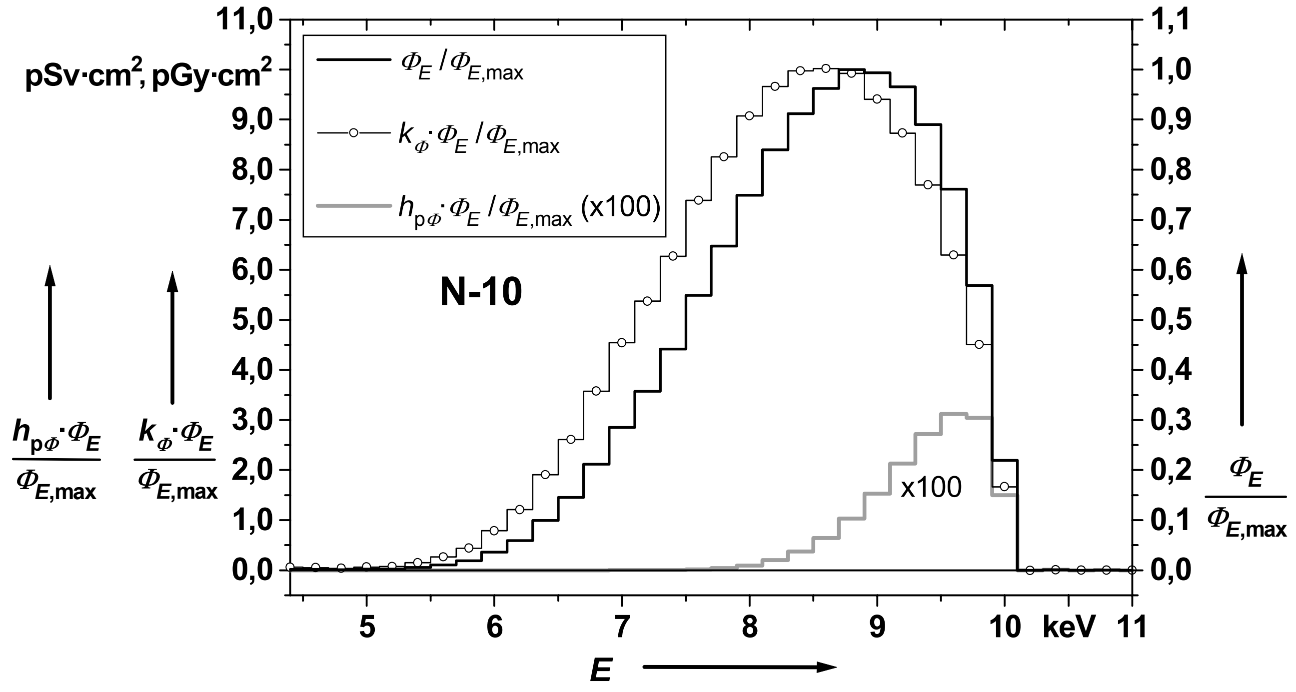

pSv·cm², pGy·cm²
$\Phi_E / \Phi_{E,\max}$
$k_\Phi \cdot \Phi_E / \Phi_{E,\max}$
$h_{p\Phi} \cdot \Phi_E / \Phi_{E,\max}$ (x100)
N-10
x100
$\frac{h_{p\Phi} \cdot \Phi_E}{\Phi_{E,\max}}$
$\frac{k_\Phi \cdot \Phi_E}{\Phi_{E,\max}}$
$\frac{\Phi_E}{\Phi_{E,\max}}$
E
keV

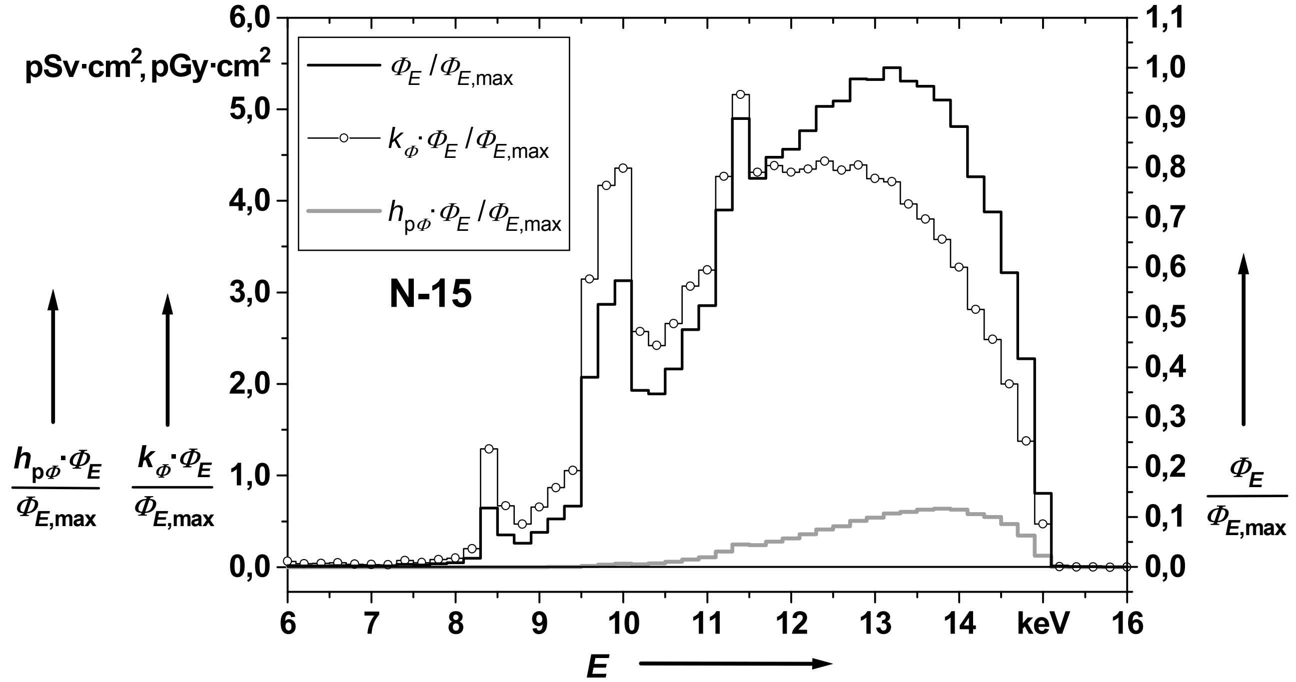

pSv·cm², pGy·cm²
$\Phi_E / \Phi_{E,\max}$
$k_\Phi \cdot \Phi_E / \Phi_{E,\max}$
$h_{p\Phi} \cdot \Phi_E / \Phi_{E,\max}$
N-15
$\frac{h_{p\Phi} \cdot \Phi_E}{\Phi_{E,\max}}$
$\frac{k_\Phi \cdot \Phi_E}{\Phi_{E,\max}}$
$\frac{\Phi_E}{\Phi_{E,\max}}$
E
keV

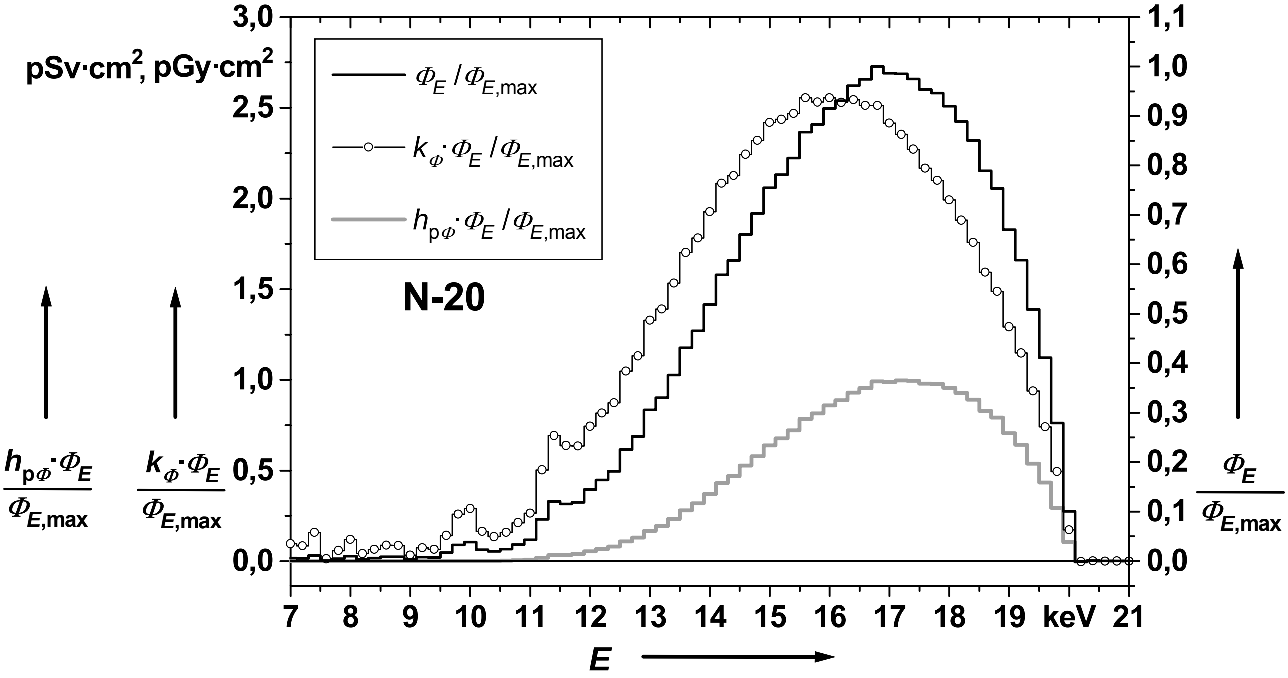

3,0
pSv·cm², pGy·cm²
2,5
2,0
1,5
1,0
0,5
0,0
$h_{p\Phi} \cdot \Phi_E / \Phi_{E,max}$
$k_{\Phi} \cdot \Phi_E / \Phi_{E,max}$
$\Phi_E / \Phi_{E,max}$
N-20
1,1
1,0
0,9
0,8
0,7
0,6
0,5
0,4
0,3
0,2
0,1
0,0
7 8 9 10 11 12 13 14 15 16 17 18 19 keV 21
E

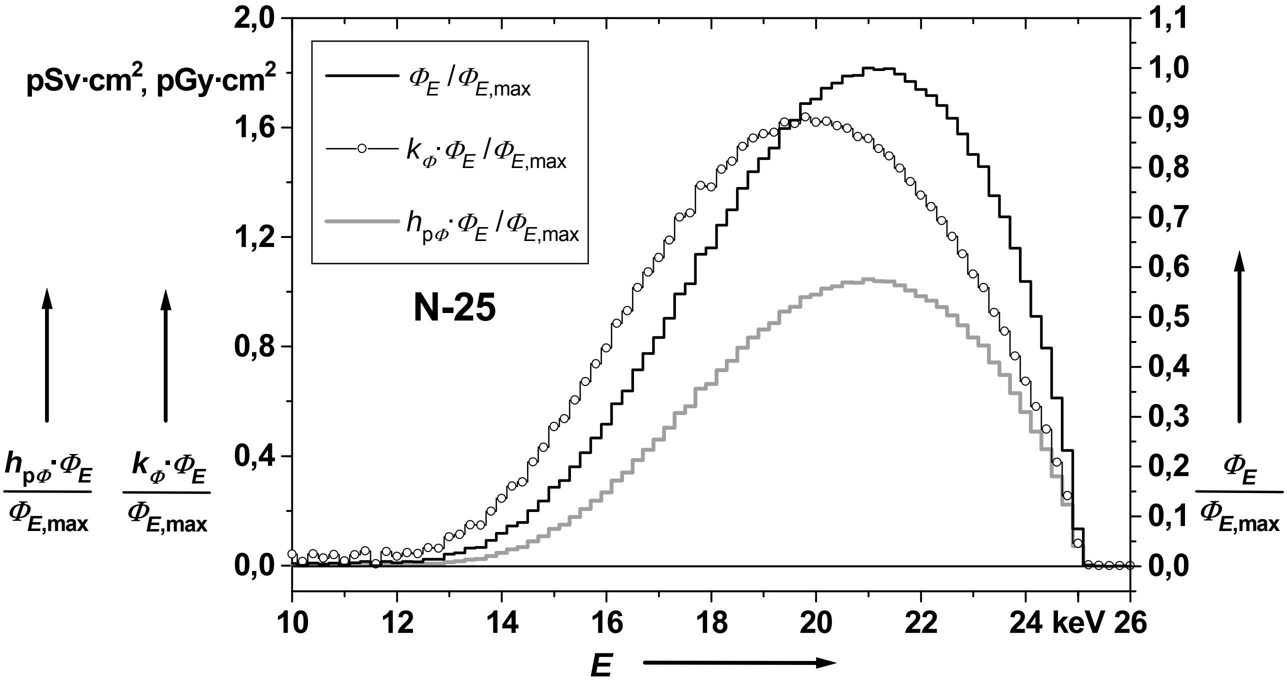

2,0
pSv·cm², pGy·cm²
1,6
1,2
0,8
0,4
0,0
$h_{p\Phi} \cdot \Phi_E / \Phi_{E,max}$
$k_{\Phi} \cdot \Phi_E / \Phi_{E,max}$
$\Phi_E / \Phi_{E,max}$
N-25
1,1
1,0
0,9
0,8
0,7
0,6
0,5
0,4
0,3
0,2
0,1
0,0
10 12 14 16 18 20 22 24 keV 26
E

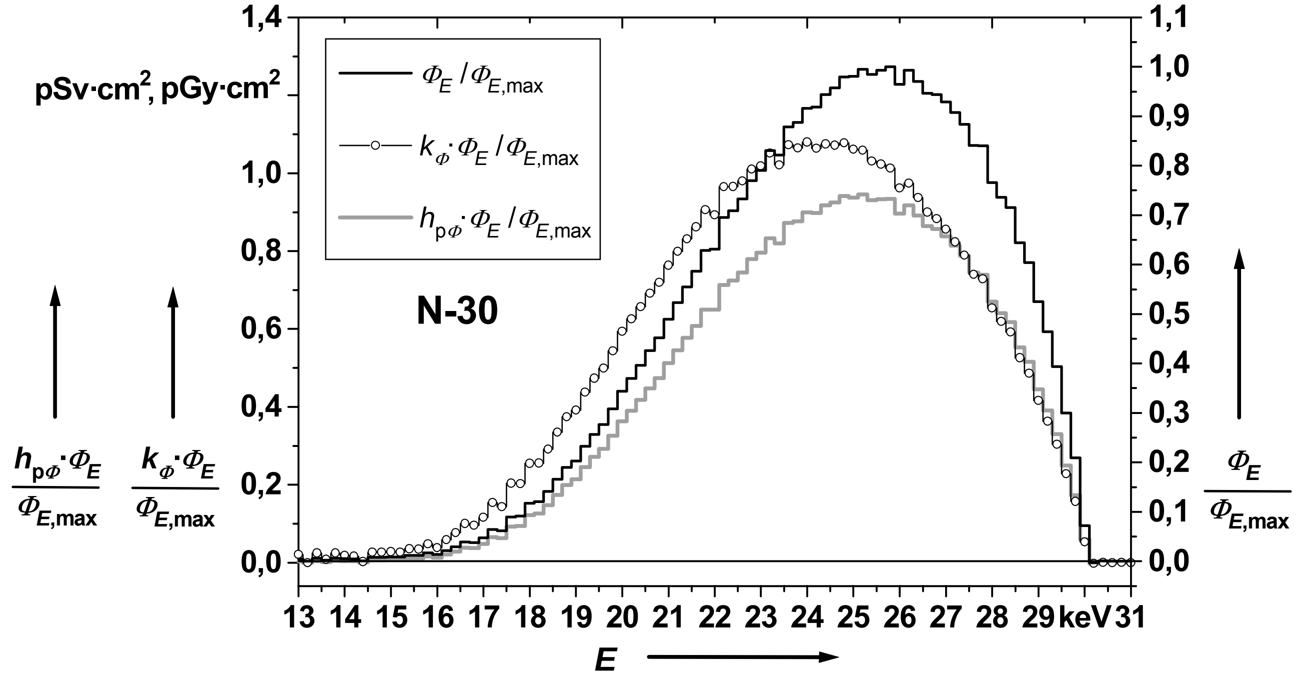

pSv·cm², pGy·cm²
N-30
Φ_E / Φ_E,max
k_Φ·Φ_E / Φ_E,max
h_pΦ·Φ_E / Φ_E,max
h_pΦ·Φ_E / Φ_E,max
k_Φ·Φ_E / Φ_E,max
Φ_E / Φ_E,max
E
keV

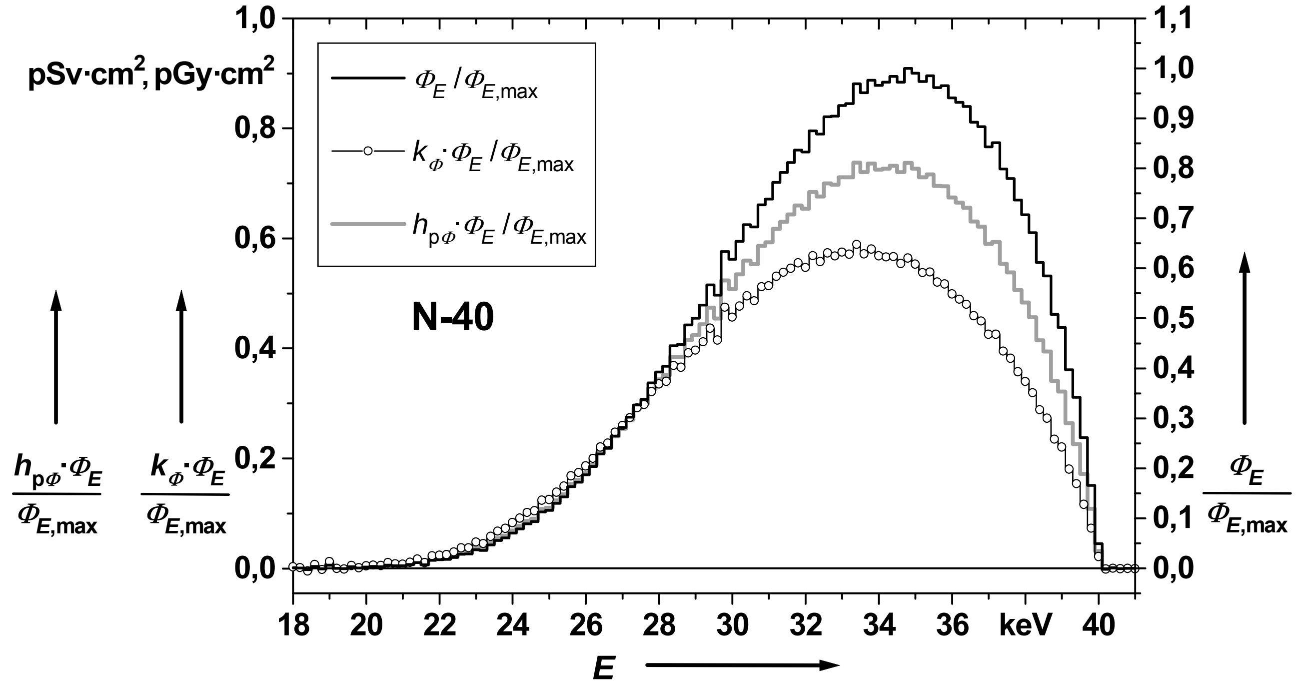

pSv·cm², pGy·cm²
N-40
Φ_E / Φ_E,max
k_Φ·Φ_E / Φ_E,max
h_pΦ·Φ_E / Φ_E,max
h_pΦ·Φ_E / Φ_E,max
k_Φ·Φ_E / Φ_E,max
Φ_E / Φ_E,max
E
keV

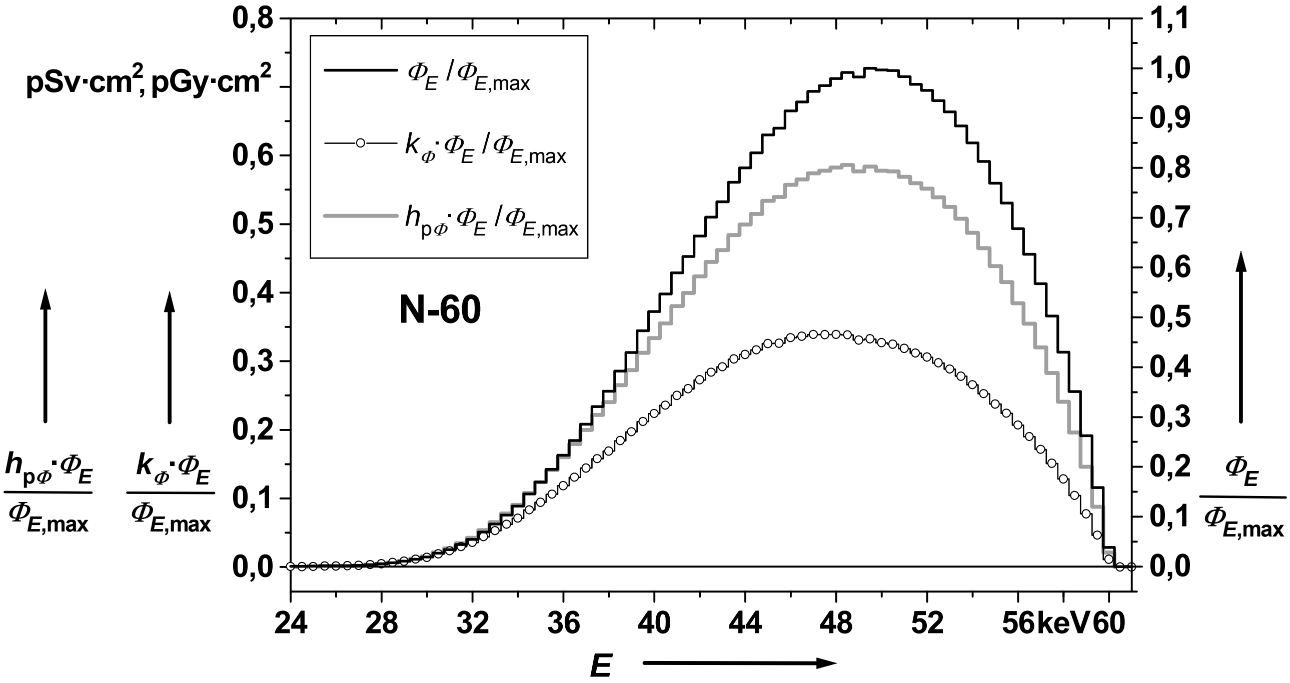
N-60
$\Phi_E / \Phi_{E,max}$
$k_\Phi \cdot \Phi_E / \Phi_{E,max}$
$h_{p\Phi} \cdot \Phi_E / \Phi_{E,max}$
pSv·cm², pGy·cm²
$\frac{h_{p\Phi} \cdot \Phi_E}{\Phi_{E,max}}$
$\frac{k_\Phi \cdot \Phi_E}{\Phi_{E,max}}$
$\frac{\Phi_E}{\Phi_{E,max}}$
E
keV

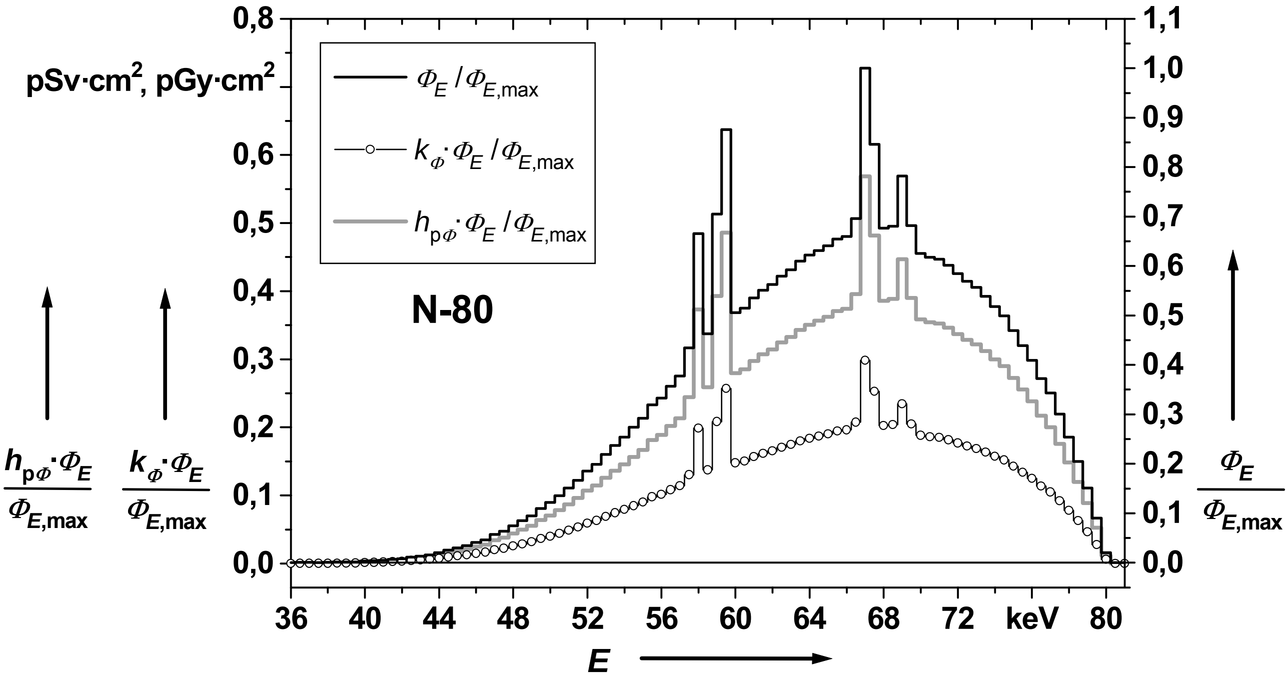
N-80
$\Phi_E / \Phi_{E,max}$
$k_\Phi \cdot \Phi_E / \Phi_{E,max}$
$h_{p\Phi} \cdot \Phi_E / \Phi_{E,max}$
pSv·cm², pGy·cm²
$\frac{h_{p\Phi} \cdot \Phi_E}{\Phi_{E,max}}$
$\frac{k_\Phi \cdot \Phi_E}{\Phi_{E,max}}$
$\frac{\Phi_E}{\Phi_{E,max}}$
E
keV

Verfügbar unter: https://doi.org/10.7795/110.20190315B

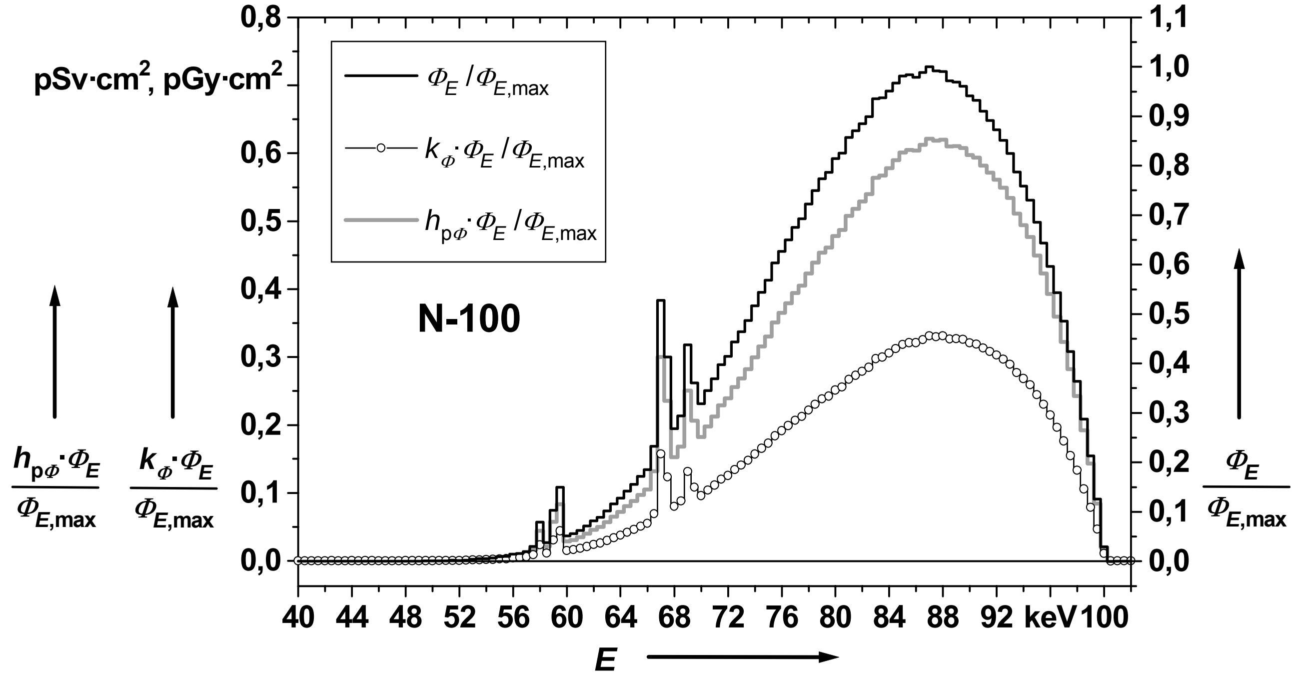

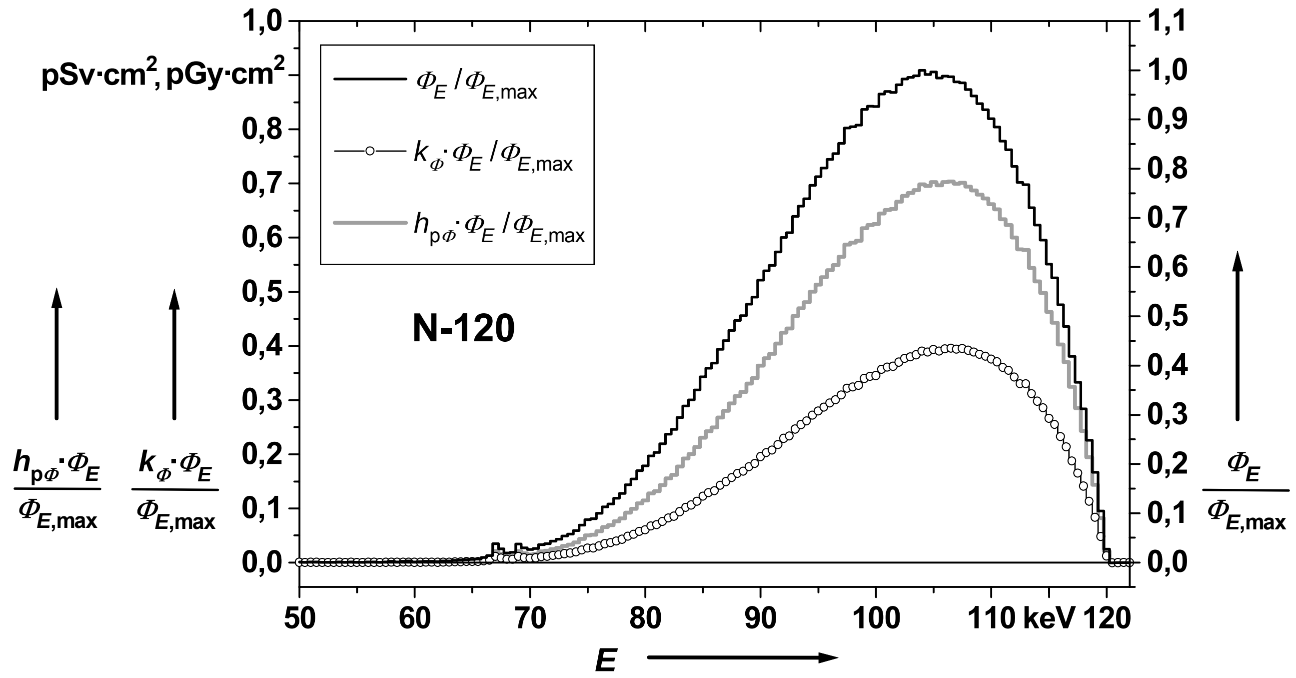

Verfügbar unter: https://doi.org/10.7795/110.20190315B

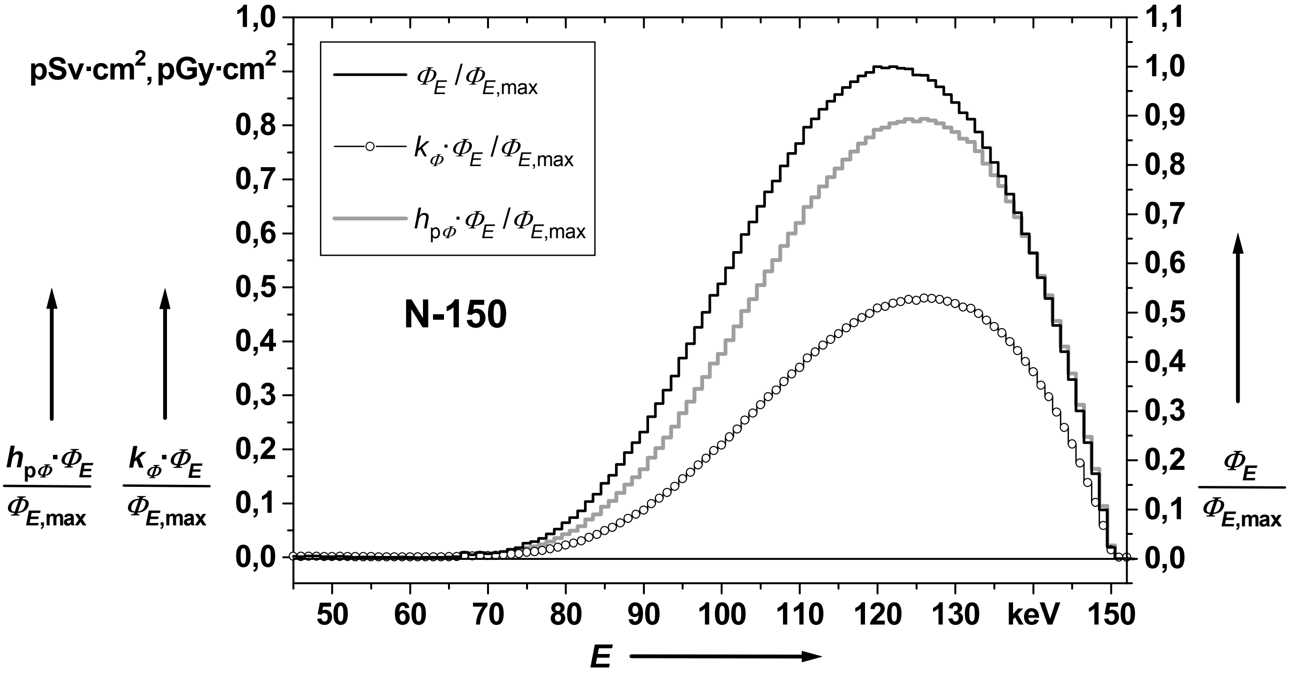

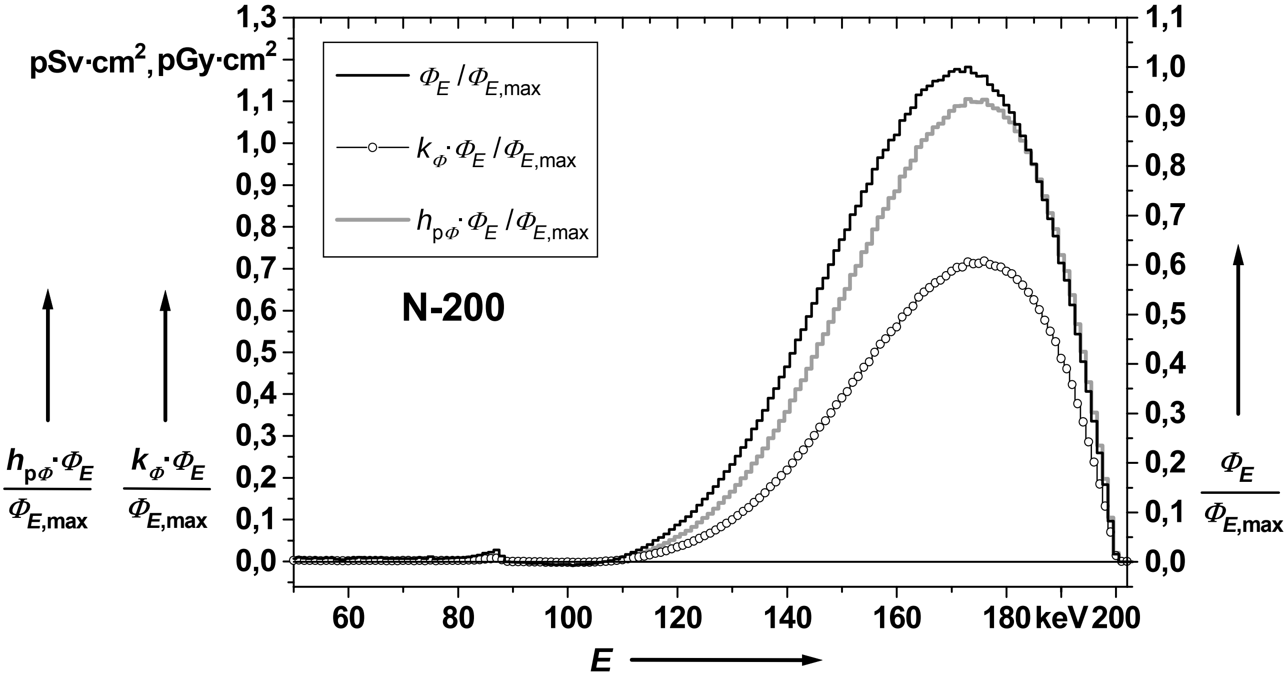

Verfügbar unter: https://doi.org/10.7795/110.20190315B

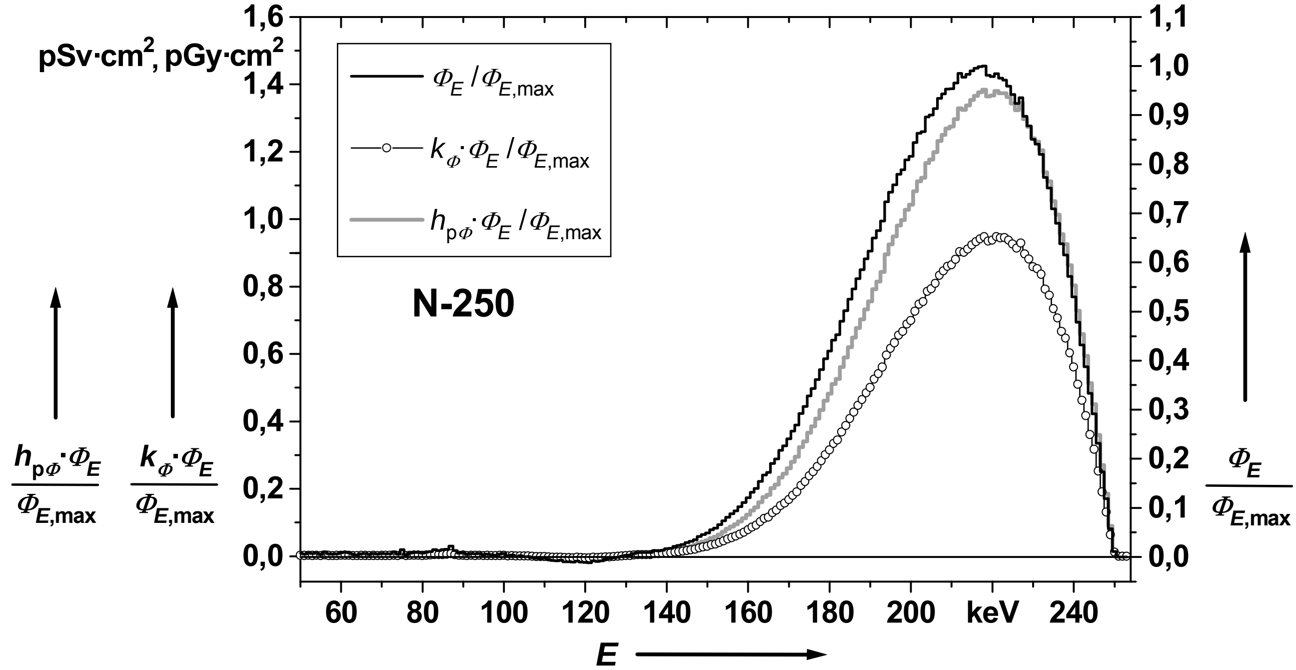

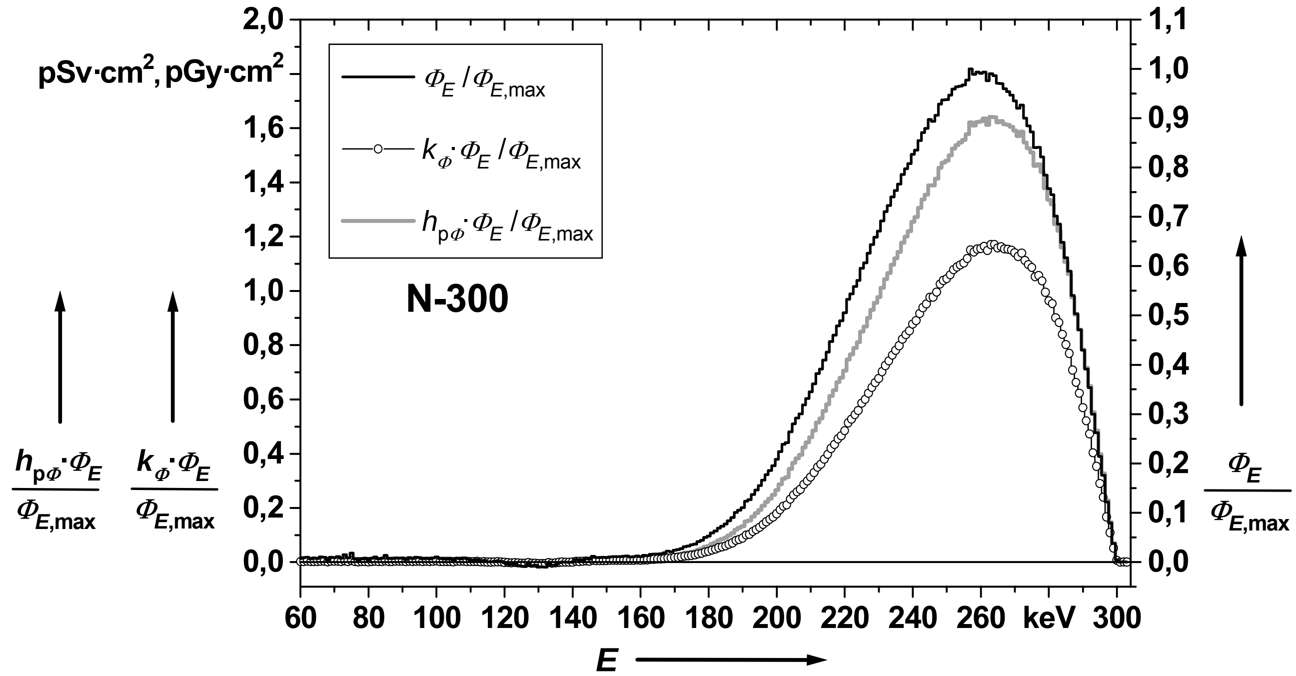

5.4 ISO wide-spectrum and DIN B-series

The radiation qualities B 7,5, B 10, B 15 and B 20 are identical with A 7,5, N-10, N-15 and N-20, respectively. The spectra of these radiation qualities are shown in Section 5.3.

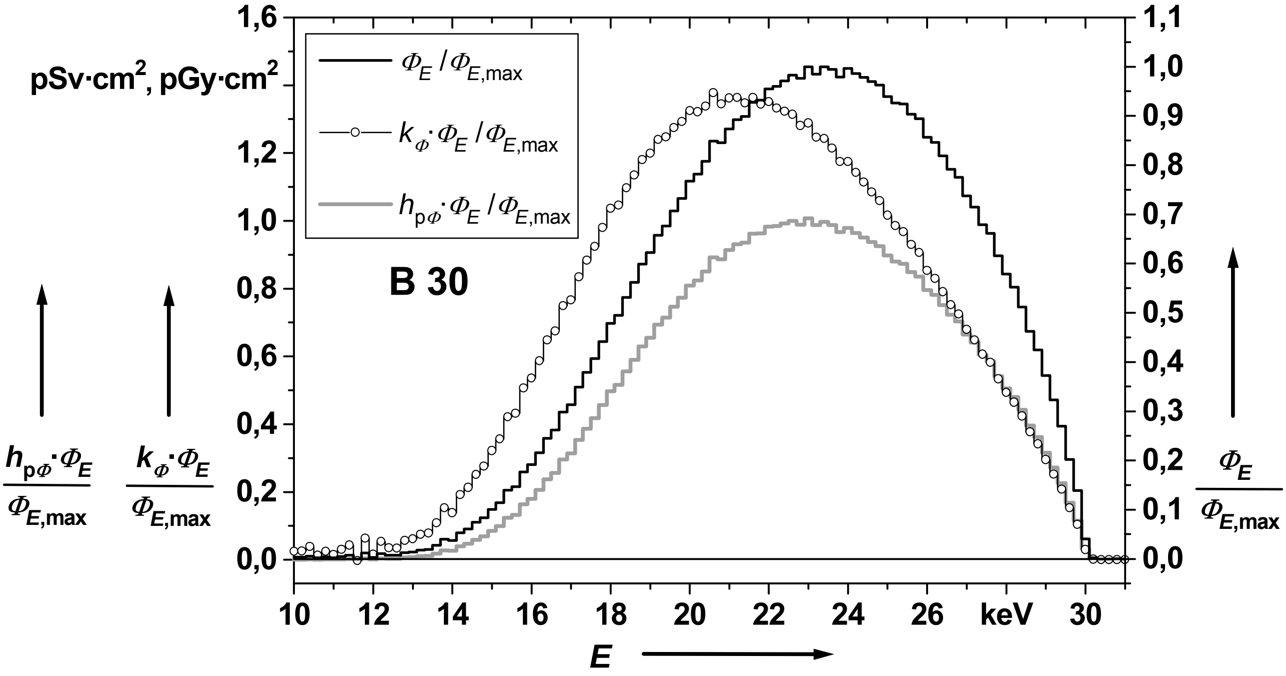

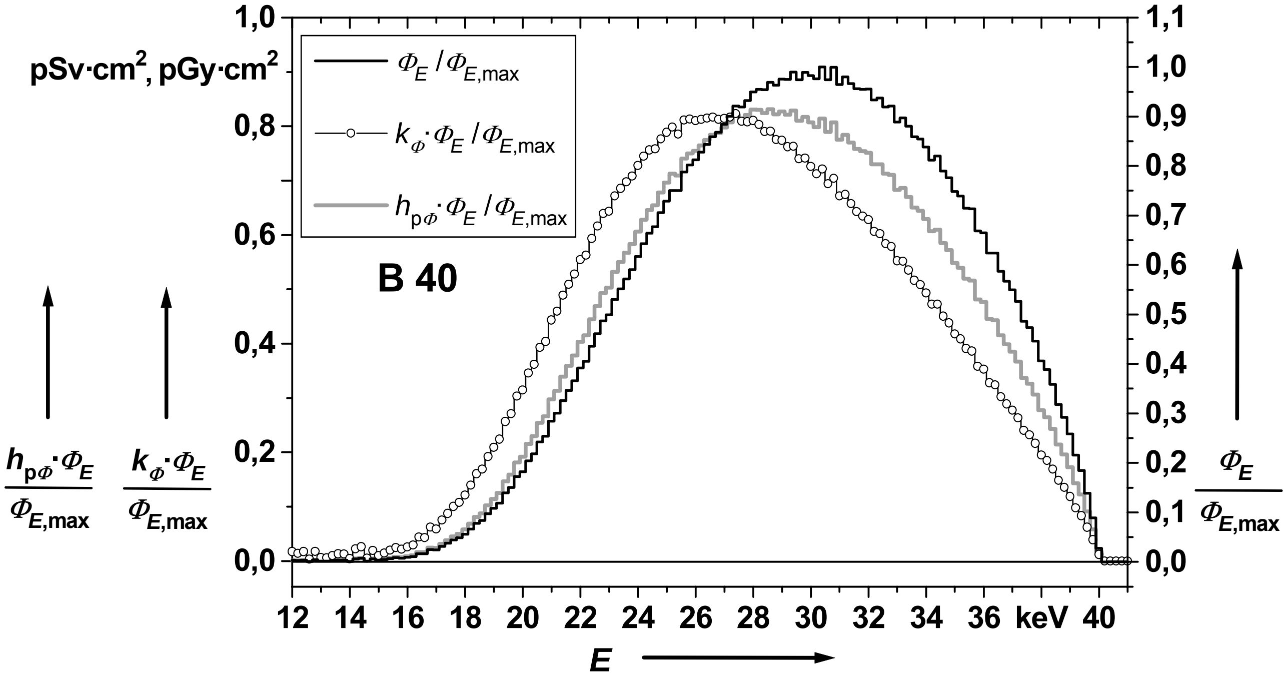

Verfügbar unter: https://doi.org/10.7795/110.20190315B

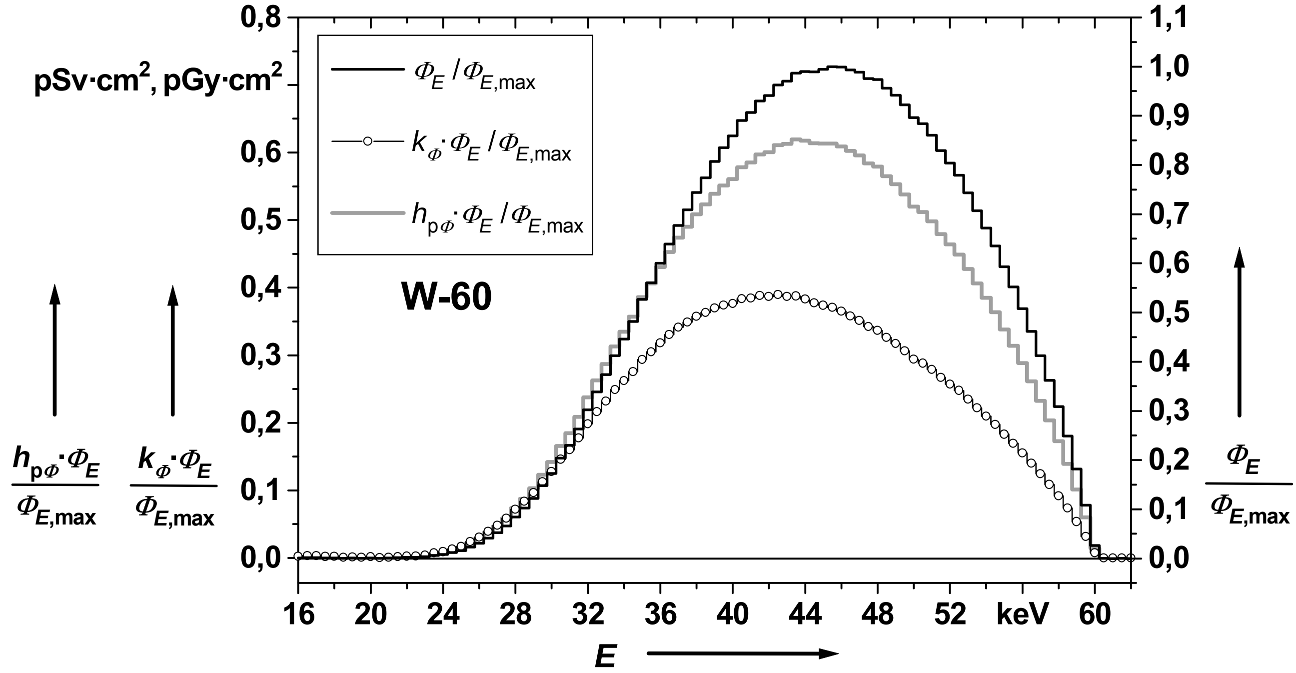

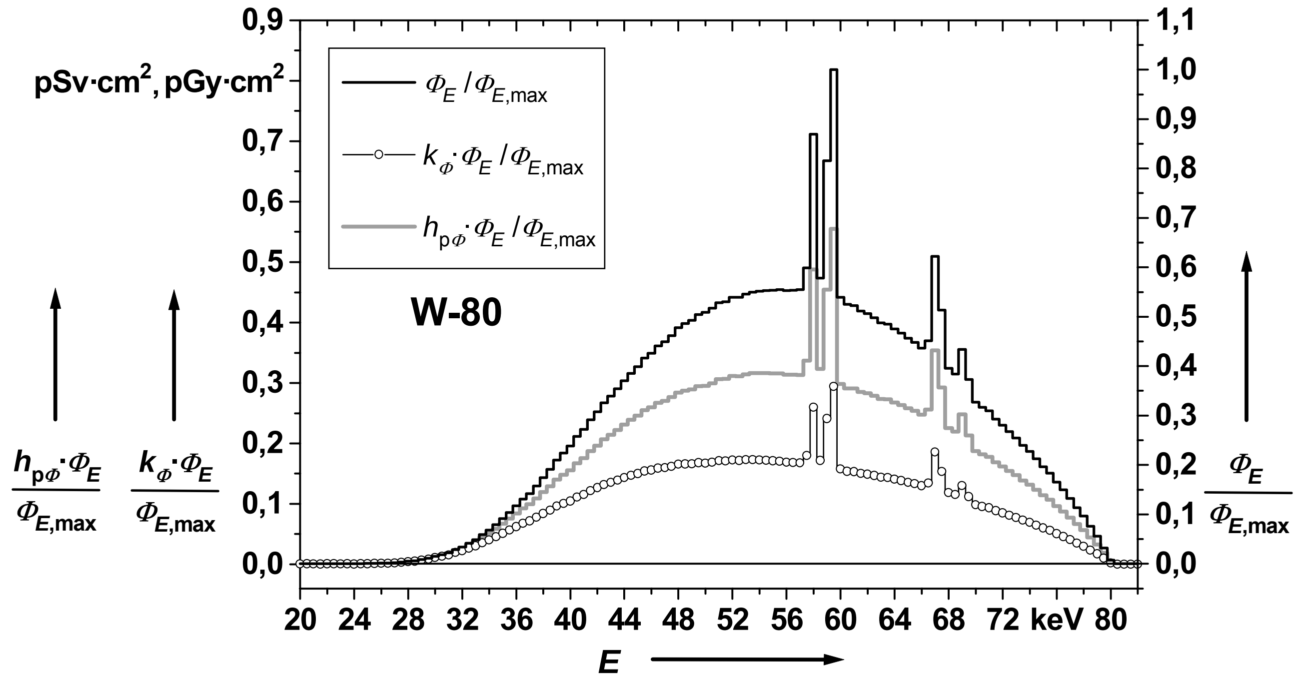

Verfügbar unter: https://doi.org/10.7795/110.20190315B

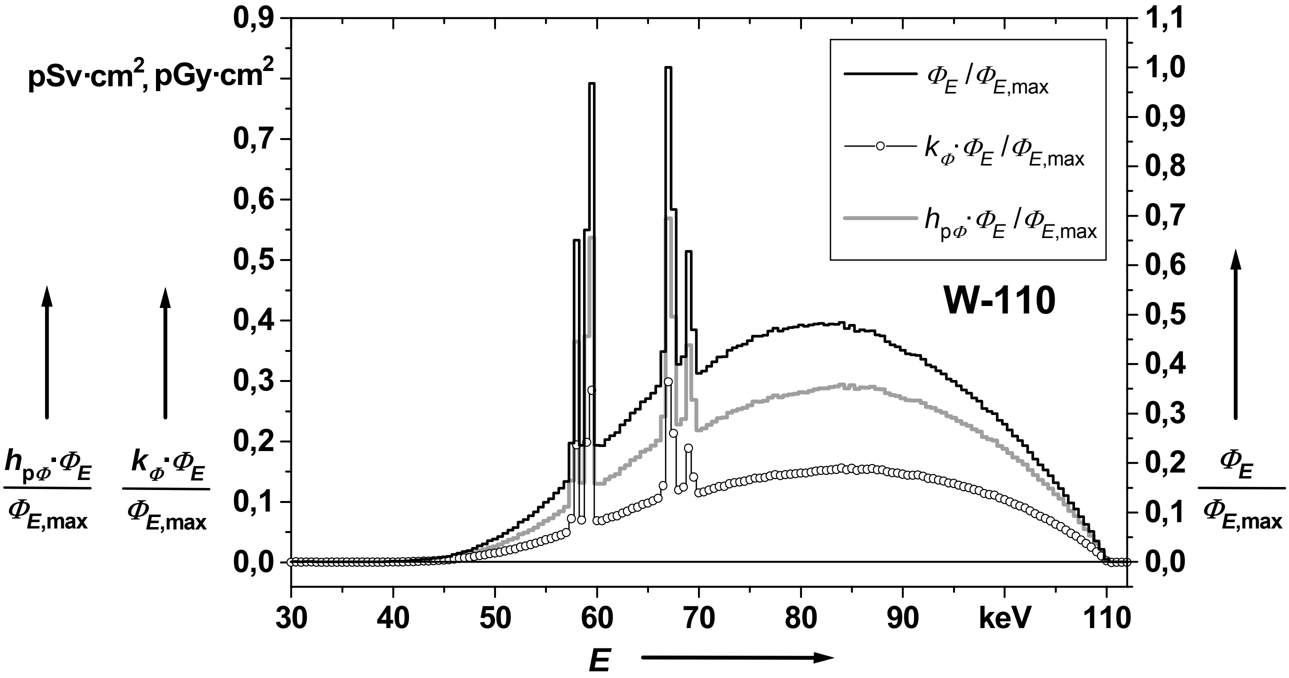

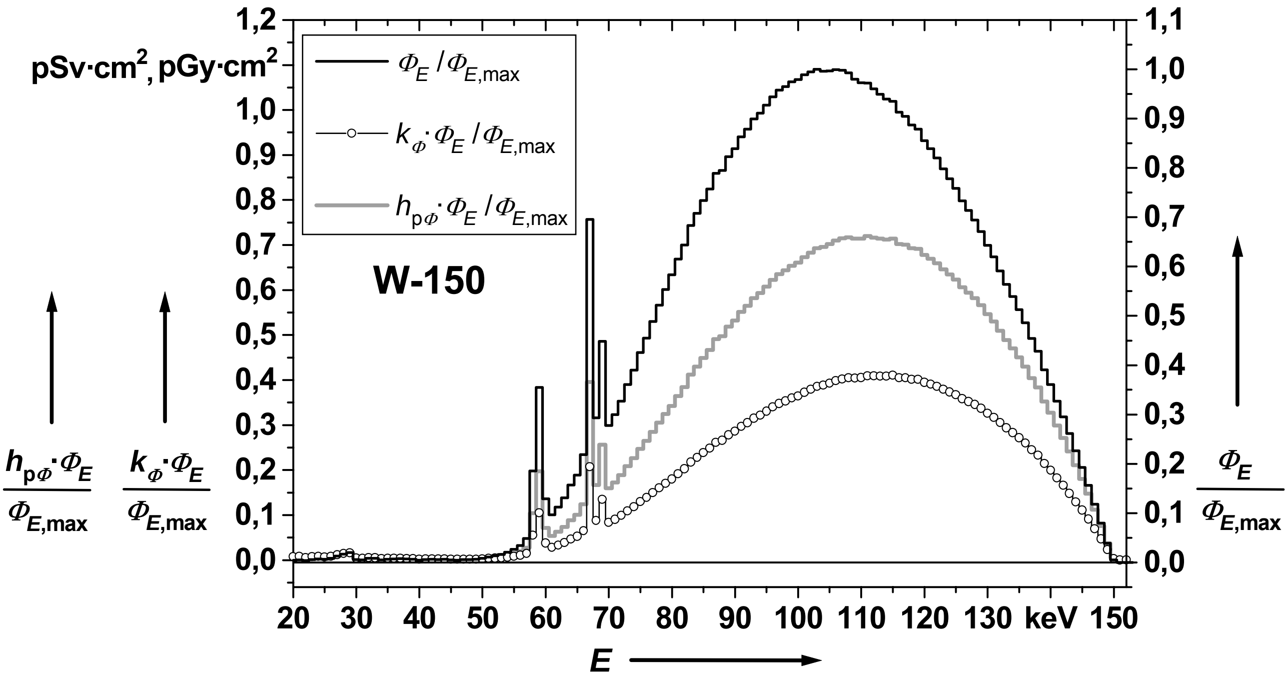

Verfügbar unter: https://doi.org/10.7795/110.20190315B

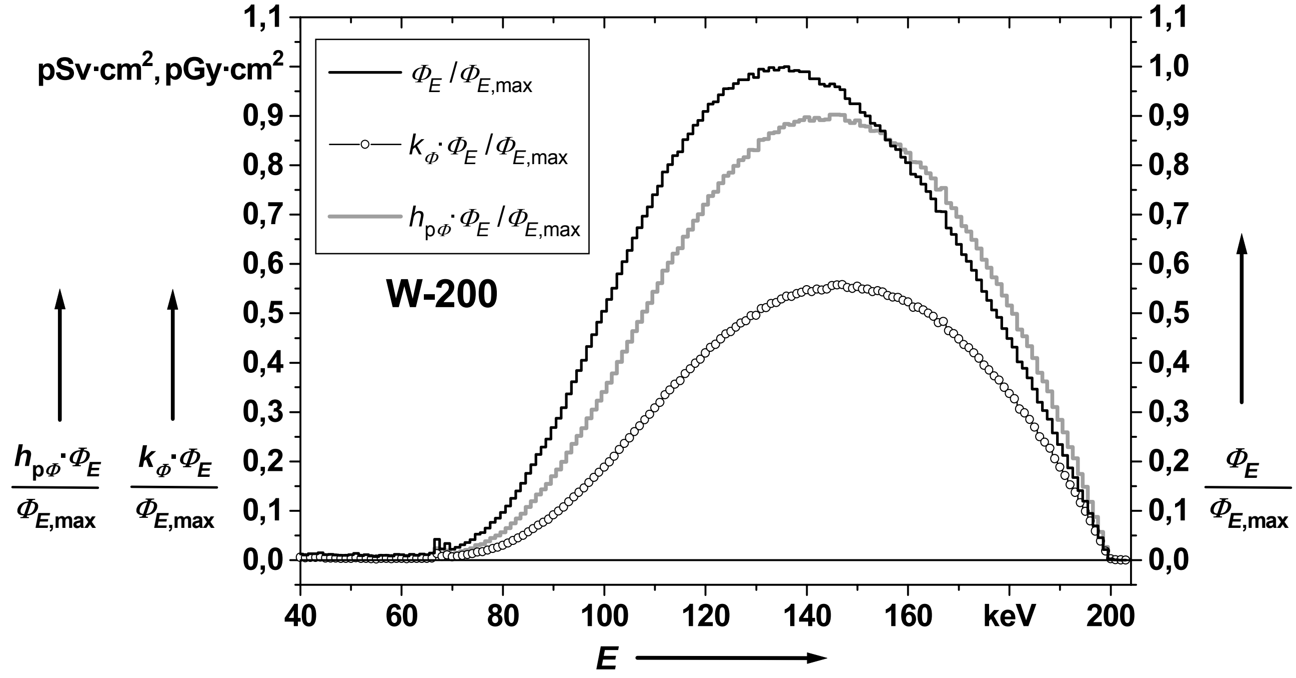

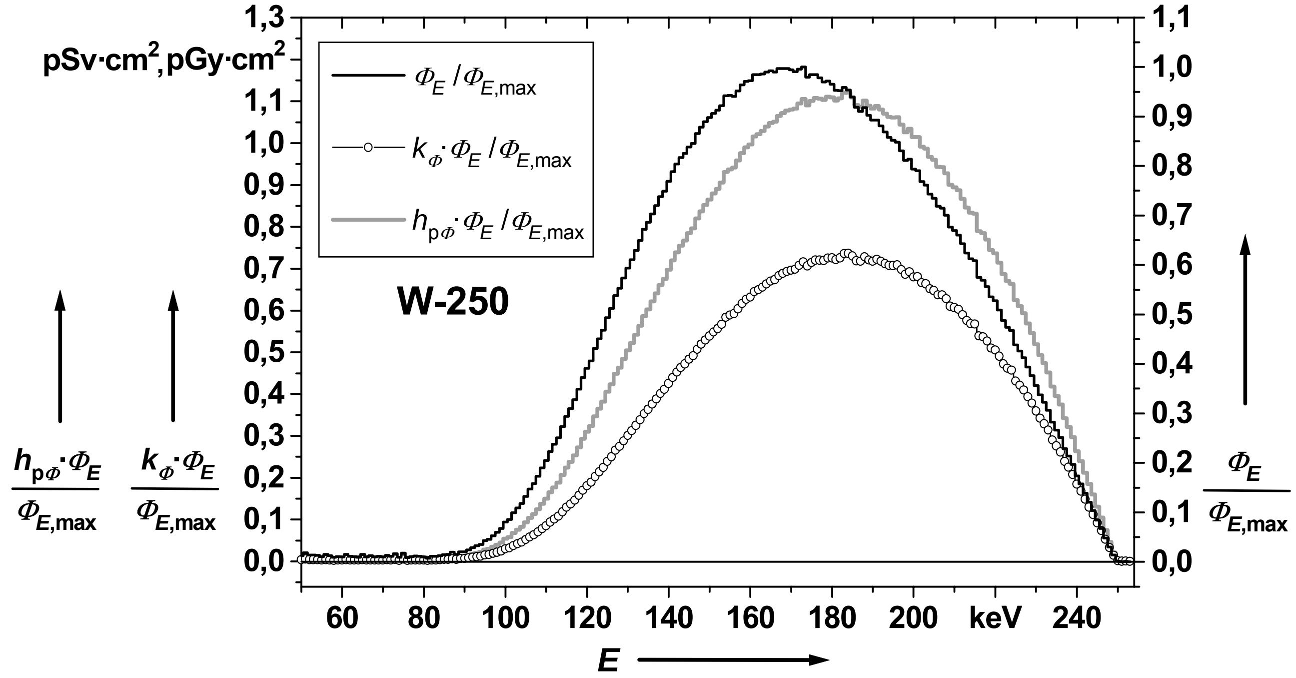

Verfügbar unter: https://doi.org/10.7795/110.20190315B

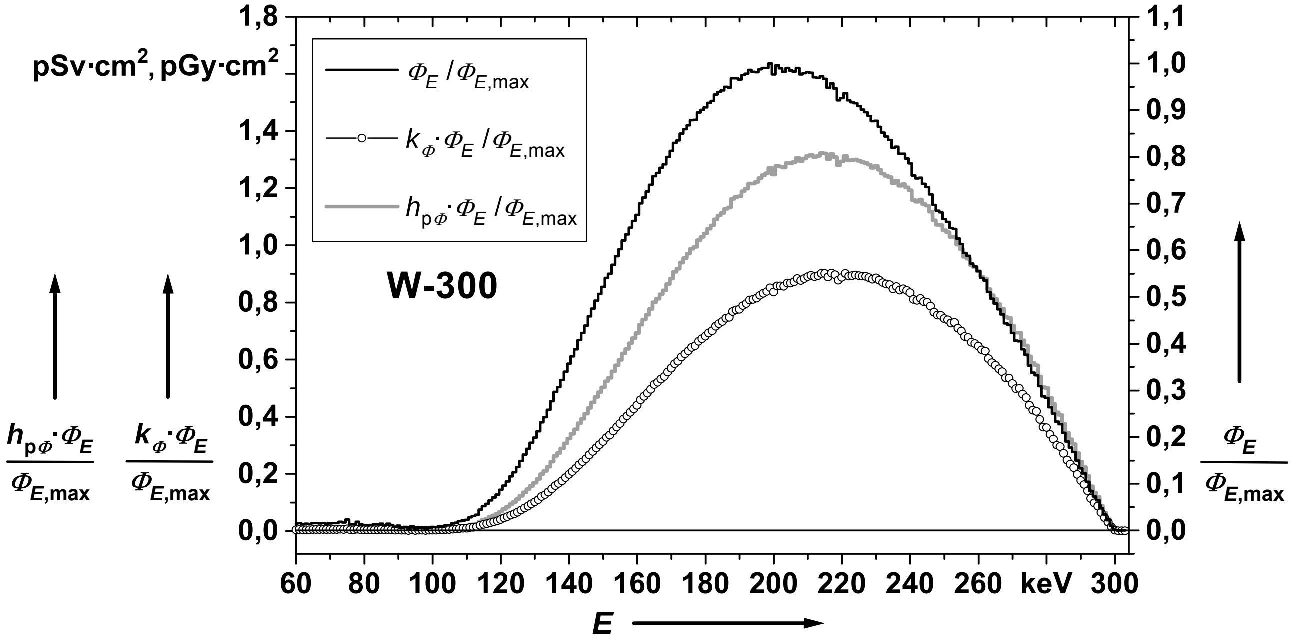

5.5 ISO high air-kerma rate and DIN C-series

The radiation quality C 7,5 is identical with A 7,5. The spectrum is shown in Section 5.3.

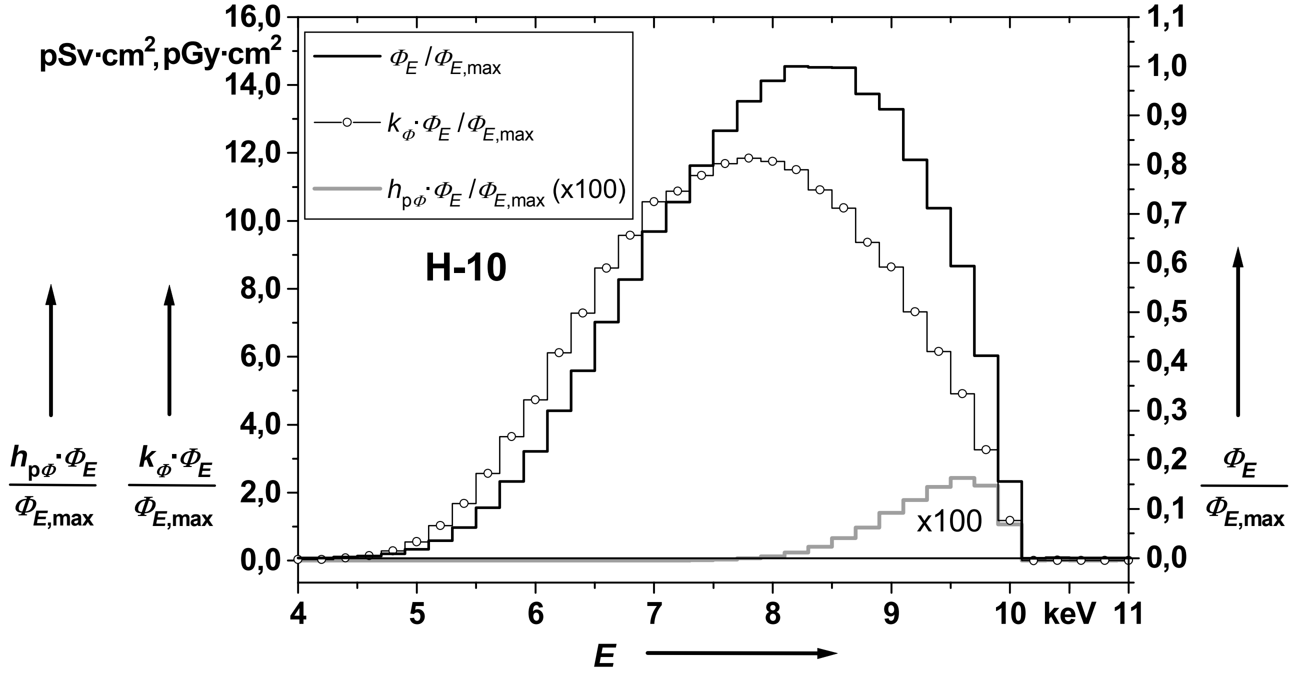

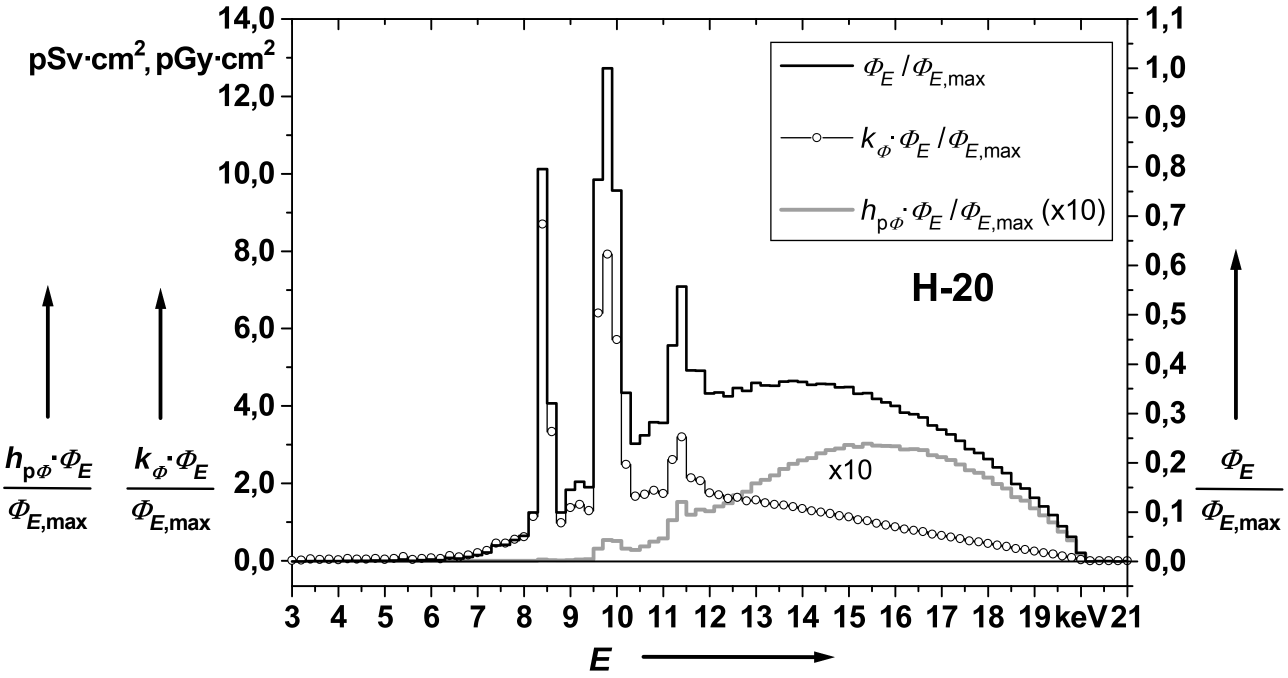
pSv·cm², pGy·cm²
$\Phi_E / \Phi_{E,\max}$
$k_\Phi \cdot \Phi_E / \Phi_{E,\max}$
$h_{p\Phi} \cdot \Phi_E / \Phi_{E,\max}$ (x10)
H-20
x10
$\frac{h_{p\Phi} \cdot \Phi_E}{\Phi_{E,\max}}$
$\frac{k_\Phi \cdot \Phi_E}{\Phi_{E,\max}}$
$\frac{\Phi_E}{\Phi_{E,\max}}$
keV
E

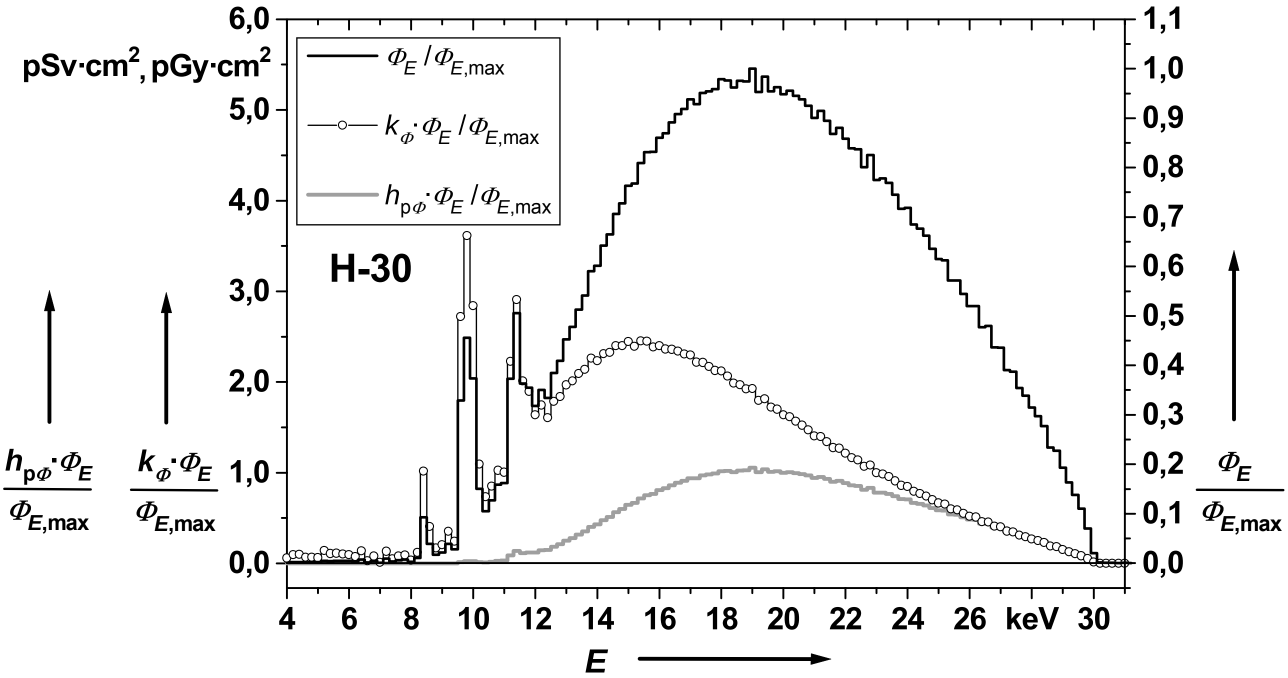
pSv·cm², pGy·cm²
$\Phi_E / \Phi_{E,\max}$
$k_\Phi \cdot \Phi_E / \Phi_{E,\max}$
$h_{p\Phi} \cdot \Phi_E / \Phi_{E,\max}$
H-30
$\frac{h_{p\Phi} \cdot \Phi_E}{\Phi_{E,\max}}$
$\frac{k_\Phi \cdot \Phi_E}{\Phi_{E,\max}}$
$\frac{\Phi_E}{\Phi_{E,\max}}$
keV
E

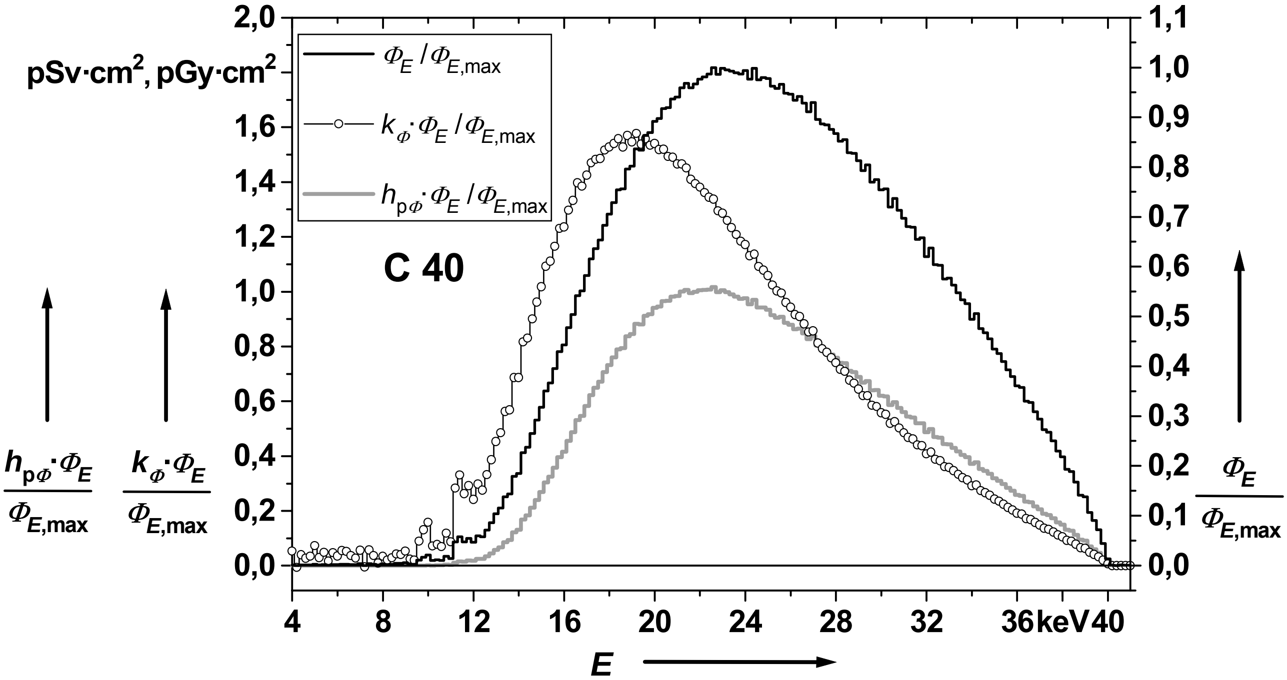

2,0
pSv·cm², pGy·cm²
1,6
1,4
1,2
1,0
0,8
0,6
0,4
0,2
0,0
$h_{p\Phi}\cdot\Phi_E$ / $\Phi_{E,max}$
$k_\Phi\cdot\Phi_E$ / $\Phi_{E,max}$
Φ_E / $\Phi_{E,max}$
$k_\Phi\cdot\Phi_E$ / $\Phi_{E,max}$
$h_{p\Phi}\cdot\Phi_E$ / $\Phi_{E,max}$
C 40
1,1
1,0
0,9
0,8
0,7
0,6
0,5
0,4
0,3
0,2
0,1
0,0
Φ_E / $\Phi_{E,max}$
4
8
12
16
20
24
28
32
36
keV
40
E

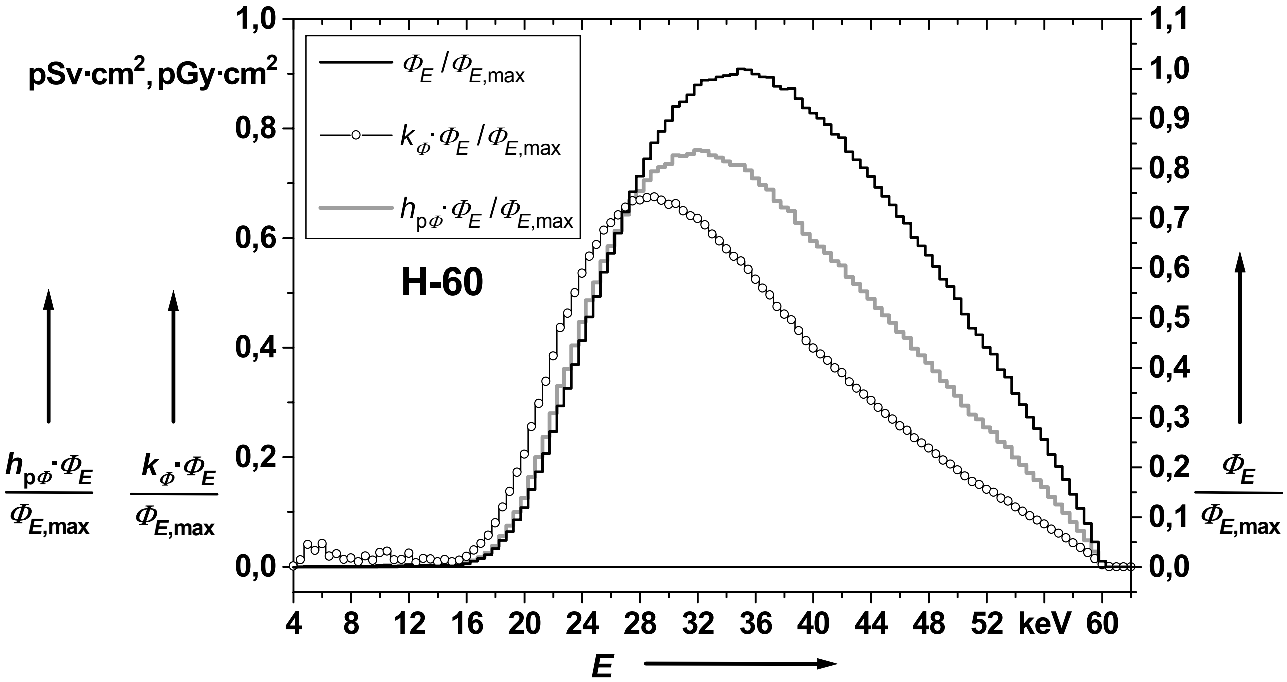

1,0
pSv·cm², pGy·cm²
0,8
0,6
0,4
0,2
0,0
$h_{p\Phi}\cdot\Phi_E$ / $\Phi_{E,max}$
$k_\Phi\cdot\Phi_E$ / $\Phi_{E,max}$
Φ_E / $\Phi_{E,max}$
$k_\Phi\cdot\Phi_E$ / $\Phi_{E,max}$
$h_{p\Phi}\cdot\Phi_E$ / $\Phi_{E,max}$
H-60
1,1
1,0
0,9
0,8
0,7
0,6
0,5
0,4
0,3
0,2
0,1
0,0
Φ_E / $\Phi_{E,max}$
4
8
12
16
20
24
28
32
36
40
44
48
52
keV
60
E

Verfügbar unter: https://doi.org/10.7795/110.20190315B

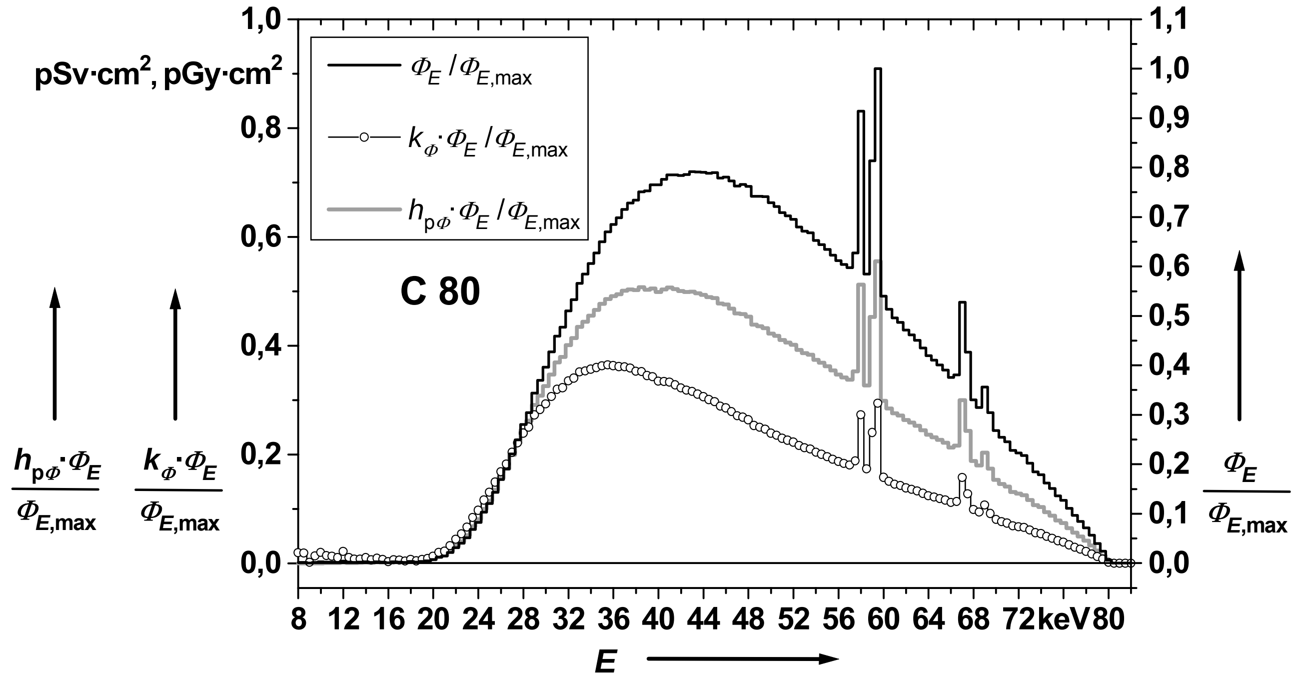

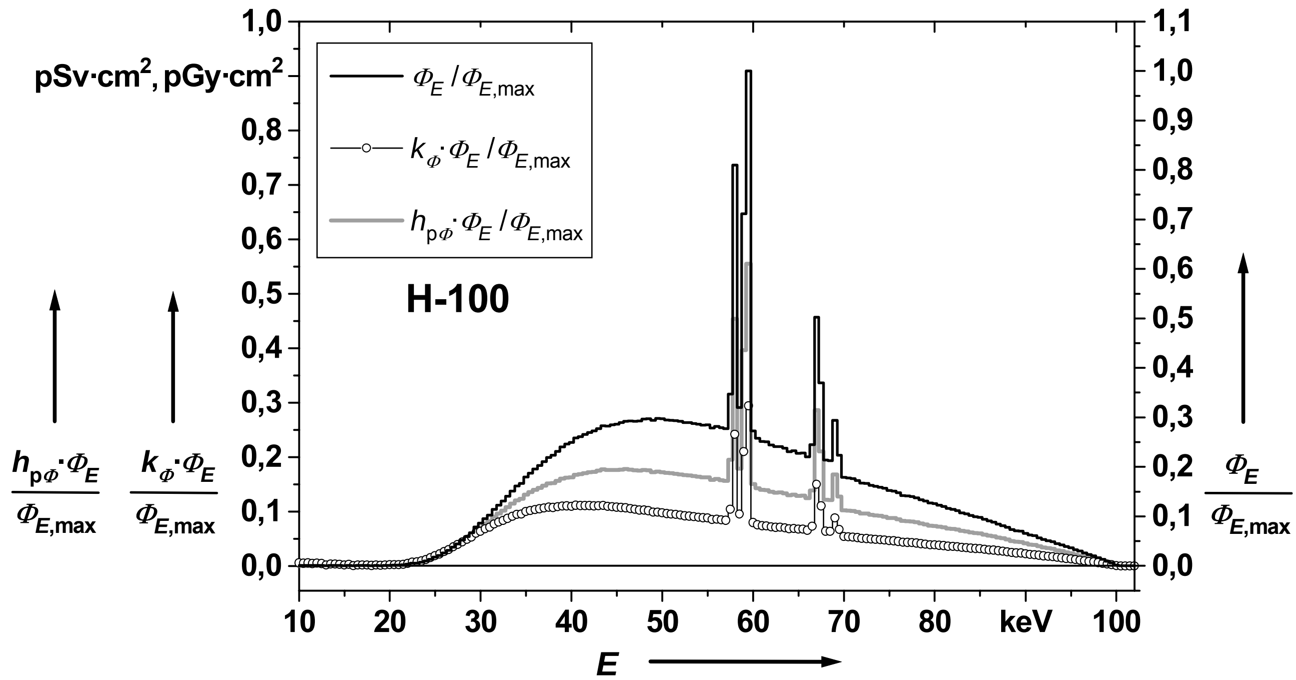

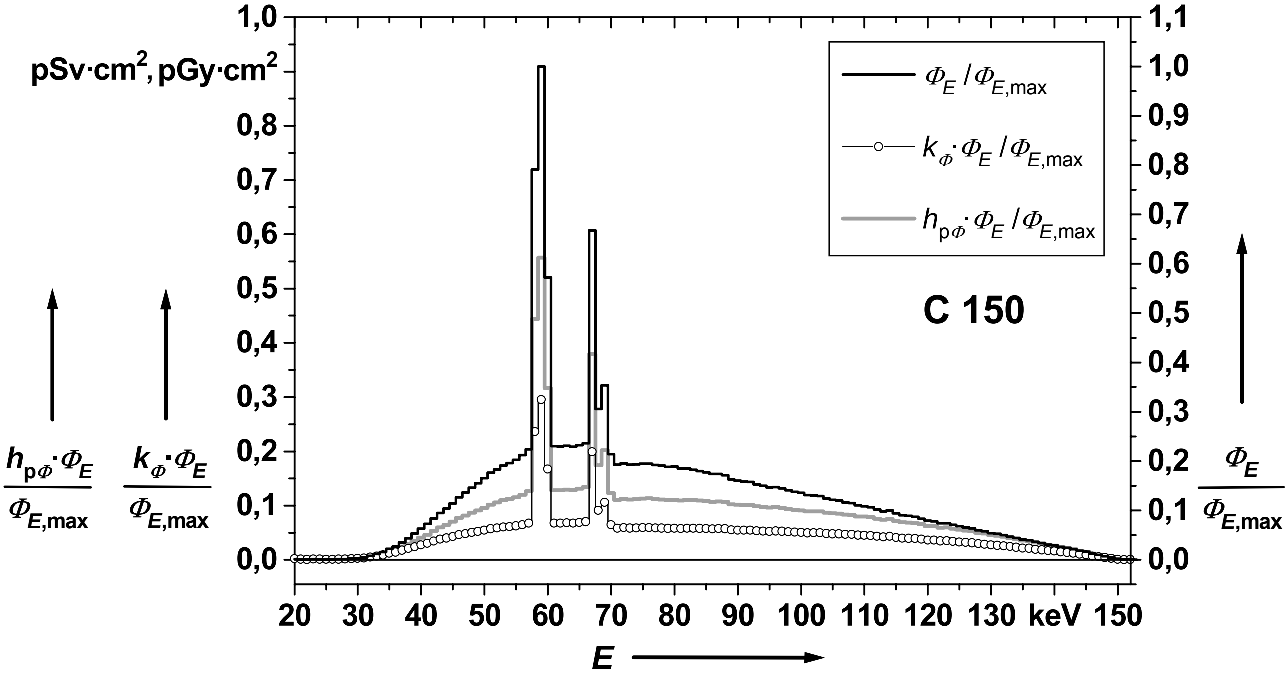
1,0
pSv·cm², pGy·cm²
0,8
0,7
0,6
0,5
0,4
0,3
0,2
0,1
0,0
$h_{p\Phi} \cdot \Phi_E / \Phi_{E,max}$
$k_\Phi \cdot \Phi_E / \Phi_{E,max}$
1,1
1,0
0,9
0,8
0,7
0,6
0,5
0,4
0,3
0,2
0,1
0,0
$\Phi_E / \Phi_{E,max}$
$\Phi_E / \Phi_{E,max}$
$k_\Phi \cdot \Phi_E / \Phi_{E,max}$
$h_{p\Phi} \cdot \Phi_E / \Phi_{E,max}$
C 150
20 30 40 50 60 70 80 90 100 110 120 130 keV 150
E

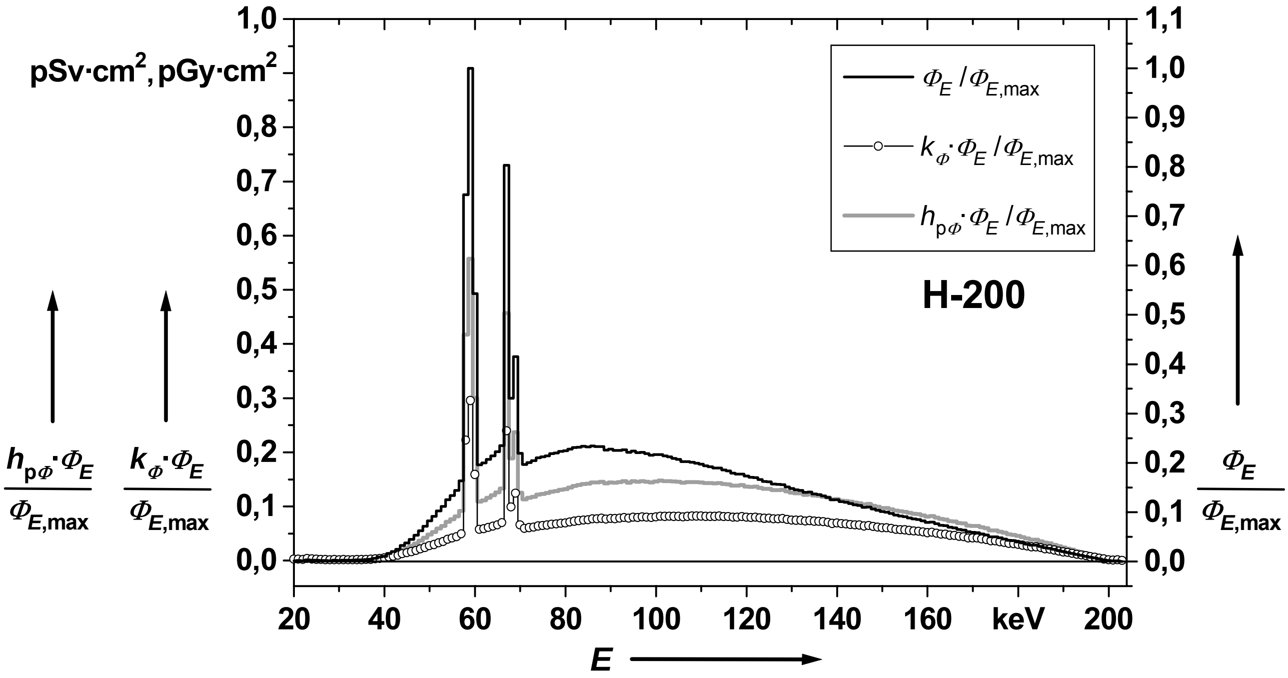
1,0
pSv·cm², pGy·cm²
0,8
0,7
0,6
0,5
0,4
0,3
0,2
0,1
0,0
$h_{p\Phi} \cdot \Phi_E / \Phi_{E,max}$
$k_\Phi \cdot \Phi_E / \Phi_{E,max}$
1,1
1,0
0,9
0,8
0,7
0,6
0,5
0,4
0,3
0,2
0,1
0,0
$\Phi_E / \Phi_{E,max}$
$\Phi_E / \Phi_{E,max}$
$k_\Phi \cdot \Phi_E / \Phi_{E,max}$
$h_{p\Phi} \cdot \Phi_E / \Phi_{E,max}$
H-200
20 40 60 80 100 120 140 160 keV 200
E

Verfügbar unter: https://doi.org/10.7795/110.20190315B

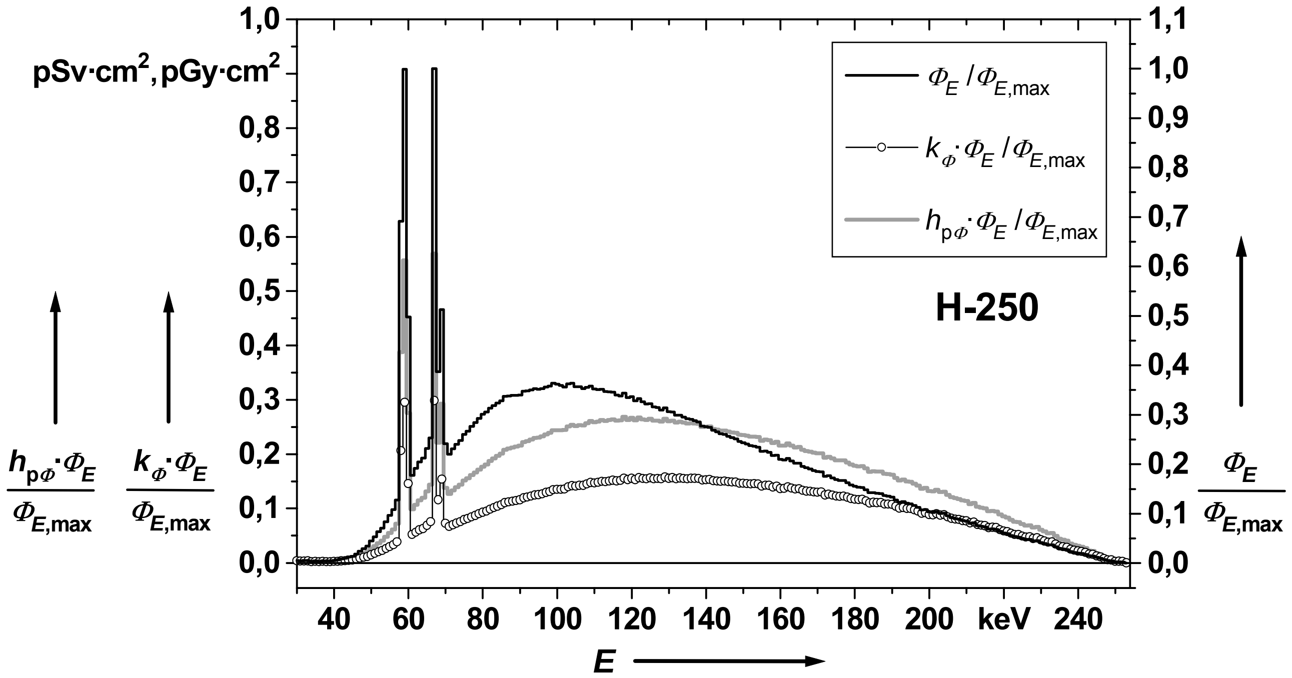

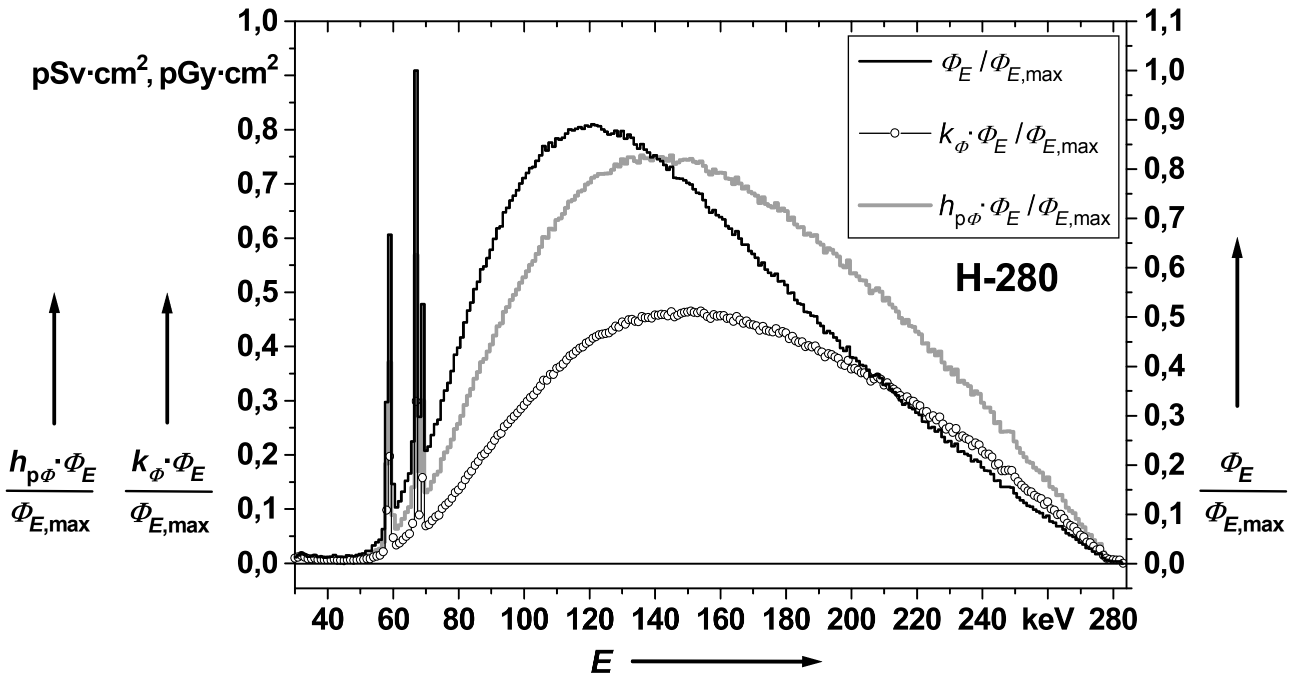

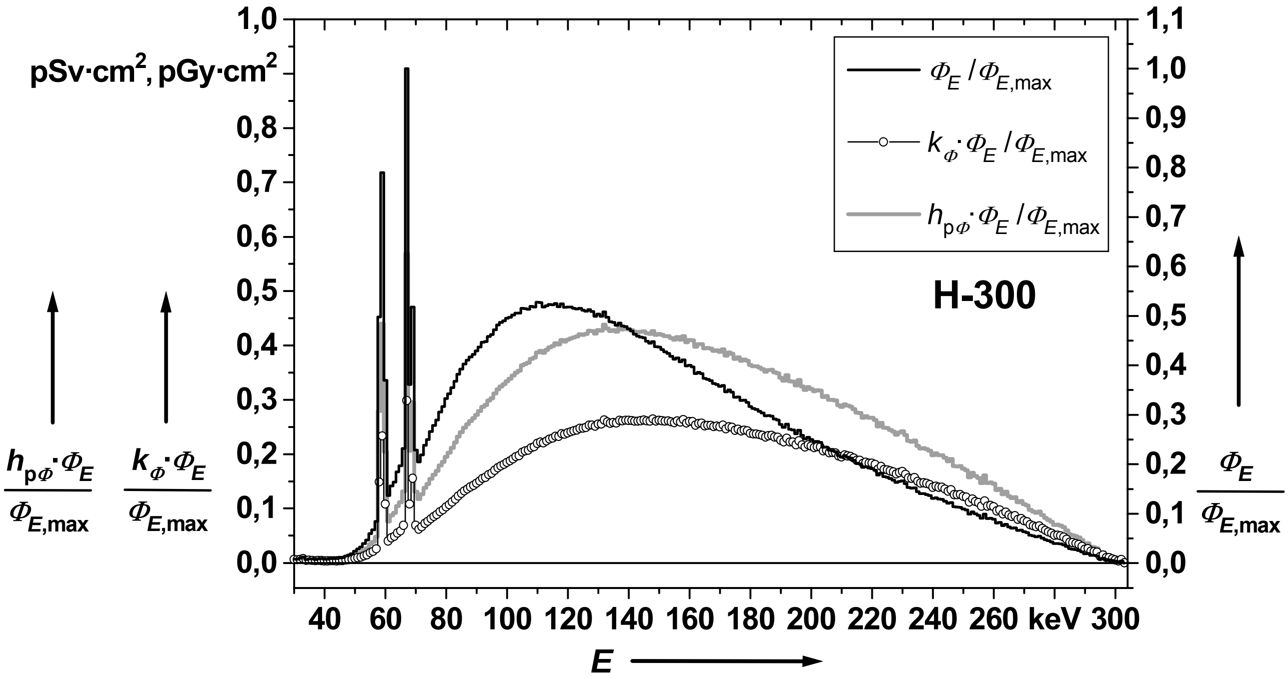

5.6 Therapy radiation qualities

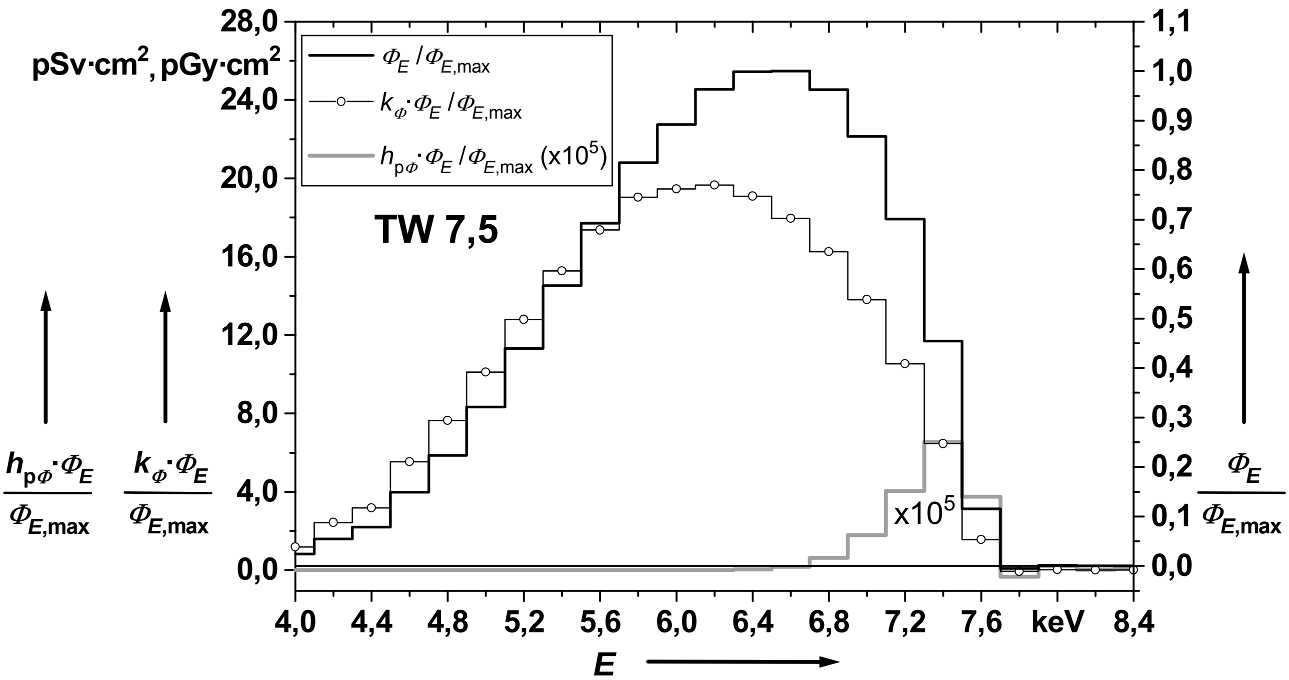

Verfügbar unter: https://doi.org/10.7795/110.20190315B

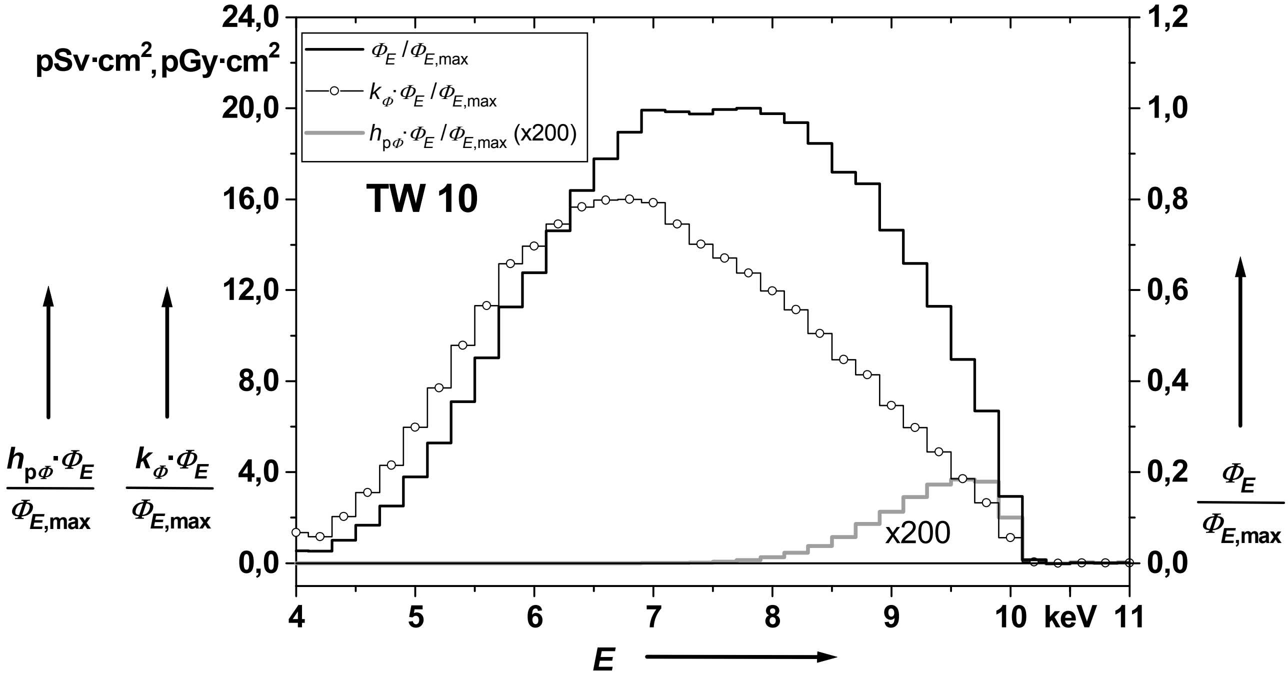

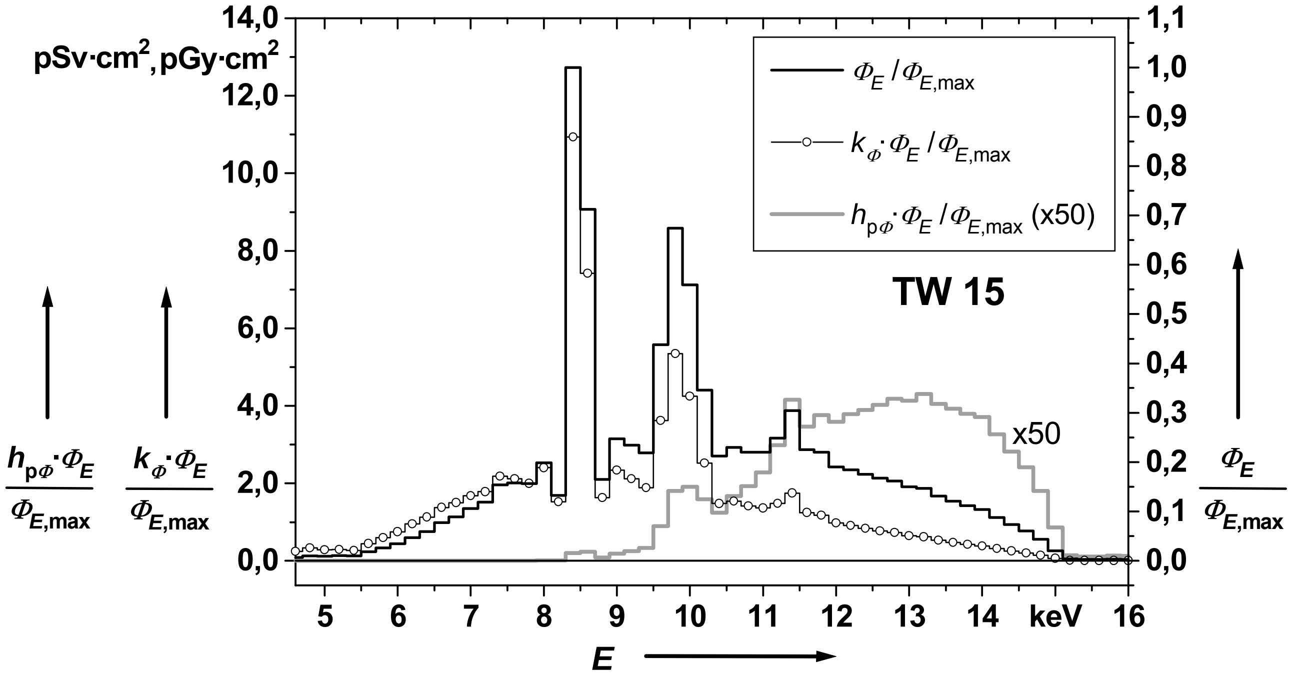

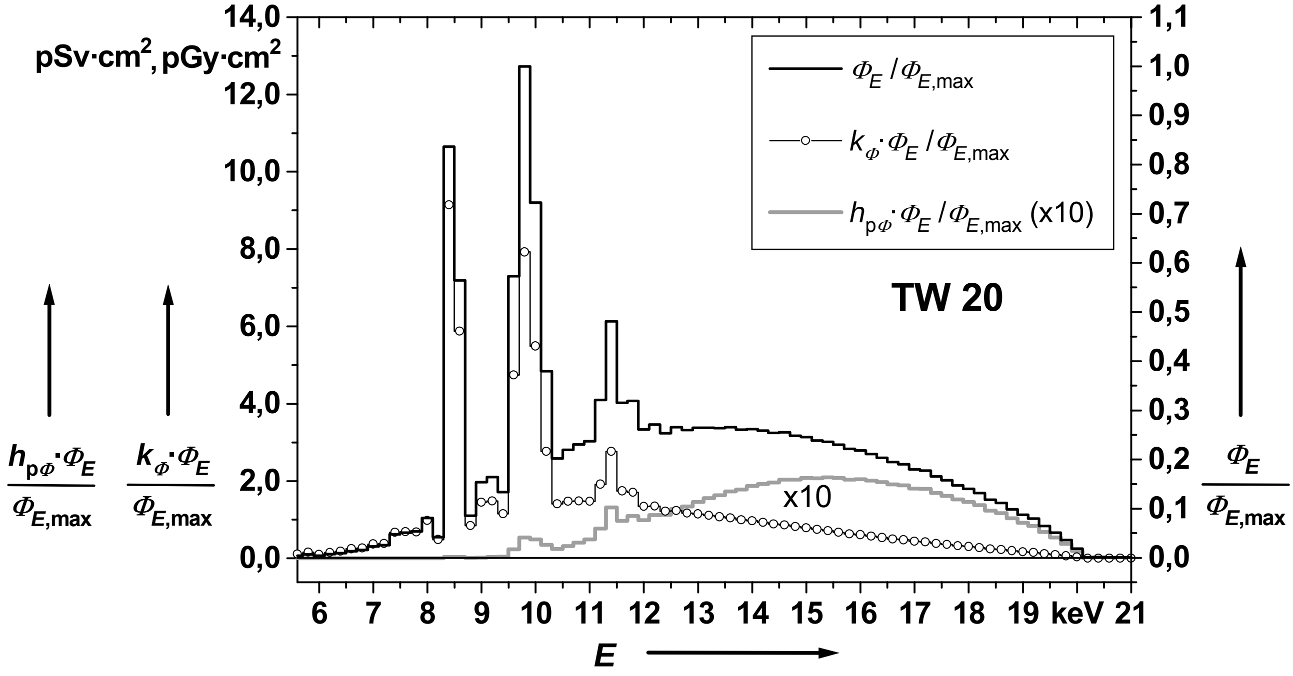
TW 20
$\Phi_E / \Phi_{E,max}$
$k_\Phi \cdot \Phi_E / \Phi_{E,max}$
$h_{p\Phi} \cdot \Phi_E / \Phi_{E,max}$ (x10)
x10
pSv·cm², pGy·cm²
$\frac{h_{p\Phi} \cdot \Phi_E}{\Phi_{E,max}}$
$\frac{k_\Phi \cdot \Phi_E}{\Phi_{E,max}}$
$\frac{\Phi_E}{\Phi_{E,max}}$
E
keV

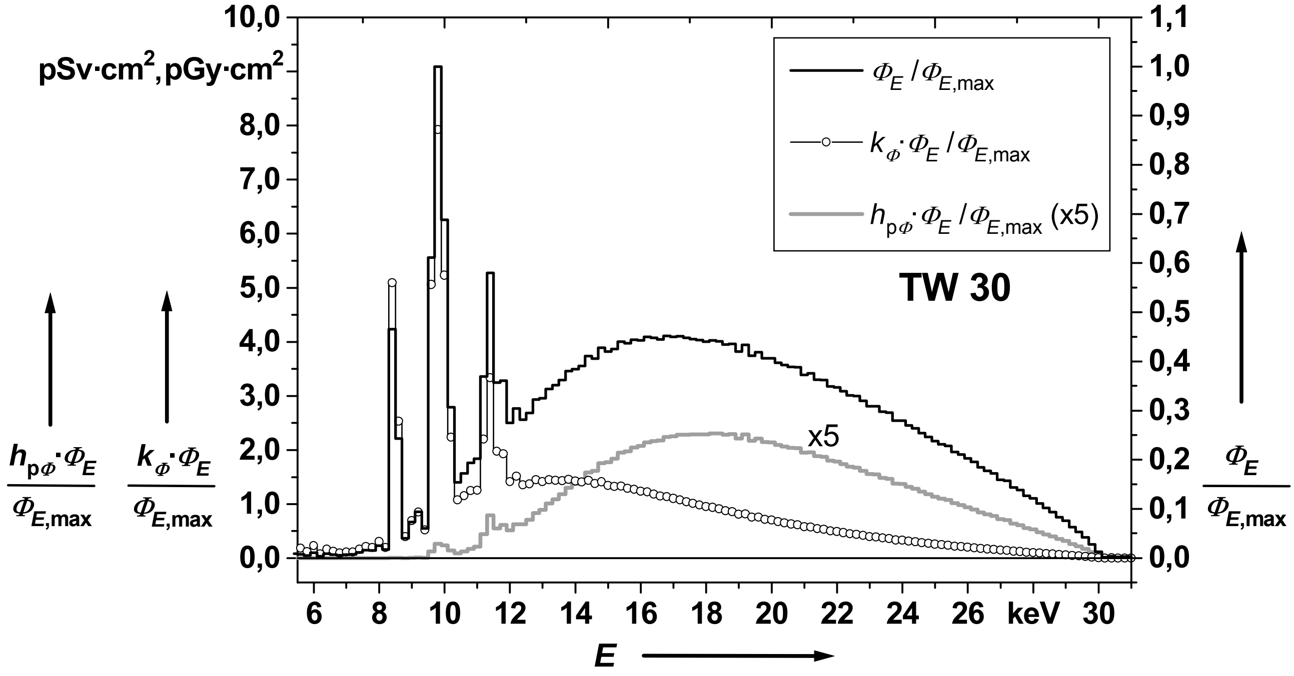
TW 30
$\Phi_E / \Phi_{E,max}$
$k_\Phi \cdot \Phi_E / \Phi_{E,max}$
$h_{p\Phi} \cdot \Phi_E / \Phi_{E,max}$ (x5)
x5
pSv·cm², pGy·cm²
$\frac{h_{p\Phi} \cdot \Phi_E}{\Phi_{E,max}}$
$\frac{k_\Phi \cdot \Phi_E}{\Phi_{E,max}}$
$\frac{\Phi_E}{\Phi_{E,max}}$
E
keV

Verfügbar unter: https://doi.org/10.7795/110.20190315B

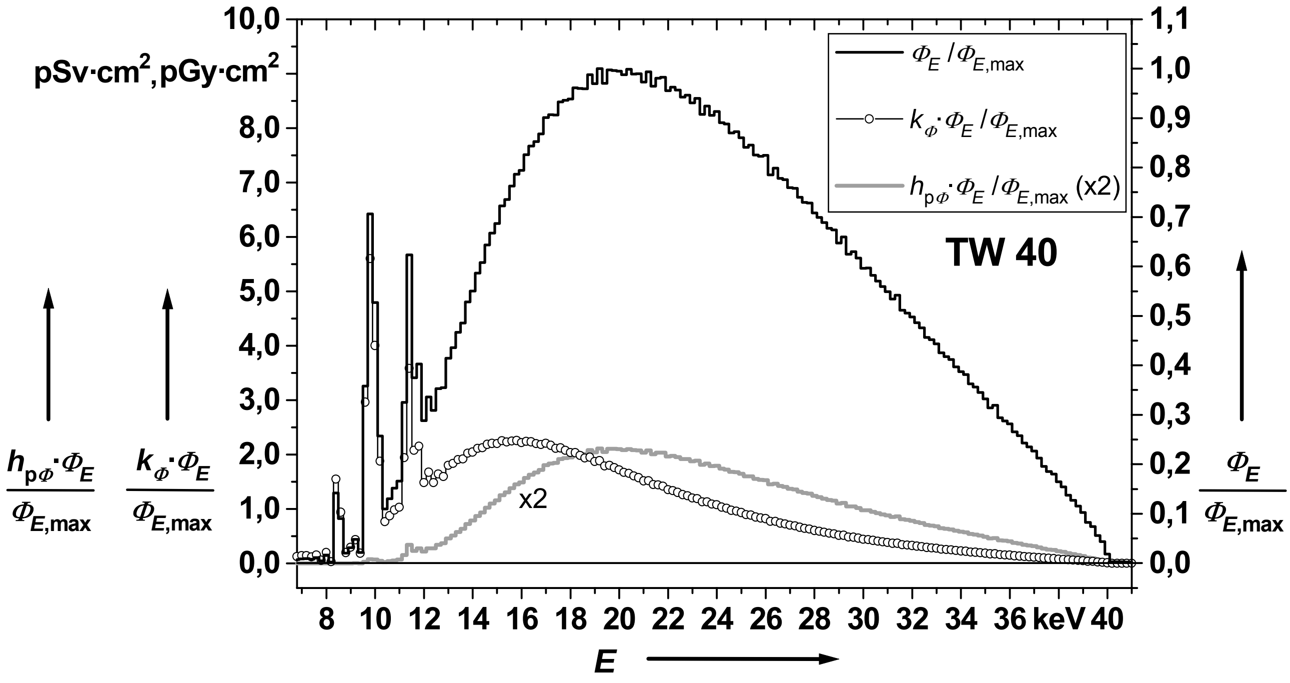

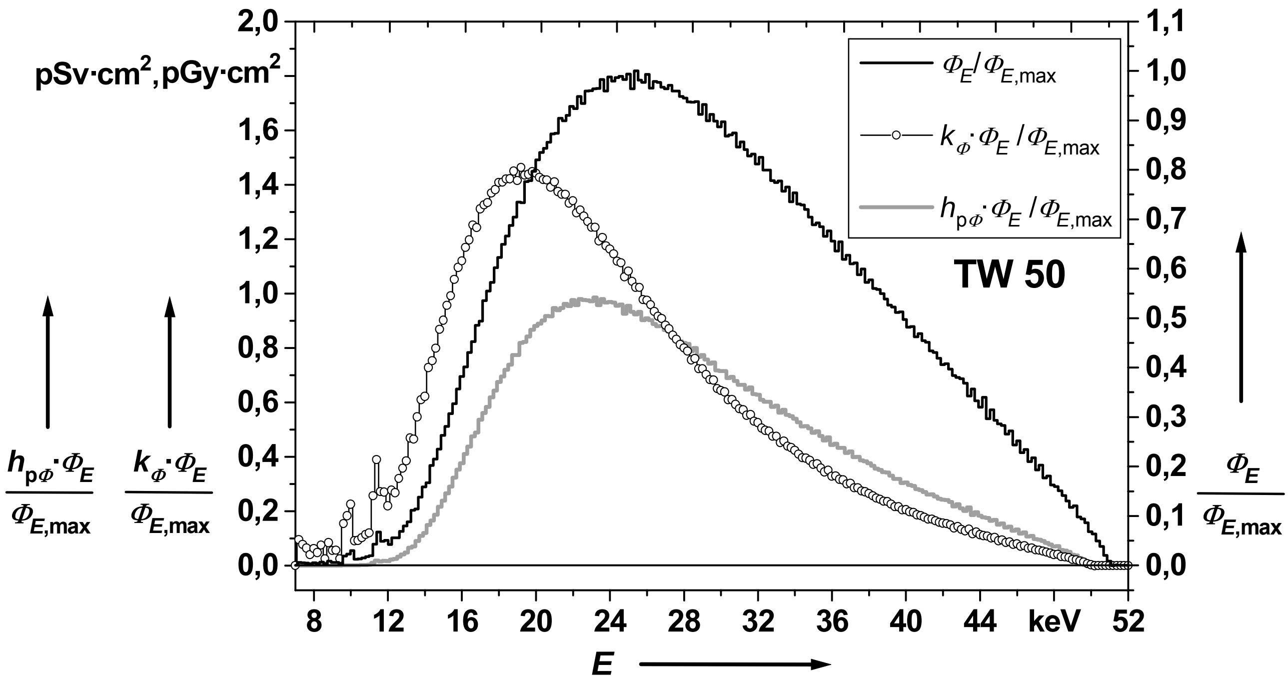

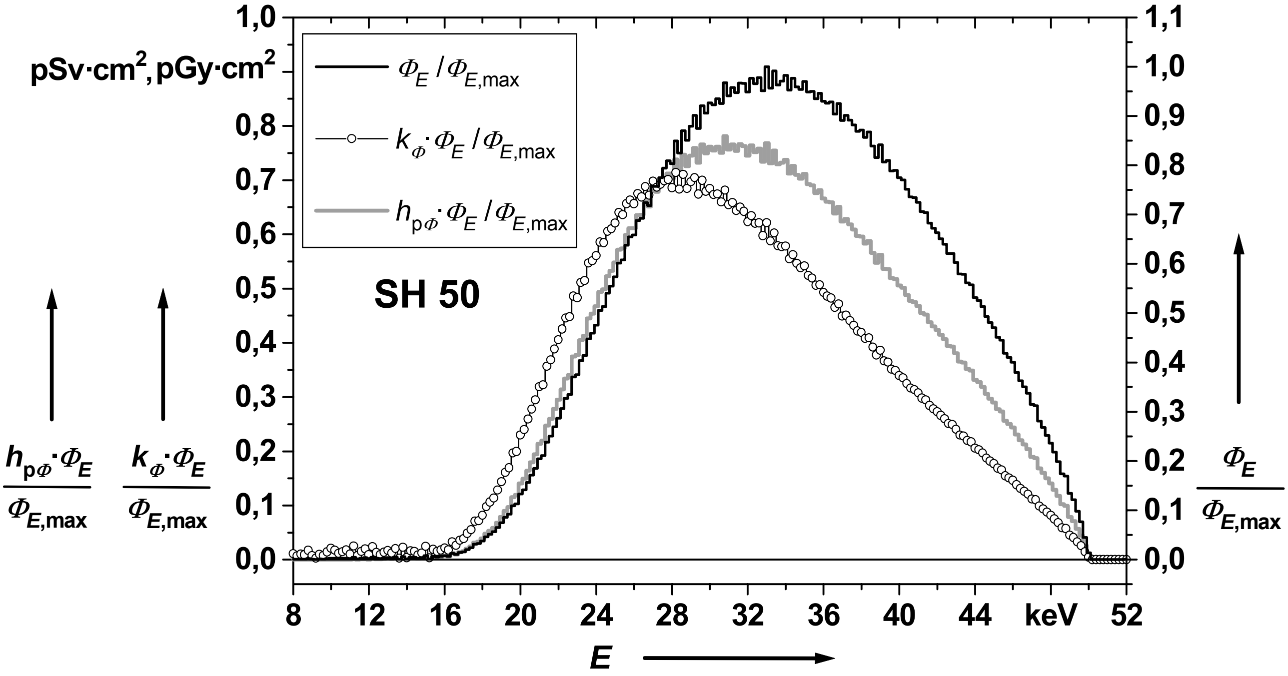
pSv·cm², pGy·cm²
$h_{p\Phi}\cdot\Phi_E / \Phi_{E,max}$
$k_{\Phi}\cdot\Phi_E / \Phi_{E,max}$
$\Phi_E / \Phi_{E,max}$
$\Phi_E / \Phi_{E,max}$
$k_{\Phi}\cdot\Phi_E / \Phi_{E,max}$
$h_{p\Phi}\cdot\Phi_E / \Phi_{E,max}$
SH 50
E
keV

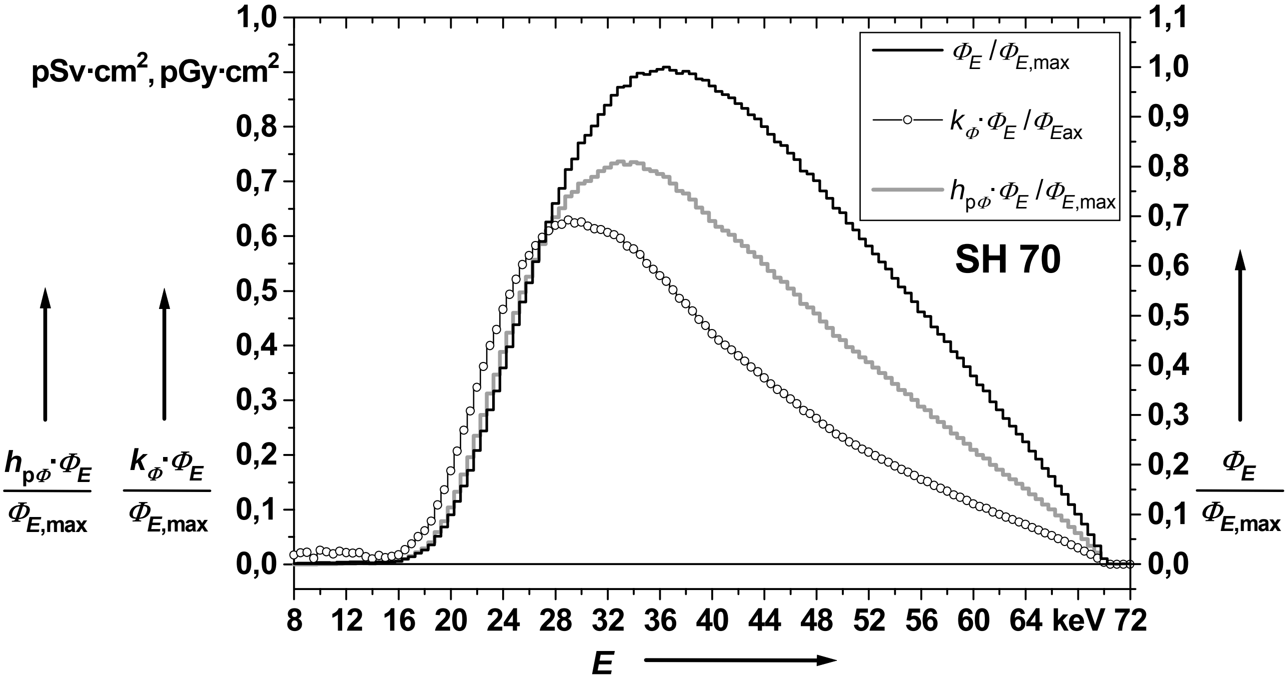
pSv·cm², pGy·cm²
$h_{p\Phi}\cdot\Phi_E / \Phi_{E,max}$
$k_{\Phi}\cdot\Phi_E / \Phi_{E,max}$
$\Phi_E / \Phi_{E,max}$
$\Phi_E / \Phi_{E,max}$
$k_{\Phi}\cdot\Phi_E / \Phi_{Eax}$
$h_{p\Phi}\cdot\Phi_E / \Phi_{E,max}$
SH 70
E
keV

Verfügbar unter: https://doi.org/10.7795/110.20190315B

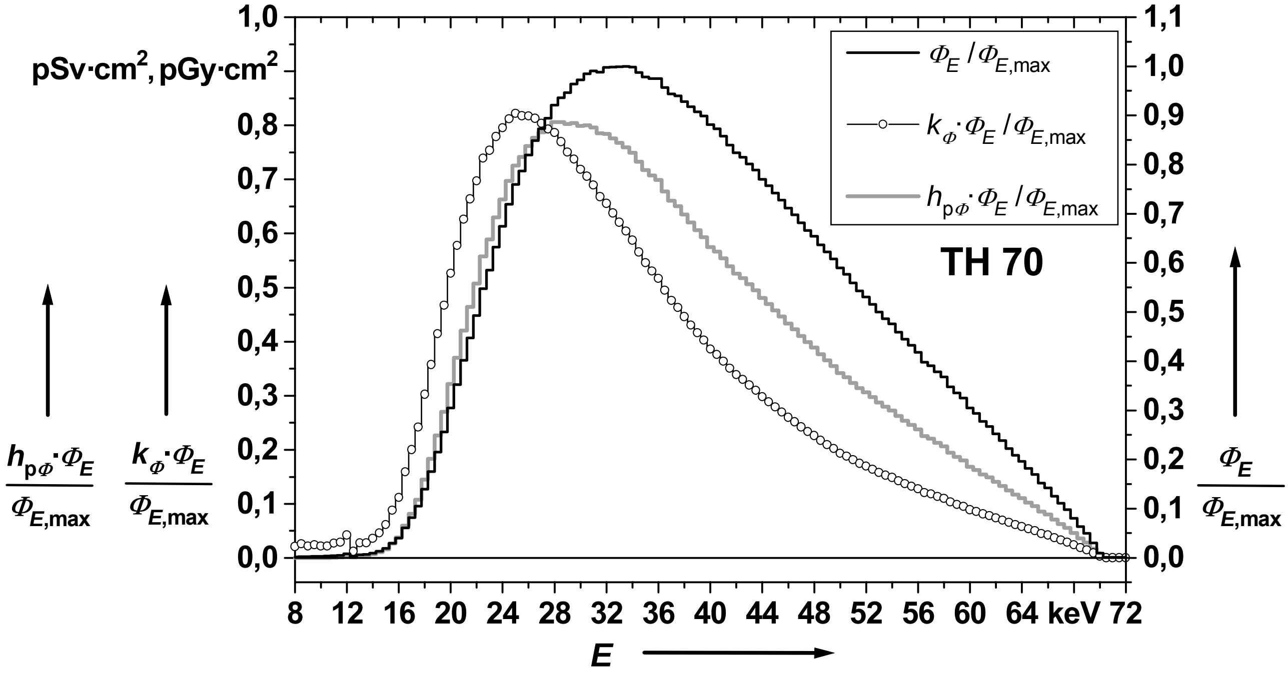

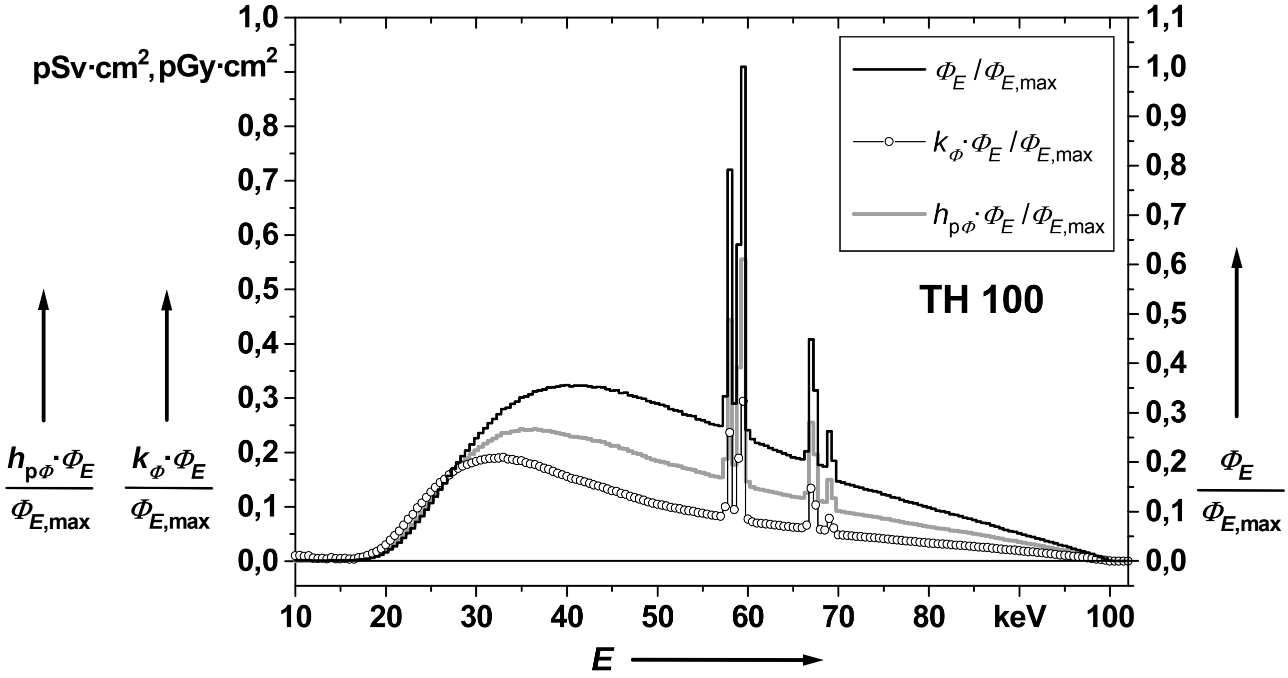

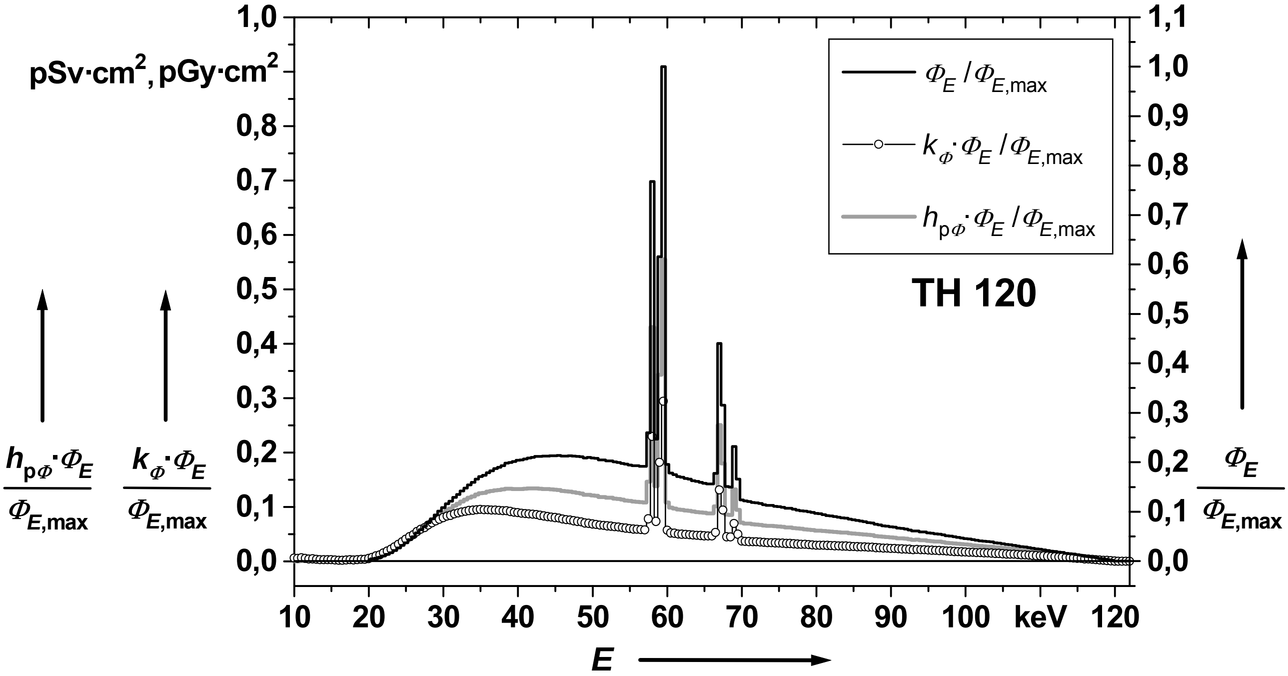

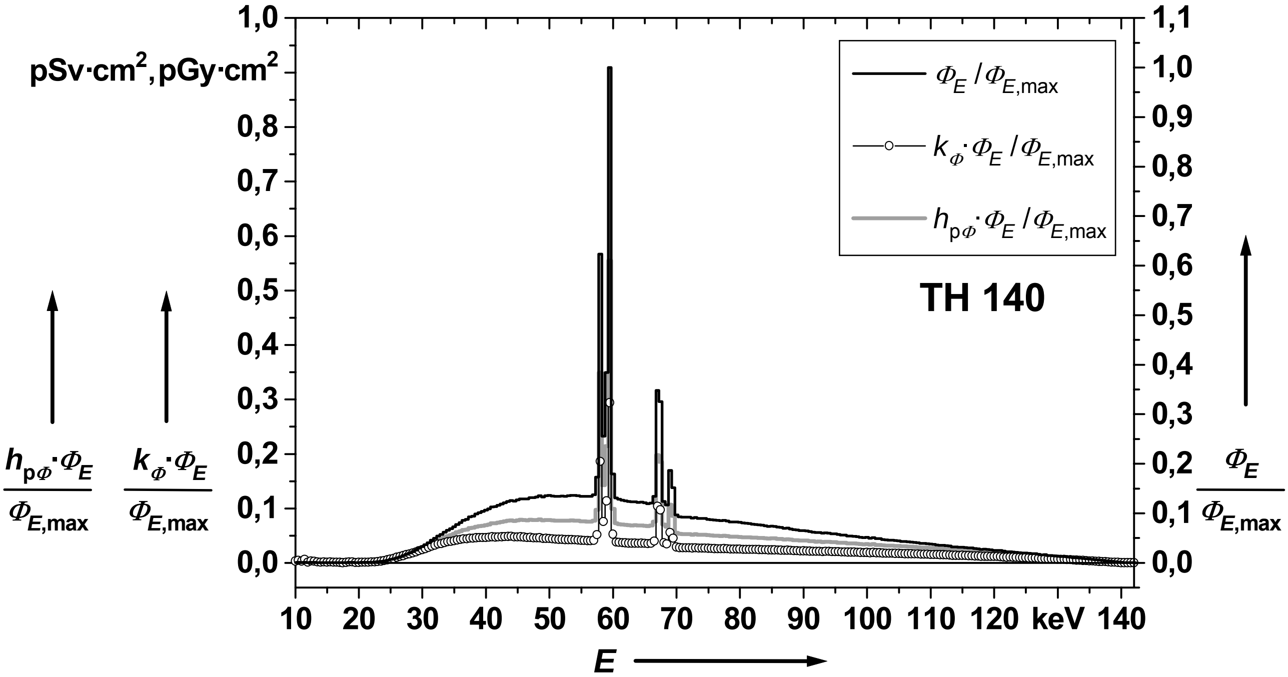

The spectra of the higher-energy therapy radiation qualities TH 150, TH 200, TH 250 and TH 280 are identical with the spectra of the radiation qualities of the DIN C-series and ISO high air-kerma rate series C 150, H-200, H-250 and H-300. These spectra are shown in Section 5.5.

Verfügbar unter: https://doi.org/10.7795/110.20190315B

5.7 Diagnostic radiation qualities

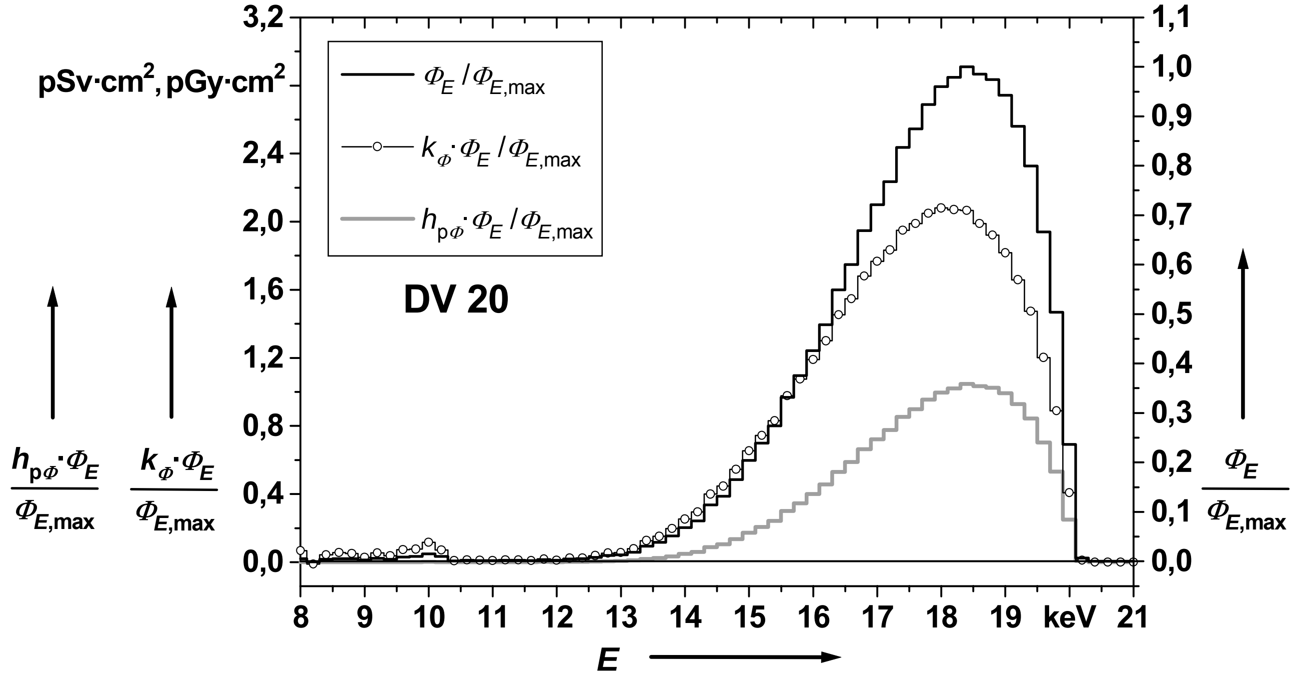

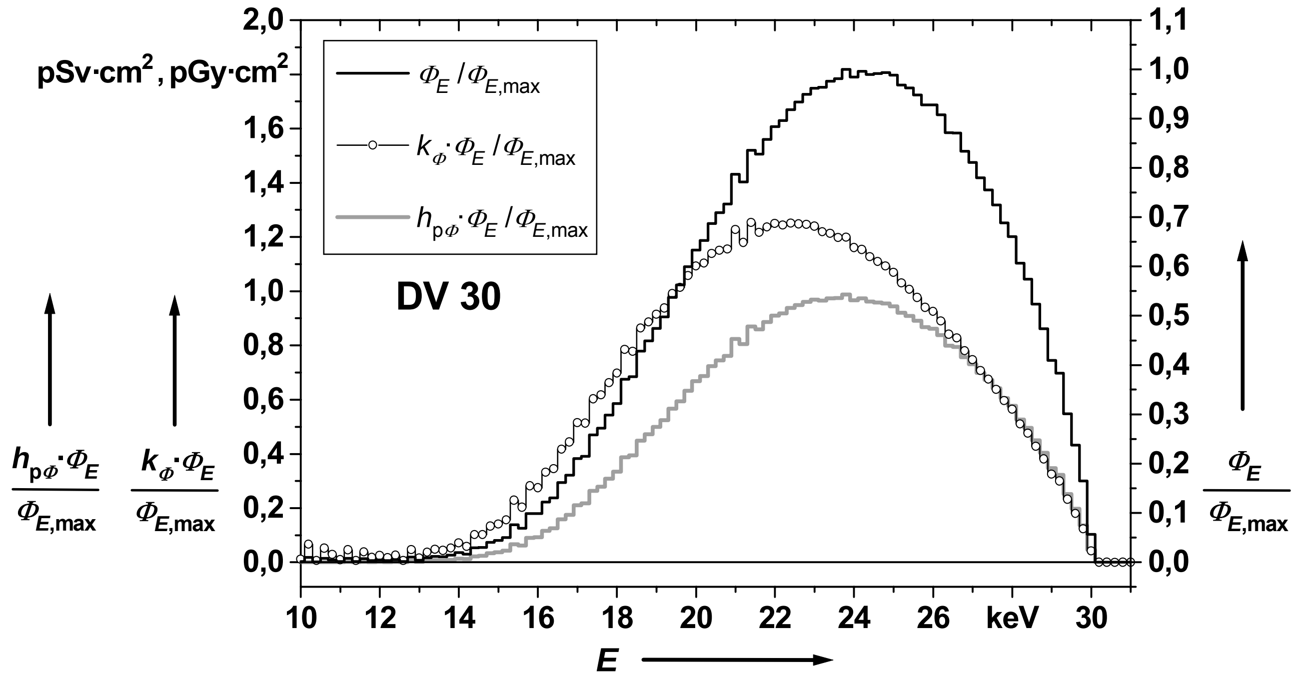

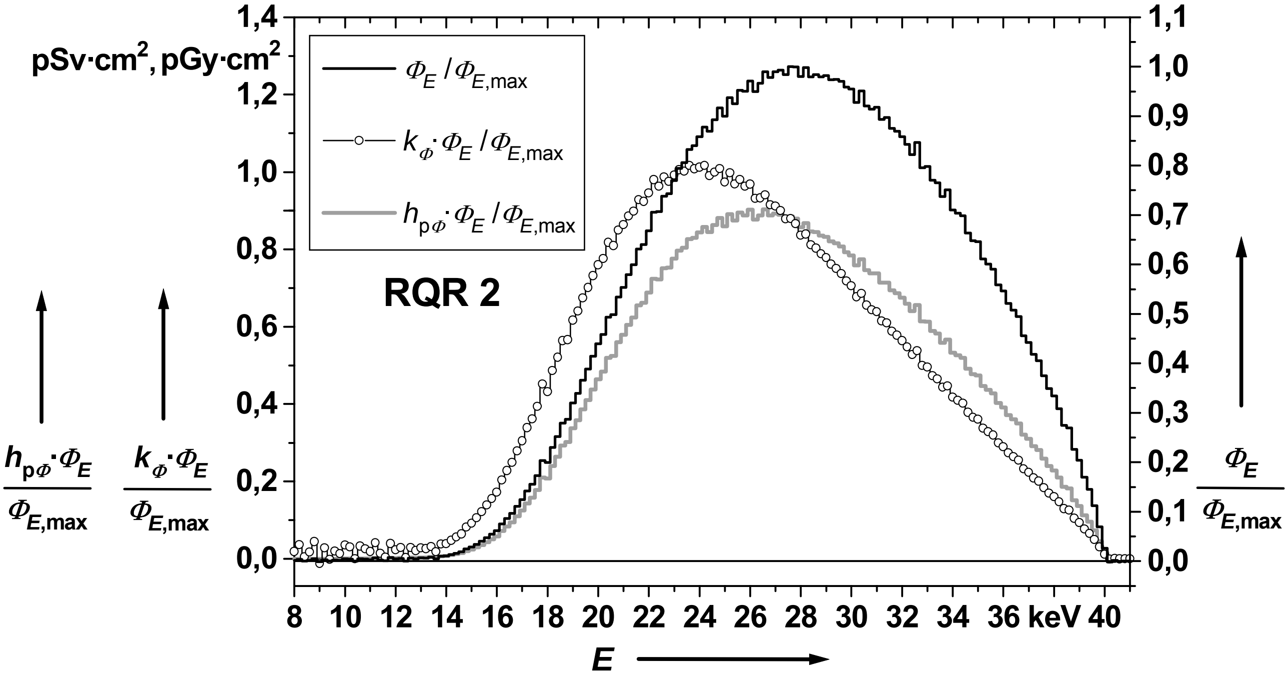

RQR 2
pSv·cm², pGy·cm²
$\Phi_E / \Phi_{E,max}$
$k_\Phi \cdot \Phi_E / \Phi_{E,max}$
$h_{p\Phi} \cdot \Phi_E / \Phi_{E,max}$
$\frac{h_{p\Phi} \cdot \Phi_E}{\Phi_{E,max}}$
$\frac{k_\Phi \cdot \Phi_E}{\Phi_{E,max}}$
$\frac{\Phi_E}{\Phi_{E,max}}$
E
keV

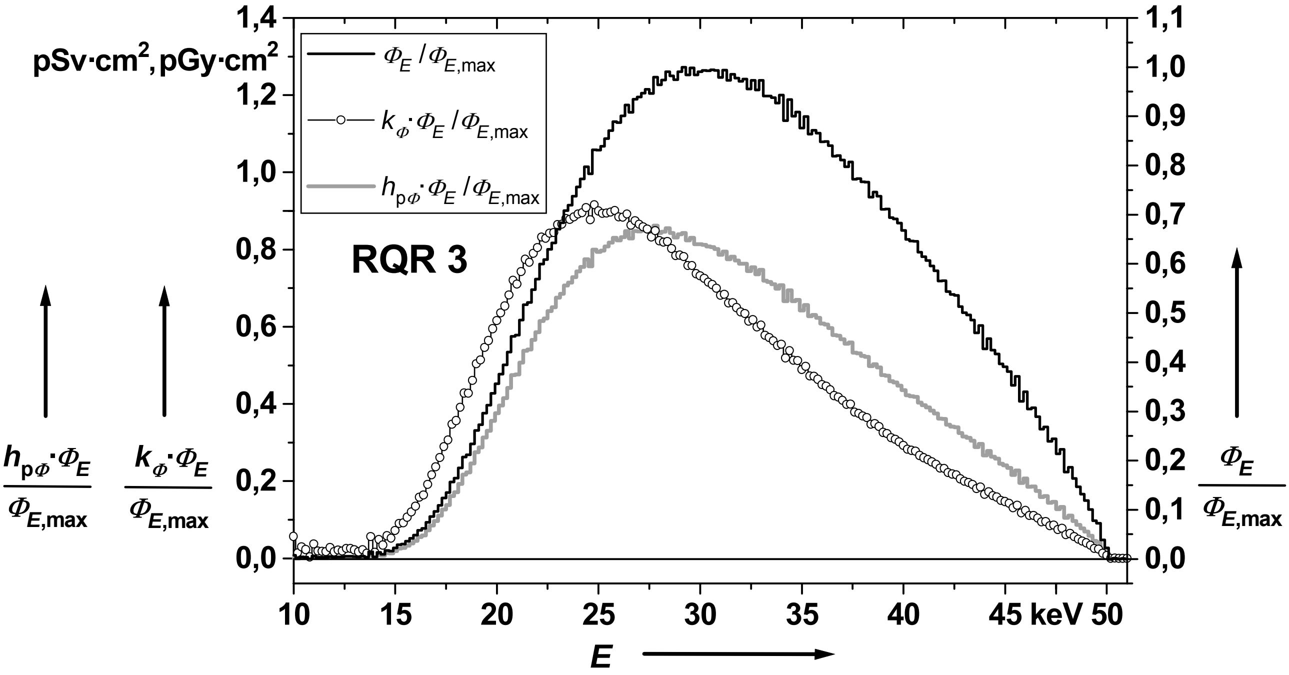

RQR 3
pSv·cm², pGy·cm²
$\Phi_E / \Phi_{E,max}$
$k_\Phi \cdot \Phi_E / \Phi_{E,max}$
$h_{p\Phi} \cdot \Phi_E / \Phi_{E,max}$
$\frac{h_{p\Phi} \cdot \Phi_E}{\Phi_{E,max}}$
$\frac{k_\Phi \cdot \Phi_E}{\Phi_{E,max}}$
$\frac{\Phi_E}{\Phi_{E,max}}$
E
keV

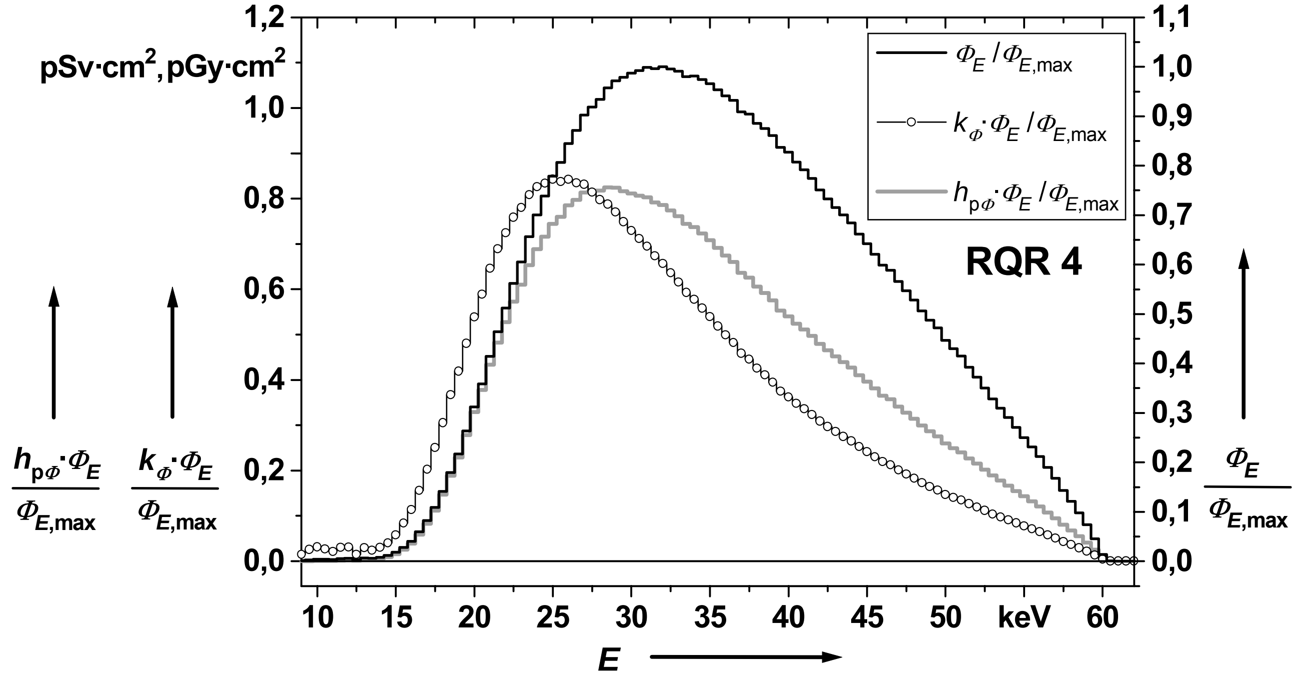
1,2
pSv·cm², pGy·cm²
1,0
0,8
0,6
0,4
0,2
0,0
1,1
1,0
0,9
0,8
0,7
0,6
0,5
0,4
0,3
0,2
0,1
0,0
Φ_E / Φ_E,max
k_Φ·Φ_E / Φ_E,max
h_pΦ·Φ_E / Φ_E,max
RQR 4
h_pΦ·Φ_E / Φ_E,max
k_Φ·Φ_E / Φ_E,max
Φ_E / Φ_E,max
10 15 20 25 30 35 40 45 50 keV 60
E

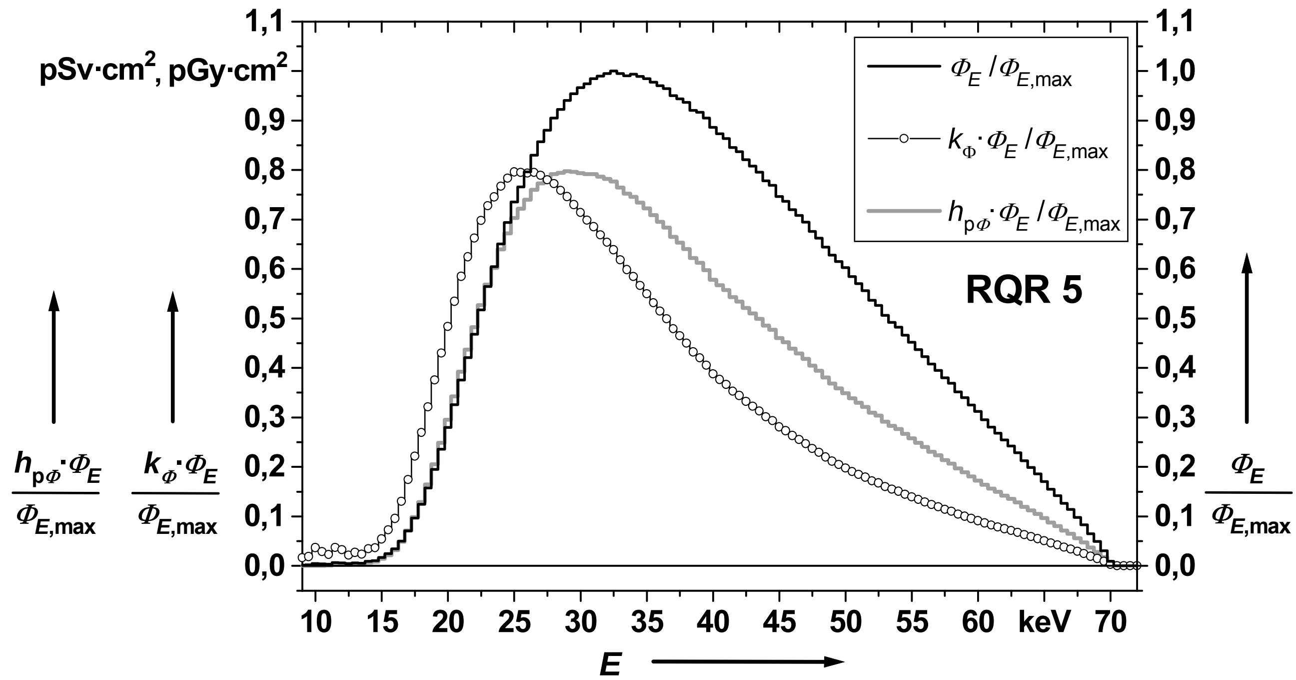
1,1
pSv·cm², pGy·cm²
1,0
0,9
0,8
0,7
0,6
0,5
0,4
0,3
0,2
0,1
0,0
1,1
1,0
0,9
0,8
0,7
0,6
0,5
0,4
0,3
0,2
0,1
0,0
Φ_E / Φ_E,max
k_Φ·Φ_E / Φ_E,max
h_pΦ·Φ_E / Φ_E,max
RQR 5
h_pΦ·Φ_E / Φ_E,max
k_Φ·Φ_E / Φ_E,max
Φ_E / Φ_E,max
10 15 20 25 30 35 40 45 50 55 60 keV 70
E

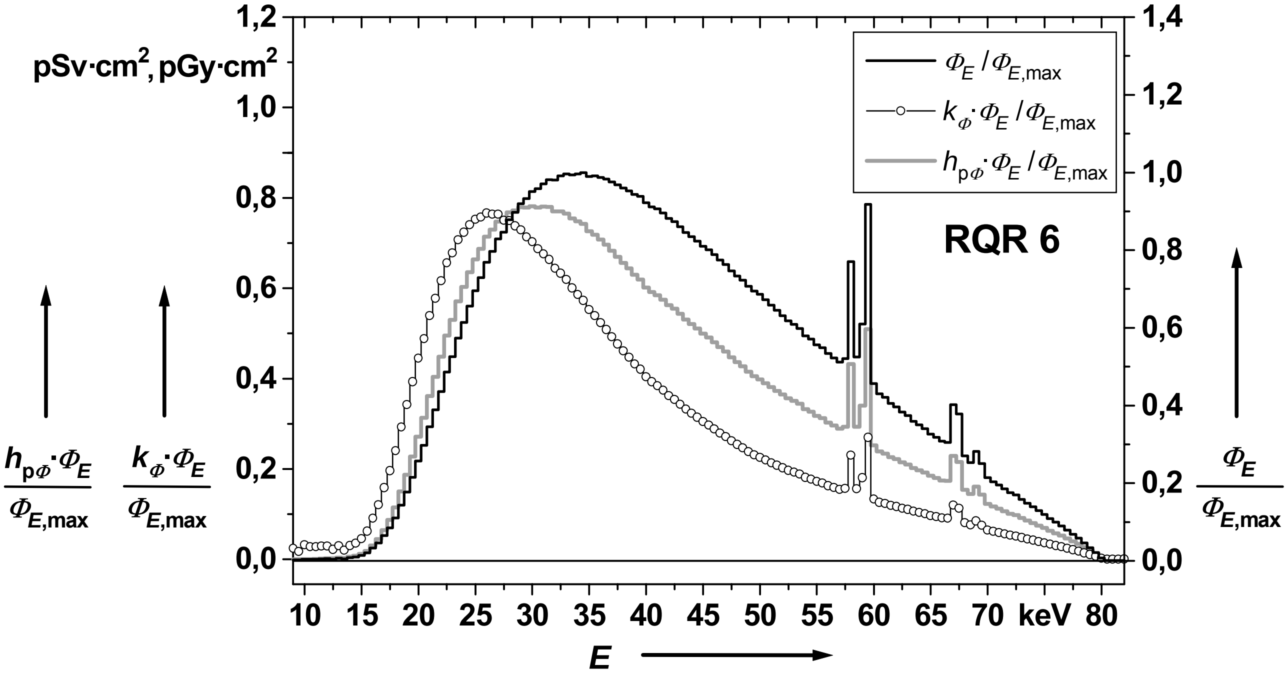

RQR 6
$\Phi_E / \Phi_{E,\max}$
$k_\Phi \cdot \Phi_E / \Phi_{E,\max}$
$h_{p\Phi} \cdot \Phi_E / \Phi_{E,\max}$
pSv·cm², pGy·cm²
$\frac{h_{p\Phi} \cdot \Phi_E}{\Phi_{E,\max}}$
$\frac{k_\Phi \cdot \Phi_E}{\Phi_{E,\max}}$
$\frac{\Phi_E}{\Phi_{E,\max}}$
E
keV

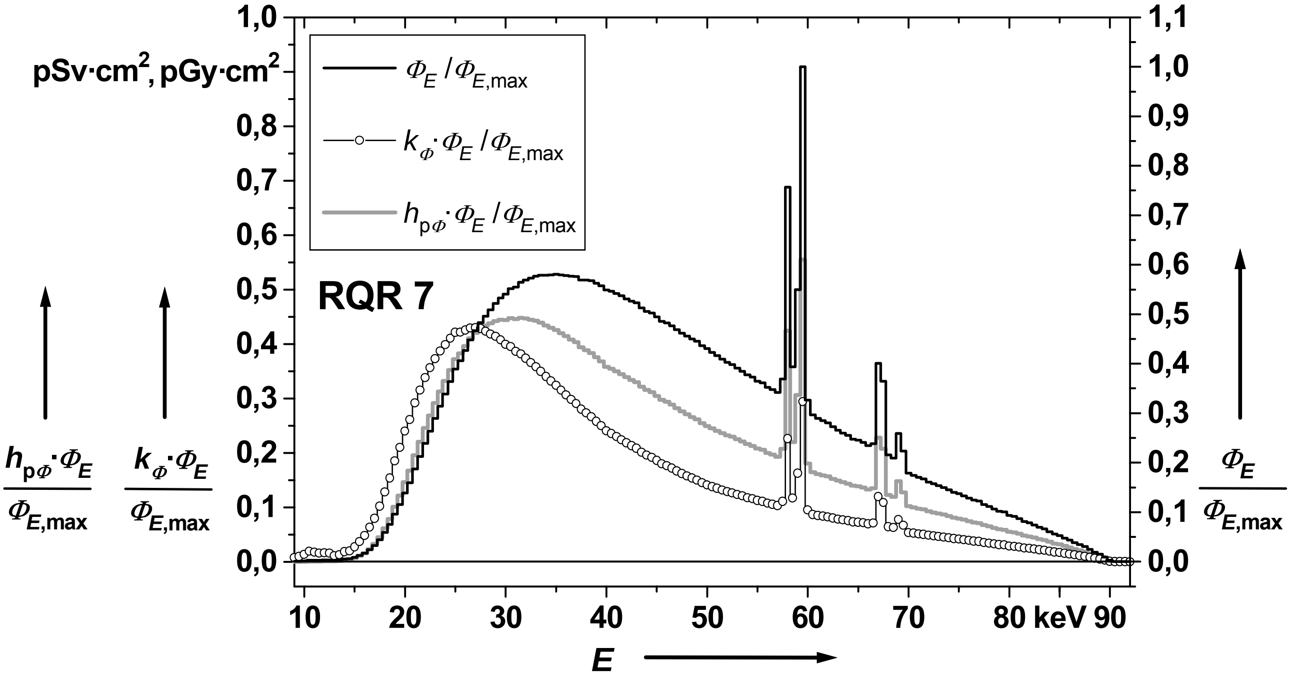

RQR 7
$\Phi_E / \Phi_{E,\max}$
$k_\Phi \cdot \Phi_E / \Phi_{E,\max}$
$h_{p\Phi} \cdot \Phi_E / \Phi_{E,\max}$
pSv·cm², pGy·cm²
$\frac{h_{p\Phi} \cdot \Phi_E}{\Phi_{E,\max}}$
$\frac{k_\Phi \cdot \Phi_E}{\Phi_{E,\max}}$
$\frac{\Phi_E}{\Phi_{E,\max}}$
E
keV

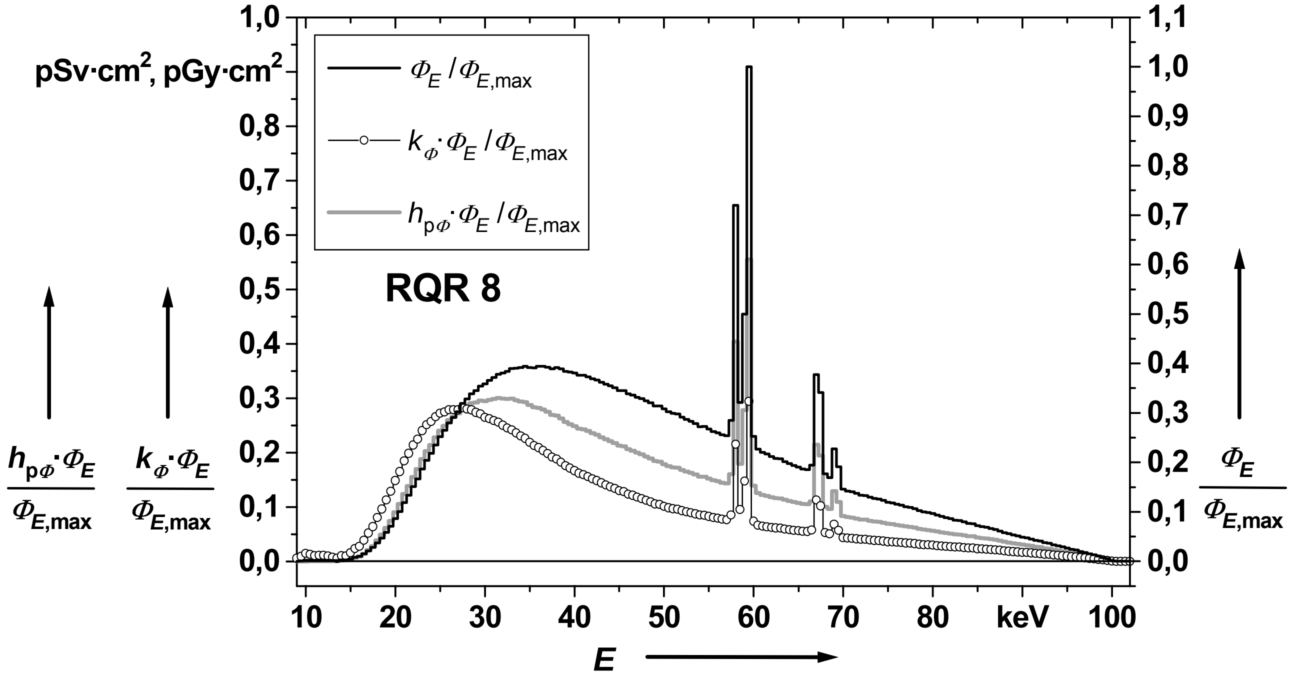

1,0
pSv·cm², pGy·cm²
0,8
0,7
0,6
0,5
0,4
0,3
0,2
0,1
0,0
$\Phi_E / \Phi_{E,\max}$
$k_\Phi \cdot \Phi_E / \Phi_{E,\max}$
$h_{p\Phi} \cdot \Phi_E / \Phi_{E,\max}$
RQR 8
$\frac{h_{p\Phi} \cdot \Phi_E}{\Phi_{E,\max}}$
$\frac{k_\Phi \cdot \Phi_E}{\Phi_{E,\max}}$
$\frac{\Phi_E}{\Phi_{E,\max}}$
1,1
1,0
0,9
0,8
0,7
0,6
0,5
0,4
0,3
0,2
0,1
0,0
10
20
30
40
50
60
70
80
keV
100
E

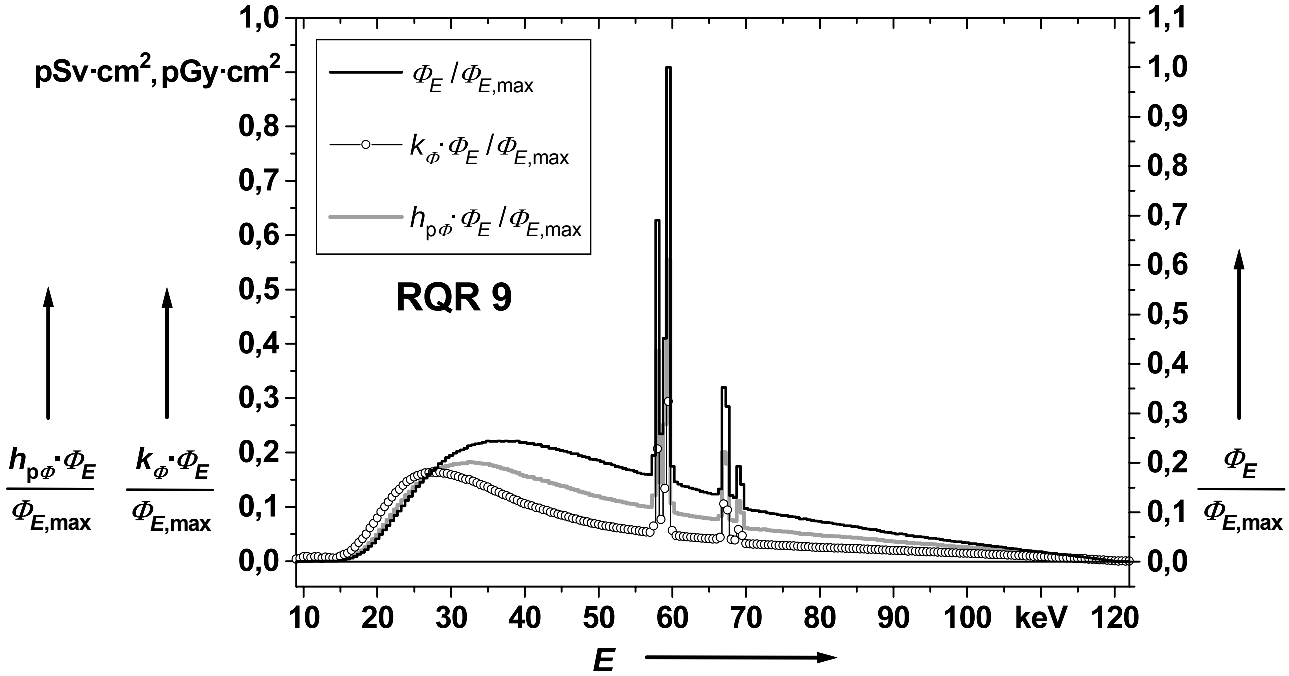

1,0
pSv·cm², pGy·cm²
0,8
0,7
0,6
0,5
0,4
0,3
0,2
0,1
0,0
$\Phi_E / \Phi_{E,\max}$
$k_\Phi \cdot \Phi_E / \Phi_{E,\max}$
$h_{p\Phi} \cdot \Phi_E / \Phi_{E,\max}$
RQR 9
$\frac{h_{p\Phi} \cdot \Phi_E}{\Phi_{E,\max}}$
$\frac{k_\Phi \cdot \Phi_E}{\Phi_{E,\max}}$
$\frac{\Phi_E}{\Phi_{E,\max}}$
1,1
1,0
0,9
0,8
0,7
0,6
0,5
0,4
0,3
0,2
0,1
0,0
10
20
30
40
50
60
70
80
90
100
keV
120
E

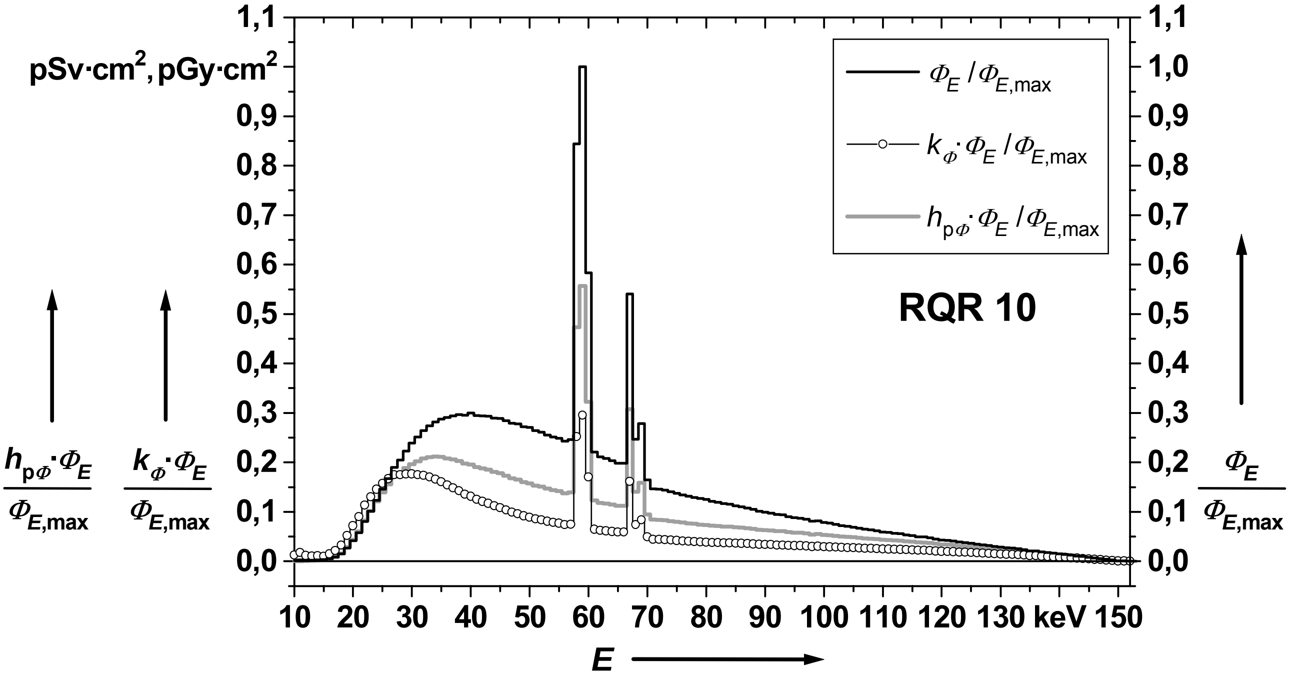

pSv·cm², pGy·cm²
$\frac{h_{p\Phi} \cdot \Phi_E}{\Phi_{E,max}}$
$\frac{k_\Phi \cdot \Phi_E}{\Phi_{E,max}}$
$\frac{\Phi_E}{\Phi_{E,max}}$
$\Phi_E / \Phi_{E,max}$
$k_\Phi \cdot \Phi_E / \Phi_{E,max}$
$h_{p\Phi} \cdot \Phi_E / \Phi_{E,max}$
RQR 10
E
keV

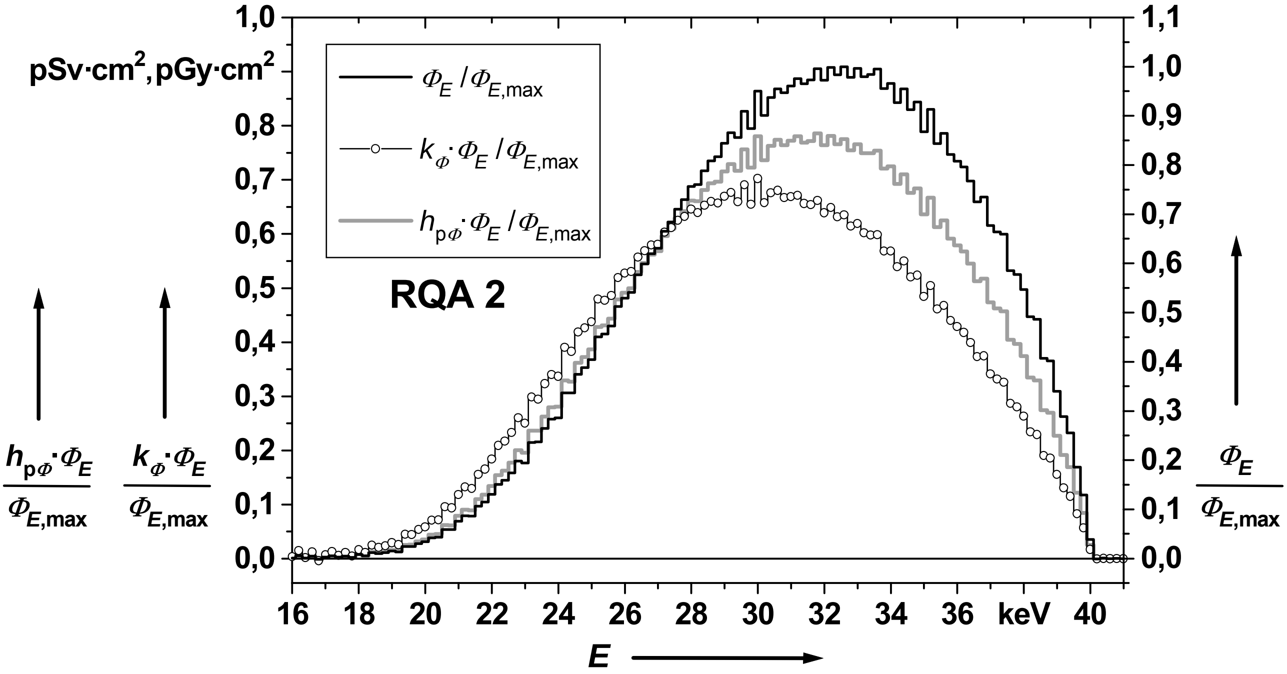

pSv·cm², pGy·cm²
$\frac{h_{p\Phi} \cdot \Phi_E}{\Phi_{E,max}}$
$\frac{k_\Phi \cdot \Phi_E}{\Phi_{E,max}}$
$\frac{\Phi_E}{\Phi_{E,max}}$
$\Phi_E / \Phi_{E,max}$
$k_\Phi \cdot \Phi_E / \Phi_{E,max}$
$h_{p\Phi} \cdot \Phi_E / \Phi_{E,max}$
RQA 2
E
keV

Verfügbar unter: https://doi.org/10.7795/110.20190315B

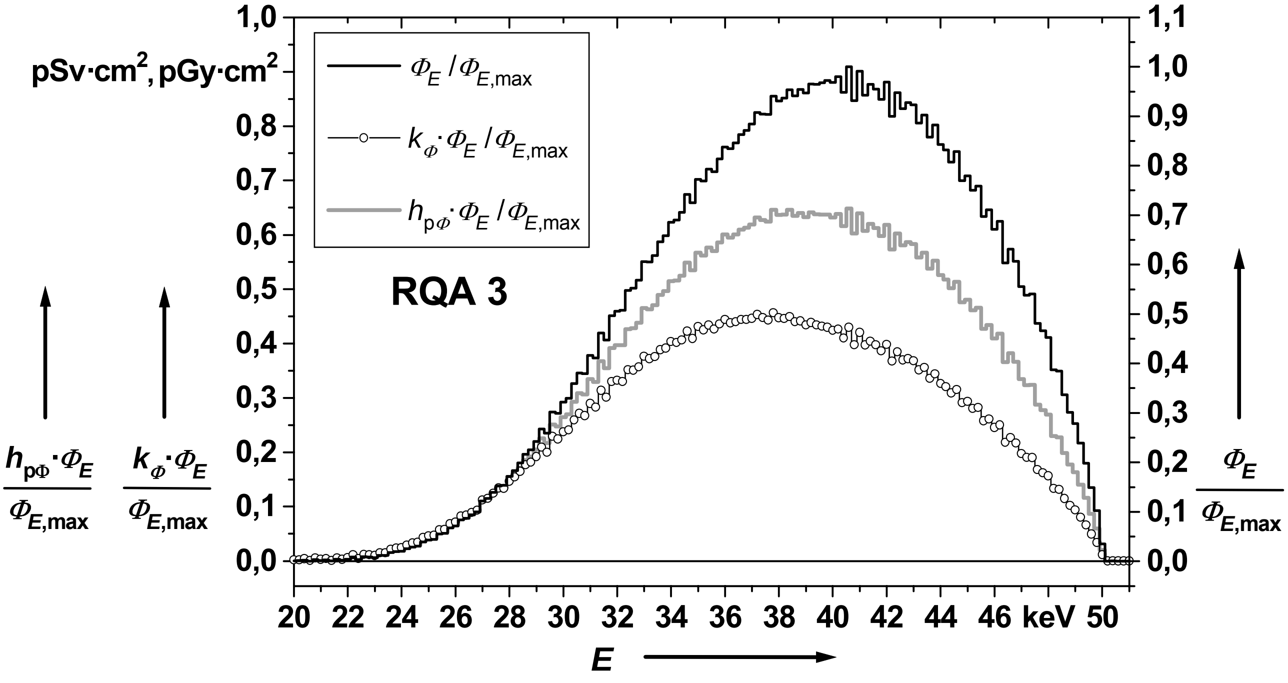

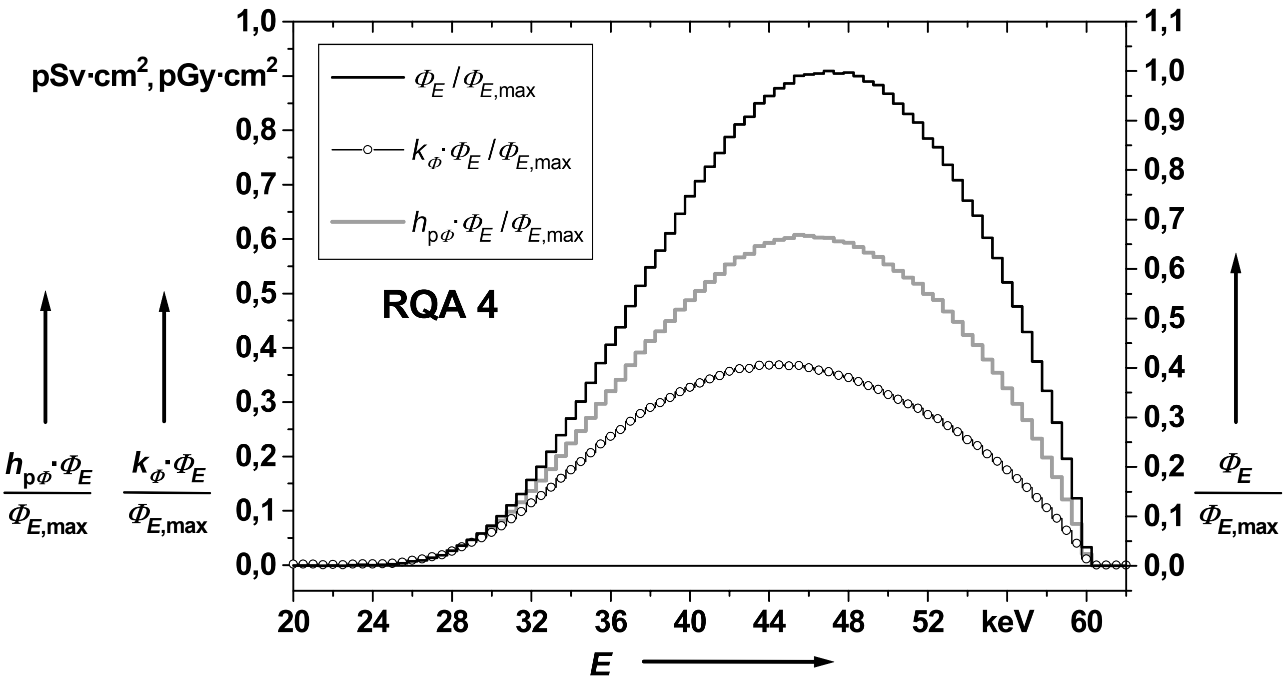

Verfügbar unter: https://doi.org/10.7795/110.20190315B

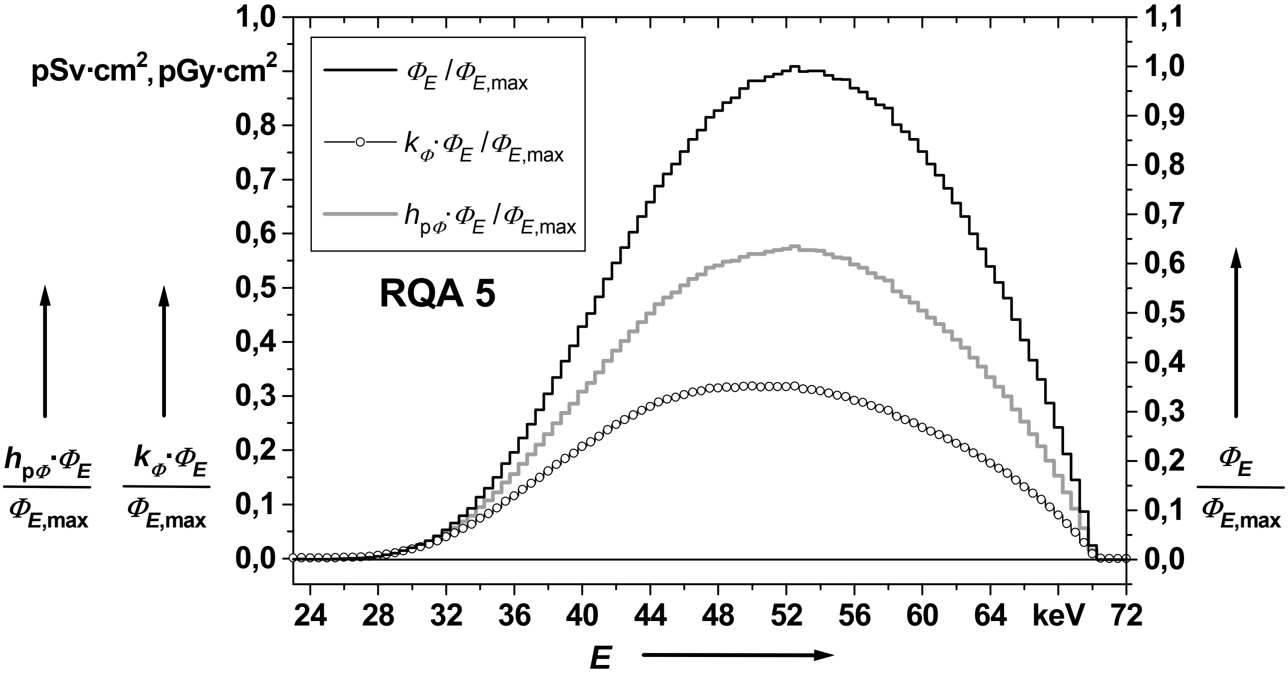

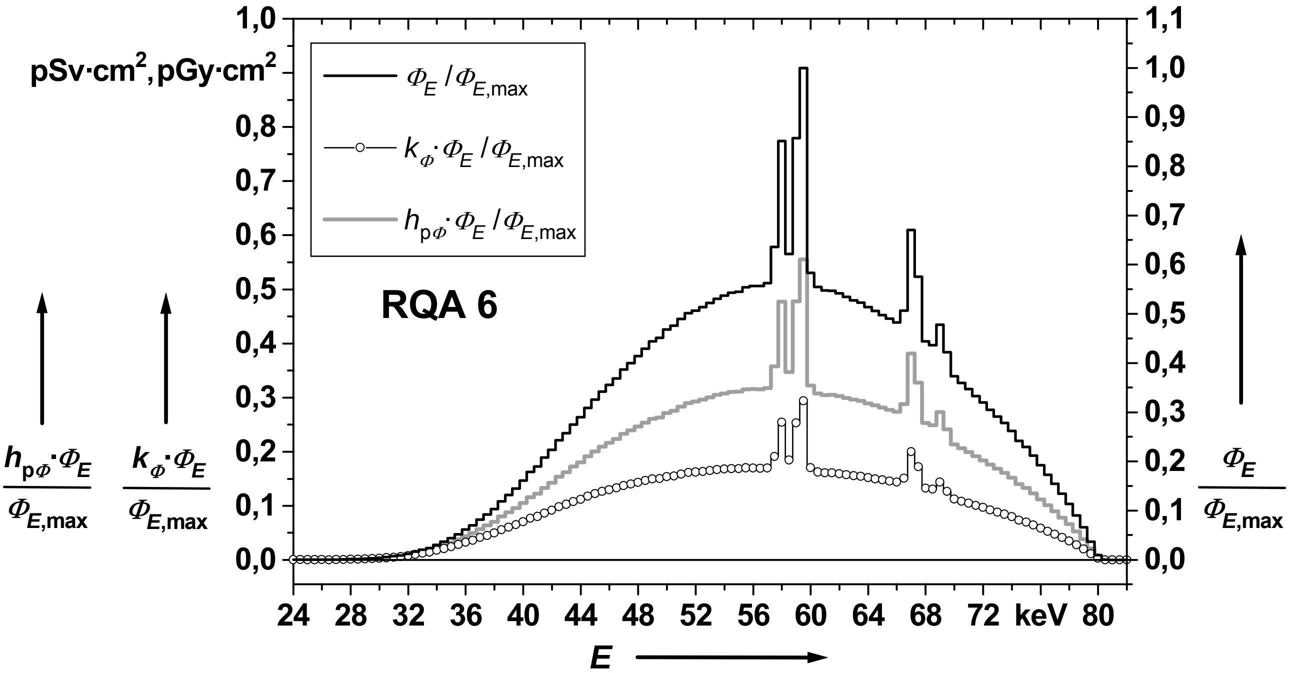

Verfügbar unter: https://doi.org/10.7795/110.20190315B

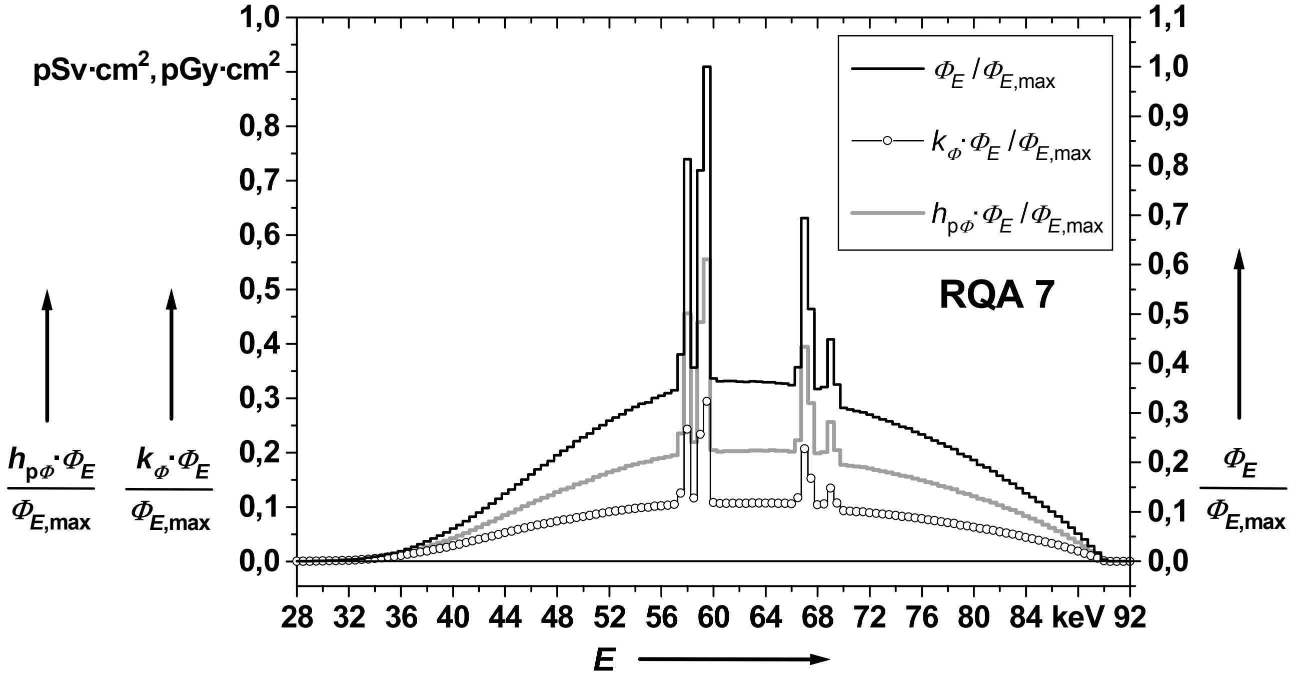

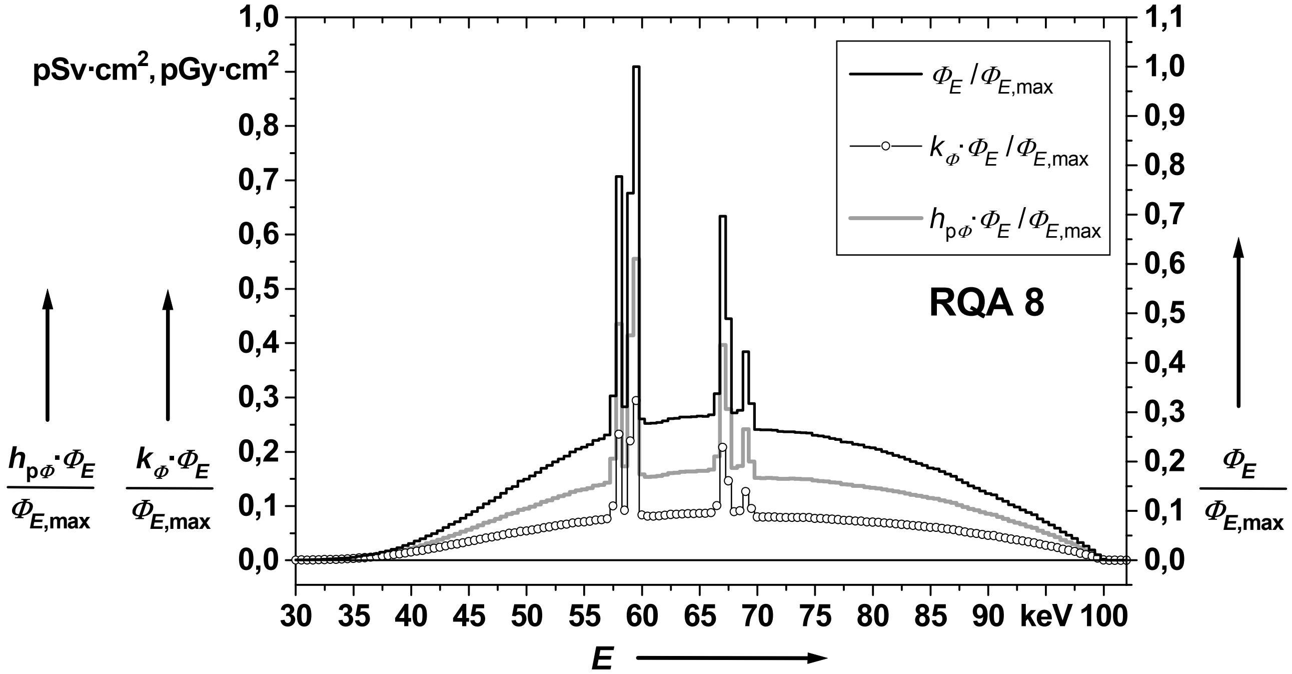

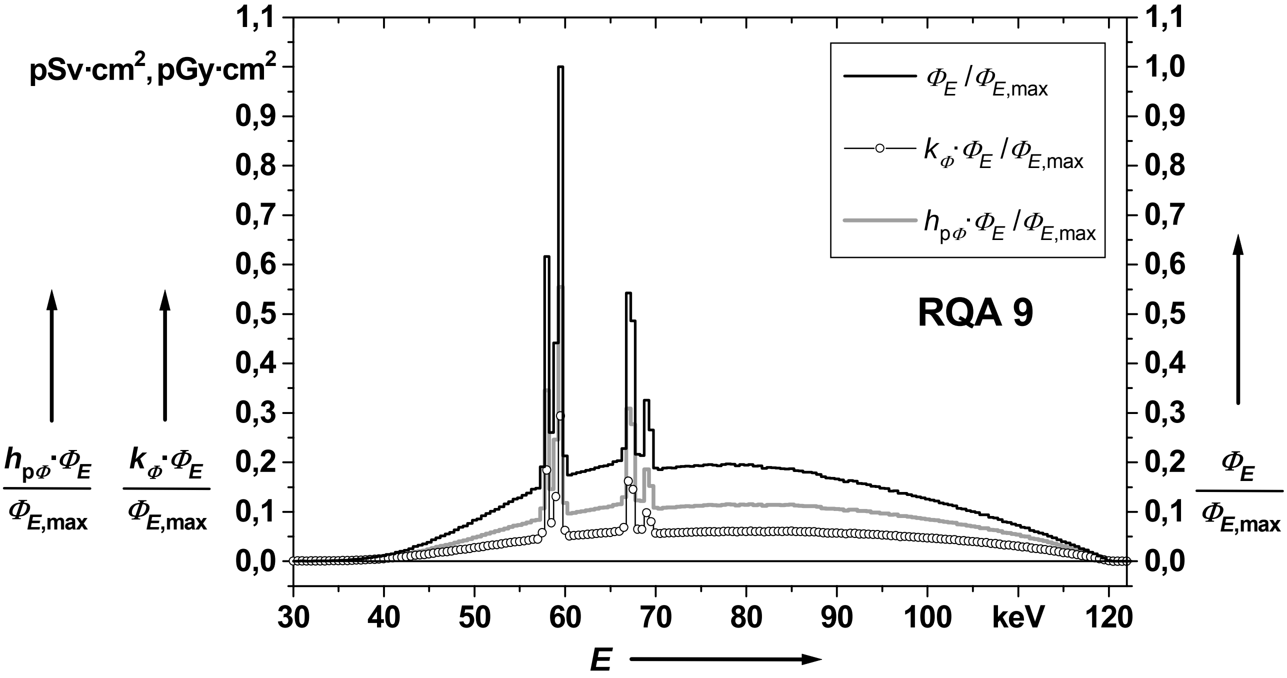

1,1
pSv·cm², pGy·cm²
$\Phi_E / \Phi_{E,max}$
$k_\Phi \cdot \Phi_E / \Phi_{E,max}$
$h_{p\Phi} \cdot \Phi_E / \Phi_{E,max}$
RQA 9
$\frac{h_{p\Phi} \cdot \Phi_E}{\Phi_{E,max}}$
$\frac{k_\Phi \cdot \Phi_E}{\Phi_{E,max}}$
$\frac{\Phi_E}{\Phi_{E,max}}$
0,0 0,1 0,2 0,3 0,4 0,5 0,6 0,7 0,8 0,9 1,0 1,1
30 40 50 60 70 80 90 100 keV 120
E

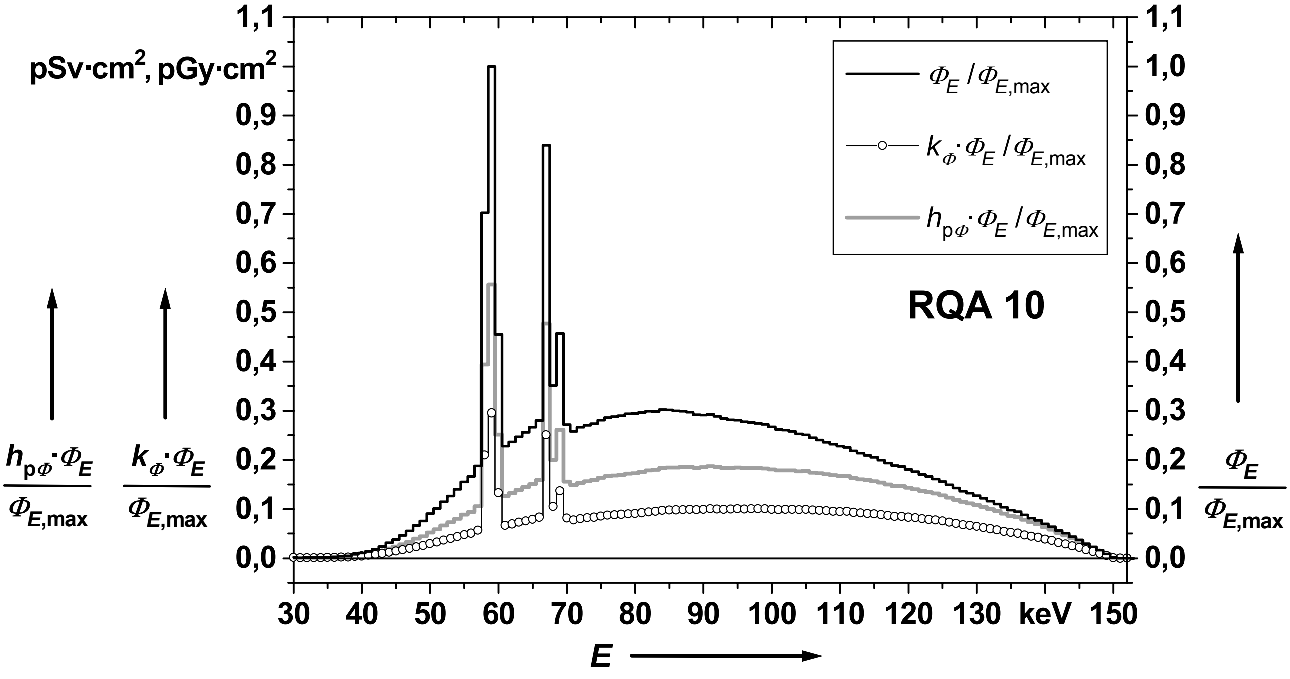

1,1
pSv·cm², pGy·cm²
$\Phi_E / \Phi_{E,max}$
$k_\Phi \cdot \Phi_E / \Phi_{E,max}$
$h_{p\Phi} \cdot \Phi_E / \Phi_{E,max}$
RQA 10
$\frac{h_{p\Phi} \cdot \Phi_E}{\Phi_{E,max}}$
$\frac{k_\Phi \cdot \Phi_E}{\Phi_{E,max}}$
$\frac{\Phi_E}{\Phi_{E,max}}$
0,0 0,1 0,2 0,3 0,4 0,5 0,6 0,7 0,8 0,9 1,0 1,1
30 40 50 60 70 80 90 100 110 120 130 keV 150
E

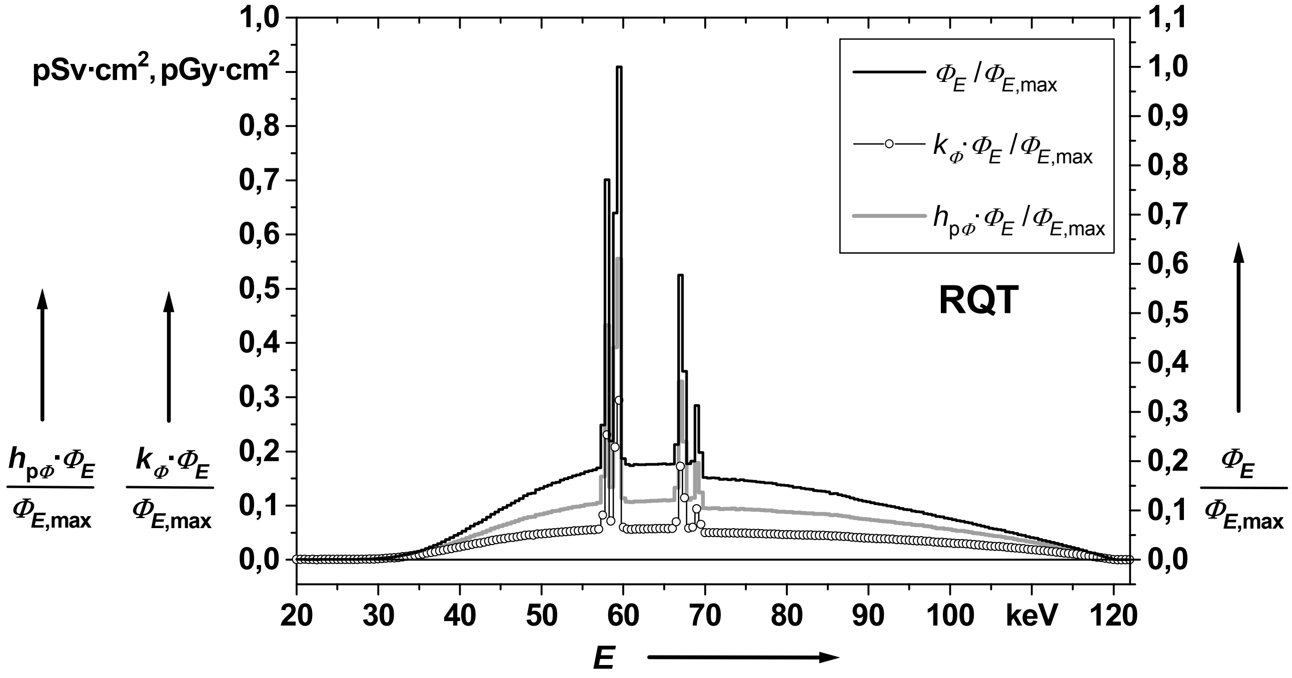

5.8 Unfiltered X-ray spectra

The unfiltered X-ray spectra with a tube voltage of 7,5 kV and 10 kV are identical with A 7,5 and H-10, respectively. They are shown in Sections 5.3 and 5.5. The unfiltered X-ray spectra generated with a tube voltage of up to 120 kV was measured at a reference distance of 1,0 m; the spectra generated with a tube voltage higher than 120 kV are given for a reference distance of 2,5 m.

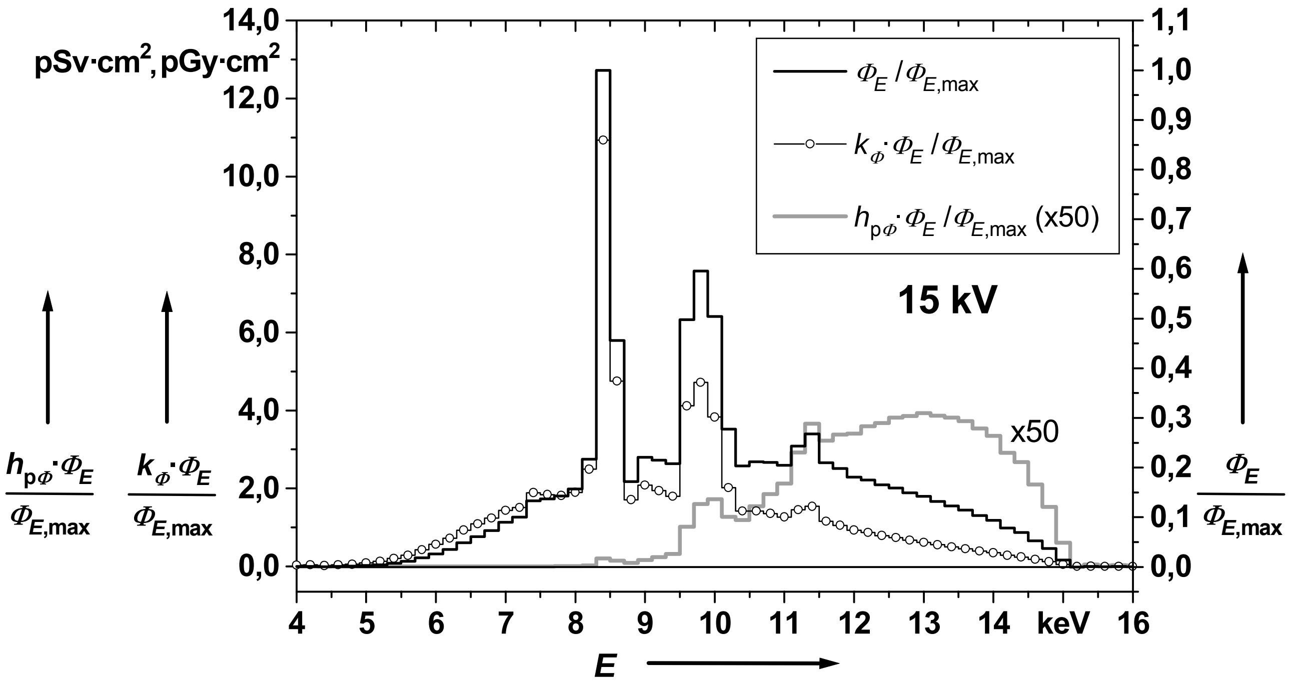

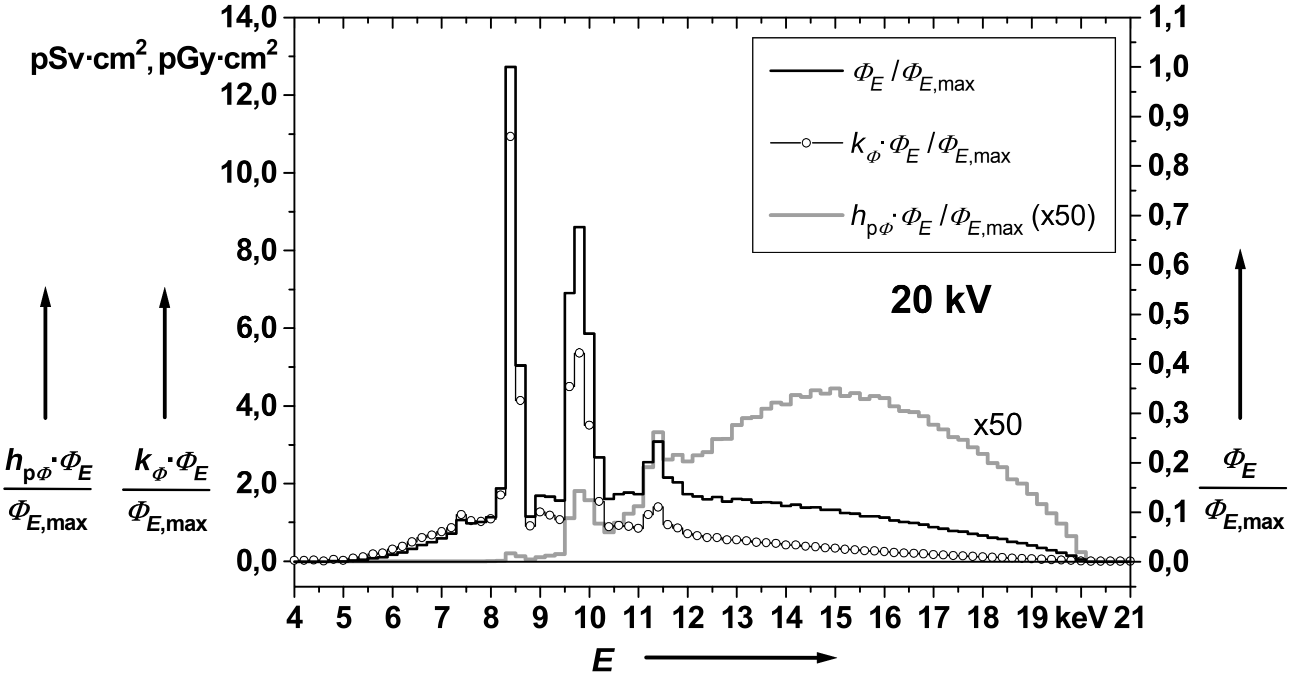

pSv·cm², pGy·cm²
$\Phi_E / \Phi_{E,\max}$
$k_\Phi \cdot \Phi_E / \Phi_{E,\max}$
$h_{p\Phi} \cdot \Phi_E / \Phi_{E,\max}$ (x50)
20 kV
x50
$\frac{h_{p\Phi} \cdot \Phi_E}{\Phi_{E,\max}}$
$\frac{k_\Phi \cdot \Phi_E}{\Phi_{E,\max}}$
$\frac{\Phi_E}{\Phi_{E,\max}}$
E
keV

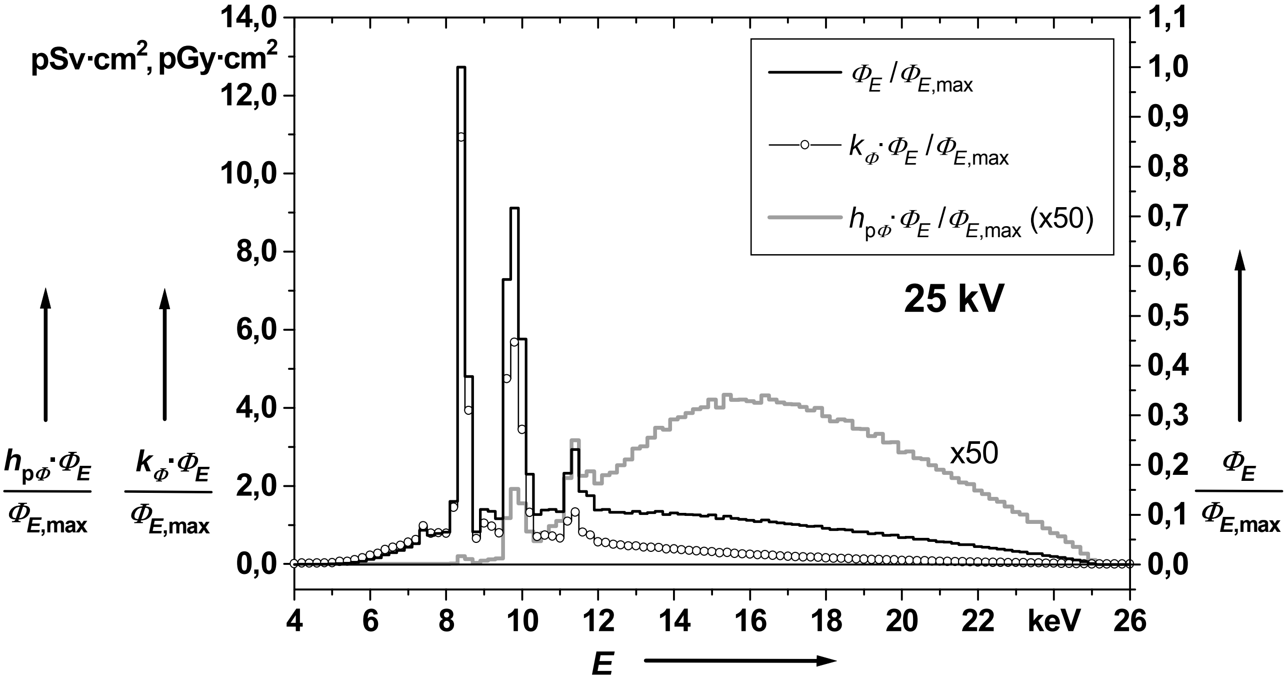

pSv·cm², pGy·cm²
$\Phi_E / \Phi_{E,\max}$
$k_\Phi \cdot \Phi_E / \Phi_{E,\max}$
$h_{p\Phi} \cdot \Phi_E / \Phi_{E,\max}$ (x50)
25 kV
x50
$\frac{h_{p\Phi} \cdot \Phi_E}{\Phi_{E,\max}}$
$\frac{k_\Phi \cdot \Phi_E}{\Phi_{E,\max}}$
$\frac{\Phi_E}{\Phi_{E,\max}}$
E
keV

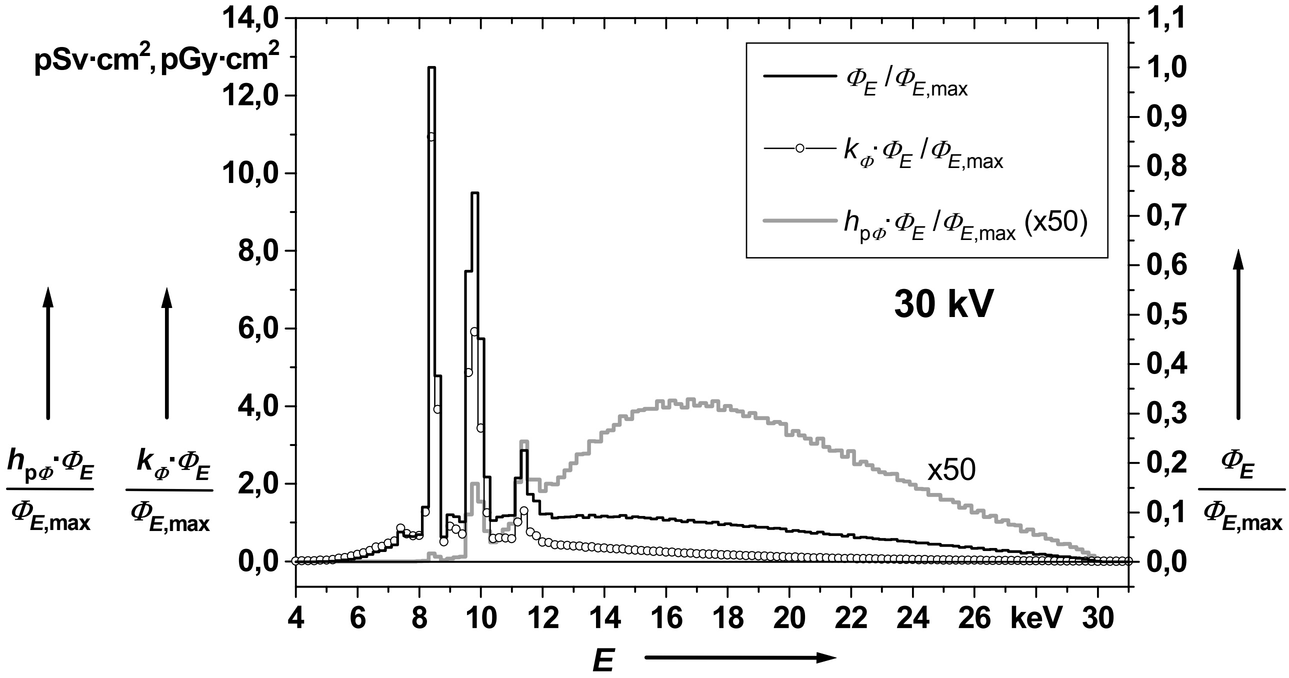

14,0
pSv·cm², pGy·cm²
12,0
10,0
8,0
6,0
4,0
2,0
0,0
1,1
1,0
0,9
0,8
0,7
0,6
0,5
0,4
0,3
0,2
0,1
0,0
$\Phi_E / \Phi_{E,\max}$
$k_\Phi \cdot \Phi_E / \Phi_{E,\max}$
$h_{p\Phi} \cdot \Phi_E / \Phi_{E,\max}$ (x50)
30 kV
x50
$\frac{h_{p\Phi} \cdot \Phi_E}{\Phi_{E,\max}}$
$\frac{k_\Phi \cdot \Phi_E}{\Phi_{E,\max}}$
$\frac{\Phi_E}{\Phi_{E,\max}}$
4 6 8 10 12 14 16 18 20 22 24 26 keV 30
E

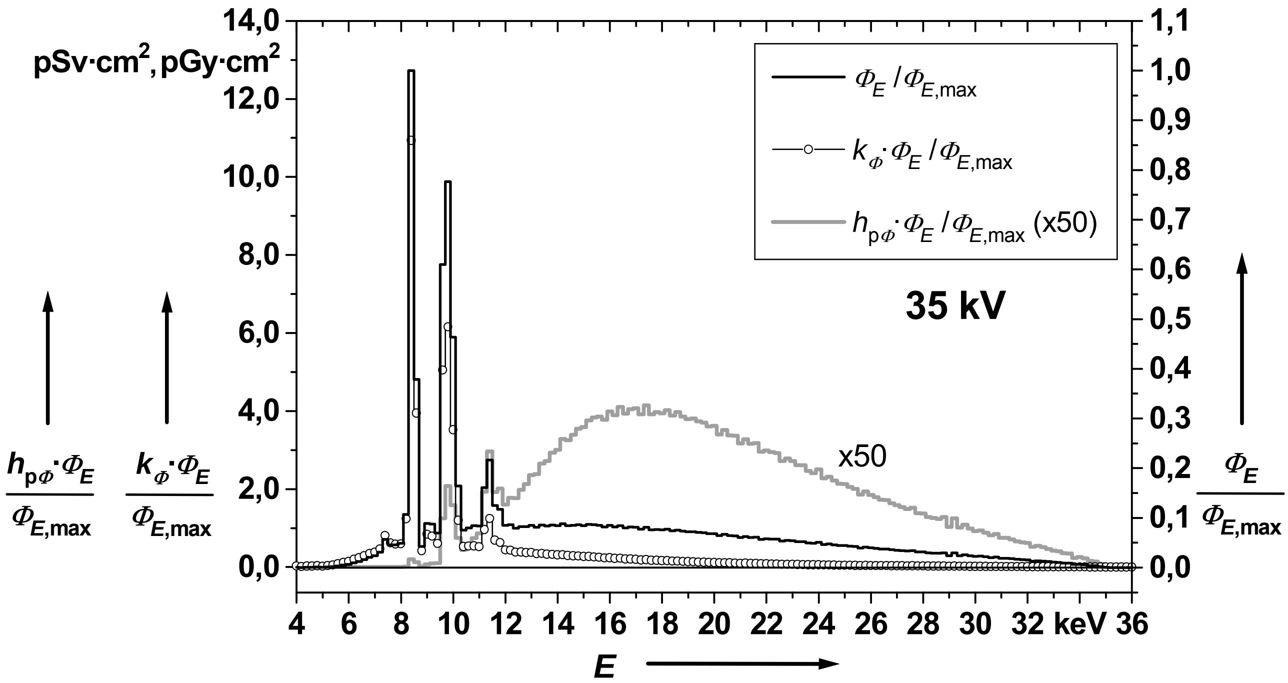

14,0
pSv·cm², pGy·cm²
12,0
10,0
8,0
6,0
4,0
2,0
0,0
1,1
1,0
0,9
0,8
0,7
0,6
0,5
0,4
0,3
0,2
0,1
0,0
$\Phi_E / \Phi_{E,\max}$
$k_\Phi \cdot \Phi_E / \Phi_{E,\max}$
$h_{p\Phi} \cdot \Phi_E / \Phi_{E,\max}$ (x50)
35 kV
x50
$\frac{h_{p\Phi} \cdot \Phi_E}{\Phi_{E,\max}}$
$\frac{k_\Phi \cdot \Phi_E}{\Phi_{E,\max}}$
$\frac{\Phi_E}{\Phi_{E,\max}}$
4 6 8 10 12 14 16 18 20 22 24 26 28 30 32 keV 36
E

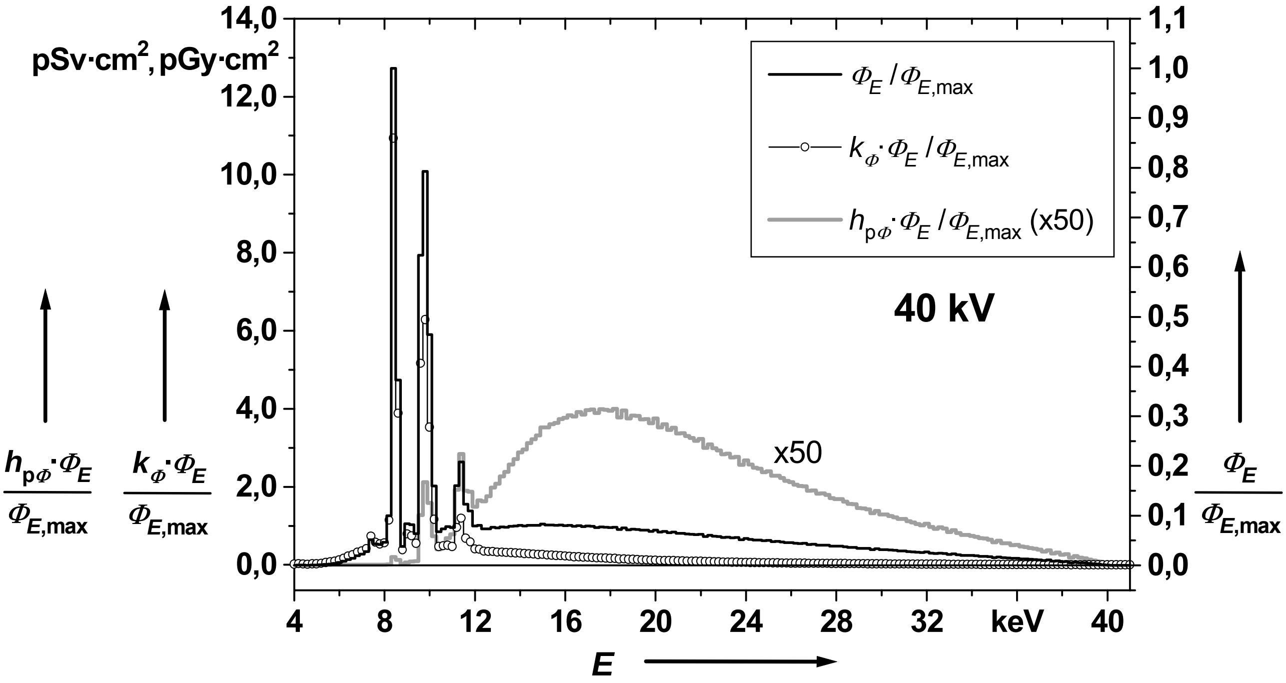

14,0
pSv·cm², pGy·cm²
12,0
10,0
8,0
6,0
4,0
2,0
0,0
1,1
1,0
0,9
0,8
0,7
0,6
0,5
0,4
0,3
0,2
0,1
0,0
Φ_E / Φ_E,max
k_Φ·Φ_E / Φ_E,max
h_pΦ·Φ_E / Φ_E,max (x50)
40 kV
x50
h_pΦ·Φ_E / Φ_E,max
k_Φ·Φ_E / Φ_E,max
Φ_E / Φ_E,max
4 8 12 16 20 24 28 32 keV 40
E

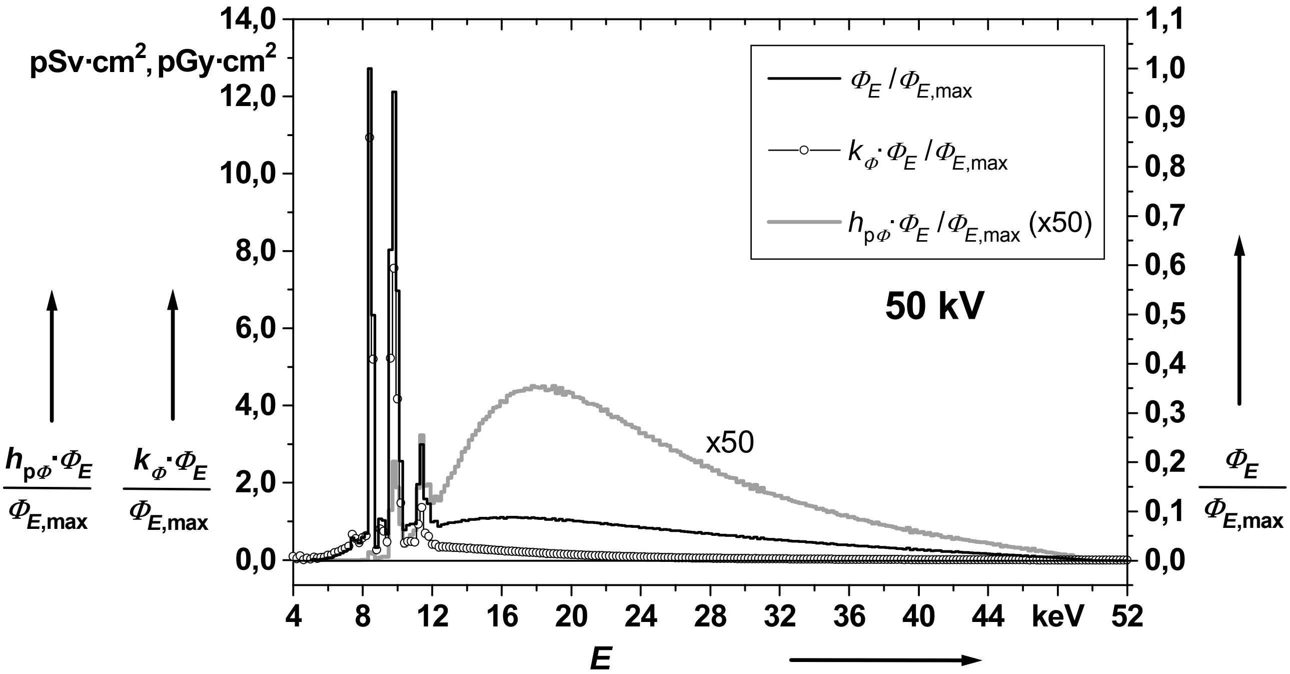

14,0
pSv·cm², pGy·cm²
12,0
10,0
8,0
6,0
4,0
2,0
0,0
1,1
1,0
0,9
0,8
0,7
0,6
0,5
0,4
0,3
0,2
0,1
0,0
Φ_E / Φ_E,max
k_Φ·Φ_E / Φ_E,max
h_pΦ·Φ_E / Φ_E,max (x50)
50 kV
x50
h_pΦ·Φ_E / Φ_E,max
k_Φ·Φ_E / Φ_E,max
Φ_E / Φ_E,max
4 8 12 16 20 24 28 32 36 40 44 keV 52
E

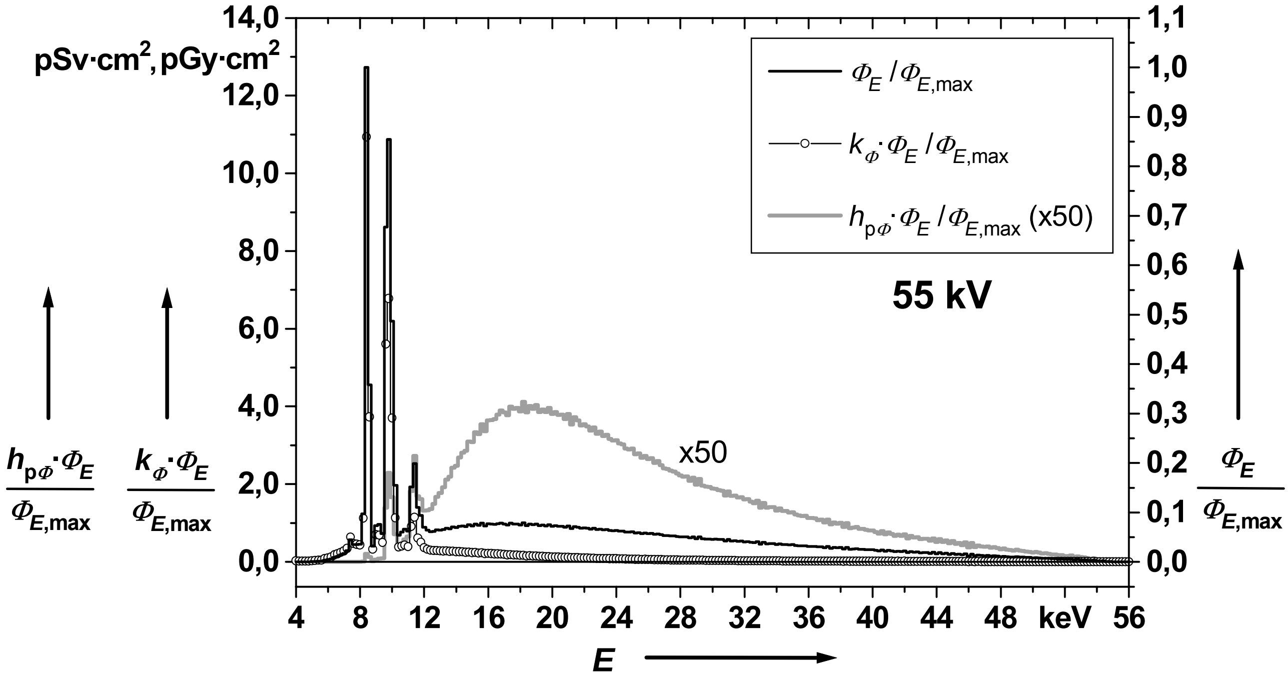
pSv·cm², pGy·cm²
14,0
12,0
10,0
8,0
6,0
4,0
2,0
0,0
1,1
1,0
0,9
0,8
0,7
0,6
0,5
0,4
0,3
0,2
0,1
0,0
$\Phi_E / \Phi_{E,max}$
$k_\Phi \cdot \Phi_E / \Phi_{E,max}$
$h_{p\Phi} \cdot \Phi_E / \Phi_{E,max}$ (x50)
55 kV
x50
$h_{p\Phi} \cdot \Phi_E / \Phi_{E,max}$
$k_\Phi \cdot \Phi_E / \Phi_{E,max}$
$\Phi_E / \Phi_{E,max}$
4 8 12 16 20 24 28 32 36 40 44 48 keV 56
E

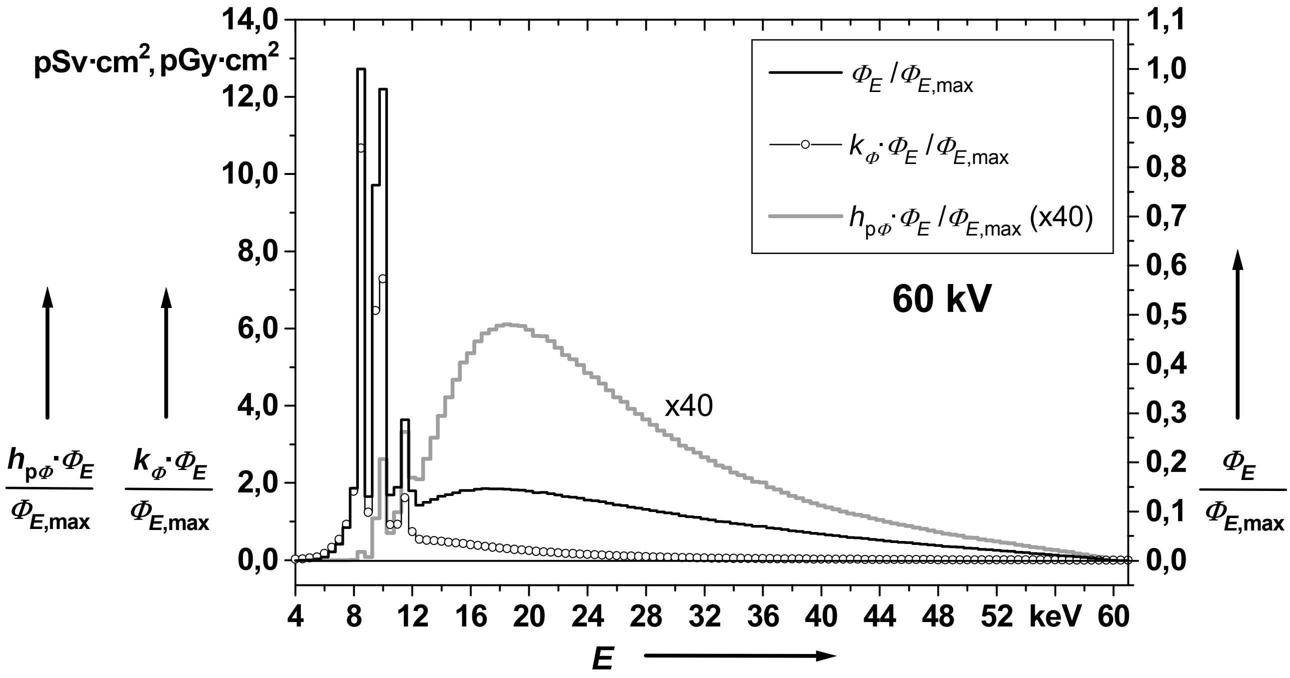
pSv·cm², pGy·cm²
14,0
12,0
10,0
8,0
6,0
4,0
2,0
0,0
1,1
1,0
0,9
0,8
0,7
0,6
0,5
0,4
0,3
0,2
0,1
0,0
$\Phi_E / \Phi_{E,max}$
$k_\Phi \cdot \Phi_E / \Phi_{E,max}$
$h_{p\Phi} \cdot \Phi_E / \Phi_{E,max}$ (x40)
60 kV
x40
$h_{p\Phi} \cdot \Phi_E / \Phi_{E,max}$
$k_\Phi \cdot \Phi_E / \Phi_{E,max}$
$\Phi_E / \Phi_{E,max}$
4 8 12 16 20 24 28 32 36 40 44 48 52 keV 60
E

Verfügbar unter: https://doi.org/10.7795/110.20190315B

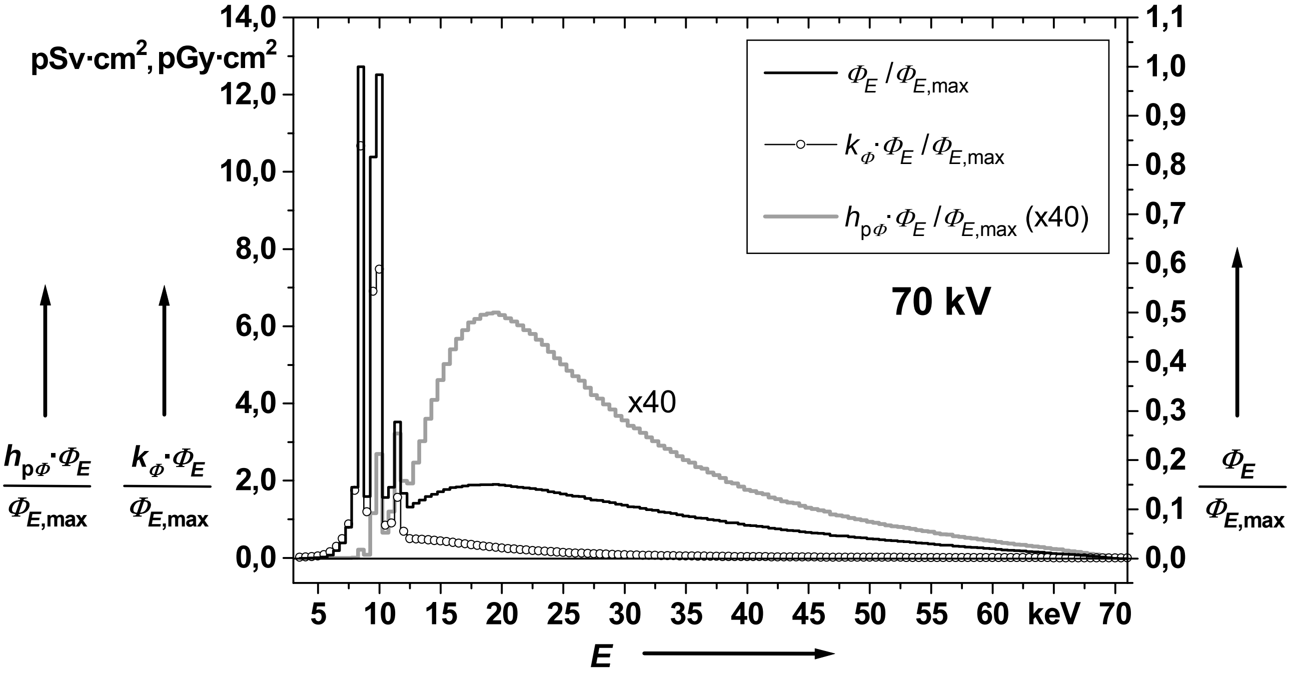

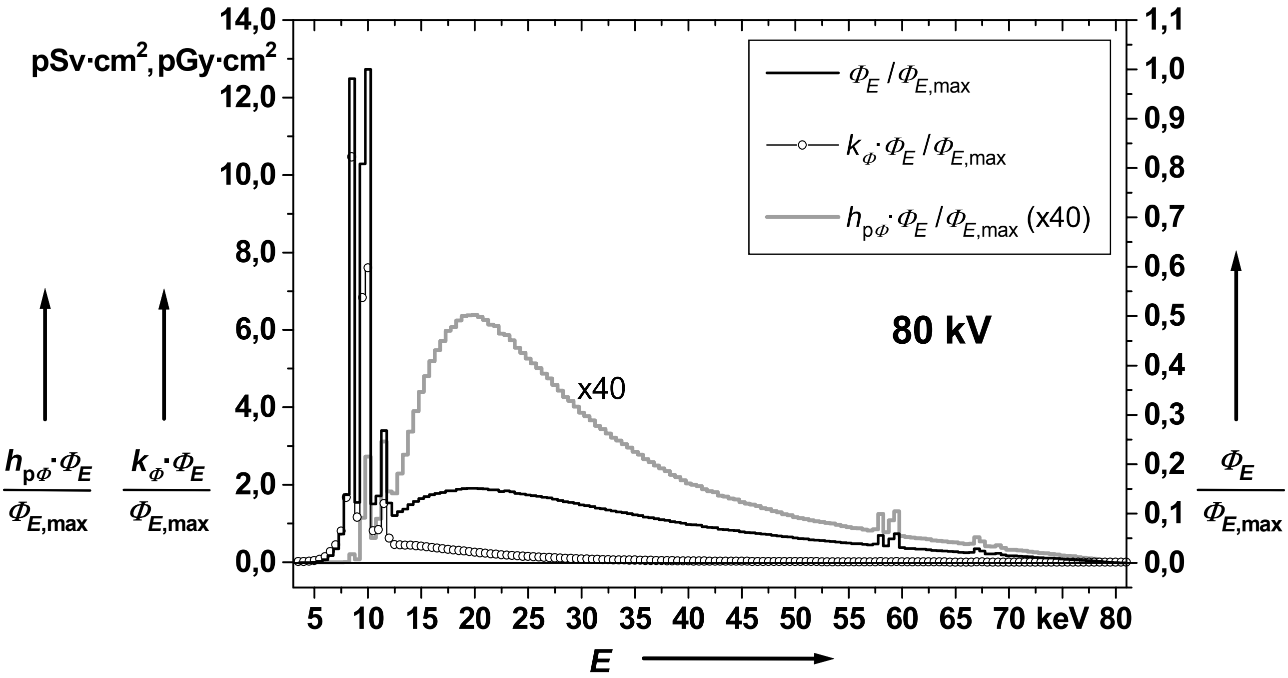

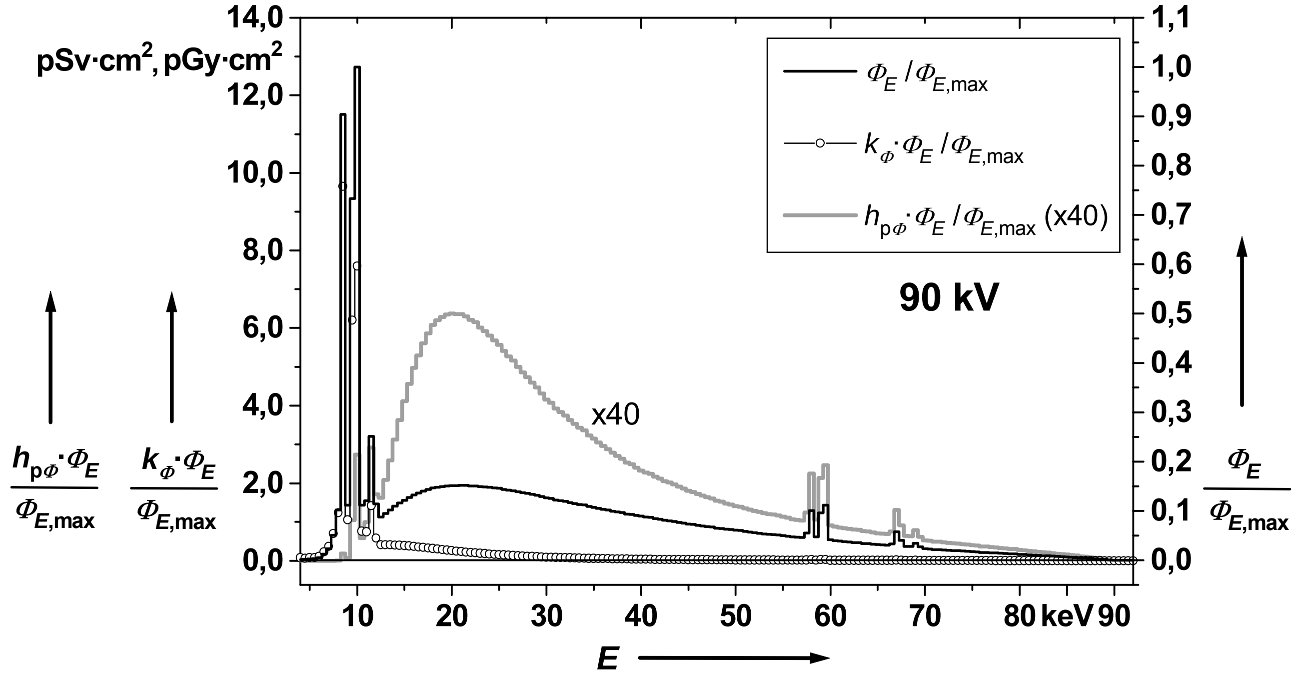

pSv·cm², pGy·cm²
14,0
12,0
10,0
8,0
6,0
4,0
2,0
0,0
1,1
1,0
0,9
0,8
0,7
0,6
0,5
0,4
0,3
0,2
0,1
0,0
$\Phi_E / \Phi_{E,max}$
$k_\Phi \cdot \Phi_E / \Phi_{E,max}$
$h_{p\Phi} \cdot \Phi_E / \Phi_{E,max}$ (x40)
90 kV
x40
$\frac{h_{p\Phi} \cdot \Phi_E}{\Phi_{E,max}}$
$\frac{k_\Phi \cdot \Phi_E}{\Phi_{E,max}}$
$\frac{\Phi_E}{\Phi_{E,max}}$
10 20 30 40 50 60 70 80 keV 90
E

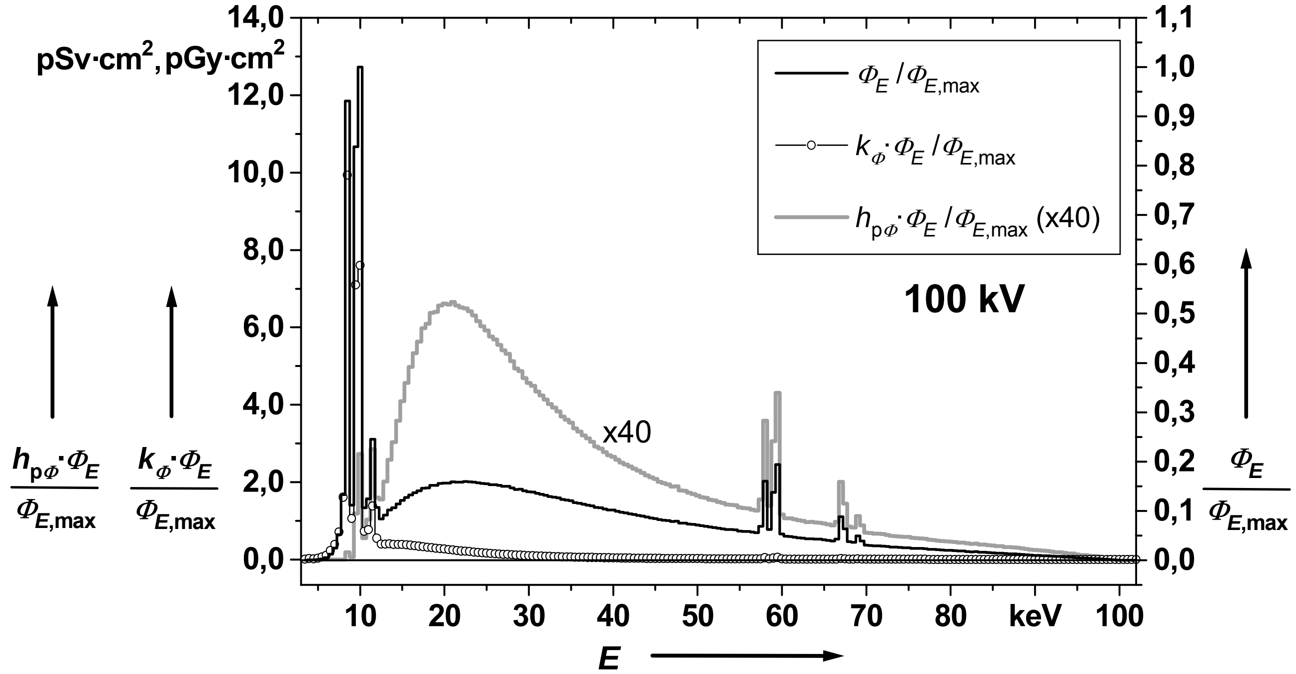

pSv·cm², pGy·cm²
14,0
12,0
10,0
8,0
6,0
4,0
2,0
0,0
1,1
1,0
0,9
0,8
0,7
0,6
0,5
0,4
0,3
0,2
0,1
0,0
$\Phi_E / \Phi_{E,max}$
$k_\Phi \cdot \Phi_E / \Phi_{E,max}$
$h_{p\Phi} \cdot \Phi_E / \Phi_{E,max}$ (x40)
100 kV
x40
$\frac{h_{p\Phi} \cdot \Phi_E}{\Phi_{E,max}}$
$\frac{k_\Phi \cdot \Phi_E}{\Phi_{E,max}}$
$\frac{\Phi_E}{\Phi_{E,max}}$
10 20 30 40 50 60 70 80 keV 100
E

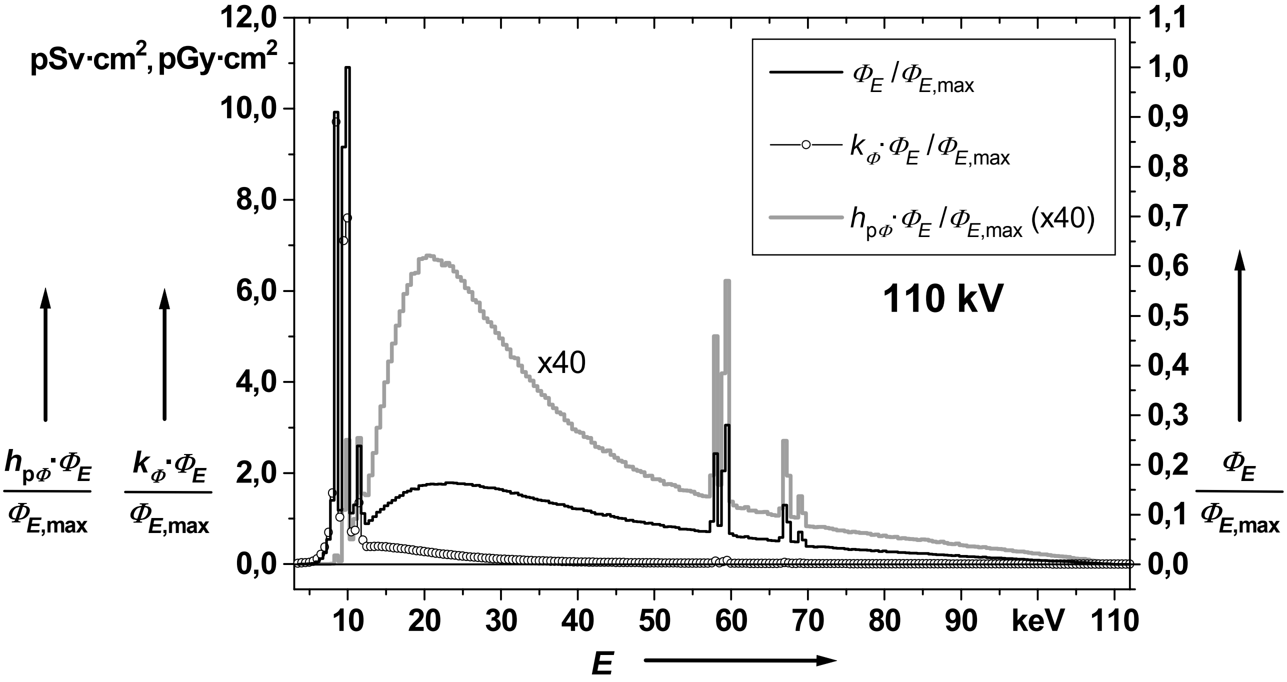

12,0
pSv·cm², pGy·cm²
10,0
8,0
6,0
4,0
2,0
0,0
1,1
1,0
0,9
0,8
0,7
0,6
0,5
0,4
0,3
0,2
0,1
0,0
$\Phi_E / \Phi_{E,\max}$
$k_\Phi \cdot \Phi_E / \Phi_{E,\max}$
$h_{p\Phi} \cdot \Phi_E / \Phi_{E,\max}$ (x40)
110 kV
x40
$\frac{h_{p\Phi} \cdot \Phi_E}{\Phi_{E,\max}}$
$\frac{k_\Phi \cdot \Phi_E}{\Phi_{E,\max}}$
$\frac{\Phi_E}{\Phi_{E,\max}}$
10 20 30 40 50 60 70 80 90 keV 110
E

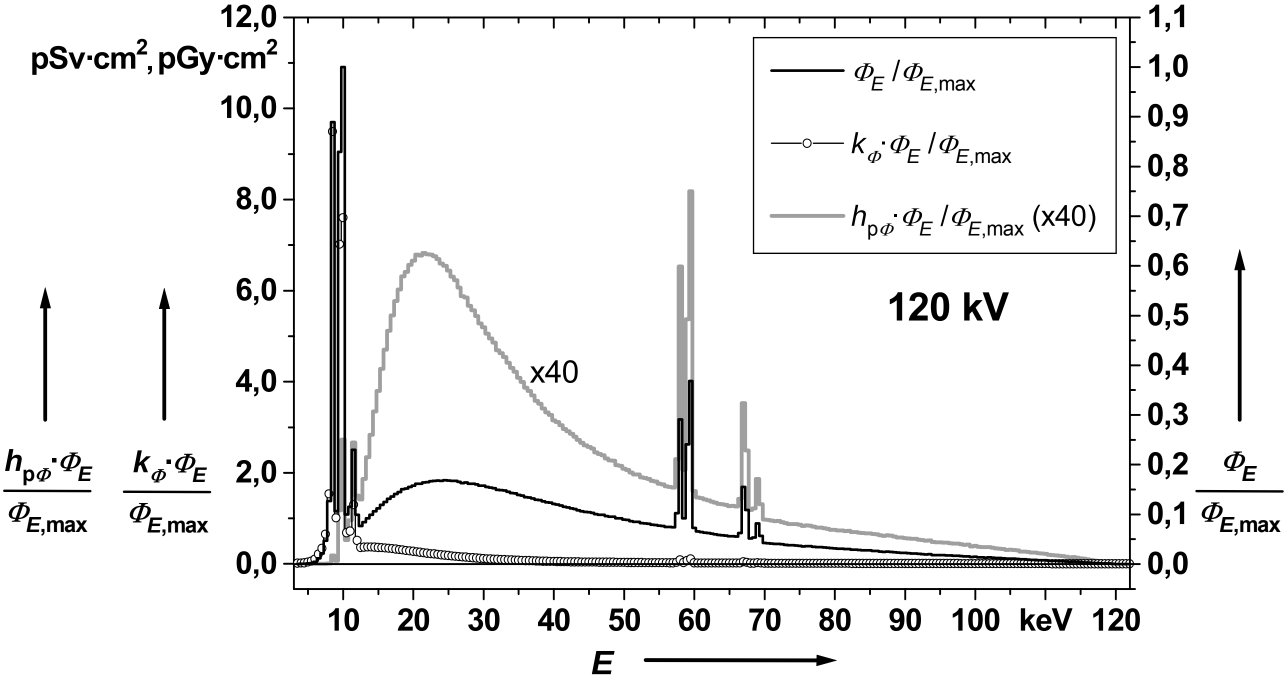

12,0
pSv·cm², pGy·cm²
10,0
8,0
6,0
4,0
2,0
0,0
1,1
1,0
0,9
0,8
0,7
0,6
0,5
0,4
0,3
0,2
0,1
0,0
$\Phi_E / \Phi_{E,\max}$
$k_\Phi \cdot \Phi_E / \Phi_{E,\max}$
$h_{p\Phi} \cdot \Phi_E / \Phi_{E,\max}$ (x40)
120 kV
x40
$\frac{h_{p\Phi} \cdot \Phi_E}{\Phi_{E,\max}}$
$\frac{k_\Phi \cdot \Phi_E}{\Phi_{E,\max}}$
$\frac{\Phi_E}{\Phi_{E,\max}}$
10 20 30 40 50 60 70 80 90 100 keV 120
E

Verfügbar unter: https://doi.org/10.7795/110.20190315B

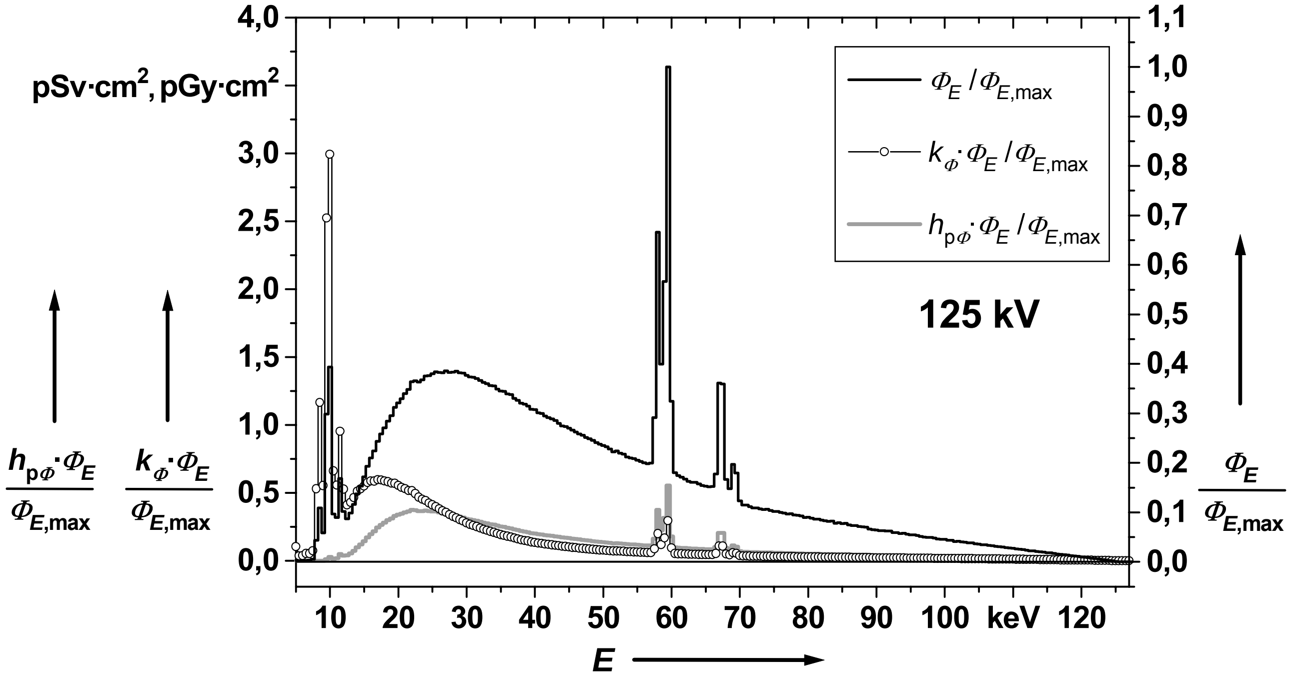

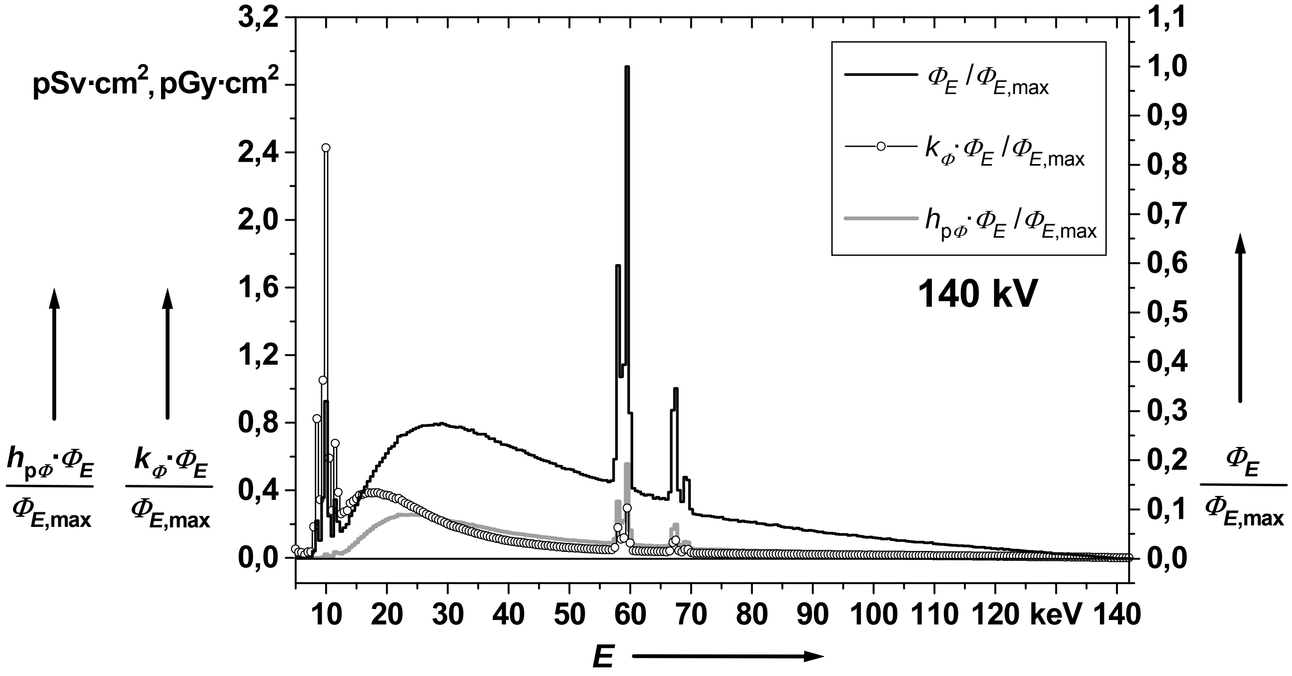

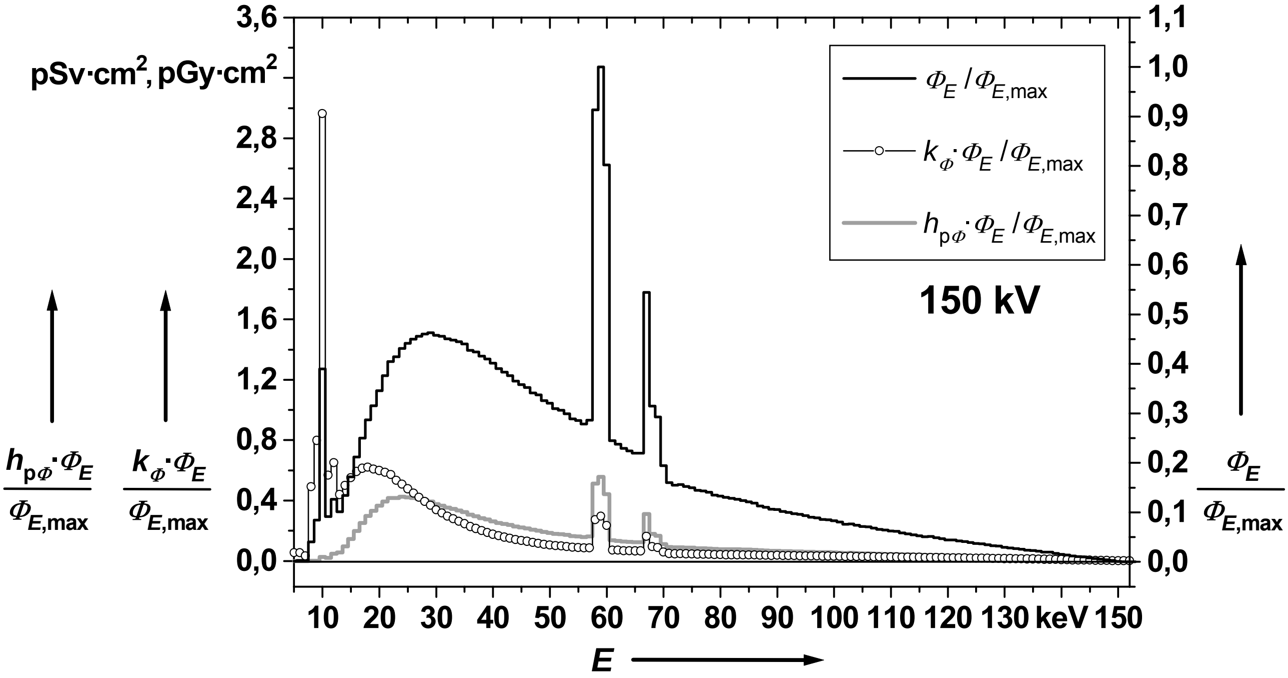

3,6
pSv·cm², pGy·cm²
2,8
2,4
2,0
1,6
1,2
0,8
0,4
0,0
1,1
1,0
0,9
0,8
0,7
0,6
0,5
0,4
0,3
0,2
0,1
0,0
Φ_E / Φ_E,max
k_Φ·Φ_E / Φ_E,max
h_pΦ·Φ_E / Φ_E,max
150 kV
h_pΦ·Φ_E / Φ_E,max
k_Φ·Φ_E / Φ_E,max
Φ_E / Φ_E,max
10 20 30 40 50 60 70 80 90 100 110 120 130 keV 150
E

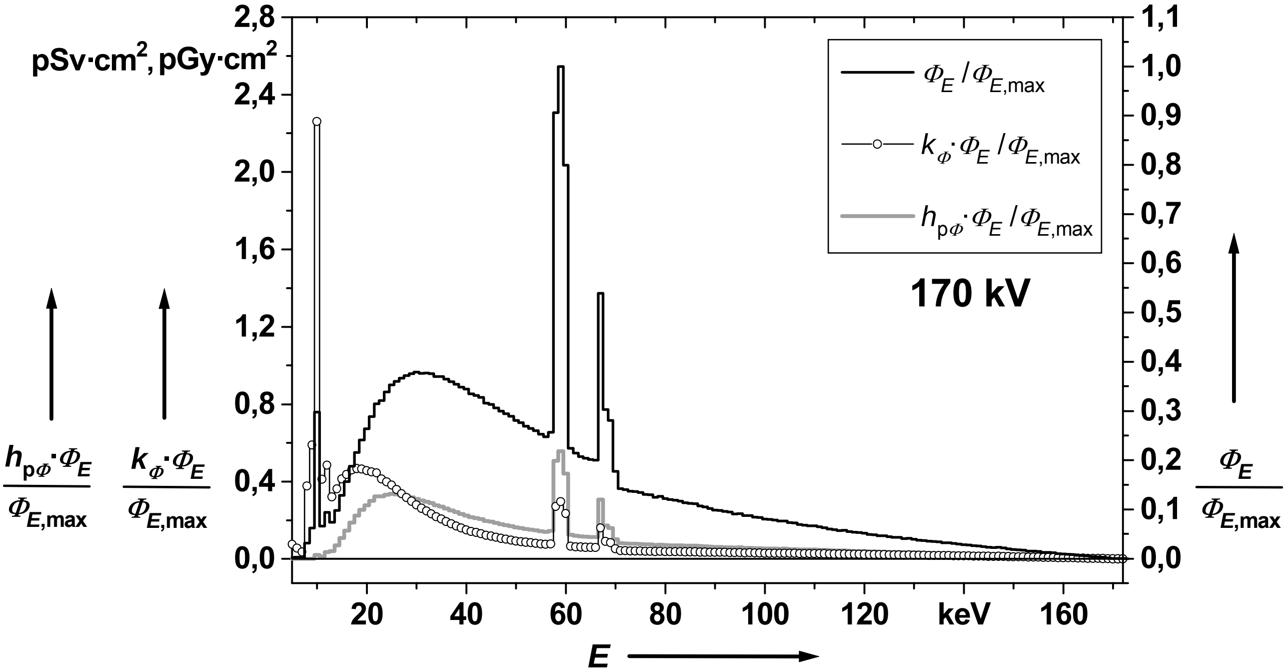

2,8
pSv·cm², pGy·cm²
2,4
2,0
1,6
1,2
0,8
0,4
0,0
1,1
1,0
0,9
0,8
0,7
0,6
0,5
0,4
0,3
0,2
0,1
0,0
Φ_E / Φ_E,max
k_Φ·Φ_E / Φ_E,max
h_pΦ·Φ_E / Φ_E,max
170 kV
h_pΦ·Φ_E / Φ_E,max
k_Φ·Φ_E / Φ_E,max
Φ_E / Φ_E,max
20 40 60 80 100 120 keV 160
E

Verfügbar unter: https://doi.org/10.7795/110.20190315B

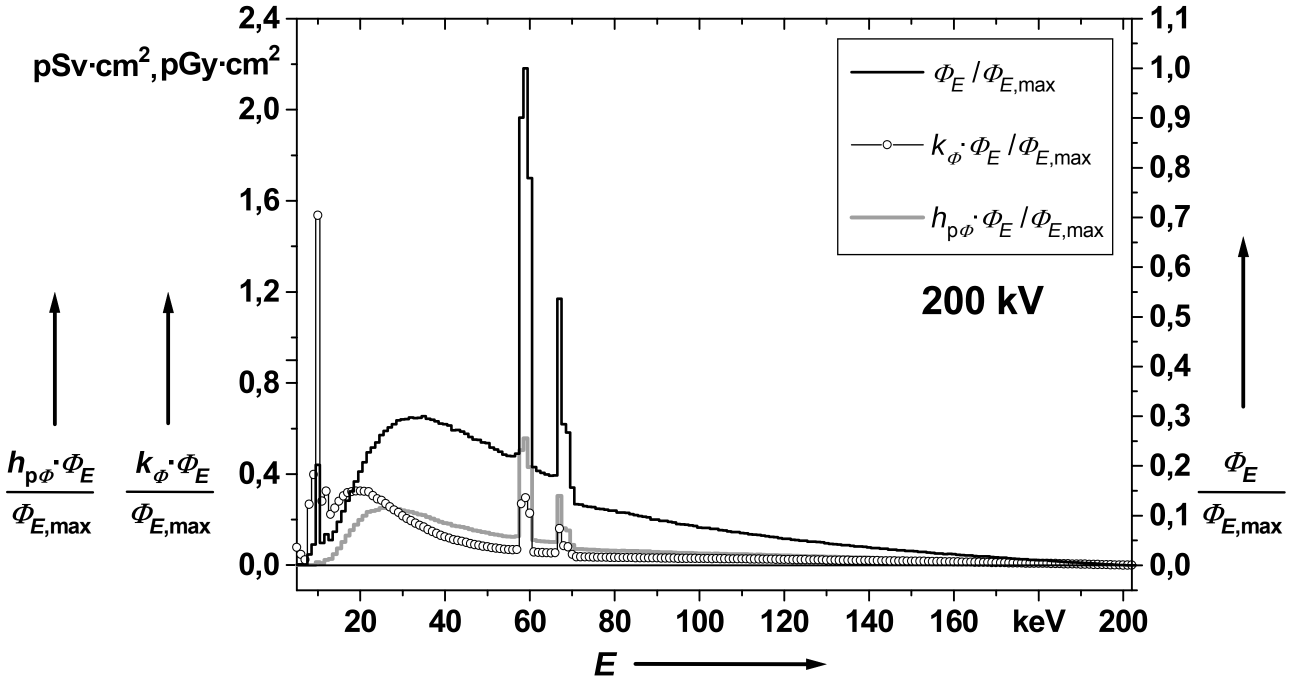

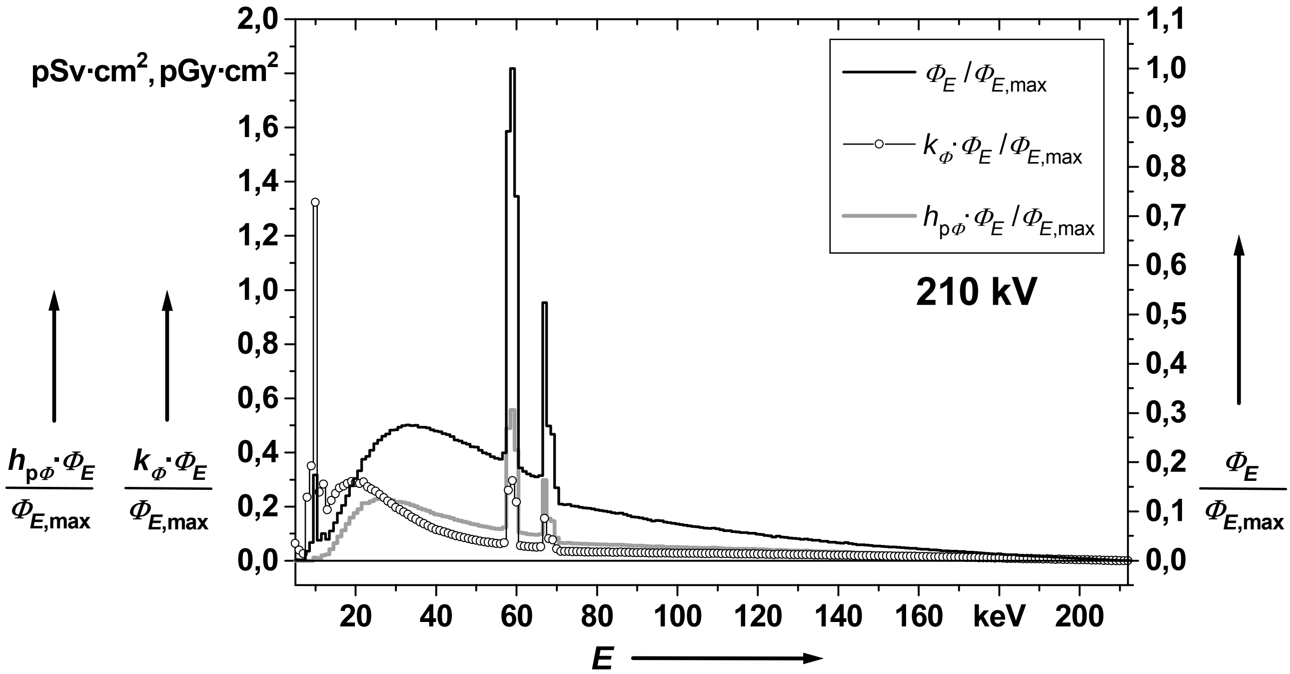

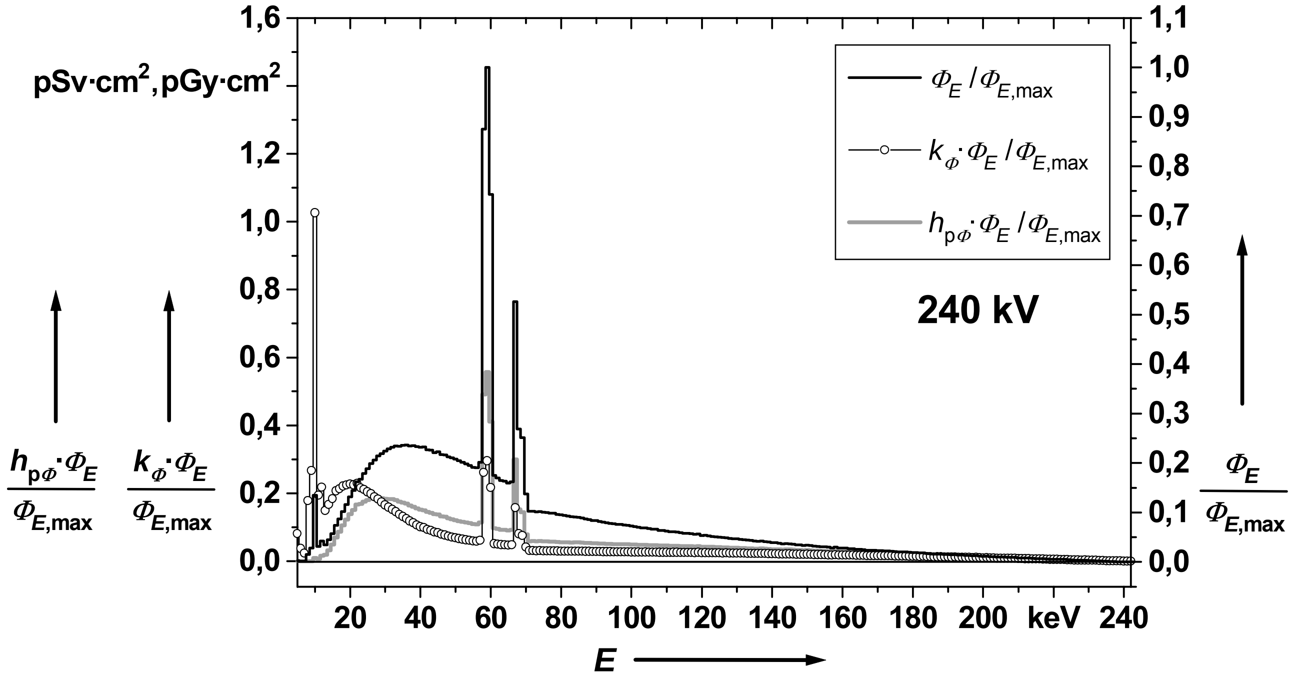
1,6
pSv·cm², pGy·cm²
1,2
1,0
0,8
0,6
0,4
0,2
0,0
$h_{p\Phi} \cdot \Phi_E$ / $\Phi_{E,max}$
$k_\Phi \cdot \Phi_E$ / $\Phi_{E,max}$
$\Phi_E / \Phi_{E,max}$
$k_\Phi \cdot \Phi_E / \Phi_{E,max}$
$h_{p\Phi} \cdot \Phi_E / \Phi_{E,max}$
240 kV
1,1
1,0
0,9
0,8
0,7
0,6
0,5
0,4
0,3
0,2
0,1
0,0
Φ_E / $\Phi_{E,max}$
20 40 60 80 100 120 140 160 180 200 keV 240
E

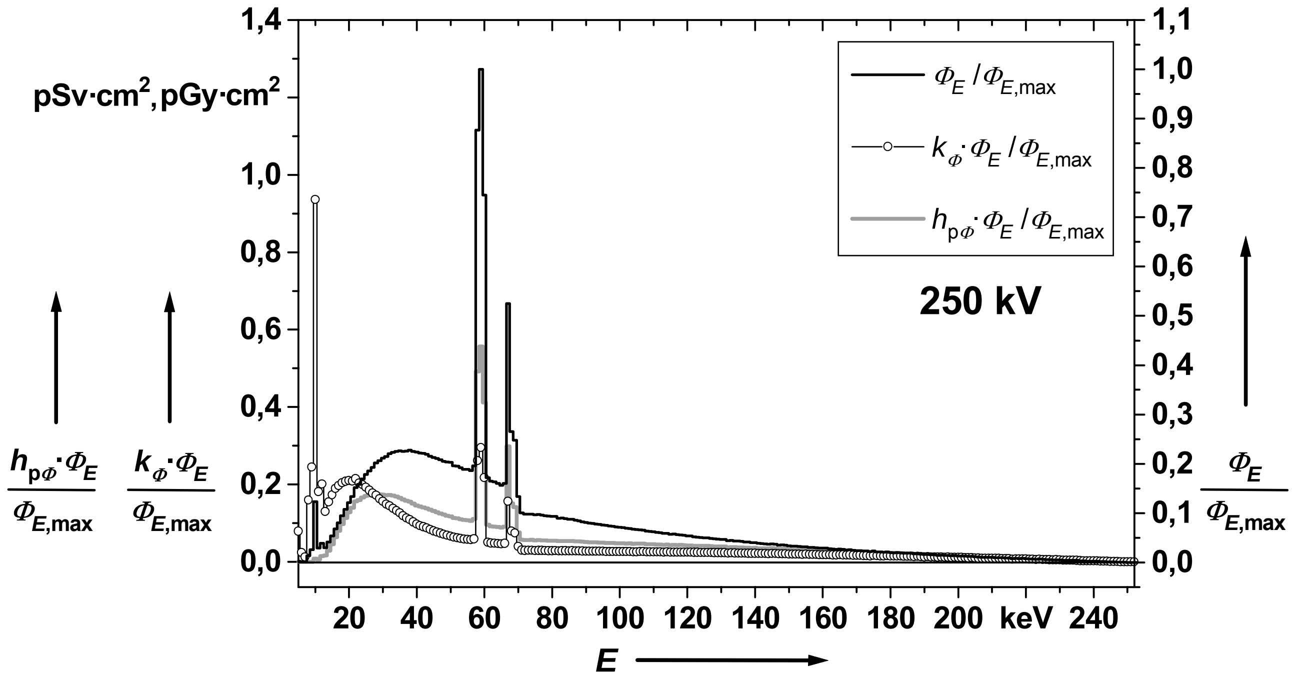
1,4
pSv·cm², pGy·cm²
1,0
0,8
0,6
0,4
0,2
0,0
$h_{p\Phi} \cdot \Phi_E$ / $\Phi_{E,max}$
$k_\Phi \cdot \Phi_E$ / $\Phi_{E,max}$
$\Phi_E / \Phi_{E,max}$
$k_\Phi \cdot \Phi_E / \Phi_{E,max}$
$h_{p\Phi} \cdot \Phi_E / \Phi_{E,max}$
250 kV
1,1
1,0
0,9
0,8
0,7
0,6
0,5
0,4
0,3
0,2
0,1
0,0
Φ_E / $\Phi_{E,max}$
20 40 60 80 100 120 140 160 180 200 keV 240
E

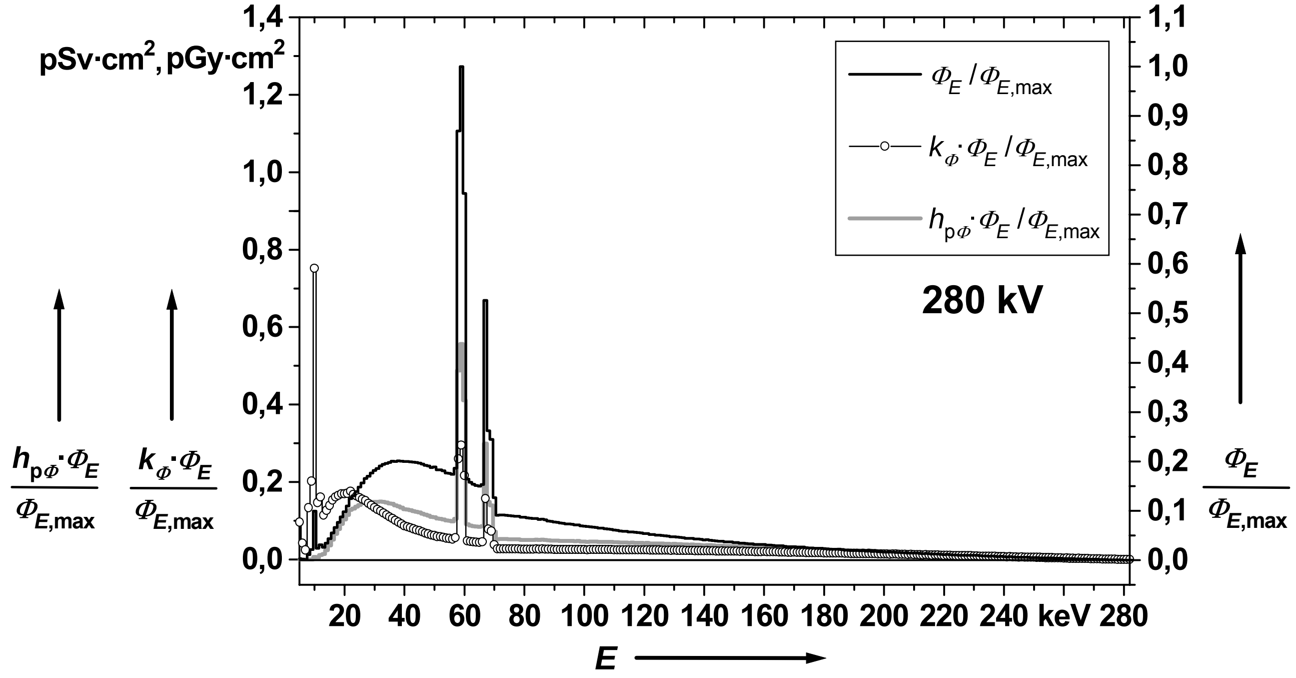

pSv·cm², pGy·cm²
1,4
1,2
1,0
0,8
0,6
0,4
0,2
0,0
1,1
1,0
0,9
0,8
0,7
0,6
0,5
0,4
0,3
0,2
0,1
0,0
Φ_E / Φ_E,max
k_Φ · Φ_E / Φ_E,max
h_pΦ · Φ_E / Φ_E,max
280 kV
h_pΦ · Φ_E / Φ_E,max
k_Φ · Φ_E / Φ_E,max
Φ_E / Φ_E,max
20 40 60 80 100 120 140 160 180 200 220 240 keV 280
E

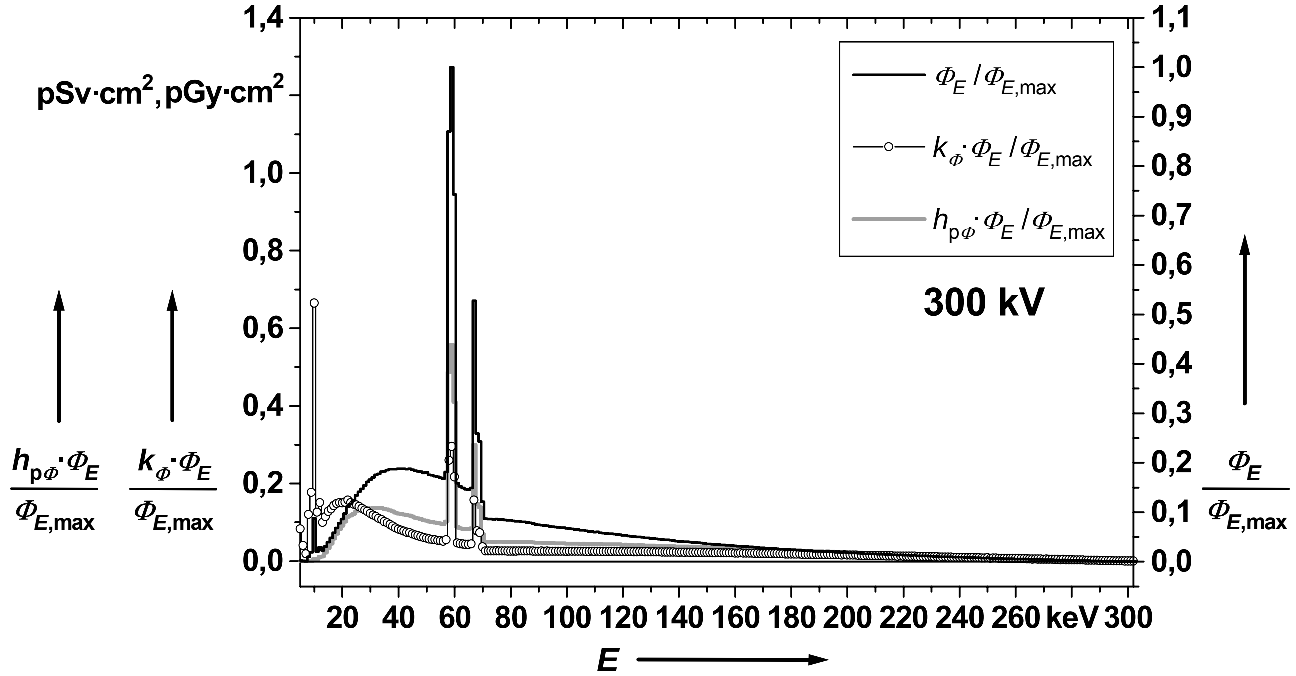

pSv·cm², pGy·cm²
1,4
1,0
0,8
0,6
0,4
0,2
0,0
1,1
1,0
0,9
0,8
0,7
0,6
0,5
0,4
0,3
0,2
0,1
0,0
Φ_E / Φ_E,max
k_Φ · Φ_E / Φ_E,max
h_pΦ · Φ_E / Φ_E,max
300 kV
h_pΦ · Φ_E / Φ_E,max
k_Φ · Φ_E / Φ_E,max
Φ_E / Φ_E,max
20 40 60 80 100 120 140 160 180 200 220 240 260 keV 300
E

6. References

[1] International Organization for Standardization, *Quantities and units – Part 0: General principles*, International Standard ISO 31-0, 1992

[2] International Organization for Standardization, *X and gamma reference radiation for calibrating dosemeters and doserate meters and for determining their response as a function of photon energy – Part 1: Radiation characteristics and production methods*, International Standard ISO 4037-1, 1997

[3] Deutsches Institut für Normung e.V., *Strahlenschutzdosimeter – Allgemeine Regeln*, DIN 6818-1, Beuth Verlag, Berlin, 1992

[4] International Electrotechnical Commission, *Medical diagnostic X-ray equipment – Radiation conditions for use in the determination of characteristics*, International Standard IEC 61267, 1994

[5] Deutsches Institut für Normung e.V., *Medizinische diagnostische Röntgeneinrichtungen, Bestrahlungsbedingungen zur Bestimmung von Kennmerkmalen*, DIN EN 61267, edition 01.97, Beuth Verlag, Berlin, 1997

[6] Deutsches Institut für Normung e.V., *Dosimeter mit Ionisationskammern für Photonen- und Elektronenstrahlung zur Verwendung in der Strahlentherapie – Regeln für die Herstellung*, DIN 6817, edition 10.84, Beuth Verlag, Berlin, 1984

[7] Deutsches Institut für Normung e.V., *Klinische Dosimetrie; Anwendung von Röntgenstrahlen mit Röhrenspannungen von 10 bis 100 kV in der Strahlentherapie und in der Weichteil-diagnostik*, DIN 6809-4, edition 12.88, Beuth Verlag, Berlin, 1988

[8] Deutsches Institut für Normung e.V., *Klinische Dosimetrie – Teil5: Anwendung von Röntgenstrahlen mit Röhrenspannungen von 100 bis 400 kV in der Strahlentherapie*, DIN 6809-5, edition 02.96, Beuth Verlag, Berlin, 1996

[9] International Commission on Radiation Units and Measurements, *Determination of dose equivalents resulting from external radiation sources*, ICRU Report 39, Bethesda, MD, 1985

[10] International Organization for Standardization, *X and gamma reference radiation calibrating dosemeters and doserate meters and for determining their response as a function of photon energy – Part 3: Calibration of area and personal dosemeters and the measurement of their response as a function of energy and angle of incidence*, International Standard ISO 4037-3, 1999

[11] PTB Testing Instructions, Vol. 11: Strahlenschutzdosimeter für Photonenstrahlung mit Energien zwischen 5 keV und 3 MeV, Physikalisch-Teschniche Bundesanstalt, 1977, ISSN 0341-7964

[12] Peaple, L.H.J., Birch, R. and Marshall, M., *Measurements of the ISO series of filtered radiations*, AERE-R13424, Environmental and Medical Sciences Division, Harwell Laboratory, Oxfordshire, May 1989

[13] Iles, W.J., *Conversion coefficients from air-kerma to ambient dose equivalent for the international standards organization's wide, narrow and low series of filtered X-radiations*, NRPB Report R206, 1987

[14] Read, L. and Hagreen, M., *The ISO narrow spectrum series of filtered X-radiations*, NPL Report RS(EXT)92, 1987

[15] Ankerhold, U., Behrens, R. and Ambrosi, P., *X-ray spectrometry of low energy photons for determining conversion coefficients from air kerma, K_a, to personal dose equivalent, $H_p(10)$, for radiation qualities of the ISO narrow-spectrum series*, Radiat. Prot. Dosim. **81**(4), 247-259, 1999

[16] Seelentag, W.W., Panzer, W., Drexler, G., Platz, L. and Santner, F., *A catalogue of spectra for the calibration of dosemeters*, GSF Report 560, 1979

[17] International Commission on Radiological Protection, *Conversion coefficients for use in radiological protection against external radiation*, ICRP Publication 74, Annals of the ICRP, Vol. 26, No. 3-4, 1987

[18] International Commission on Radiation Units and Measurements, *Conversion coefficients for use in radiological protection against external radiation*, ICRU Report 57, Bethesda, MD, 1 August 1998

[19] International Commission on Radiation Units and Measurements, *Measurement of dose equivalents from external photon and electron radiations*, ICRU Report 47, Bethesda, MD, 15 April 1992

[20] Böhm, J., Alberts W.G., Swinth, K.L., Soares, C.G., McDonald, J.C., Thompson, I.M.G. and Kramer, H.-M., *ISO recommended reference radiations for the calibration and proficiency testing of dosemeters and dose rate meters used in radiation protection*, Radiat. Prot. Dosim. **86**(2), 87-105, 1999

[21] International Organization for Standardization, *X and gamma reference radiation for calibrating dosemeters and doserate meters and for determining their response as a function of photon energy – Part 4: Calibration of personal dosemeters and dose equivalent (rate) meters in low energy X and gamma reference radiation fields*, International Standard ISO/WD 4037-4, under prepraration

[22] Engelke, B.-A., Oetzmann, W. and Struppek, G., *Die Meßeinrichtungen der Physikalisch-Technischen Bundesanstalt zur Darstellung der Einheiten der Standard-Ionendosis, Photonen-Äquivalentdosis und Luftkerma*, PTB Report, PTB-Dos-16, 1988

[23] Hubbell, J.H. and Seltzer, S.M., *Tables of X-ray mass attenuation coefficients and mass energy absorption coefficients 1 keV to MeV for elements Z=1 to 92 and 48 additional substances of dosimetric interest*, NIST, NISTIR 5632, 1995

[24] Deutsches Institut für Normung e.V., *Begriffe in der radiaologischen Technik – Teil 2: Strahlungsphysik*, DIN 6814-2, Beuth Verlag, Berlin, 1997

[25] Photcoef AIC Software, Grafton MA 01515, 1993
The database of the Photcoef program used the data published by the National Bureau of Standards (Berger, M.J. and Hubell, J.H., *XCOM: photon cross sections on a personal computer*, National Bureau of Standards, NBSIR 87-3597, 1987), the Los Alamos Scientific Laboratory (Storm, E. and Israel, H.I., *Photon cross sections from 0.001 to 100 MeV*, Los Alamos Scientific Laboratory, LA-3753, UC-34-Physics, TID-4500, 1967) and the Kaman Sciences Corporation (Veigele, W.J., Briggs, E., Bates, L., Henry, E.M. and Brackwell, B., *X-Ray cross section compilation from 0.1 keV to 1 MeV*, Kaman Sciences Corporation, DNA 2433 F, KN-71-431(R), 1971).

[26] International Commission on Radiation Units and Measurements, *Quantities and units in radiation protection dosimetry*, ICRU Report 51, Bethesda, MD, 1 September 1993

[27] International Commission on Radiation Units and Measurements, *Photon, electron, proton and neutron interaction data for body tissues*, ICRU Report 46, Bethesda, MD, 1992

[28] Ankerhold, U., Behrens, R., Ambrosi, P., *A prototype ionisation chamber as a secondary standard for the measurement of personal dose equivalent, $H_p(10)$, on a slab phantom*, Radiat. Prot. Dosim. **86**(3), 167-174, 1999

[29] International Organization for Standardization, *Guide to the Expression of Uncertainty in Measurement*, first published in 1993 in the name of BIPM, IEC, IFCC, ISO, IUPAC, IUPAP and OIML, corrected and reprinted 1995, Geneva, Switzerland